GEOPHYSICS

VOL. XXIII, NO. 4 OCTOBER, 1958

Deep-Hole Geophone Studies ..... *Franklyn K. Levin and Ralph D. Lynn* 639
Generation of Seismic Waves by Weight Drops ..... *S. N. Domenico* 665
Key Variables of Gravity ..... *Frederick E. Romberg* 684
Terrain Corrections for an Inclined Plane in Gravity Computations ..... *C. H. Sandberg* 701
Para- and Diamagnetic Susceptibilities in Non-Fluctuating Weak Fields ..... *William Schriever* 712
Results of Airborne Magnetometer Profile from Brownsville, Texas, to Guatemala City .. *W. B. Agocs* 726
Interrelationships Between Magnetic Anomaly Components ..... *James Affleck* 738
Magnetic Analysis by Logarithmic Curves ..... *Ralph D. Hutchison* 749
Some Effects of Formation Anisotropy on Resistivity Measurements in Boreholes ..... *K. S. Kunz and J. H. Moran* 770
Getting the Most out of Present Seismic Instruments .... *Joseph W. Hammond and James E. Hawkins* 795
An Empirical Velocity Determination in Southern Oklahoma ..... *Donald R. Oksa* 823
Revised Date of Issue for GEOPHYSICS ..... *The Editor* 838

DEPARTMENTS

Patents 839
Reviews and Publications Received 848
Discussions and Communications
Letters to the Editor 854
Contributors 865
Society Round Table
Committees 872
Local Sections 873
Society Affiliations 875
Membership Applications Received 875
Constitutional Amendments 876
Announcements 877
Personal Items 878
Calendar of Meetings 882

Published by the
Society of Exploration Geophysicists

FOR SEISMIC EXPLORATION

NATIONAL GEOPHYSICAL CO., INC.
8800 Lemmon Avenue
Dallas, Texas

DALLAS
DENVER
HOUSTON
MIDLAND

•
CALGARY

NATIONAL GEOPHYSICAL CO. OF CANADA, LTD.
Calgary, Alberta, Canada

for international surveys contact

namco INTERNATIONAL INCORPORATED
P. O. Box 13127, Dallas, Texas
Phone Fleetwood 2-2671

GEOPHYSICS

Published by the Society of Exploration Geophysicists

LAWRENCE Y. FAUST 1957-1959 Editor

Amerada Petroleum Corp., Box 2040, Tulsa 2, Okla.

ASSOCIATE EDITORS (1957-1959)

G. E. ARCHIE — Well Logging
Shell Oil Co., Box 2099, Houston 1, Texas

MILTON B. DOBRIN — Experimental Seismology
Triad Oil Co., Ltd., 535 7th Avenue W., Calgary, Alberta, Canada

JOHN C. HOLLISTER — Mining Geophysics
Department of Geophysics, Colorado of Mines, Golden, Colorado

PAUL L. LYONS — Seismic Theory
Sinclair Oil and Gas Co., Box 521, Tulsa 2, Okla.

L. L. NETTLETON — Gravity and Magnetic Prospecting
Gravity Meter Exploration Co., 340 M. Esperson Building, Houston 2, Texas

O. F. RITZMANN — Patents
The Gulf Companies, Gulf Building, Pittsburgh 30, Pennsylvania

IRWIN ROMAN — Electrical Prospecting
Geophysics Branch, U.S. Geological Survey, Washington 25, D.C.

EDGAR J. STULKEN — Seismic Field Techniques and Operations
Geophysical Service Inc., 100 Exchange Park North, Dallas 35, Texas

Manuscripts of papers submitted for publication in GEOPHYSICS should be sent directly to the Editor, with the exceptions noted below.

Reviews of geophysical literature published outside of this journal should be sent to the Chairman of the Reviews Committee.

Announcements, news items, and personal items should be sent to the business manager (see next page).

Form of Manuscript and instructions for its preparation may be found in GEOPHYSICS, v. 19, p. 141-153. Reprints of this style guide may be obtained from the business manager (see next page) upon request.

Responsibility for all statements and opinions made in GEOPHYSICS must be assumed by the repective authors.

Discussions and Letters to the Editor are welcomed by the Editor.

Subscriptions are given to all members of the Society in good standing as part payment for their dues. For non-members and organizations the subscription rate is $10.00 per year in the United States and its possessions and $10.50 per year in all other countries.

Change of Address Notice should be sent to the Business Manager (see next page). Claims for non-receipt must be sent within 3 months of date of publication to be filled gratis.

Single Copy price is $2.50 to members and $3.00 to non-members. For foreign shipment add 20¢ per copy. Subscriptions and single copy orders should be sent to the business manager (see next page).

Microcard copies of all back issues of GEOPHYSICS are available through the business office—prices upon request.

Advertising rates will be furnished by the Business Manager upon request. No advertisements will be accepted for prospecting methods based on hypotheses which are at variance with the accepted principles of physics.

Permission to Copy text material from GEOPHYSICS is limited to one page and is granted on the express condition that reference be made to the source of the material. Larger text excerpts and illustrations from GEOPHYSICS may not be reproduced without written permission of the Editor.

Indexed regularly by Engineering Index, Inc. and by The Applied Science and Technology Index.

Published by George Banta Company, Inc., Menasha, Wisconsin. Issued five times a year in January, April, July, October and December. Second-class postage paid at the Post Office at MENASHA, WISCONSIN, under the Act of March 3, 1879. Acceptance for mailing at the special rate of postage provided for in the Act of February 28, 1925, embodied in paragraph 4, Section 538, P. L. & R., authorized March 19, 1941. Copyright 1958 by the Society of Exploration Geophysicists.

Society of Exploration Geophysicists

The *Society of Exploration Geophysicists* had its beginning in 1930 when it was organized in Houston, Texas as the *Society of Petroleum Geophysicists*, the name being changed to its present form in 1936. The Society is dedicated to the advance of the science of geophysics and the art of geophysical prospecting. Through its journal GEOPHYSICS it supplies a medium for the dissemination of new knowledge in the field.

BUSINESS OFFICE

COLIN CAMPBELL, *Business Manager*
H. L. FARRIS, *Editorial Assistant*
Box 1536, Tulsa 1, Oklahoma

COUNCIL

OFFICERS (1957-1958)

O. C. CLIFFORD, JR. — *President*
The Atlantic Refining Co., Box 2819, Dallas 21, Texas

BEN F. RUMMERFIELD — *Vice-President*
Century Geophysical Corp., Jenkins Building, Tulsa 3, Oklahoma

HOWARD E. ITTEN — *Secretary-Treasurer*
Empire Geophysical, Inc., 6000 Camp Bowie Boulevard, Fort Worth, Texas

LAWRENCE Y. FAUST — *Editor*
Amerada Petroleum Corp., Box 2040, Tulsa 2, Oklahoma

ROY F. BENNETT — *Past President*
Sohio Petroleum Co., Skirvin Tower, Oklahoma City, Oklahoma

R. C. DUNLAP, JR. — *Prior Past President*
Geophysical Service Inc., 100 Exchange Park North, Dallas 35, Texas

DISTRICT REPRESENTATIVES

Ark-La-Tex Geophysical Society
Jackson S. Young (1958)
Herbert J. Ferber (1959)

Canadian Society of Exploration Geophysicists
F. A. Hale (1958)
P. I. Bediz (1959)
Harry McGrew (1959)

Casper Geophysical Society
W. H. Hawkes (1959)

Dallas Geophysical Society
Martin C. Kelsey (1958)
Glen M. Conklin (1959)
Paul E. Nash (1959)

Denver Geophysical Society
A. Haig (1958)
Leslie C. Spenser (1959)

Fort Worth Geophysical Society
H. E. Itten (1958)
A. E. McKay (1959)

Houston Geophysical Society
Richard H. Parker (1958)
J. E. McGee (1959)
W. H. Taylor (1959)

Jackson Geophysical Society
Mark D. Butler (1958)

Montana Geophysical Society
R. E. Whitmore (1959)

New Mexico Geophysical Society
F. A. Grimm (1959)

Geophysical Society of Oklahoma City
Richard M. Davis (1958)

Pacific Coast Section, SEG
Robert E. Plumb (1958)
James A. Kurfess (1958)
E. M. Curry (1959)

Permian Basin Geophysical Society
Lorenz Shock (1958)
C. N. Page (1958)
G. A. Grimm (1959)

Geophysical Society of South Texas
W. Lee Moore, Jr. (1959)

Southeastern Geophysical Society
L. W. Cobena (1958)
Edwin A. Malone (1959)

Southwest Louisiana Geophysical Society
E. L. Ricketts (1959)

Geophysical Society of Tulsa
J. M. Crawford (1958)
W. M. Erdahl (1959)
Paul L. Lyons (1959)

Utah Geophysical Society
R. J. Lacy (1959)

Please mention GEOPHYSICS when answering advertisers

MODERN ALTIMETER SURVEYS

AMERICAN PAULIN SYSTEM

MICRO
SURVEYING ALTIMETER

Intervals as close as ONE FOOT

Models available in all ranges.

ENGLISH or METRIC.

Designed for rugged field use under all climatic conditions.

Price in U.S.A.
MICRO MODELS $300
TERRA MODELS $250

FIELD INSTRUMENT

BETTER ALTIMETER SURVEYS AT LOWER COST

WRITE FOR DESCRIPTIVE CATALOG

MICRO SURVEYING BAROGRAPH

- CHART READING IMMEDIATELY AVAILABLE
- ACCURATE, SENSITIVE, (Same as our Micro Altimeter)
- EASILY READ
- DEPENDABLE
- LIGHT WEIGHT — EASILY PORTABLE

PRICE IN U.S.A.: $790 complete READY FOR USE

PRECISION RECORDER REPLACES BASE OPERATOR

MADE IN U.S.A.

BASE INSTRUMENT RECORDER
MODEL SMB-5

AMERICAN PAULIN SYSTEM

1524 SOUTH FLOWER STREET • LOS ANGELES 15, CALIFORNIA, U.S.A.

THE WORLD'S LEADING MANUFACTURER OF SURVEYING ALTIMETERS

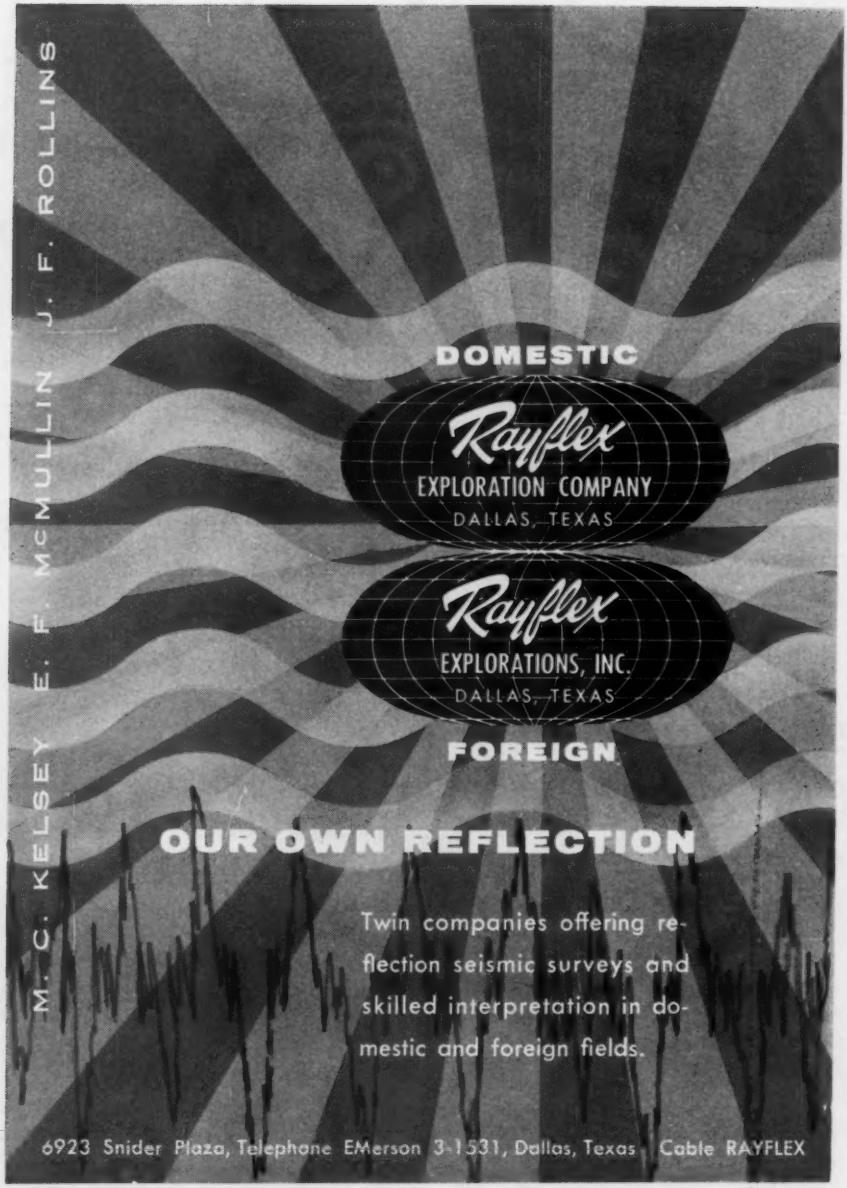
M. C. KELSEY E. F. McMULLIN J. F. ROLLINS
DOMESTIC
Rayflex
EXPLORATION COMPANY
DALLAS, TEXAS
Rayflex
EXPLORATIONS, INC.
DALLAS, TEXAS
FOREIGN
OUR OWN REFLECTION
Twin companies offering reflection seismic surveys and skilled interpretation in domestic and foreign fields.
6923 Snider Plaza, Telephone EMerson 3-1531, Dallas, Texas Cable RAYFLEX

NOW OPERATING!
Century's
Seismic Data Reduction Center

The Oil Industry's FIRST General Contract Seismic Reduction Service

What Century's SEISMIC Data Reduction Service Means To You . . .

- A cross section of seismic records corrected without distortion for normal move-out, weathering and elevation differences.
- The ability to work heretofore "no record" areas by improving signal-to-noise ratio through compositing and/or filter discrimination.
- A means of analyzing subsurface stratigraphic and lithologic conditions.
- More discrimination and integration in your oil finding efforts.
- A clearer and more comprehensive presentation of seismic data to administrators and geologists who are not geophysicists.

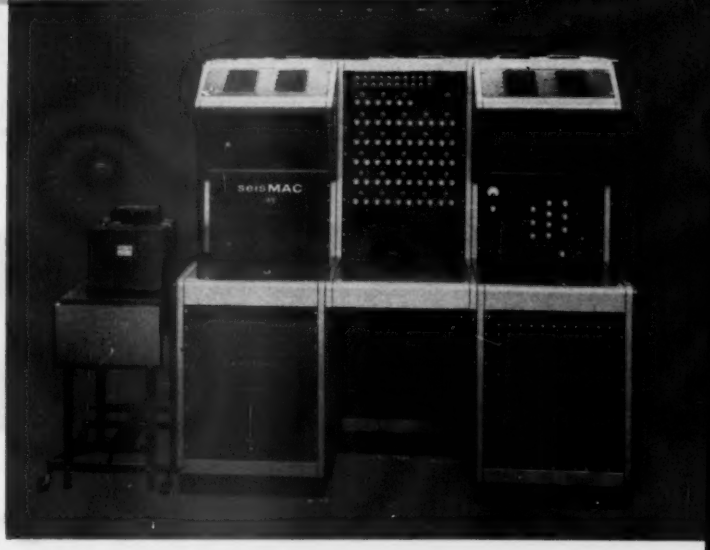

For Full Information Phone

CHerry 2-8121 TULSA, OKLAHOMA

AMhurst 9-5571 CALGARY, ALBERTA

CENTURY GEOPHYSICAL CORPORATION
JENKINS BUILDING TULSA, OKLAHOMA

CENTURY GEOPHYSICAL CORPORATION OF CANADA
1105 7th AVENUE WEST, CALGARY, ALBERTA, CANADA

Du Pont announces...

the new "ELCORD"

(TRADEMARK)

the first practical, flexible, accurate means for Sequential Shooting and Matching Velocities

BETTER SIGNAL, LESS NOISE, NO "GHOSTS"

Here's real news for seismic operators!

Now you have a new tool for improving the signal-to-noise ratio and eliminating "ghost" reflections—a tool that's *practical, flexible* and *accurate!*

Sequential shooting and matching velocities are widely accepted methods of accomplishing these ends. Now the new "ELCORD" Delay Unit by Du Pont gives you the accuracy and convenience to make those methods practical in *your* operations.

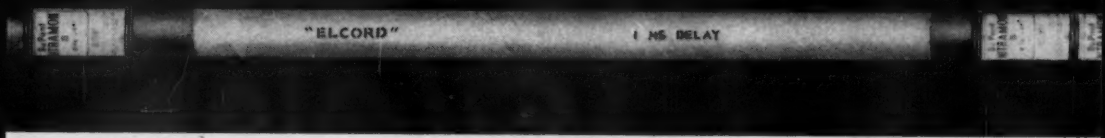

Practical!

Designed for use with Du Pont "Nitramon" S, "ELCORD" Delay Units can be coupled quickly and easily into rigid charges that can be loaded even in badly blocked holes. They're unaffected by water. Can be "slept" indefinitely. Impervious to heat or cold. Highly insensitive to shock and friction. Immune to static electricity. Firing is by means of a "Nitramon" S Primer at the top of the charge. No other primers are necessary because an "ELCORD" Delay Unit will detonate either "Nitramon" S or another unit.

Please mention GEOPHYSICS when answering advertisers

Delay Unit

Flexible!

"ELCORD" Delay Units are five feet long and can be assembled into charges of any desired length. Greater spacings between the "Nitramon" S sections, in multiples of five feet, may be obtained by screwing two or more units together. Delays of 0.50, 0.75, 1 and 2 milliseconds provide matched velocities between 2,500 and 10,000 ft./sec. The amount of explosive per delay can be varied from one pound to whatever is wanted, merely by changing the number of "Nitramon" S cans between the "ELCORD" Delay Units.

Accurate!

All devices previously offered for sequential shooting and matching velocities have been inherently inaccurate, and some have been subject to wide variation depending on borehole conditions such as hardness of the material in which the hole is drilled, presence or absence of water, etc. By contrast, "ELCORD" Delay Units are accurate to ±3% and are unaffected by borehole conditions. When you match velocities with "ELCORD" Delay Units, you know exactly what you are doing.

TRY IT NOW...in your problem areas

With the new convenience and accuracy provided by "ELCORD" Delay Units, Sequential Shooting and Matching Velocities are now more attractive than ever for seismic exploration where conventional methods do not give satisfactory results.

Your Du Pont representative can give you full details. Or write: Explosives Department, E. I. du Pont de Nemours & Co. (Inc.), Wilmington 98, Delaware.

DU PONT

Better Things for Better Living...*Through Chemistry*

DU PONT SEISMIC PRODUCTS

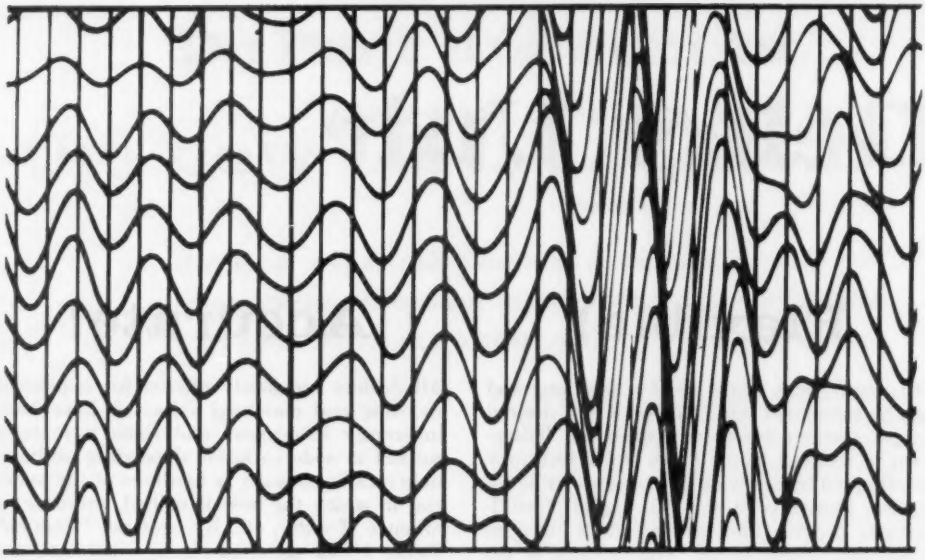

Get perfect recordings of every shot with Seismo-Writ

Here's why Du Pont Seismo-Writ is better in these four ways.

SPEED. Seismo-Writ can be *processed* quicker. Even if extreme underexposure forces over-development, you still get a good, clear, easy-to-read trace. You can process Seismo-Writ in developer temperatures up to 125°F.

STABILITY. Seismo-Writ has minimum curl and won't crack. It's easy to handle, roll and store. It won't soften, even under toughest field conditions.

CLARITY. Seismo-Writ is free from stain and fog. You get highest density, both in timing lines and in reflection traces.

SAFETY. Seismo-Writ is wrapped in a heat-sealed, moisture-proof inner pouch and packaged in a durable waterproof canister. This package assures maximum protection—even if dropped into water, it will float, and its bright red color makes for easy spotting and recovery.

E. I. du Pont de Nemours & Co. (Inc.)
Photo Products Department
Nemours 2420-17, Wilmington 98, Del Ga-10

Please send me your booklet, "Seismo-Writ Photorecording Paper"

Name _____

Firm _____

Street _____

City _____ State _____

DU PONT
REG. U. S. PAT. OFF.

Better Things for Better Living . . . *through Chemistry*

YOU ARE INVITED

to participate in a 'live' demonstration of SSC's remarkable Optical Analog Computer, at the 1958 S.E.G. Convention in San Antonio, October 13-16, 1958.

SSC will have a working Optical Analog Computer in their display area, booths 43-46.

To participate, bring in geologic cross sections whose gravity response would be of interest. Within time limitations, we will present to the Computer these geological concepts and determine their simulated gravity curves.

In order to handle as many demonstrations as possible, we suggest that these cross sections be limited to two-dimensional profiles of the geology. The scale should be 1 to 1 vertical to horizontal, with a range of $1'' = 1000'$ to $1'' = 4000'$. Please be prepared to indicate your ideas of the density contrasts.

Seismograph Service Corporation P.O. BOX 1590, TULSA, OKLAHOMA, U.S.A.

UNITED
GEOPHYSICAL

continuous progress

UNITED'S Geophysical Leadership in advanced research and development, modern equipment and facilities, scientific methods and techniques and world wide service is constantly being augmented by UNITED'S ElectroDynamic Division outstanding achievements in research development, engineering, testing and instrumentation. For the finest Geophysical Service any place in the world rely on UNITED Geophysical Surveys.

UNITED
Geophysical Corporation

SEISMOGRAPH • GRAVIMETER • MAGNETOMETER

P. O. BOX M, 1200 SOUTH MARENGO AVENUE, PASADENA 15, CALIFORNIA • 1430 NORTH RICE AVENUE, HOUSTON, TEXAS • 422 NORTH MAIN STREET, TULSA, OKLAHOMA • 531 8th AVENUE WEST, CALGARY, ALBERTA, CANADA • EDMONTON-REGINA • APARTADO 1085 CARACAS, VENEZUELA • RUA URUGUAIANA 118-9°, RIO DE JANEIRO, BRAZIL • 194 RUE DE RIVOLI, PARIS, FRANCE

UNITED ELECTRODYNAMICS
Environmental Test facilities
—an important step in instrument leadership.

GI Seismic Recorder and Data Processing Equipment

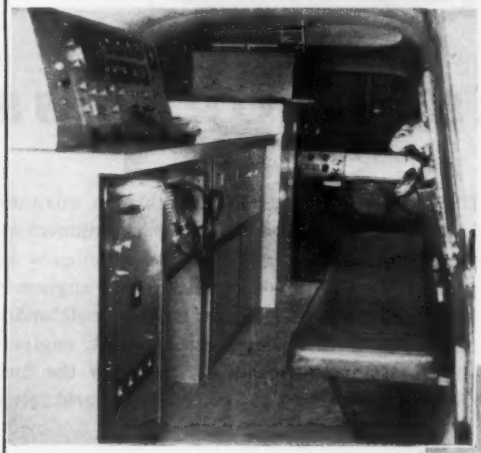

The field recorder uses special tapes 8½ inches wide. The machine normally may record 114 channels before tape changes. Gear drive and a special recorder synchronizing device assures time accuracy better than one millisecond. Refraction equipment is built in for weathering measurements.

Play back analyzing equipment will compensate for fixed and dynamic corrections. Electronic and mechanical computing devices are used to introduce corrections into the records. Flexibility of processing is provided to meet the requirements of the various areas that will be encountered.

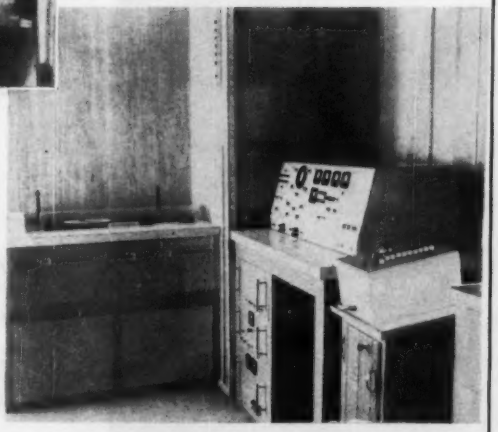

Complete Seismic Survey & Interpretation Service

GEOPHYSICAL INTEGRATORS INC.

CREWS AVAILABLE FOR FOREIGN & DOMESTIC SEISMIC SURVEYS

BOX 887 SAN ANGELO, TEXAS PHONE 26821

THE WORLD IS OUR STOMPING GROUNDS

TI | seisMAC* brings new speed . . . accuracy . . . flexibility to seismic data processing!

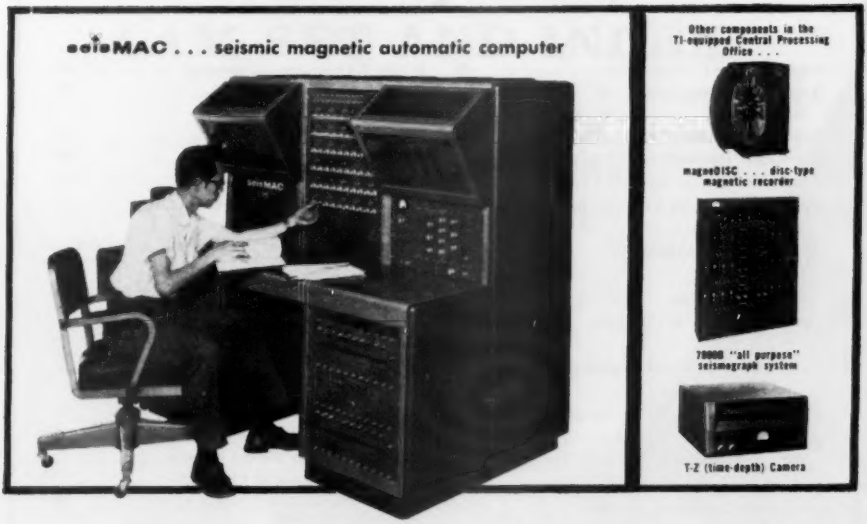
seisMAC . . . seismic magnetic automatic computer
Other components in the TI-equipped Central Processing Office . . .
magneDISC . . . disc-type magnetic recorder
"all purpose" seismograph system
T-Z (time-depth) Camera

The seisMAC, seismic magnetic automatic computer, developed by Texas Instruments Incorporated, is an analog data reduction machine controlled by a digital programmer. seisMAC provides for constant (weathering and elevation) and variable (normal moveout) corrections to be made to any number of seismic traces played back from the magneDISC or other magnetic recorder.

seisMAC, in conjunction with the other individual blocks used in the TI Central Processing Office (or a mixture of equipments, if desired), makes possible the preparation of either time or depth record sections with all the original character of seismic data preserved and the presentation enhanced. Some of the outstanding advantages of seisMAC which permit the presentation of data in its most comprehensible form for final interpretation by the geologist-geophysicist team are:

1. Constant and variable time corrections are made automatically.
2. Unlimited repeatability of data within one millisecond accuracy.
3. Provides 100 millisecond constant plus 100 millisecond variable corrections with no frequency, phase or amplitude distortion.
4. Adaptable with most magnetic transports.
5. Completely automatic during the processing — no adjustments need be made during the operation cycle.
6. No moving heads or cams to become misaligned — seisMAC is the first all-electronic system.
7. Immediate adaptability to any spread or velocity change.
8. Each trace is time-corrected sequentially and independently — no proportioning of a single NMO function for correcting inner traces.
9. Signal remains in analog form with digital programming — high speed processing, accuracy, and repeatability are inherent in the system.

For more complete information on the seisMAC and the TI-equipped Central Processing Office, write for Bulletin No. ___S-318.

*TRADEMARK REGISTRATION APPLIED FOR

TEXAS INSTRUMENTS INCORPORATED
INDUSTRIAL INSTRUMENTATION DIVISION
3609 BUFFALO SPEEDWAY · HOUSTON, TEXAS · CABLE: HOULAB

Seismation®

7246

GEOPHYSICS ADVERTISERS

Aero Service Corporation 59
American Association of Petroleum Geologists 30
American Cyanamid Company 43
American Institute of Physics 24
American Paulin System 3
Arnold Magnetics Corporation 35
Askania-Werke 49
Atlas Powder Company 15

Thomas J. Bevan 78
Bible Geophysical Company 77

Century Geophysical Corporation 5
Clevite Corporation .....74 & 75
Compagnie Générale de Géophysique .. 66
Continental Geophysical Company 63
Custom Fabrication Corporation 26

Dallas Geophysical Society 26
Bert & Ralph Duesing 36
DuPont Explosives .....6 & 7
DuPont Photo Products 8

Eastman Kodak Company 25
Economic Geology 26
Elder Trailer and Body, Incorporated . 23
Electrodynamic Instrument Corporation 48
Electro-Technical Labs .....13 & 62
European Association of Exploration Geophysicists 38

Fortune Electronics, Incorporated 76

General Geophysical Company 31
Geophysical Associates International .. ..Insert after 16
Geophysical Integrators Incorporated .. 10
Geophysical Service Incorporated 4th cover
W. & L. E. Gurley 47

Hale Instruments Incorporated 64
Hall-Sears, Incorporated 53–56
Herb J. Hawthorne Incorporated 27

Independent Exploration Company 65

Klaus Exploration Company 41
Koenig Iron Works 29

Mayes-Bevan Company 37
Mayhew Supply Company 50
E. V. McCollum & Company 61
McCollum Exploration Company 39

National Geophysical Company ..2nd cover

Olsen Seismograph Supplies 52

Petty Geophysical Engineering Company 67
Prakla 42

Robert H. Ray Company 57
Rayflex Exploration Company 4
Republic Exploration Company 45
Rogers Geophysical Companies 71
Ruska Instrument Corporation 60

Schlumberger Well Surveying Corporation 68
Seismic Engineering Company 28
Seismic Explorations Incorporated ... 51
Seismograph Service Corporation ....3rd cover & insert after 8
Seismos GmbH 72
Society of Exploration Geophysicists . 36
Society of Exploration Geophysicists—Safety Committee 32
Southwestern Industrial Electronics Company .....Insert after 30

Techno Instrument Company 70
Tex-Tube Supply Company 58
Texas Instruments Incorporated 11, 40, 46, 69
Texas Seismograph Company 24
Tidelands Exploration Company 33
Triad Transformer Corporation 73
Trija Publishing Company 52

United Geophysical Corporation 9

Wallace & Tiernan Incorporated 34
Western Geophysical Company 16
World-Wide Instruments, Incorporated 44

Electro-Tech Adds Versatility with the . . . .

UNIVERSAL
CAM SET AND INDEX

for use on their DS-7 Magnetic Tape Recorder And Playback Unit

✓ No need for separate cams for each area and spread set-up.

✓ Can be added to all existing DS-7 Units.

DS-7 Recorder and Playback Unit—

Purchase—$8750 with cam set

Rent—$550/mo. (with 90% of rental applying toward purchase, minimum rental four months)

Cam Index Mechanism—$375

Can be installed in field by user

Special Cam Sets—$250/set

One universal cam set plus index allows use with multiple combinations of velocity data and normal split-spread setups.

ELECTRO-TECH

ELECTRO-TECHNICAL LABS
DIVISION OF MANDREL INDUSTRIES
P. O. BOX 13343 HOUSTON 19, TEXAS

LEADERS IN THE FIELD OF SEISMIC INSTRUM

NEW PRODUCTS

RUGGED AERIAL CAMERA

The Mast Development Company, Inc. Model 110, 10″ focal length Polaroid Spotting Camera was developed for aerial reconnaissance photography. It has both civilian and military telephoto applications where instant photographs are needed.

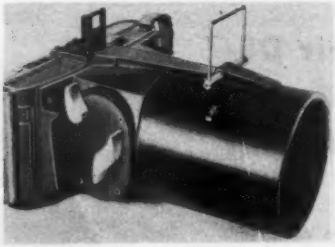

This hand-held long-range Camera uses 8 exposure Polaroid roll film in a standard Polaroid Camera back and provides 60 second in-camera development of exposures. Each 3″ x 4″ positive opaque photograph can be checked before leaving the location.

Additional features of this versatile Camera are its easily maneuverable weight of only 8 pounds and its sturdy cast aluminum housing which extends beyond the lens and allows all-weather or open aircraft use.

The Model 110 has a 10″ focal length f/5.6 Raptar telephoto lens. Two Wratten Series 8 coated glass filters, a K-2 (yellow) and a K-25A (red), are available as optional equipment.

The aperture of the Graflex K-20 behind-the-lens shutter can be adjusted from f/5.6 to f/32. The shutter speeds are 1/125, 1/250, and 1/500 of a second. The shutter winding knob and trigger are conveniently located on the right side of the cast aluminum housing.

The open type viewfinder consists of two collapsible elements

Overall dimensions of the Model 110 are 5⅜″ high, 9⅝″ wide, and 11″ long.

Additional information may be obtained by writing to **Mast Development Company, Inc., 2212 East 12th Street, Davenport, Iowa.**

PORTABLE GENERATOR

There are no extras on Pacific Mercury electric plants. Standard equipment includes the features the survey indicated were desired by the industry—electric starter, shock-absorbing feet, built-in carrying handles, trickle charger and extra plug-in receptacles including standard, two-way and three-way plug units. No adapter is required. Again, at no extra cost, all AC models from 2.5 kw and larger are available with standard or duel voltage to meet the needs of the industry.

Pacific Mercury now has a full staff of sales supervisors in all areas of the country.

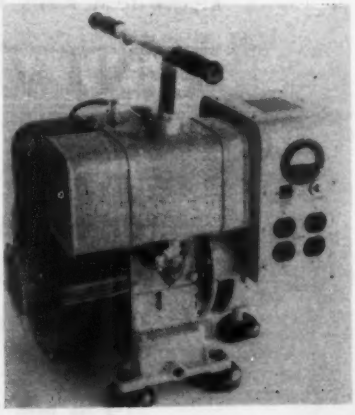

These staff members are available without cost for technical assistance to all users of Pacific Mercury electric plants. Too, Briggs & Stratton agencies across the country offer complete service on all Pacific Mercury engines.

In full production now, **Pacific Mercury** electric plants are available on immediate delivery from the company's sales headquarters at **14052 Burbank Boulevard, Van Nuys, California.**

HAND SIZE LABELER

The improved portable hand embosser, named Roovers MIDGIE LABELER, which quickly makes individual label strips in any desired lengths, provides the answer to virtually every kind of labeling problem. This device, now being introduced for national distribution, embosses clearly marked permanent raised character lettering and numbers on strips of corrosion-resistant monel, stainless steel, aluminum, copper, lead and now vinyl plastic. These labels may be used for any purpose where an indestructible metal tag is desired.

These strips are one-half inch wide. They are handy for numerous household, business and commercial purposes where an indestructible metal tag is needed for such items as wires, cables, chemicals being processed, tools, stock shelves, parts bins, letter files, motors, screens, storm windows, plants, trees, and a variety of other uses, according to **D. Blackstone, Product Development Manager, of Roovers-Lotsch Corporation, Brooklyn 18, N.Y.**

Wherever you prospect...
you'll find an ATLAS DISTRIBUTOR

We look at it this way: If you can get there, we can get a full line of explosives, blasting agents and accessories to you. For best results and best readings, rely on your Atlas Distributor.

ATLAS EXPLOSIVES FOR SEISMIC PROSPECTING

Atlas Powder Company, Wilmington 99, Delaware

Please mention GEOPHYSICS when answering advertisers

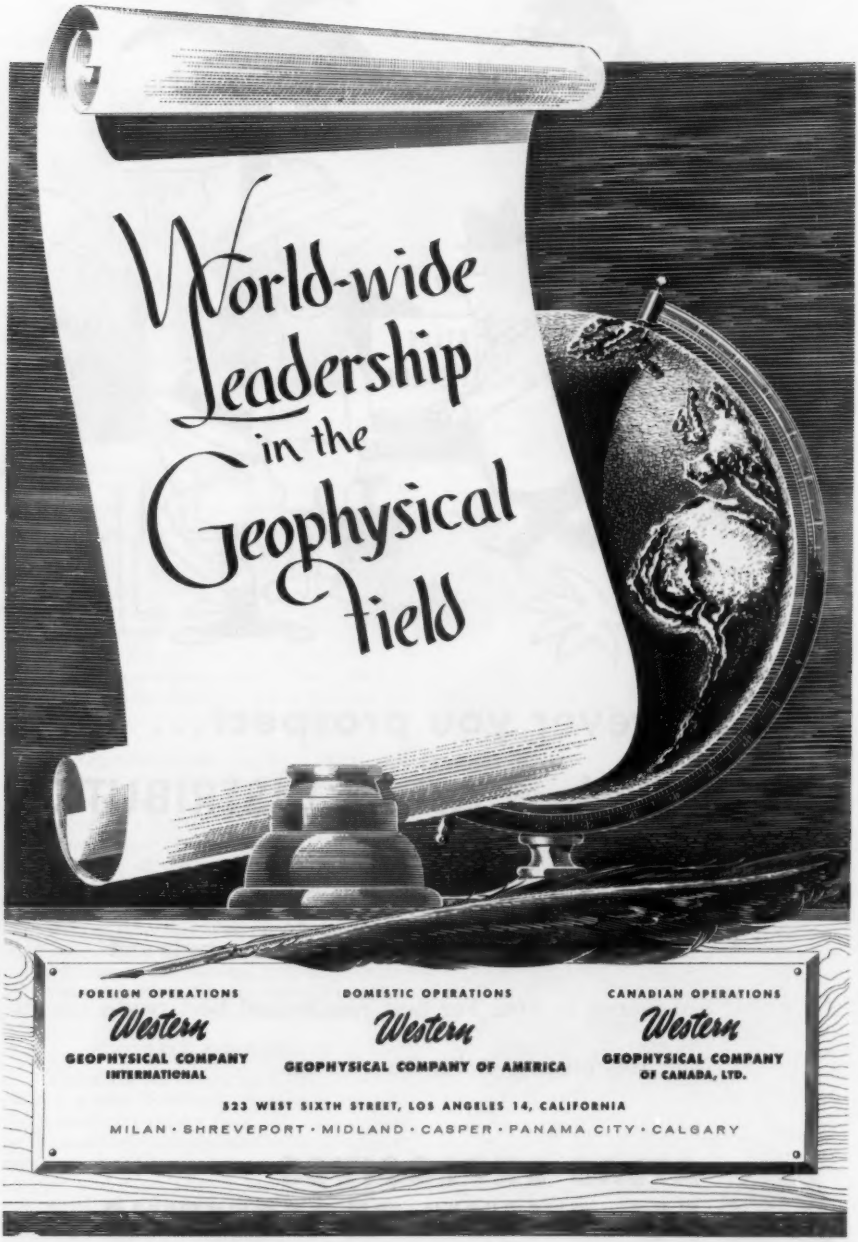
World-wide
Leadership
in the
Geophysical
Field
FOREIGN OPERATIONS
Western
GEOPHYSICAL COMPANY
INTERNATIONAL
DOMESTIC OPERATIONS
Western
GEOPHYSICAL COMPANY OF AMERICA
CANADIAN OPERATIONS
Western
GEOPHYSICAL COMPANY
OF CANADA, LTD.
523 WEST SIXTH STREET, LOS ANGELES 14, CALIFORNIA
MILAN • SHREVEPORT • MIDLAND • CASPER • PANAMA CITY • CALGARY

Before you step off into a new province, make certain you have the basic facts. The fastest and most economical way to determine underlying geology in a new area is with an aero magnetic survey. The proper interpretation of magnetic data at GAI lets you take a good quick look before you leap. GAI makes and interprets gravity, magnetic, and seismic surveys anywhere in the world.

Geophysical Associates International,
3621 West Alabama,
Houston 27, Texas, U.S.A.

gai

GMX

Dr. L. L. Nettleton
E. Joe Shimek
Dr. Nelson C. Steenland

VOLUME XXIII OCTOBER, 1958 NUMBER 4

GEOPHYSICS

DEEP-HOLE GEOPHONE STUDIES*

FRANKLYN K. LEVIN† AND RALPH D. LYNN†

ABSTRACT

Seismic surveys have been made in eight widely separated wells with two types of wall-coupled geophones. These geophones accurately detected and reproduced elastic waves traveling in the earth.

Both direct (initial) pulses from shots and reflection events were studied. The complexity introduced into the initial pulses by secondary reflections varied from well to well. Amplitude decayed as the negative 2.4 power of travel time. Pulse-broadening caused by selective absorption of high frequencies was found. Different wells showed amounts of broadening ranging from nearly complete to that indicating little absorption of high seismic frequencies.

Reflections from interfaces below the geophone were traced to their origin in the earth. At three wells, the same reflections were found on surface seismograms giving an identification of surface-detected reflections and of reflector depth. Multiple reflections were distinguished from direct reflections and were found to mask the latter at four wells. In one case, multiple reflections were identified with events on surface records.

Reflection coefficients found for direct reflections averaged 0.36.

Accurate velocity surveys of the wells resulted from this work.

INTRODUCTION

Although understanding elastic pulse behavior in the earth is fundamental to exploration with the reflection seismograph, few investigators have studied the subject. Ricker (1953) and McDonal et al. (1958) examined pulses traveling through the relatively uniform Pierre shale. Jolly (1953) investigated pulses propagating through a more common type of earth section. With a special well geophone, he detected seismic pulses far below the surface. The present study is a continuation of Jolly's work. We shall report results from seven additional wells and shall describe a new type of geophone used in six of them. The location of the wells, the pertinent information about them, and the data for the well discussed by Jolly (Coleman Stephens No. 2) are given in Table I.

INSTRUMENTS AND FIELD PROCEDURES

With a few exceptions, the instruments and procedures for this study were identical with those of Jolly. The major exception was the well geophone, two

* Paper read at the 11th Annual Midwestern Meeting at Tulsa on April 18, 1958. Manuscript received by the Editor June 14, 1958.

† Jersey Production Research Company, Tulsa, Oklahoma.

types of which were used. The first resembled that described by Jolly, but it differed in several respects. The principal difference lay in the lock-in section, which consisted of one motor-driven arm that could be retracted and extended from the surface. With this instrument, we could survey going down or coming up the well. Also, the variable reluctance detector of Jolly's original geophone was replaced with a 4-cps dynamic unit. Finally, the preamplifier design was changed to give improved high-frequency response. Two geophones of this type were

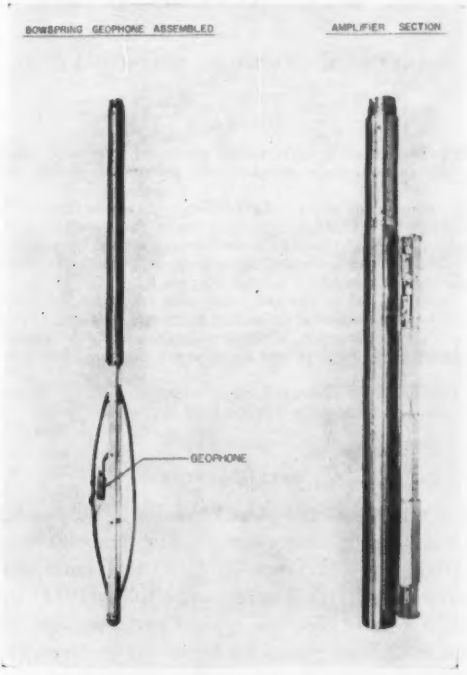

FIG. 1. Bow-spring deep-hole geophone.

built and run in tandem in one well (Walter Morris No. 1). Difficulty in locking the geophones at the desired depth and unduly long survey times led to the design of our present unit, the bow-spring deep-hole geophone.

Like the locking-arm geophones, the bow-spring deep-hole geophone consists of detector, lock-in and preamplifier sections (Figure 1). The detector is a 17-cps dynamic seismometer in a heavy case. It is carried at the center of one of two bow-springs and is coupled to the borehole wall at two points. A slip joint at each end of the bow-spring section provides mechanical decoupling from the remainder of the instrument. The preamplifier has an overall gain of about 275 and an

output impedance of about 300 ohms. The frequency response is flat from about 17 to 500 cps. It is limited by the frequency of the seismometer and by the electrical capacity of the logging cable. The preamplifier is powered by mercury batteries and is controlled from the surface.

Either type of wall-coupled geophone accurately measures earth particle velocity amplitudes. Under identical conditions, locking-arm and bow-spring instruments give the same results. However, for operational ease, we favor the

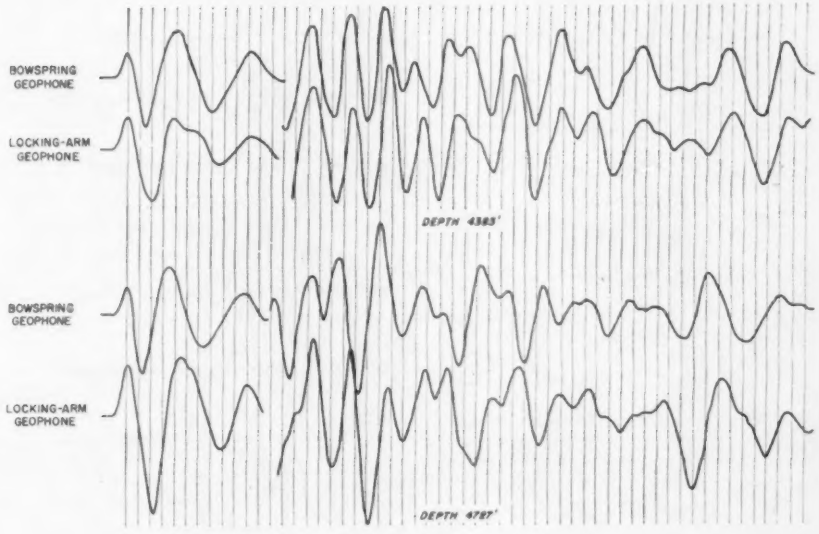

FIG. 2. Comparison of signals from bow-spring and locking-arm deep-hole geophones.

bow-spring geophone. Figure 2 is a comparison of signals from the two instruments. For the lower pair of traces, the charges were not at exactly the same depth; a corresponding time difference is apparent.

THE INITIAL PULSE

Two types of data resulted from deep-hole geophone studies. By examining the initial shot pulses, we could determine how travel through an earth section modified simple seismic pulses. Also, we could detect reflections, track them to their source in the earth, and differentiate them from multiple reflections.

The initial pulses from shots detected in the wells of Table I changed shape in a regular manner with depth, but there were differences between pulses from different wells (Figures 3 to 11). Some pulses were simple and resembled Ricker wavelets (Figure 7) with their shape independent of detector depth. Others,

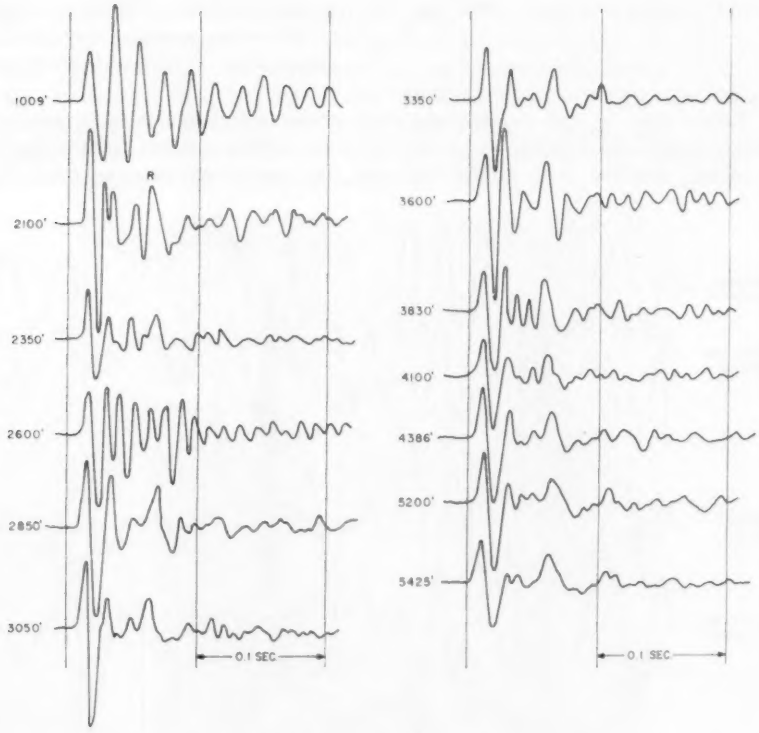

FIG. 3. Initial seismic pulses from hole shots—Coleman-Stephens No. 2.

initially simple, became complexes of several cycles (Figure 9). In addition, all pulse changes between these extremes occurred.

Two mechanisms contributed to the shape changes. First, high frequencies were attenuated more than low frequencies so that the pulses broadened. Secondly, the pulses added cycles or distinct secondary events. A principal source of secondary energy was the reflection from the surface. Van Melle and Weatherburn (1953) called this event the ghost reflection. Ghost reflections generated by reflection from the base of the weathered zone were not detected here, since we shot just below that depth. Surface-generated ghost reflections appear in Figures 3, 5, and 8, where they are marked with *R*. By far the most spectacular example occurred at the Navajo Tribe No. 1 (Figure 8). It was a perfect inverted image of the initial pulse, and its average amplitude was 0.85 that of the initial pulse. Since the effective initial pulse consisted of the actual initial pulse and the ghost reflection, reflections in the vicinity of the Navajo Tribe No. 1 were double.

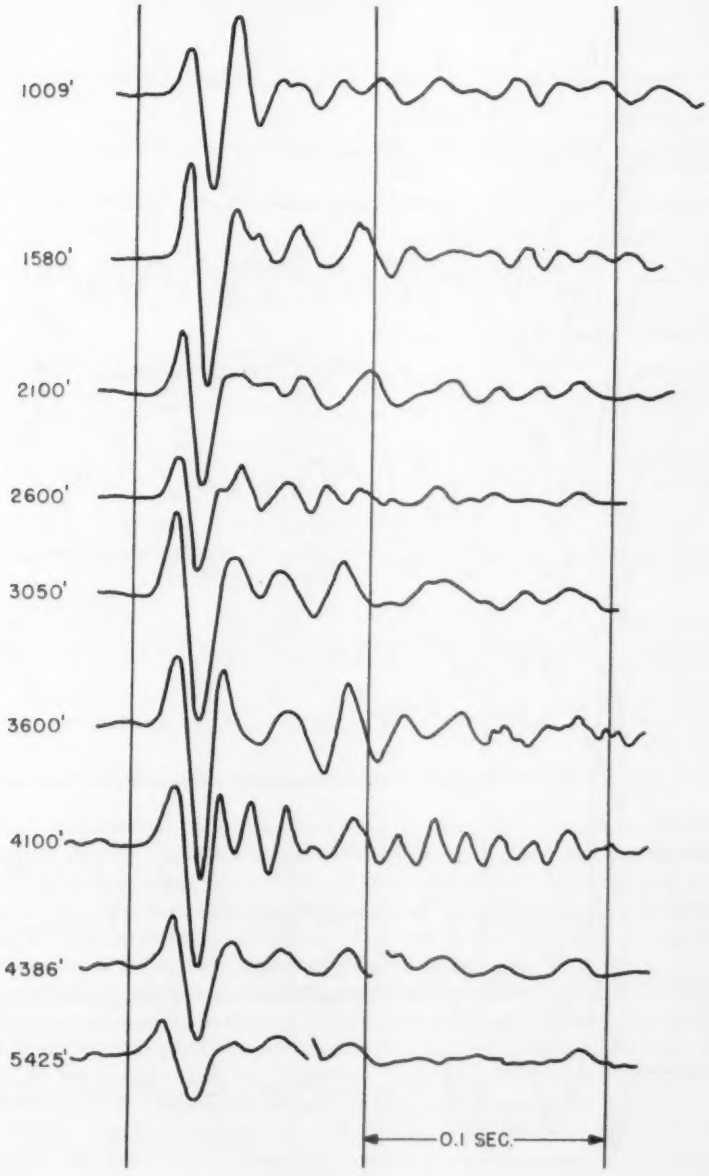

FIG. 4. Initial seismic pulses from air shots—Coleman-Stephens No. 2.

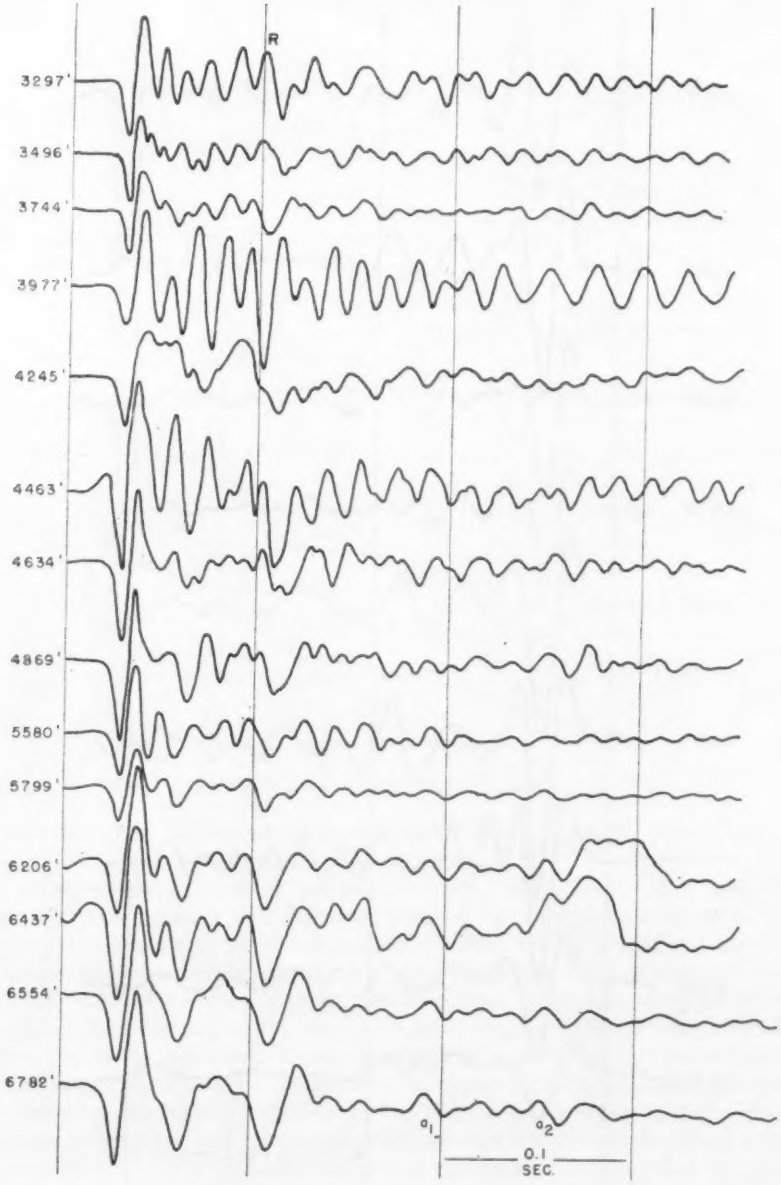

FIG. 5. Initial seismic pulses—Walter Morris No. 1.

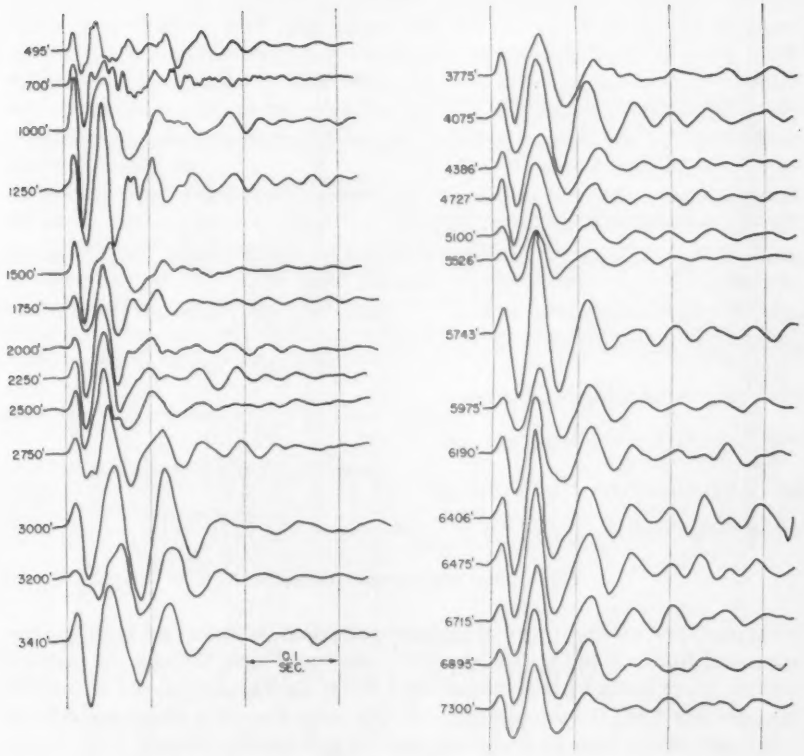

FIG. 6. Initial seismic pulses—Mayme Morrissey No. 1.

Ghost reflections at the other two wells (Figures 3 and 5) were smaller than those at the Navajo Tribe No. 1, the average ratio of ghost reflection amplitude to initial pulse amplitude being 0.46 and 0.44 respectively. Although the ghost reflections were less obviously inverted images of the initial pulses, in both cases the travel times were twice the uphole time. Air shots (Figure 4), as expected for sources above the surface, produced no ghost reflections.

In addition to ghost reflections, interbed and intrabed reflections affected the initial pulse shape by modifying and extending the initial pulse. The amount of complication introduced by interbed and intrabed reflections varied from well to well. At the Gothic Nose No. 1 (Figure 9), for depths greater than 2,000 ft, two distinct events (designated a_1 and a_2) appeared immediately following the direct arrival. The first of these was 0.50, the second 0.35 times as large as the initial pulse. Because of data scatter, the numerical values are not too significant. a_1 and a_2 arose as reflections within massive low-speed beds from 2,020 to 2,245 ft.

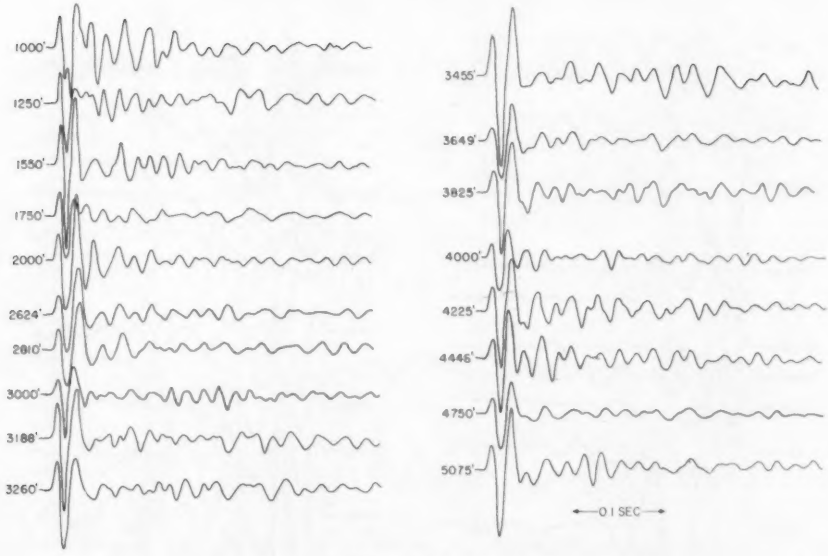

FIG. 7. Initial seismic pulses—Hurley No. 1.

In agreement with the theory of multiple reflections, a_1 and a_2 are erect and are separated from the initial pulse by twice the travel time through the beds involved. Wave forms from depths above 1,900 ft do not show a_1 and a_2 (see, for example, the 1,883-ft form of Figure 9). The large sizes of a_1 and a_2 are difficult to explain on the basis of reasonable velocity and density values.[1]

Although the largest secondary event at the Walter Morris No. 1 was the ghost reflection, there were minor secondaries, indicated as a_1 and a_2 on Figure 5. a_1 arose as a multiple reflection within a massive high-speed layer, predominantly limestone, dolomite, and anhydrite from 4,633 to 5,798 ft; a_2 is the corresponding event generated by the ghost reflection. As expected for multiple reflections, a_1 and a_2 have the same polarities as the initial pulse and ghost reflection respectively; and their time separation from their generating pulses, 0.15 sec, is twice the travel time through the massive layer. Also, both a_1 and a_2 disappear near the top of the layer. The ratios of amplitudes a_1 to the initial pulse and a_2 to the ghost reflection are 0.14 and 0.32. In theory, if the multiply reflected

[1] The persistence of events a_1 and a_2 at the Navajo Gothic Nose No. 1 emphasizes the atypical nature of two of the records, one recorded at 2,883 ft, the other recorded at 4,333 ft, on neither of which a_1 and a_2 appear. Poor coupling of the geophone to the borehole wall, presumably caused by hole washouts, was responsible for the record peculiarities. In later work, the well caliper log was used to avoid setting the geophone in washouts.

pulses were identical with their generators, the two ratios should be the same. However, the high frequency loss shown by the traces from 5,799 and 6,206 ft occurred within the massive layer. Since the ghost reflection had already lost high frequencies in the weathered zone, it was less affected than the initial pulse. Trapping of high frequencies within the massive layer is the probable cause of the phenomenon.

The effect of multiple reflections upon the initial pulse was most marked at the Sarah Harman No. 1 (Figure 11). If the initial energy is defined as both the first arrival and the secondary events moving with it, the initial energy duration was more than 0.2 sec at the Sarah Harman. Except for loss of high frequencies, all wave forms recorded from 1,576 to 5,892 ft were essentially the same. Some of the secondary events were large; at 5,892 ft, the event marked a_1 is 0.47 times

FIG. 8. Initial seismic pulses—Navajo Tribe No. 1.

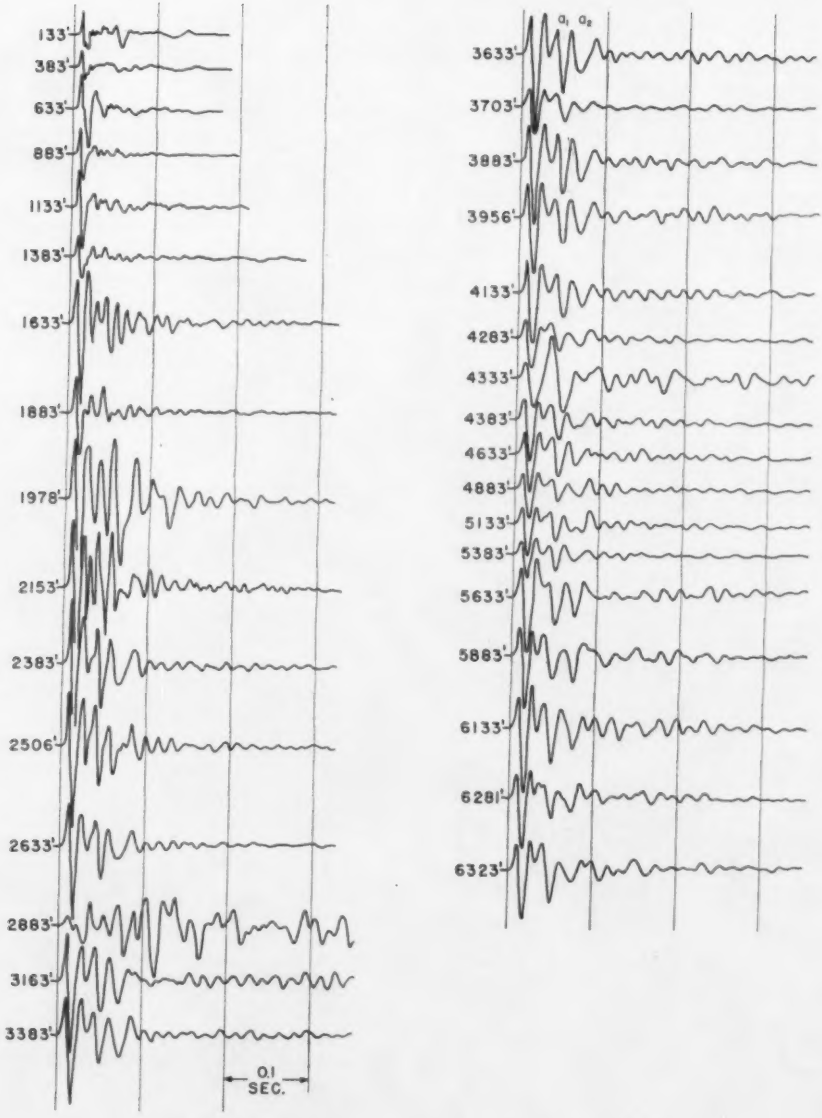

FIG. 9. Initial seismic pulses—Navajo Gothic Nose No. 1.

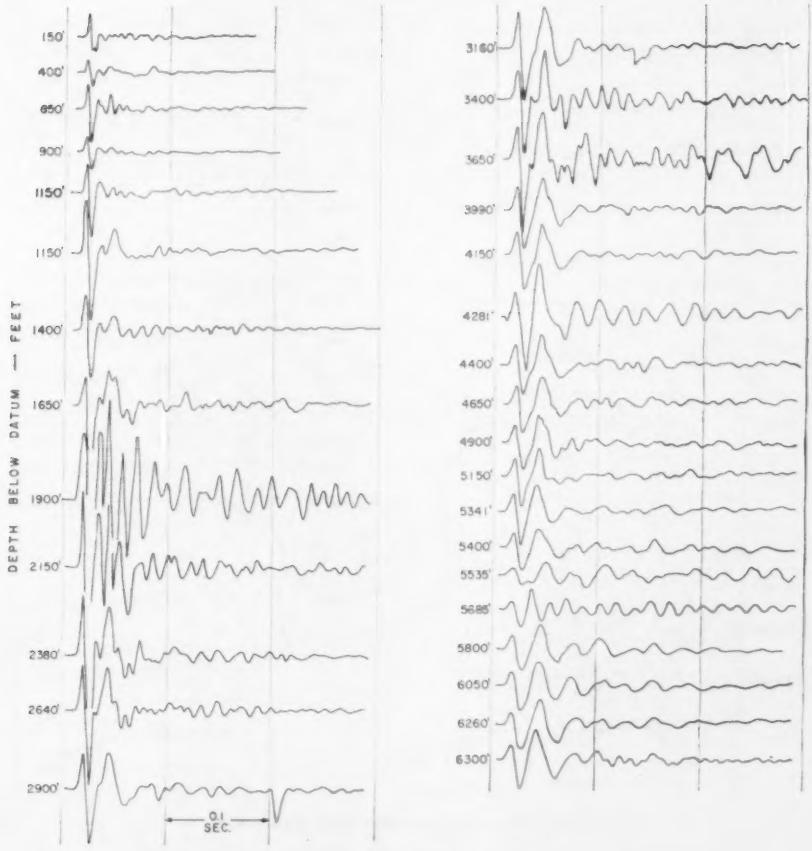

FIG. 10. Initial seismic pulses—Navajo White Mesa No. 2.

as large as the initial pulse. Other secondaries were smaller but persisted at all depths. Apparently the major generators of secondary events were three anhydrite and gypsum layers, each 30 to 40 ft thick, in the depth range of 900 to 1,600 ft. These layers, embedded in a thick shale section, had been cased off and did not appear on the electric or continuous velocity logs, but they showed as major features on the neutron log of the Sarah Harman well.

Of the eight wells listed in Table I, only three have initial pulses uncomplicated by ghost reflections or multiple reflection energy. It is the complete complex—initial pulse, ghost reflection, and multiples—that impinges upon an

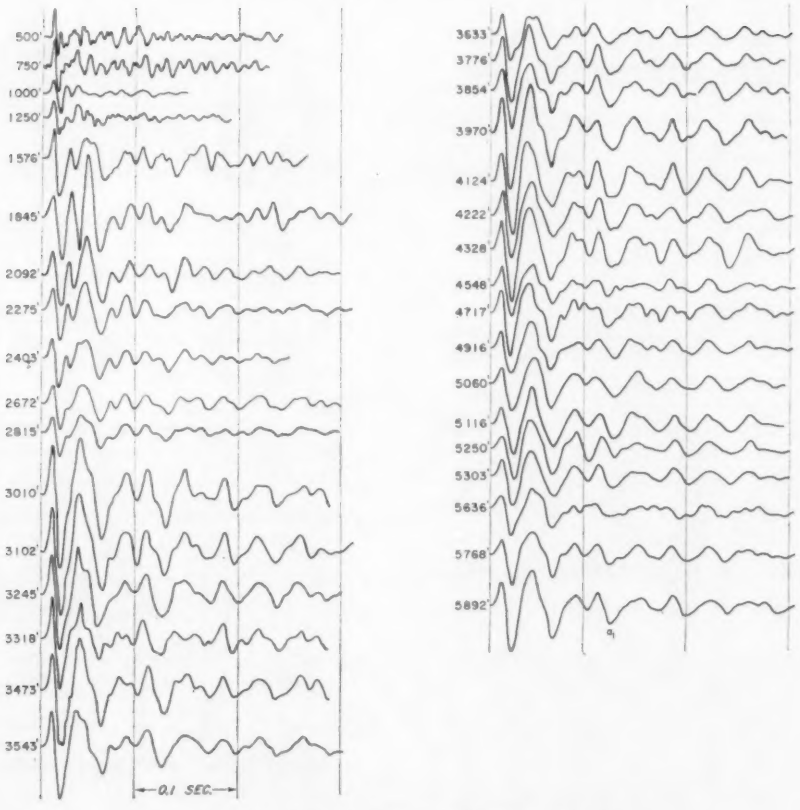

FIG. 11. Initial seismic pulses—Sarah Harman No. 1.

TABLE I

WELLS SURVEYED WITH DEEP HOLE GEOPHONES

Name	Location	County	State	Depth (ft)	Casing (ft)	Date Surveyed
Coleman Stephens No. 2	35-T2N-R2W	Garvin	Oklahoma	5,503	520	9-28-50
Walter Morris No. 1	36-T18N-R8W	Webster	Louisiana	9,636	3,001	10-30-52
Mayme Morrissey No. 1	6-T161N-R92W	Burke	North Dakota	7,321	618	4-16-55
Hurley No. 1	7-5N-11ECM	Texas	Oklahoma	5,100	1,496	5-16-55
Navajo Tribe No. 1	4-41N-28E	Apache	Arizona	6,382	911	9-20-55
Navajo Gothic Nose No. 1	33-T41S-R22E	San Juan	Utah	5,573	1,360	11-25-55
Navajo White Mesa No. 2	22-T42S-R24E	San Juan	Utah	5,606	1,386	12-19-55
Sarah Harman No. 1	20-T4N-11ECM	Texas	Oklahoma	5,916	1,592	3-20-56

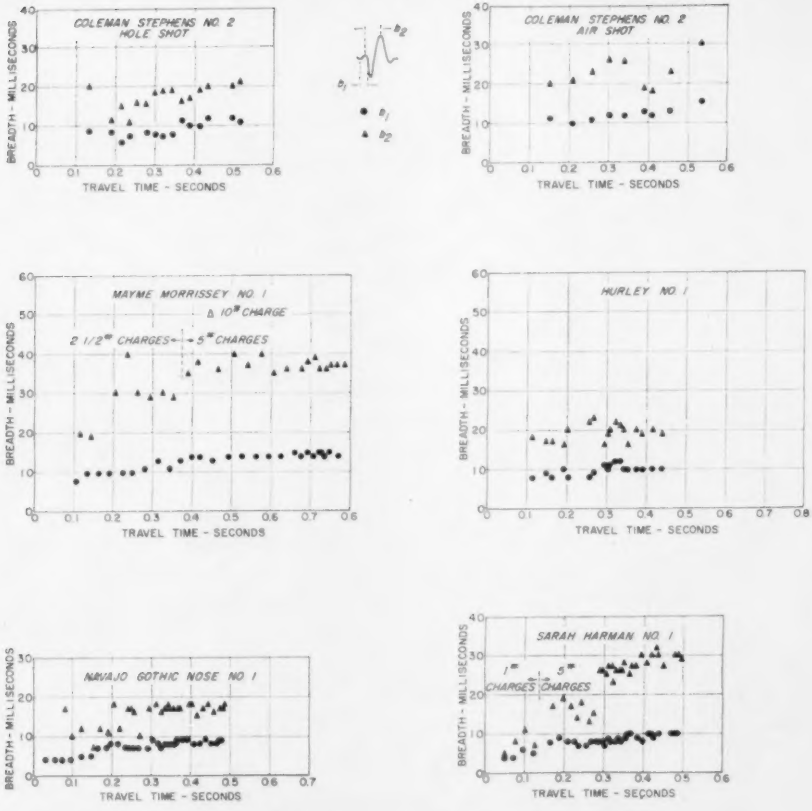

FIG. 12. Pulse breadth versus travel time—typical examples.

interface and is reflected. If the pulse complication shown here is typical, isolated "wavelet" reflections must be rare indeed.

Figures 3 to 11 illustrate qualitatively the tremendous variation in the shape of initial pulses from shots. To describe the pulses quantitatively, we give their frequency spectra and amplitudes. Plots of pulse breadth against travel time indicate in a crude manner the change in frequency content due to travel through the earth. Figure 12 shows typical breadth-time plots for some of the wells of Table I.

Pulse breadth behavior was much the same at each well: The breadths increased with increasing travel times. The magnitude of the effect varied from well to well and was more marked for b_2, the peak-to-peak breadth, than for b_1, the

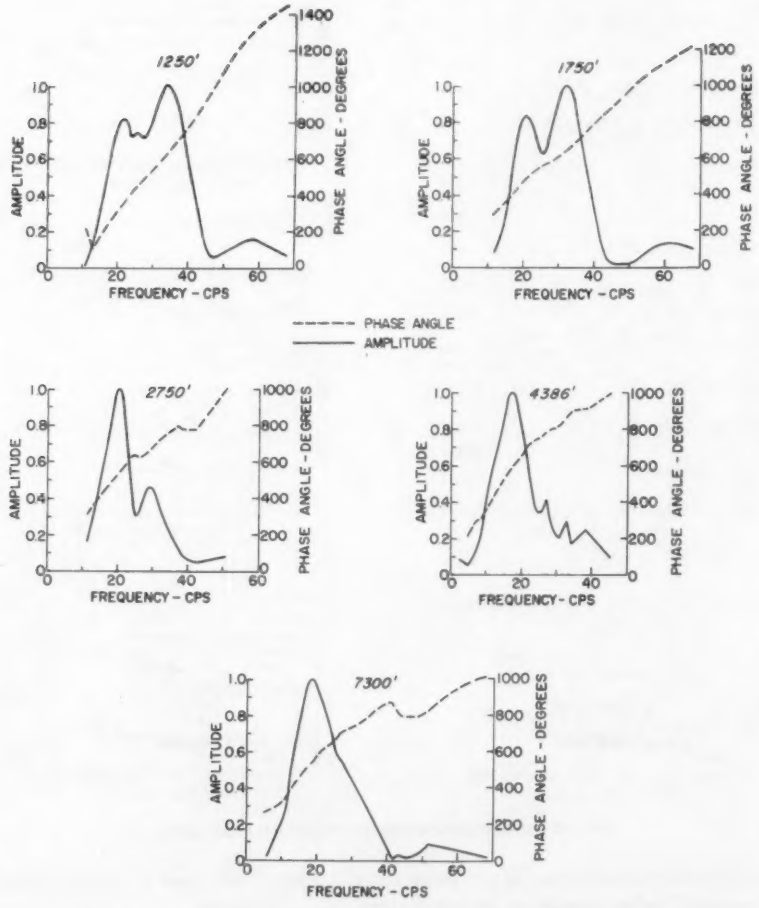

FIG. 13. Frequency spectra of initial pulses—Mayme Morrissey No. 1.

half-breadth. The b_1's changed only slightly, the range in an extreme case being 4 to 10 milliseconds. On the other hand, b_2's as high as 50 milliseconds and as low as 5 milliseconds were measured, and a 20-millisecond change was recorded at one well. The variation of pulse breadth with travel time was negligible at the Hurley No. 1 and Navajo Tribe No. 1, small at the other two Navajo wells and the Coleman Stephens No. 2, and considerable at the Mayme Morrissey No. 1 and Sarah Harman No. 1.

A comparison of hole and air shot breadths is interesting. At the Coleman

Stephens No. 2, air shot breadths were larger than those from hole shots (Figure 12), even though the air charges were only half the size of those fired in holes. The amplitudes of the pulses from the air shots were 1/30 of those from the hole shots.

Although charge size appears to affect pulse breadth, the data on this factor were too incomplete to permit us to correct the measured breadths to a standard charge.

Since breadth-time plots did not supply sufficiently detailed information on the frequency content of the initial pulses, we found the frequency spectra of the pulses. Figures 13 and 14 are spectra of initial pulses at several depths for the two wells of Table I showing a systematic frequency change with depth: Mayme Morrissey No. 1 and Sarah Harman No. 1. The changes at other wells were less marked.[2] Indeed, spectra from the Hurley No. 1 were single-peaked, bell-shaped, and nearly independent of depth. The corresponding initial pulses (Figure 7) were wavelet forms.

Spectra from the Mayme Morrissey No. 1 (Figure 13) and Sarah Harman No. 1 (Figure 14) showed selective attenuation of high frequencies.[3] For the Mayme Morrissey, the spectrum at 1,250 ft was two-peaked; this degenerated into a single-peaked curve at 7,300 ft, the maximum at 40 cps decreasing relative to the one at 20 cps and eventually vanishing completely. Similarly, for the Sarah Harman, a large peak near 55 cps in the 1,845-ft curve was all but gone at 5,892 ft. A peak at 40 cps, absent on the 1,845-ft spectrum, became prominent at greater depths.

It is not immediately obvious why in some areas there is marked attenuation of high frequencies; in others, relatively little selective attenuation. Logs of the Mayme Morrissey No. 1 indicated a geologic column consisting mostly of low-velocity shales. Such a section might absorb high frequencies more readily than one made up of high-speed carbonates. On the other hand, the Hurley and Sarah Harman wells were near each other and, although on opposite sides of a fault, cut similar geologic sections. The phenomena observed here are still obscure.

Another factor in a quantitative description of initial pulses was investigated, i.e., pulse amplitude. Figure 15 is a typical plot of log amplitude against log travel time. As in Jolly's Figure 4, the least square straight lines fit the data reasonably well. The values of the slopes (attenuation constants) are tabulated in Table III. The average values of -2.38 and -2.26 are lower than the -2.5 predicted by Ricker (1953) for a homogeneous isotropic medium and found experimentally in his Pierre shale work. Little significance can be assigned to the average slope values, since data points from the individual wells scatter, and

[2] Because of the uncertainty as to what comprises the initial pulse, the time at which the form being analyzed was cut off was chosen arbitrarily. This was unfortunate, but apparently unavoidable.

[3] The spectra were not sufficiently consistent with depth to permit us to determine the attenuation law of frequency with depth. Small differences caused by different shots for each pulse and different coupling at each depth were responsible for the observed data scatter.

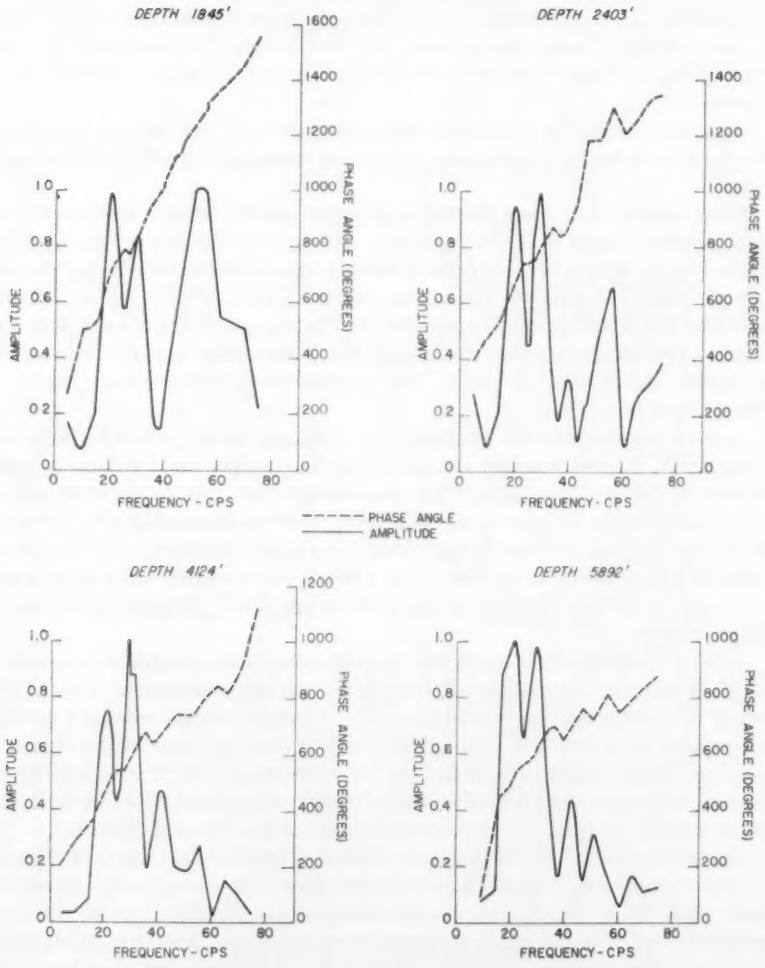

FIG. 14. Frequency spectra of initial pulses—Sarah Harman No. 1.

slopes for wells within an area do not always agree. Thus, the two Panhandle wells, Hurley No. 1 and Sarah Harman No. 1, have similar attenuation constants, but the three Navajo wells do not. In fact, both the highest and lowest slopes occur for wells only 15 miles apart—the Navajo Tribe No. 1 and the Navajo Gothic Nose No. 1. In the absence of a suitable theory, no prediction of the exact attenuation expected in complex materials can be made, nor can explanation be offered for attenuation constant variations.

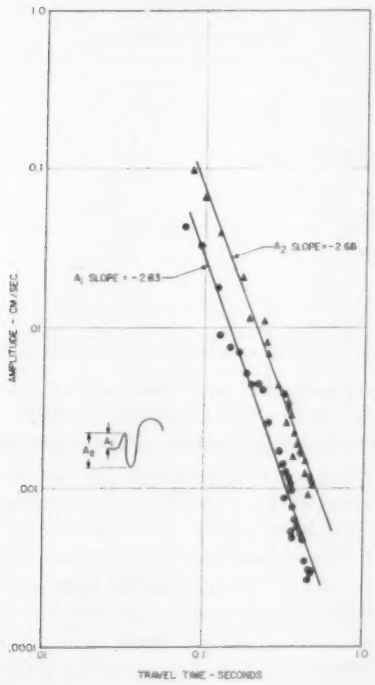

FIG. 15. Earth particle velocity of initial event versus travel time—Navajo Gothic Nose No. 1.

Although an investigation of absolute amplitude variations from well to well was not part of the deep-hole studies, the initial pulse amplitudes at 0.4 sec are listed, purely for reference, in Table II.

TABLE II

ABSOLUTE AMPLITUDE AT 0.4 SECOND

Well	Charge (lbs)	Amplitude at 0.4 Sec cm/sec
Coleman-Stephens No. 2	5*	2.2×10^{-3}†
Walter Morris No. 1	1	2.5×10^{-3}
Mayme Morrissey No. 1	5	1.3×10^{-3}
Hurley No. 1	5	2.7×10^{-3}
Navajo Tribe No. 1	5	1.4×10^{-4}
Navajo Gothic Nose No. 1	15	5.6×10^{-4}
Navajo White Mesa No. 2	15	7.5×10^{-4}
Sarah Harman No. 1	5	2.2×10^{-3}

* Hole shot; 2½ lb air shot.
† Hole shot; 6.5×10^{-5} air shot.

TABLE III

ATTENUATION CONSTANTS

Well	n from A_1	n from A_2
Coleman-Stephens No. 2	−2.6	−2.7
Walter Morris No. 1	−2.5	—
Mayme Morrissey No. 1	−2.4	−2.3
Hurley No. 1	−2.2	−1.9
Navajo Tribe No. 1	−1.9	−1.9
Navajo Gothic Nose No. 1	−2.8	−2.7
Navajo White Mesa No. 2	−2.3	−2.2
Sarah Harman No. 1	−2.3	−2.1
Average	−2.38	−2.26

REFLECTIONS AND MULTIPLE REFLECTIONS

The examining and tracking of reflections involve events arriving after the initial pulse. They reach the geophone after reflection from one or more interfaces. This technique used has been described in detail by Jolly (1953), and Figures 16 and 17 illustrate the method, using data from the Mayme Morrissey.[4] On plots of the deep-hole geophone traces for each depth, reflections from interfaces below the geophone follow time-depth curves which are mirror images of the initial pulse curves. The two curves form a symmetrical pair around the intersection time; the intersection occurs at the depth of the reflector.

At three wells—Coleman Stephens No. 2, Mayme Morrissey No. 1, and White Mesa No. 2—direct reflections relatively free of multiples were present. (Results from the Coleman Stephens No. 2 were presented by Jolly.) Major breaks characterized the velocity log from the Mayme Morrissey No. 1. Some of these were bounded discontinuties, 100 ft or more thick, produced by sandstone beds in shale or shale beds in a carbonate section. One break was the transition from a predominantly shale section to one containing carbonates. The important reflections correlated with the important velocity changes, the changes here being large enough to minimize intrabed interference. At the White Mesa No. 2, the strong reflections correlated with thick shale and sand beds in a carbonate section. As for the Mayme Morissey and Coleman Stephens wells, the prominent seismic events appeared to come from marked geologic changes of reasonable thickness.

There was some ambiguity in defining the reflecting interface. Both the initial pulse and the reflection consisted of several cycles; a correct depth resulted only if the corresponding cycles of the events were chosen. The choice was complicated by two factors. First, simple reflections from isolated reflectors are uncommon. Usually the observed event is a complex coming from several nearby reflectors, and the shape of the complex is not necessarily the shape of the initial pulse. Secondly, even if the reflection is an isolated event, its phase depends upon the

[4] Breaks in the traces indicate changes of 10 or 20 db in the flat amplifier gains.

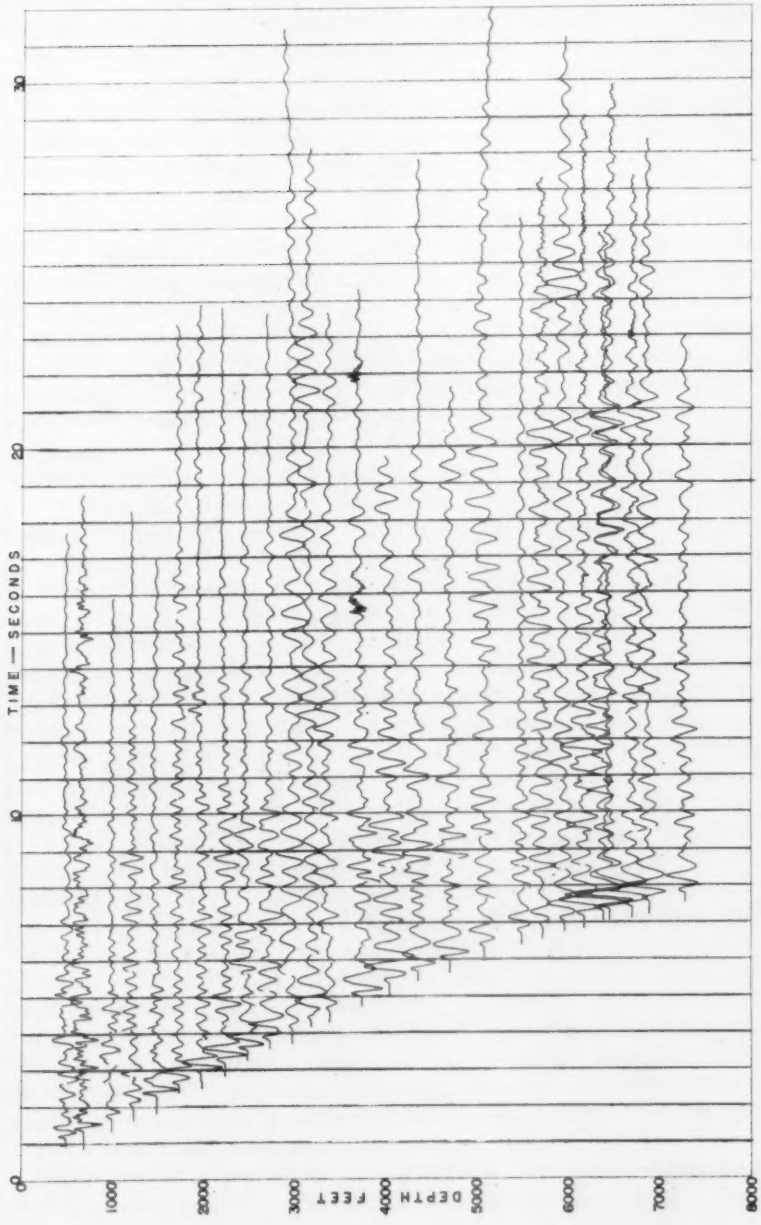

FIG. 16. Deep-hole geophone traces for all depths—Mayne Morrissey No. 1.

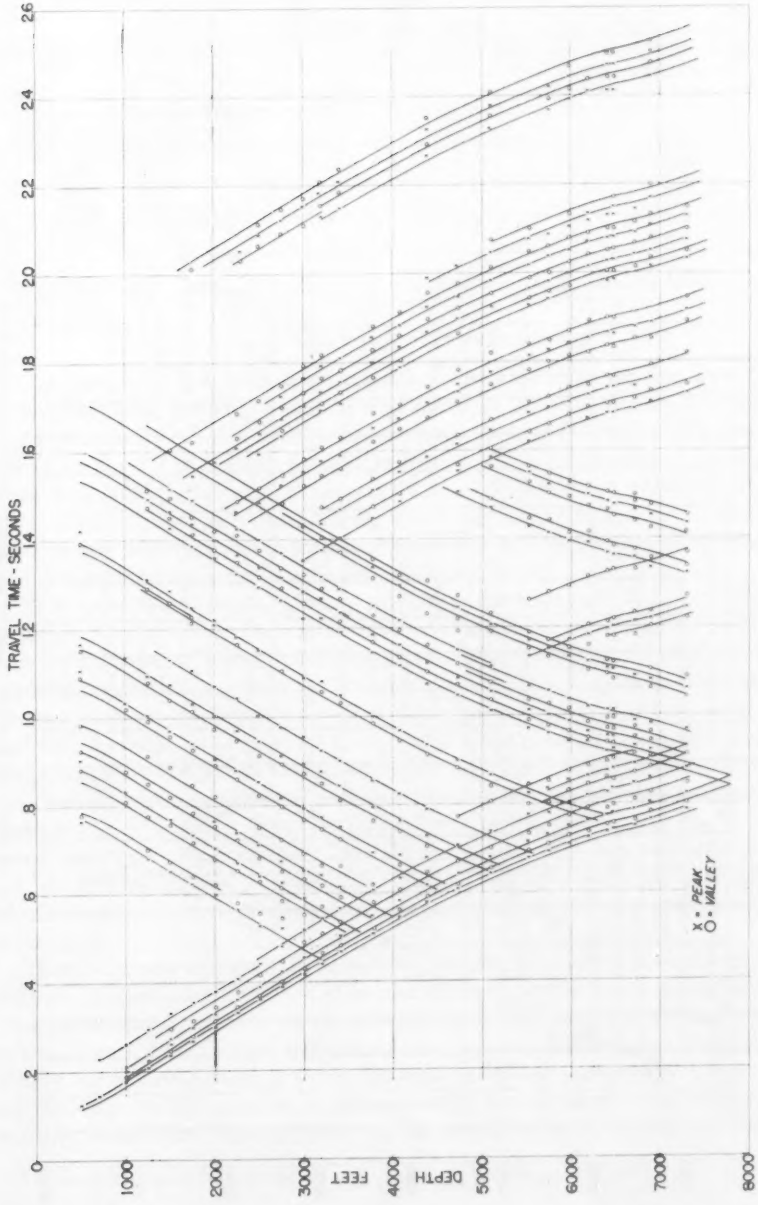

FIG. 17. Peak and valley plot for each geophone depth—Mayme Morrissey No. 1.

reflector order, i.e., upon whether the medium with higher acoustic impedance lies over the one with lower acoustic impedance, or vice versa. Our criterion for choosing the intersection was empirical: A high-amplitude reflection peak was taken to correspond to a high-amplitude initial-event peak or valley. Once the intersection was found, the velocity log sometimes tested its validity, since for prominent velocity breaks, the phase was fixed. A depth uncertainty of 100 ft in locating a reflector is possible.

On the time-depth plots of Figures 16 and 17, reflections from interfaces below the well bottom are evident. To find the corresponding reflectors, the initial pulse and reflection curves were extrapolated until they crossed, extrapolation being along mirror image curves. Although the correct curve was not known, reasonable extensions of the measured curves could be drawn for a reflector not too much deeper than the well. Figure 17 shows an extrapolation for a distinct reflection; the interface involved is about 500 ft beneath the last survey point. In this sense, the deep-hole geophone explores below the total well depth.

Using the technique described by Jolly (1953, Figure 7), effective reflection coefficients were found for 23 reflections from 5 wells. The average value was 0.36, with a range from 0.14 to 0.66. Since prominent reflections are followed most easily, reflection coefficients larger than the average for all geologic interfaces are to be expected.

When the intersection of a direct reflection and the initial pulse could be found, the depth of the reflector was known. If, further, the reflections seen on a surface seismogram made near the well could be identified with those found on well survey records, a depth of origin could be assigned to each reflection of the surface record. For the Coleman Stephens No. 2, Mayme Morrissey No. 1, and White Mesa No. 2, surface and well reflections were tied. Jolly presented the Coleman Stephens data; results from the other two wells are seen in Figures 18 and 19. Since the reflections occurred as discrete events unevenly distributed in time, there is little doubt that the identification is correct.

Besides direct reflections moving along mirror image curves, Figures 16 and 17 show events traveling parallel to, but displaced from, the initial pulses. These events are multiple reflections, arrivals that have been reflected at least once from a bed below and once from a bed above the deep-hole geophone. They hit the geophone from above. Because of their origin, they cannot appear until the geophone is below the upper reflector. In practice, except for extraordinarily good reflectors such as thick anhydrite or gypsum beds, the upper reflector is the surface or base of the weathered layer. Compared with a surface detector, the deep-hole geophone is unusually sensitive to multiple reflections. A surface detected multiple is reflected at least twice from an interface below the well geophone and consequently is smaller by the reflection coefficient of that interface than the same multiple detected in the borehole.

Depth-time plots from all the wells of Table I, except the Coleman-Stephens No. 2, showed multiples. Doubtlessly careful examination of the Coleman-

FIG. 18. Comparison of surface and deep-hole geophone signals—Mayme Morrissey No. 1.

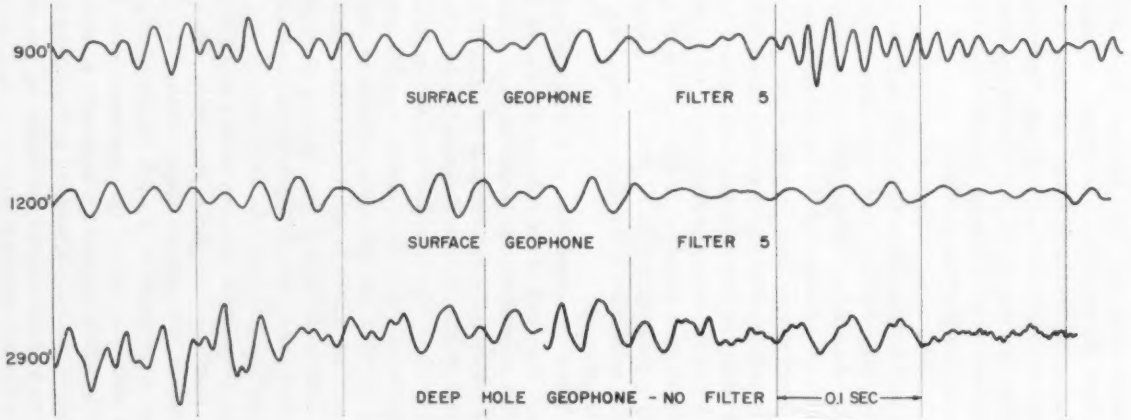

FIG. 19. Comparison of surface and deep-hole geophone signals—Navajo White Mesa No. 2.

Stephens records would also have revealed multiple reflections, but the analysis was completed before the general prevalence of multiply reflected energy was suspected. Determination of a reflector depth as the intersection of mirror image curves depends on having distinct reflection arrivals. When strong multiples are present, the reflections cannot be followed, since the overlap regions of the depth-time curves are confused. All degrees of confusion occurred. At the Mayme Morrissey No. 1 and Navajo White Mesa No. 2, multiples were present; but they appeared so late that direct reflections could be followed. At the Walter Morris No. 1, Hurley No. 1, Navajo Tribe No. 1, and Navajo Gothic Nose No. 1, there was more or less continuous interference of direct and multiple reflections. The

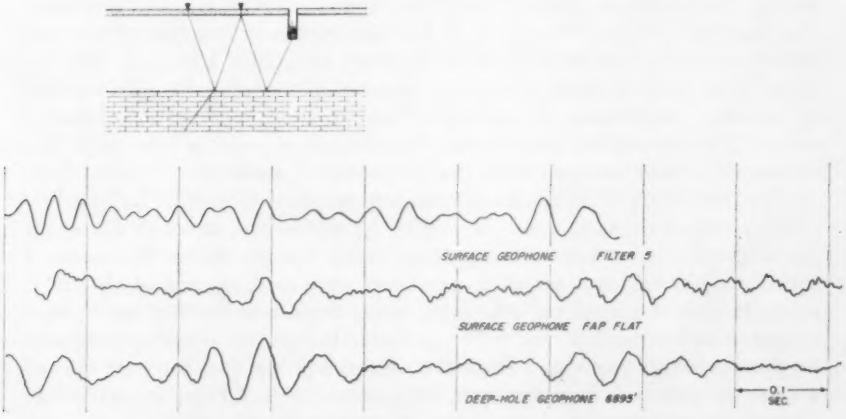

FIG. 20. Comparison of surface and deep-hole geophone signals showing multiple reflections—Mayme Morrissey No. 1.

upper reflectors at the Walter Morris were associated with a massive high-speed layer between 4,633 and 5,798 ft. At the Hurley well the upper reflectors were probably anhydrite and gypsum beds above the first geophone depth, while at the two Navajo wells probable sources of multiple reflections were the surface and massive low-speed beds which gave rise to secondary arrivals following the initial pulse. The Sarah Harman No. 1 represents a limiting case: No direct reflections were visible and all cycles moved with the initial pulse. As explained above, three anhydrite and gypsum beds were responsible for this complexity.

Where the prominent direct and multiple reflections were separated in time, the multiples as well as the direct reflections found with the well geophone could be identified on surface traces. Figure 20 is the identification of multiples for the Mayme Morrissey No. 1; the event-spacing is such that displacement of the

traces by even one cycle is impossible. Thus, wall-coupled deep-hole geophones not only can tell where reflections arise in the earth, they may also tell which events seen on seismograms are multiples.

INCIDENTAL RESULTS OF DEEP-HOLE GEOPHONE STUDIES

In the deep-hole geophone program, the emphasis was on the study of pulse propagation and reflection properties. Analysis of the experimental data gave, in addition, results not related directly to the program's purposes. Some of the by-products were of practical value, the most important being related to velocity surveying.

Wall-coupled deep-hole geophones give velocity survey data of an excellent quality. First kicks are sharper than those from a conventional well geophone. The superior kicks are due partly to the high-frequency response of the geophones, partly to noise levels 20 to 30 db below those from a hanging detector. Lower noise levels allow surveying with substantially smaller charges. Not only are powder costs reduced, but shot holes hold up under repeated shooting. For several of our surveys all depth points involved one or two shot holes only. The elimination of shot hole parameter changes promoted consistency of record data.

The consistency of time picks on deep-hole geophone records, as indicated by repeat points at the same depth, is usually ± 1 millisecond, although discrepancies as great as 3.5 milliseconds have been noted. For the Walter Morris No. 1 survey, two locking-arm deep-hole geophones were used, approximately 230 ft apart. In spite of operational difficulties, travel times from fourteen depths were measured and reduced to datum by two methods. Interval velocities computed for those intervals involving a single shot recorded on the dual detectors showed a 4 percent variation; those involving two separate shots, a 17 percent variation. Though the total number of points was too small to be conclusive, the data suggest more accurate interval velocities for dual geophones. Also, the number of depths surveyed in a given time may be doubled. These advantages must be weighted against a more complex operational procedure and a greater chance of cable and instrument loss.

In addition to a lower noise level, a wall-coupled geophone has several minor advantages as compared with a free-hanging detector. The latter is sensitive to tube waves, and is therefore unsuitable for studying arrivals later than the initial pulse. On the other hand, wall-coupled geophones are insensitive to tube waves, and they do not show reversed kicks. They are excellent for making fundamental studies of elastic pulses in the earth and for obtaining additional information from routine velocity surveys.

We corrected deep-hole geophone amplitudes for shot variations, using as a correction signal the output of a surface monitor geophone placed to one side of the working area. Figure 21 shows plots of monitor amplitude as a function of ordinal shot number for some of the wells. (At the remaining wells, shot-hole conditions

were not constant.) We can draw two conclusions from the figure and associated data. First, except at the White Mesa No. 2, seismic "punch" did not depend on shot number. Secondly, water tamping, i.e., the amount of water over the charge, markedly influenced the "punch." At the White Mesa No. 2, the charges were in sandstone; at the remaining wells, in shaly material. Sandstone is subject to

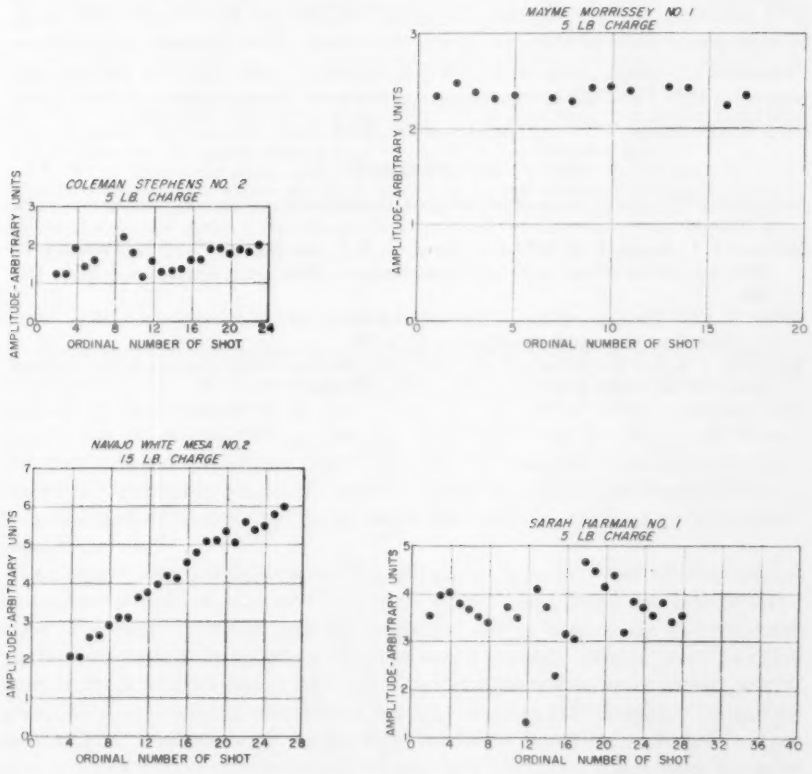

FIG. 21. Monitor geophone amplitude versus ordinal number of shot.

crushing (Ricker, 1956), whereas shale apparently is not. To a good approximation, the amplitudes at the White Mesa No. 2 were proportional to shot number from shot 4 to shot 20.

The influence of water tamping is apparent on the plot from the Sarah Harman No. 1. At the time the well was surveyed, the Oklahoma Panhandle was suffering from a severe drought and we had difficulty keeping water in the shot holes.

Whenever water was added to cover the charge, the "punch" went up only to decline on the following shots. The resulting saw-tooth pattern is evident.

ACKNOWLEDGMENT

Among the numerous members of the Geophysical Research Section involved in the deep-hole geophone studies, special mention should be made of Mr. R. N. Jolly and Miss Halcyon McNeil. Mr. Jolly directed the field work at the Coleman-Stephens No. 2 and Walter Morris No. 1 wells and completely analyzed the data from the latter. Miss McNeil did most of the calculations for the last five wells of Table I and all of the frequency analyses. A great measure of the project's success is due to the carefulness of her work.

REFERENCES

Jolly, R. N., 1953, Deep-hole geophone study in Garvin County, Oklahoma: Geophysics, v. 18, p. 662–670.

McDonal, F. J., Angona, F. A., Mills, R. L., Sengbush, R. L., Van Nostrand, R. G., and White, J. E., 1958, Attenuation of shear and compressional waves in Pierre shale: Geophysics, v. 23, p. 421–439.

Ricker, N., 1953, The form and laws of propagation of seismic wavelets: Geophysics, v. 18, p. 10–40.

———, 1956, Shooting in sand: Geophysics, v. 21, p. 537.

Van Melle, F. A., and Weatherburn, K. R., 1953, Ghost reflection caused by energy initially reflected above the level of the shot: Geophysics, v. 18, p. 793–804.

GEOPHYSICS, VOL. XXIII, NO. 4 (OCTOBER, 1958), PP. 665–683, 11 FIGS.

GENERATION OF SEISMIC WAVES BY WEIGHT DROPS*

S. N. DOMENICO†

ABSTRACT

A series of experiments designed to evaluate the weight-drop technique was conducted in West Texas. These tests demonstrated the general nature of the seismic waves generated by a weight drop and the effectiveness of compositing drops in providing useful reflection information.

At the first of two test sites discrete waves from single drops consisted of a refracted wave, an air-earth coupled wave, reflected wave segments, and fragmentary waves which were likely dispersive surface waves. A 72-seismometer array provided appreciably more reflected wave segments on records from single drops and also on records from the composite of these drops than did a single seismometer. Additional testing revealed that records prepared from weight drops along three parallel lines 100 ft apart recorded at the same seismometer station are appreciably different. Compositing of the drop lines in general did not provide reflections superior to the best on individual lines.

At the second test site record quality appeared significantly superior to that at the first site. Discrete waves on records from single drops recorded by a 36-seismometer array were of the same types as those observed previously. However, the air-earth coupled wave, prominently developed at the first site, did not appear. Compositing of drops provided two prominent reflections which were correlatable over a 5-mile traverse.

INTRODUCTION

Perhaps the earliest experimental study of the generation of seismic waves by weight drops was that reported by Hubert (1925). Employing weights of 20, 50 and 117 kg dropped from heights of 1 to 11 m, he observed at least nine distinct seismic events on the seismograms. He established that (1) the arrival times, ranging from 0.07 to 3.20 sec, and character of these events are independent of the masses and initial height of the falling weights, and (2) the observed amplitudes are proportional to the square root of the potential energy of the suspended weight.

In recent years magnetic recording techniques have provided efficient means to procure seismic records routinely from weight drops along continuous traverses. The field technique may be considered the inverse of the conventional method employing shotpoints and seismometer spreads. One or more parallel lines of drops at intervals of 15 to 30 ft replace the seismometer spread, and a group of seismometers (seismometer station) replaces the shotpoint. Magnetic recordings at a seismometer station from successive drops are corrected in time to a common datum (static correction) and to a zero or common drop distance (dynamic correction). Successive recordings then are composited ordinarily in groups ranging from 12 to as many as 96 per trace.

From recent experimental studies Neitzel (1958) reports that the efficiency of a weight drop in producing a reflection from the Devonian formation in West Texas is approximately one thousand times the efficiency of a dynamite shot. His

* Paper read at the 11th Annual Midwestern Exploration Meeting at Tulsa on April 17, 1958. Manuscript received by the Editor April 30, 1958.

† Pan American Petroleum Corporation, Canadian Division, Calgary, Alberta, Canada.

data show that the predominant frequency of the seismic transient produced by a weight drop is appreciably lower than that of a seismic transient produced by a dynamite shot. Employing magnetic recording equipment, he found that record quality in an area probably is determined primarily by the severity of ground roll generated by the weight drops; and he demonstrated that effects of ground roll are minimized by the optimum seismometer configuration at the recording station, by the proper length of the drop pattern, and by the proper horizontal offset between the drops and seismometer station.

During January of 1956 the Pan American Petroleum Corporation directed a series of experiments in West Texas designed to evaluate the weight-drop technique. The purpose of this paper is to discuss portions of these tests which are believed to demonstrate the general nature of the seismic waves generated by a weight drop and the effectiveness of compositing drops in providing useful reflection data through the relative attenuation of undesirable waves. In addition to drop compositing, recordings from a single seismometer are compared to those from an areal array of seismometers to establish the effectiveness of the latter in providing additional cancellation of these waves. The variation of reflection quality with various drop distances is also investigated.

EQUIPMENT

Weight Truck

The energy source for the experimental work discussed here was a three-ton steel weight measuring 3 ft by 5 ft by 8 inches. This weight was suspended approximately 9 ft above the ground at the rear of a heavy-duty truck. Release of the weight was initiated by a radio signal transmitted from the recording truck. An inertia switch mounted above the weight closed upon impact and initiated a second radio signal which was transmitted to the recording truck. The latter signal was recorded to indicate the time of initiation of the seismic energy (equivalent to the "time-break" in conventional methods).

Recording Truck

The recording truck contained two amplifier channels and a frequency modulating magnetic recorder. This allowed the simultaneous recording on magnetic tape of two seismometer stations. A switch on the drum which closed upon each revolution activated a radio signal that initiated the release of the weight. Recordings were made through a single section filter with 50 percent amplitude response points at 18 and 92 cps.

Drop Compositing Equipment

Field magnetic tapes and associated data sheets were forwarded to a central location where magnetic recording equipment capable of compositing recordings from individual drops had been installed. This compositing was performed after static and dynamic time corrections to a regional reference surface were in-

troduced. In the test areas selected here, static corrections were based on measurements of weathered layer variation available from conventional records previously obtained by the company. Dynamic or "normal-moveout" corrections were based on velocity surveys from wells in the immediate vicinity of the test areas. From 4 to 48 recordings from individual drops were composited into a single recording in the tests described here.

Playback of the fully corrected and composited traces to galvanometers for a paper record was through a single-section filter with 50 percent amplitude response points at 18 and 64 cps. On some of the test records 50 percent mix was used; that is, for a composite of 24 drops per trace, each trace consisted of the last 12 drops of the preceding trace plus the first 12 drops of the succeeding trace. This is called a drop composite of 24/12, the numerator denoting the number of drops per trace and the denominator the number of drops retained from the preceding trace. For a traverse containing 96 drops between seismometer stations, this compositing scheme provides seven traces (four of which are independent) on a record recorded at a single station.

DESCRIPTION AND RESULTS OF TESTS

Location of Test Sites

The experimental work described here was performed at two test sites in West Texas shown in Figure 1. Test Site I in Pecos County, Texas, is 14 miles southeast of the town of Fort Stockton, and Test Site II in Crane County, Texas, is about 13 miles northwest of the town of Crane. Topography in the immediate vicinity of Test Site I is that of an even plain sloping gently to the northeast. Topography at Test Site II is characterized by sand dunes tens of feet in height.

Test I at Test Site I

Description.—The field layout for the first test at Test Site I is shown in Figure 2a. It consisted of a single drop line extending 3,000 ft from the seismometer station which contained a single seismometer placed between two groups of 36 seismometers each. Seismometers within each group were spaced 50 ft parallel and 40 ft perpendicular to the drop line. A total of 300 drops at 10-ft intervals was made beginning 10 ft and ending 3,000 ft from the single seismometer. The single seismometer and the two seismometer groups connected in parallel, a total of 72 seismometers, were recorded separately through the two amplifier channels on each drop. Records were prepared for single drops recorded by the single seismometer and simultaneously by the 72-seismometer array. The playbacks are illustrated in Figures 3 and 5 respectively. These recordings then were composited (after weathered layer and normal moveout corrections) to provide additional records with 48 drops per trace and 50 percent mix (drop composite of 48/24) for the single seismometer, illustrated in Figure 7a, and for the 72-seismometer array as shown in Figure 7b.

This test provided (1) a display of the full complement of waves from single drops and a single seismometer, (2) a qualitative measure of the attenuation of undesirable waves relative to reflected waves from single drops effected by the 72 seismometers in an areal array, and (3) a demonstration of the effectiveness of drop compositing in the further reduction of the undesirable waves.

Results.—Single drops recorded at a single seismometer at Test Site I (Figure 3) revealed at least four types of discrete waves. A refracted wave (*P*) travelling in an underlying limestone bed, approximately 100 ft below the surface, at a velocity of 12,300 ft/sec is followed from the critical distance at approximately

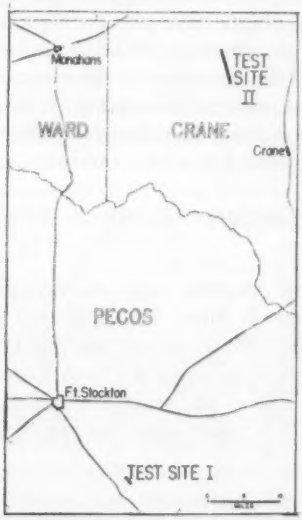

FIG. 1. Location of Test Site I in Pecos County and of Test Site II in Crane County, Texas.

130 ft to the end of the drop line. Fragmentary repetitions of the refracted wave, that is, waves of nearly identical apparent velocity, appear at record times as late as 1.9 sec. These are tentatively identified as multiple reflections at the ground surface of the primary refracted wave. Similar phenomena have been observed by Pommier and Richard (1957) in an area in the northern portion of the Sahara on conventional records; that is, records from subsurface dynamite shots and a surface spread of seismometers.

A second prominent wave (*A*) identified as an air-earth coupled wave, appears well developed at 1,200 ft and is followed easily to the end of the drop line. This wave travels at nearly the velocity of sound in air (1,140 ft/sec). The "quiet" zone or zone of relatively low amplitude following the initial two or three cycles of this wave is created largely by automatic gain circuitry in the amplifier and

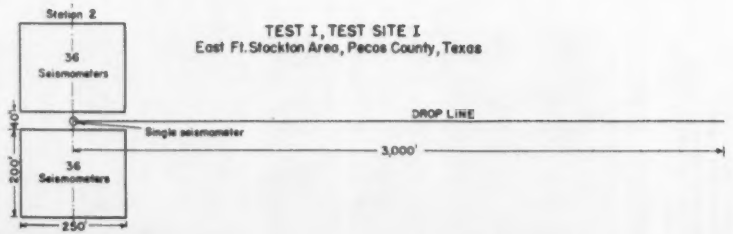

FIG. 2a. Configuration of drop lines and seismometers for Test I at Test Site I. Drops were made at 10-ft intervals along the drop line. The single seismometer and the two seismometer groups connected in parallel (total of 72 seismometers) were recorded separately on each drop.

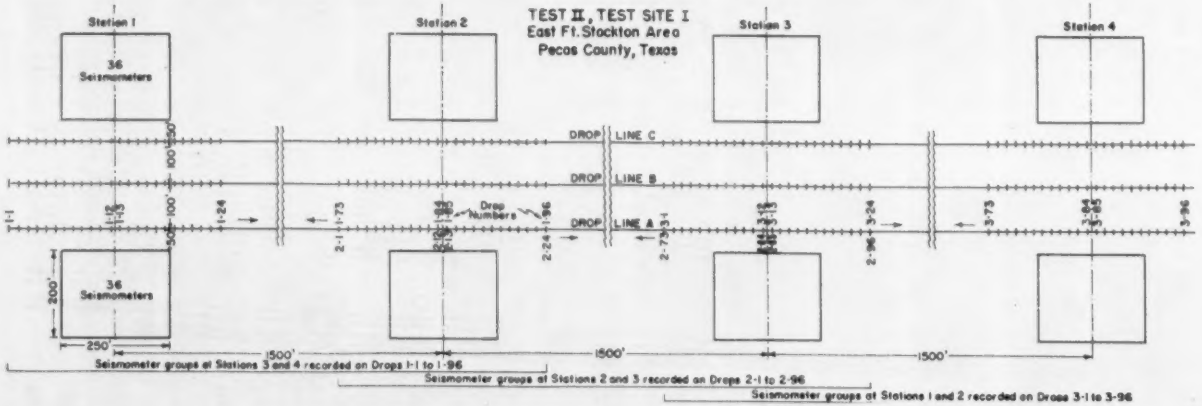

FIG. 2b. Configuration of drop lines and seismometer groups for Test II at Test Site I. Seismometer groups connected in parallel at each station were recorded on drops at 20.8-ft intervals along each of the three drop lines in the order shown below the diagram.

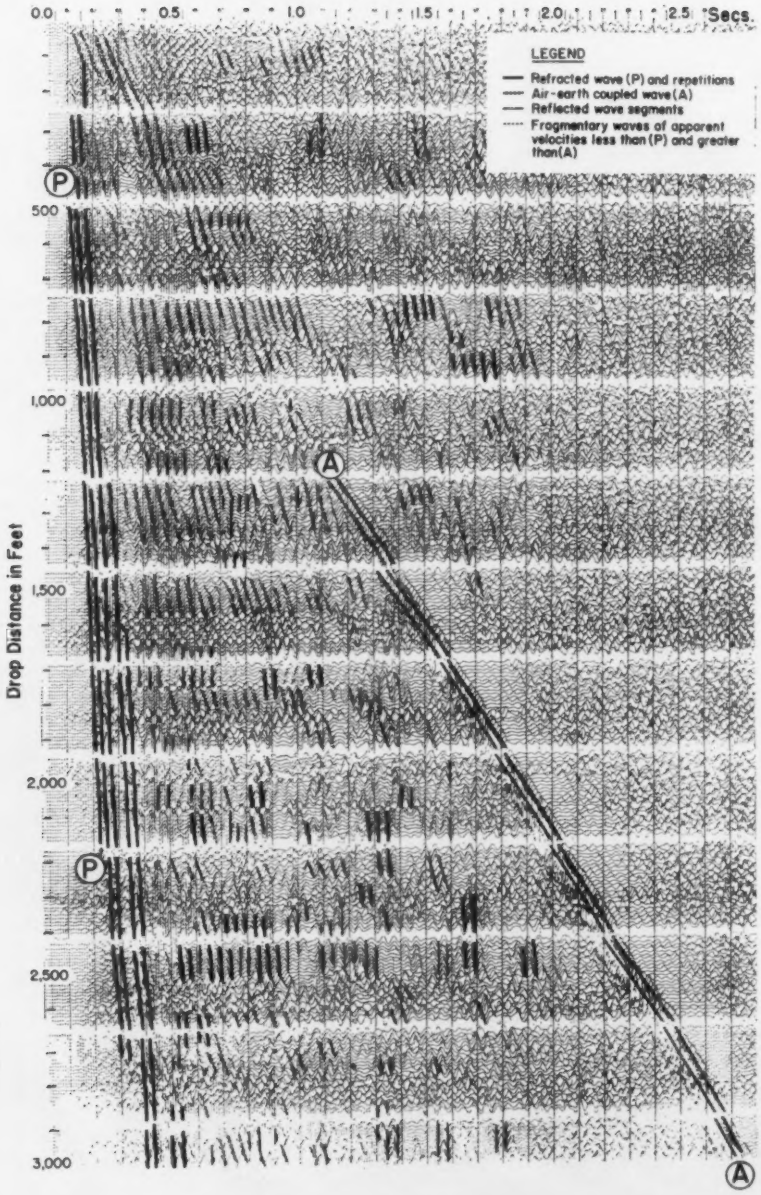

FIG. 3. Records for Test I at Test Site I. Each trace represents a single drop recorded at the *single seismometer* shown in Figure 2a.

attests to the large amplitude of this event relative to the amplitude of immediately preceding events. Press and Ewing (1951), applying theoretical results of Lamb on the effect of a travelling disturbance, have shown that atmospheric compressional waves are coupled to Rayleigh wave motion in the earth when the phase velocity of a discrete frequency in the Rayleigh wave equals the velocity of sound in air. For the case of dynamite shots either on or above the earth's surface recorded by a surface spread of seismometers, the Rayleigh wave begins at the arrival of the direct air wave and thereafter exhibits a constant frequency and phase velocity. Since these conditions appear duplicated here, it appears probable that the weight drop generates sufficient acoustic energy in the atmosphere to set up an air-earth coupled wave.

Other discrete waves in general are not correlatable continuously over more than 18 traces. These are identified as reflected wave segments which exhibit negligible moveout (infinite apparent velocity) and fragmentary waves of apparent velocity less than that of the refracted wave (*P*) and greater than that of the air-earth coupled wave (*A*). The latter are likely dispersive surface waves.

On a time-distance graph of these waves (Figure 4), the positions of reflected waves appearing on the record for a drop composite of 48/24 (Figure 7a) prepared from these drops also are shown. Of the reflections shown in Figure 7a, only the reflection trough (a) is correlatable over more than two independent traces. (Alternate traces on the record are independent, that is, composed entirely of different drops.) This reflection is coincident with only one reflected wave segment from single drops (Figure 4) and apparently arises primarily from the relative attenuation of other waves. The alignment exhibited by the remaining troughs (*e*, *m*, and *n*) in Figure 7a is likely accidental since these are correlatable only over two independent traces. It is noteworthy, however, that these events cross the time-distance domain of the prominent air-earth coupled wave (*A*) with negligible change in form.

Records from the same single drops as those in Figure 3 but recorded by the 72-seismometer array rather than by a single seismometer are shown in Figure 5. The same types of waves are observed here. However, approximately 25 percent more reflected wave segments are present, and in general these are correlatable over appreciably more traces. As in the case of the single seismometer, a time-distance graph of waves recorded by the 72-seismometer array was prepared (Figure 6).

The improvement in record quality effected by the 72-seismometer array over that of a single seismometer for a drop composite of 48/24 is evidenced by the records shown in Figures 7a and 7b. A total of ten reflected wave segments, six of which are correlatable over more than two independent traces, occur on the record with 72 seismometers per trace (Figure 7b), whereas only four reflected wave segments occur on the record with a single seismometer per trace (Figure 7a). The positions of the reflected wave segments appearing on the record of Figure 7b are shown on the time-distance graph (Figure 6) of waves from single drops

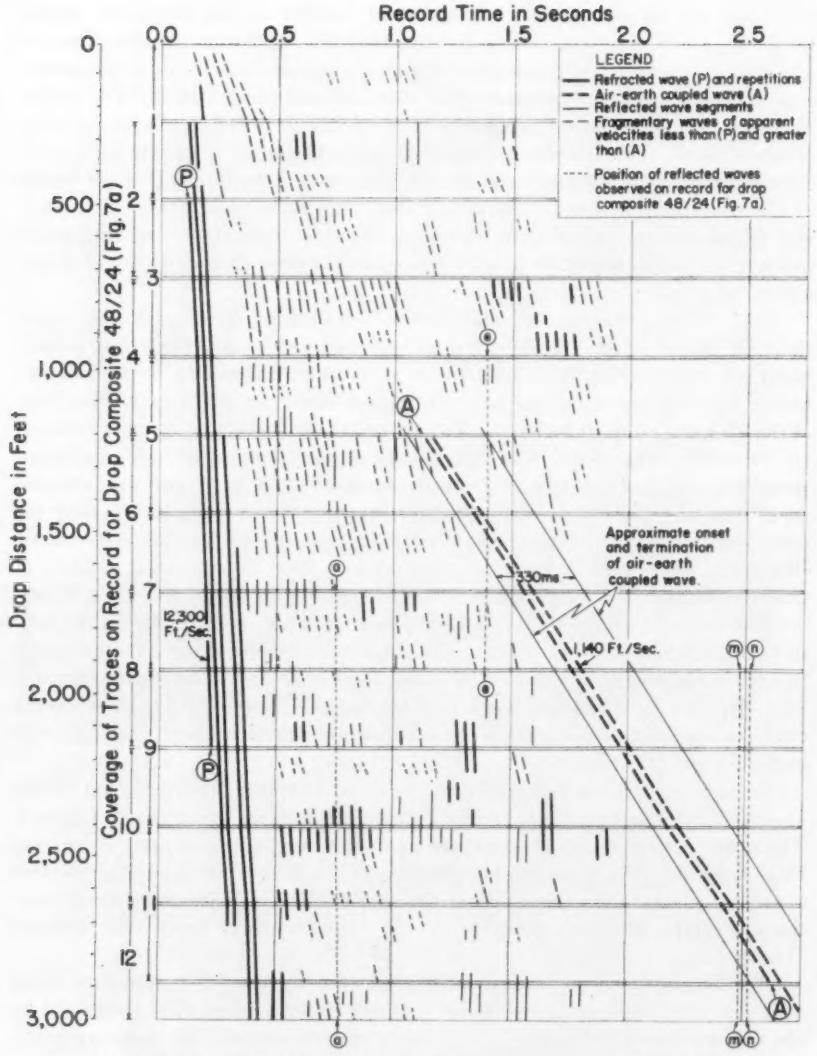

FIG. 4. Time-distance graph of correlatable events evident on the records from a single seismometer shown in Figure 3. The positions of reflected events appearing on the record for a drop composite of 48/24 (Figure 7a) also are shown.

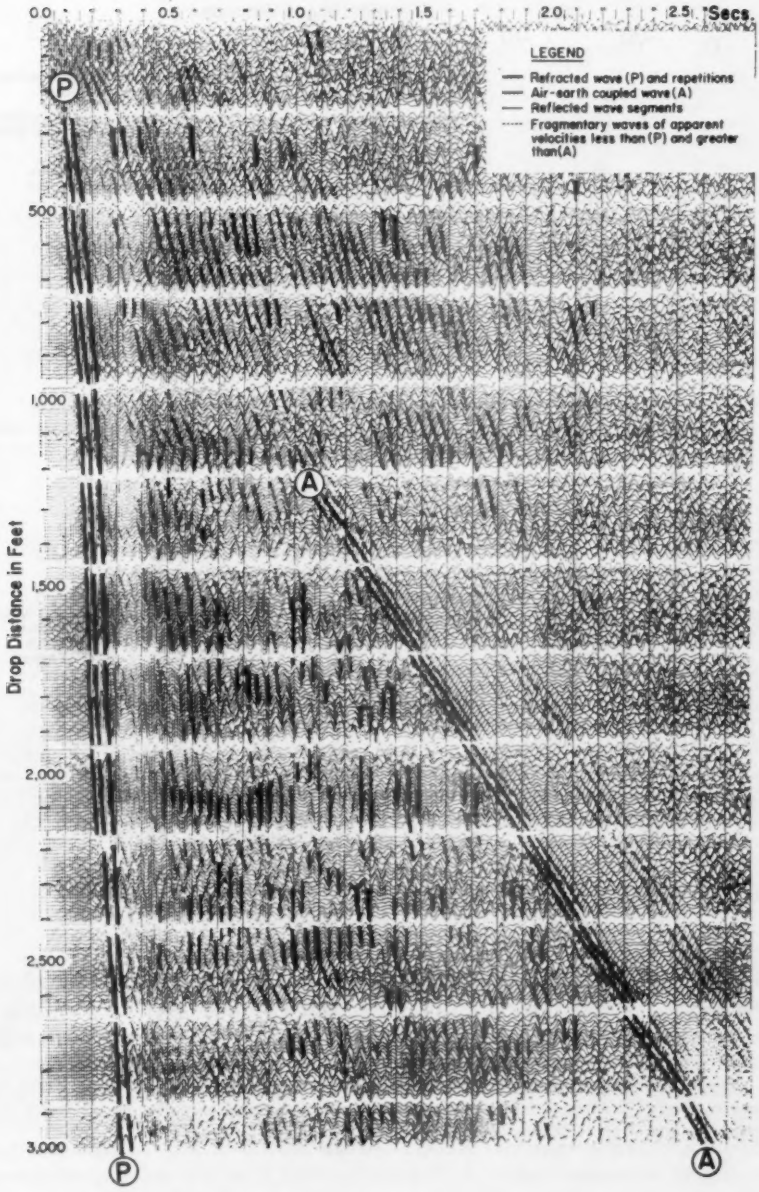

FIG. 5. Records for Test I at Test Site I. Each trace represents a single drop recorded at the *two seismometer groups* (72 seismometers) shown in Figure 2a.

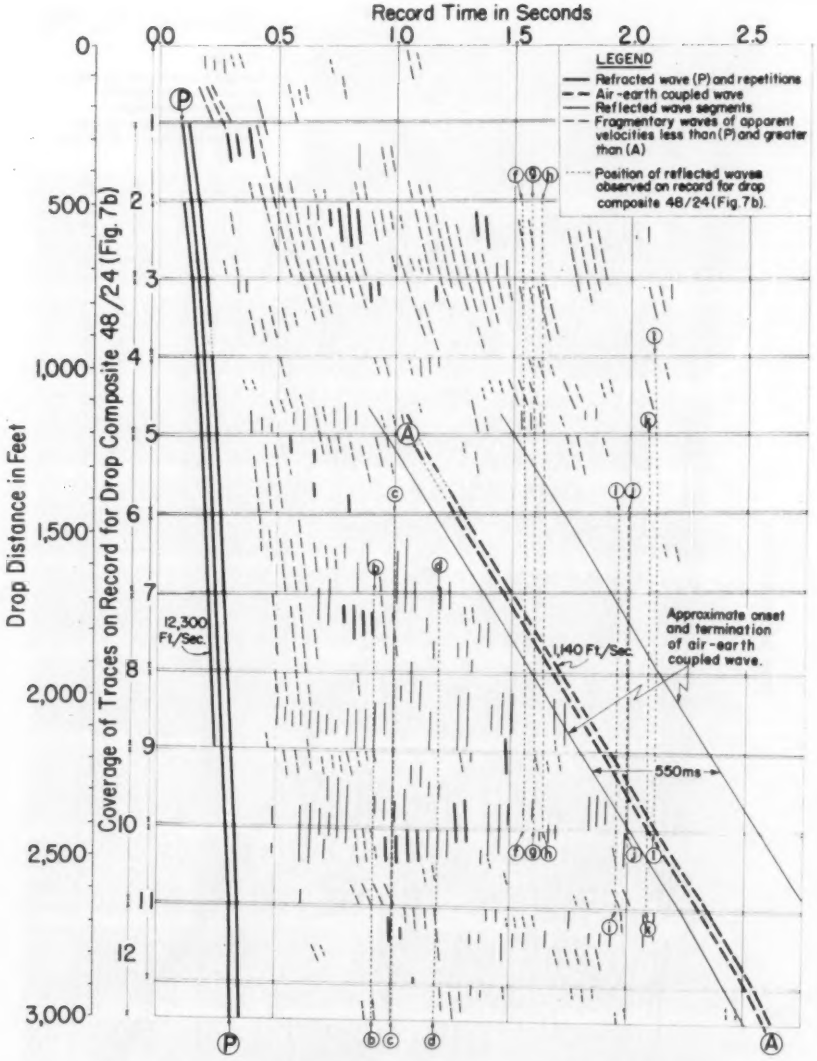

FIG. 6. Time-distance graph of correlatable events shown on records of Figure 5 from *two seismometer groups* (72 seismometers). The positions of reflected events appearing on the record for a drop composite of 48/24 (Figure 7b) also are shown.

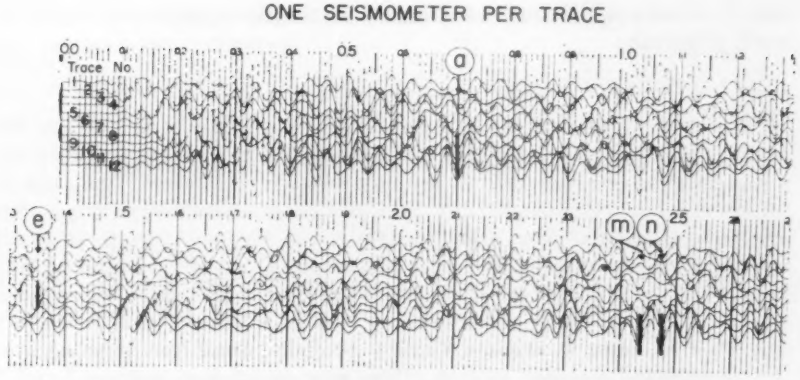

FIG. 7a. Record for Test I at Test Site I. Each trace represents the composite of 48 consecutive drops with 50 percent mix (drop composite of 48/24) recorded at the *single seismometer* shown in Figure 2a.

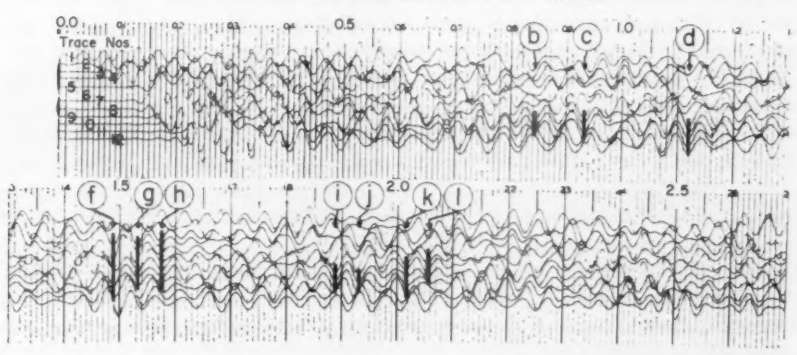

FIG. 7b. Record for Test I at Test Site I identical to that shown in Figure 7a, except that drops were recorded at the *two seismometer groups* (72 seismometers) shown in Figure 2a.

recorded by the 72-seismometer array. Reflections from the drop composite, in general, are not coincident with reflected wave segments from single drops. This observation, similar to that noted in Figure 4, suggests that the relative attenuation of other waves by means of drop compositing is responsible for the differences. Again it is observed that these reflections from the drop composite of 48/24 cross the time-distance domain of the air-earth coupled wave (A) with minor changes in wave form. The wave (A) persists for approximately 220 milliseconds longer than the same wave recorded by a single seismometer (Figure 3)

since it is being recorded by seismometers within the array over a distance of 250 ft (Figure 2a).

Test II at Test Site I

Description.—The field layout for the second test at Test Site I (Figure 2b) consisted of four seismometer stations 1,500 ft apart, each station containing two seismometer groups each with 36 seismometers spaced internally the same as for Test I above. Three parallel drop lines, 100 ft apart, were used. The recording and drop sequence is given below the diagram in Figure 2b. Drops at 20.8-ft intervals were made along each of the three lines, first commencing 12 drop positions to the left of the center of Station 1 at 1–1 and ending 12 drop positions to the right of the center of Station 2 at 1–96 for a total of 96 drops on each line while recording at Stations 3 and 4. Secondly, drops were repeated from 2–1 to 2–24 and extended to 2–96. These were recorded at Stations 2 and 3. Finally, drops were made in the same manner between Stations 3 and 4 while recording at Stations 1 and 2.

After correction for the weathered layer and normal moveout, consecutive drops were composited 24 to each trace with 50 percent mix, or a drop composite of 24/12. A single record was made for each line and seismometer station, each record (Figure 8) consisting of seven traces, alternate traces of which are independent. The three lines recorded at the same seismometer station were then composited to provide additional records (also shown in Figure 8) with 72 drops per trace and 50 percent mix, or a drop composite of 72/36. This procedure provides three sets of interlocking records, all of *common subsurface coverage* from Station 2 to Station 3, but each with *different drop-line dimensions*, that is, distance from ends of the drop line to the recorded seismometer station (equivalent to spread dimensions in conventional methods). Drop-line dimensions for the three sets of interlocking records are, respectively, 0-1,500-0 ft ("long" traces interlocking), 3,000-1,500-3,000 ft ("short" traces interlocking), and 3,000-4,500-3,000 ft ("long" traces interlocking). The 12-drop extension of drop lines beyond station centers provides common subsurface coverage for the interlocking traces on each pair of interlocking records.

This test provided (1) a comparison of records obtained individually on parallel drop lines, (2) a method to gauge the effectiveness of compositing drop lines in improving record quality, and (3) a means to determine variation in record quality from changes in drop-line dimensions.

Results.—Records from single drop lines of dimensions 0-1,500-0 ft recorded at Seismometer Stations 2 and 3 shown in Figure 8 demonstrate marked differences in the definition of reflections between drop lines.

Reflection troughs *o* and *p* recorded at Station 2 are continuous over appreciably more traces on Drop Line A than on Drop Lines B and C. Reflection troughs *r* and *s* are defined best at Station 2 on Drop Line B, and trough *t* is most pronounced at Station 3 on Drop Line B. Records from single drop lines

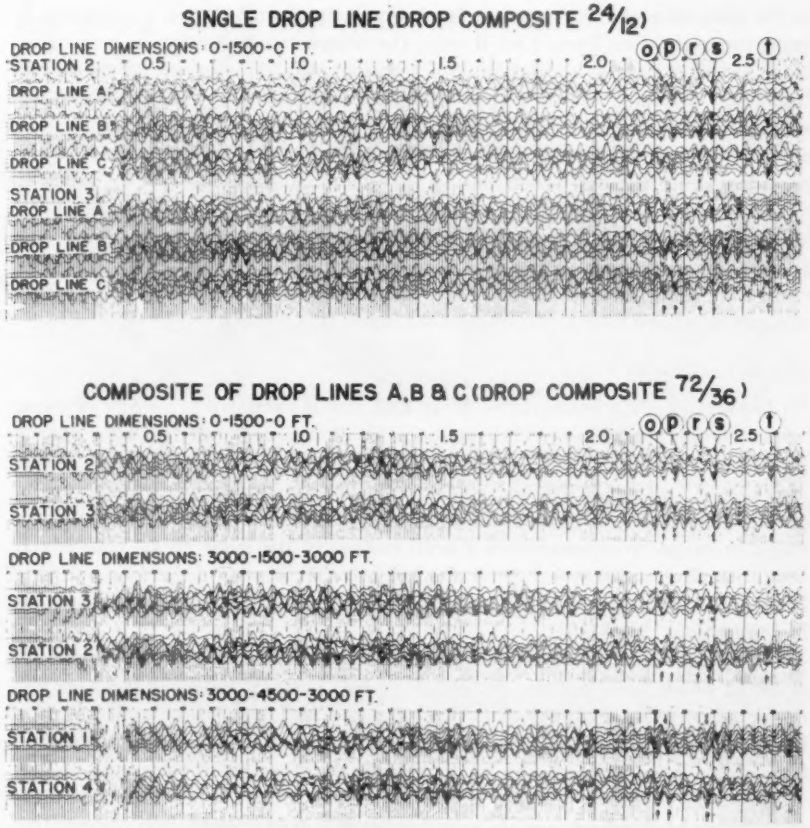

FIG. 8. Records for Test II at Test Site I. Records are shown for a drop composite of 24/12 along Drop Lines A, B, and C of dimensions 0–1,500–0 ft. In addition three records are shown for the composite of Drop Lines A, B, and C (drop composite of 72/36) at dimensions 0–1,500–0, 3,000–1,500–3,000 and 3,000–4,500–3,000 ft, respectively.

of other dimensions (3,000-1,500-3,000 and 3,000-4,500-3,000 ft) exhibited similar differences in reflection quality between parallel drop lines and for brevity are not reproduced here.

The composite record of Drop Lines A, B, and C of dimensions 0-1,500-0 ft shown in Figure 8 indicates that negligible improvement in definition of reflection has been obtained through this compositing. The quality of reflections in general appears no better than the best quality on the individual lines. Reflection troughs *o* and *p* at Station 2 are developed equally well on Drop Line A as

on the composite of the three drop lines. Similarly, troughs *r* and *s* at Station 2 are as pronounced on Drop Line B as on the composite. An exception is trough *t* which is better defined at Station 3 on the composite than on any of the single drop lines. Although the improvement through compositing drop lines appears minor, it should not be overlooked that the over-all quality of the composite is superior to that of any single drop line, since reflections on the former nearly equal in quality the best reflections on the individual lines.

The variations of reflection quality with changes in drop line dimensions for records of the composite of the drop lines does not appear pronounced. Reflection troughs *o* and *p* are defined nearly equally well at all dimensions. Troughs *r* and *s* are slightly better developed at dimensions 3,000-1,500-3,000 ft, whereas trough *t* is defined best at dimensions 0-1,500-0 ft.

Test at Test Site II

Description.—Experimental work at Test Site II consisted of a single traverse line extending 5 miles in a northwest-southeast direction (Figure 1). Drops were at 20.8-ft intervals along a single drop line between seismometer stations at 2,000-ft intervals. A total of 120 drops, inclusive of 12-drop extensions beyond station centers, were made between stations. Each seismometer station consisted of a single group of 36 seismometers spaced internally the same as at Test Site I. Drop-line dimensions were 2,000-4,000-2,000 ft, that is, ends of the drop line were 2,000 and 4,000 ft from the recorded station (equivalent of in-line offset spreads in conventional methods).

After the necessary corrections, records were prepared for a drop composite of 24/12 which provided nine traces per record. Further testing in this area was restricted by other commitments. However, in addition to the record for a drop composite of 24/12 at one of the seismometer stations, records also were prepared for a single drop per trace and for four drops per trace (drop composite of 4/0) as shown in Figure 9. Similar to Test I at Test Site I, preparation of these records provided a display of the complement of waves prior to drop compositing and a qualitative measure of the effectiveness of drop compositing in the attenuation of undesirable waves relative to the reflected waves.

Results.—Records for one drop per trace, shown in Figure 9, exhibit a refracted wave travelling at a velocity of 11,500 ft/sec, surface waves with an apparent velocity of 2,900 ft/sec, and fragmentary reflected waves (troughs *a* through *i*). On the record for a drop composite of 4/0 (four drops per trace) prepared from these drops, it is observed that reflection troughs *a* through *d* have been effectively masked by other waves. However, reflection troughs *e* through *i* may be identified. On the final record for a drop composite of 24/12 (24 drops per trace with 50 percent mix), a well defined Devonian reflection at about 1.1 sec was followed continuously along the entire traverse. Another less pronounced pre-Cambrian reflection at about 1.5 sec was correlatable over most of the traverse. Reflection troughs *e*, *f*, and *g* become well defined over the entire drop

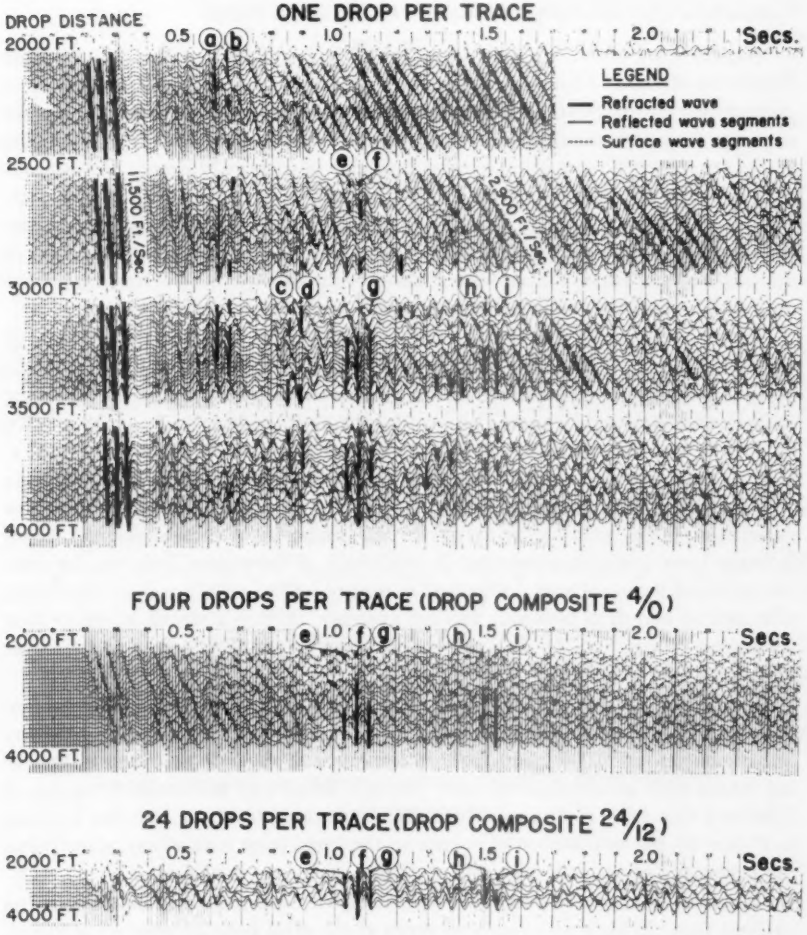

FIG. 9. Records from Test Site II. Traces on the upper four records represent single drops at 20.8-ft intervals along a line extending 2,000 to 4,000 ft from the recording seismometer station containing 36 seismometers. The bottom two records were obtained by compositing these drops four to a trace and 24 to a trace, respectively.

line. Similarly, trough *h* is well developed, even where surface waves dominate the traces from single drops at distances from 2,000 to approximately 3,300 ft. Thus, although some fragmentary reflections appearing on traces from single drops are obscured through drop compositing, others have developed sufficiently to be used for subsurface mapping.

Comparison of Interlocking Traces

As described above, on Test II at Test Site I and also at Test Site II, drop lines were extended 12-drop positions beyond seismometer station centers. After compositing drops 24 to a trace, these extensions provided common subsurface coverage for interlocking traces on each pair of tying records, that is, interlocking traces are recorded from interchanged positions of source (24 drops) and receiver (seismometer array). It follows from this reciprocal relationship that seismic events on interlocking traces should be identical, providing the initiation and also the reception of the energy are identical for the two traces. Thus, the degree of duplication of events on interlocking traces becomes a qualitative measure of the uniformity of initiation and reception conditions along a seismic traverse.

Interlocking traces selected from records for Test II at Test Site I (Figure 8) are reproduced in Figure 10. As shown in the field configuration diagram at the bottom of the figure, the average distance between the 24 drops and the recording seismometer station, consisting of two groups of 36 seismometers each, is 1,500 ft. Traces are shown for the 24-drop composite along Drop Lines A, B, and C and for the composite of these drop lines. It is noted that negligible duplication of amplitude and phase is evident for events appearing on the trace pairs. The duplication is not good on the traces for the composite of three drop lines where it might have been reasoned that the inclusion of these drop lines on the composite would have reduced differences in energy initiation. Since the interchange of recording and drop positions was not absolute, there is a strong inference that the source of much of the interference lies close to the drop points and receiver positions.

Interlocking traces selected from records obtained at the first four seismometer stations along the traverse at Test Site II are reproduced in Figure 11. Drop line dimensions of 2,000-4,000-2,000 ft employed at this site provided interlocking traces with an average distance between drops and seismometer station of 2,000 and also 4,000 ft. In contrast to the interlocking traces at Test Site I shown in Figure 10, the duplication of events on the trace pairs is excellent, attesting to the constancy of the initiation and reception of energy in this area.

It was not possible to establish conclusively the causes of this difference at the two test sites. At both sites repeated drops at the same position resulted in identical recordings. Possibly, the tens of feet of sand cover at Test Site II in contrast to the relatively thin soil cover at Test Site I constituted a major factor. The thick sand cover may have provided a more homogeneous near-surface medium for the initiation and reception of energy in contrast to possible radical changes in the material below the relatively thin soil cover at Test Site I. Record quality at Test Site II proved considerably better than that at Test Site I which, at least in part, must be attributed to the difference in constancy of the initiation and reception of energy at the two sites.

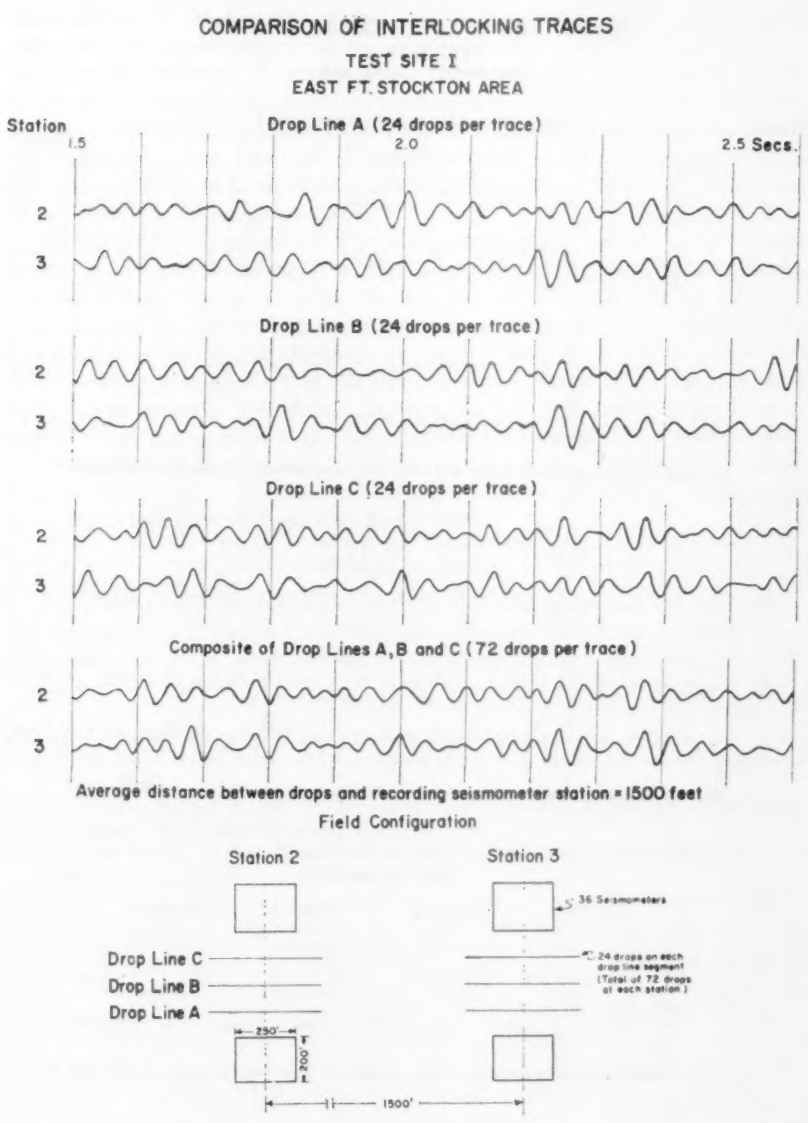

FIG. 10. Comparison of interlocking traces reproduced from records taken at Test Site I.

FIG. 11. Comparison of interlocking traces reproduced from records taken at Test Site II.

CONCLUSIONS

Undesirable waves generated by weight drops in general may be attenuated sufficiently to provide useful reflection data by employing an areal array of

seismometers at the recording station and by compositing drops along a single drop line. Although compositing of parallel drop lines provided small improvement in the definition of reflections, the over-all quality of the record for the composite of the drop lines appeared superior to records for individual drop lines, since the former usually retains the best reflections appearing on records from the single drop lines. Variation of reflection quality with changes in drop-line dimensions (distance from ends of the drop line to the recorded seismometer station) did not appear pronounced.

Difference in the uniformity of initiation and reception conditions at two test sites is evidenced by the degree of duplication of events on interlocking traces. Events on interlocking traces at the first site bear little if any resemblance, whereas those on interlocking traces at the second site are nearly identical. Although the causes of this difference at the two sites could not be established conclusively, it is suggested that a thick sand cover at one site may have provided a more homogeneous near-surface medium for the initiation and reception of energy in contrast to possible radical changes in the material below the relatively thin soil cover at the other site. The evidence may suggest that to achieve satisfactory duplication in the more difficult areas, the composition of considerably more than three lines of drops may be required.

ACKNOWLEDGMENTS

The author expresses his appreciation to the management of the Pan American Petroleum Corporation for permission to present this material. He is especially indebted to Dr. M. B. Widess for his many helpful suggestions.

REFERENCES

Hubert, F., 1925, Earth tremors by falling weights: Zeit. Geophysik, v. 1, p. 197.

Neitzel, Edwin B., 1958, Seismic reflection records obtained by dropping a weight: Geophysics, v. 23, p. 58–80.

Pommier, G., and Richard, H., 1957, Supermultiplication des charges et des sismographes au Sahara (Zone nord): Geophysical Prospecting, v. 5, p. 282–299.

Press, F., and Ewing, M., 1951, Ground roll coupling to atmospheric compressional waves: Geophysics, v. 16, p. 416–430.

GEOPHYSICS, VOL. XXIII, NO. 4 (OCTOBER, 1958) PP. 684–700, 8 FIGS.

KEY VARIABLES OF GRAVITY*

FREDERICK E. ROMBERG†

ABSTRACT

There is an inherent difficulty in converting gravity data into geologic information because the problems have to be solved indirectly. This difficulty has given rise to an intellectual gap between people who interpret gravity data and those who apply the results. With a view to bridging this gap, a check list of variables important to the correlation of gravity and geology is offered. This should help the non-specialist to obtain a better idea of where gravity will give him useful information. Remarks are made on the role each variable plays in the interpretation process and on the accuracy with which each may be used in computations. The effect of target depth on residual and derivative interpretation methods is examined. Examples are given showing the extent to which information about geologic structures can be got from gravity.

INTRODUCTION

Any given map of the observed gravity can be caused by an infinite number of possible geologic structures. It is impossible for the geophysicist to say from gravity alone: "*This* gravity is evidence of *that* structure." Gravity can be interpreted only when the geologic possibilities have been reduced in number to relatively few. Let the geologists say: "*These* things we know about our prospect; can you tell us whether the structure is *this* way or *that* way?" Then the geophysicist can help him.

The crux of applying gravity to detailed problems in exploration is in knowing enough about the geology of a prospect to be able to ask questions that gravity can answer. To get the most information from gravity, the person who asks the questions has to be both a geologist and a geophysicist. He has to be geologist enough to keep in mind all conditions that lead to the discovery of oil. He must also be geophysicist enough to see where any of these conditions may cause gravity anomalies.

It is seldom that the two specialities, of petroleum geologist and gravity interpreter, are adequately combined in a single person. It follows that to exploit gravity successfully, there must be a clear meeting of minds between the geologist who knows about a prospect and the geophysicist who can extract information from gravity. Until now, exploration has been hindered by the failure of geologists and geophysicists to pool their knowledge on particular prospects. This paper is intended to help bridge that gap in understanding. It is supposed to set up a common body of knowledge and a common language to be used by the two professions. It is designed to be a check list to be used when the following questions are asked:

1) Can a given type of structure be found with gravity?

* Paper read at the 27th Annual Meeting of the Society at Dallas on November 13, 1957. Manuscript received by the Editor April 16, 1958.

† Geophysical Service Inc., Houston, Texas.

2) What structural knowledge can be obtained from a given set of gravity data?

No attempt will be made to show how to compute the gravity anomalies caused by geologic structures. These computations can be laborious, but they are straightforward; and it may be said that the theory of making them is complete enough for the purpose. Facility with them can be acquired only after training and practice, together with a feeling for the short cuts which can be made without detriment to the geologic conclusions. A discussion of this process is far beyond the scope of this paper. The main problem of gravity in exploration is not how to compute gravity anomalies, but how to get the right data and make the right assumptions before the computations are begun.

Another way to say this is that the problems of gravity cannot be solved by formulas or by machine methods. What is needed is not a standard practice or routine; what is needed is an attitude or mode of thinking that will enable new problems to be stated so that they can be solved. Every prospect is different, in some way, from the others; each problem offers special features and fresh avenues; each gravity map has to be considered individually. The routine approach in gravity has been found unrewarding, from the standpoint of geologic knowledge gained. To state the problem in any particular case requires, besides geologic knowledge, a special kind of physical information in quantitative terms. These terms will be called "key variables," and they will constitute our check list for the study of new prospects.

THE EXPLORATION PROCESS

The Target:

The first step in applying gravity to an exploration problem is to set up a target. The geologist goes about his business by assuming that if a certain structural (or stratigraphic) condition exists, it may lead to the discovery of oil. He then asks the geophysicist the question: "Is such a condition present on the prospect?" The geophysicist's job is to devise ways to answer that question.

Often enough, of course, the target is at first generalized, so the geologist merely asks for any geologic information he can get about, say, a basin—or, indeed, he may merely ask whether a basin exists. This does not imply that a target is absent; it merely marks a state in its development. At any rate, as soon as the target, general or specific, has been set up, then the question poses itself: "Will the target give gravity anomalies which are recognizable?" There are two ways to answer this question, empirical and theoretical.

The Empirical Method:

A geophysicist who has seen many gravity maps will recall a number of known structures which gave good gravity anomalies and also a number of gravity anomalies which turned out to be evidence of structure. If the target

structure resembles those in the experience of the geophysicist, then it is fair for him to say that it will give a similar gravity anomaly. If the target does not resemble any whose gravity anomaly he has seen, he naturally suggests the experiment of observing gravity over a known structure which does resemble the target. Thus, if his experience to date does not answer the question for him, he simply proposes to add some experience which does.

There are two reasons why the empirical method may not work. The first is that the individual who is to decide whether gravity will give him the information he needs may not have either the necessary experience nor the authority to get it. The second is that, in practice, targets are often either structures more difficult to find than the structures that have already been discovered, or they are details of structures which were not perceptible by the techniques hitherto in use. In either case the empirical method of deciding whether the target can be found with gravity will break down.

The Theoretical Method

When the empirical method breaks down, the question of whether gravity will give evidence of the target structure has to be answered with the help of theory.

The theoretical approach to whether a target structure can be found with gravity is to compute its probable gravity anomaly. This is done by describing the target structure in terms of physical variables. Once the structure has been correctly described, it is a relatively simple matter to compute its anomaly. Much has been written describing the anomalies given by simplified or ideal target structures, and many examples have been published showing the correspondence between computed and observed anomalies. The assignment is now to describe actual targets correctly from the geologic data at hand.

Our next step is to make a list of the physical variables that are important in describing anomalies and to discuss how successfully, in practice, values of these variables can be assigned to target or model structures. It should be remembered that the variables apply to regional as well as to local structures—to the exploration of whole basins as well as to the search for small oil traps.

KEY VARIABLES IN GEOLOGIC STRUCTURES

In computing the gravity anomaly of a given structure, five principal variables have to be considered. These are *volume*, *density contrast*, *depth*, *shape*, and *isolation*. Without estimated values for all five, it will not be possible to say whether gravity is likely to give evidence of the structure. Other attributes, such as dip, age, or rock character, so important to geology, are unimportant in gravity exploration except as they bear on the five key variables.

It is, of course, clear why each of the key variables is important. The magnitude of the gravity anomaly given by a structure depends directly on its *volume* times its *density contrast*. The size of the anomaly decreases as the square of the *depth*, and its sharpness with the depth itself. These relations, however,

hold only so long as the structure has a concentrated *shape*. If the shape is diffuse the observed anomaly will be reduced in magnitude and sharpness. Finally, if the structure is not sufficiently well *isolated* from other structures, similar or not, which give similar anomalies, its own anomaly will not be resolved from the others and will not, therefore, be evident to the explorer.

Some remarks ought to be made about the relative accuracy with which values for the key variables can be assigned to target structures. It is usually easy enough to estimate the *volume* of targets accurately enough for the purpose. For economic reasons the importance of the target structure is usually proportional to its volume, so a proper estimate of the volume is usually inherent in choosing the target.

The *depth* of a target structure is also fairly easily estimated, except for two difficulties. First, the *size* (amplitude or number of milligals) of a gravity anomaly is much more sensitive to changes in depth than to changes in volume; thus an error in the estimated depth of the target has a more serious effect on the anomaly than an error in the volume. This difficulty is offset in many cases by the fact that structures like folds and faults have density contrasts over a range of depths from shallow to deep. Folds and faults often give gravity anomalies that are clearly due (from their shape) to density contrasts shallower than those which are perceived by geologic logging methods. The extent to which this effect occurs is not known. It may be due to differential compaction of shales. Rosaire (1938) has said that it is sometimes due to chemical changes. At any rate, it is difficult to estimate in such cases the controlling depth of density contrast of a target structure and, therefore, the probable size of its gravity anomaly.

The *shape* of a target structure is important. Even though its depth may be small and its volume large, it will not give a large anomaly unless it is concentrated. This is a problem in looking for ores and minerals other than petroleum, since they frequently occur in tabular bodies, extensive, but so thin that their gravity effects are scattered. In general, however, the shape of a target structure can be assumed correctly enough for the purpose of computing its anomaly.

The *isolation* of target structures is as important as any of the other variables. It is obvious that unless a gravity anomaly is sufficiently well isolated from other anomalies it cannot be properly identified. Nettleton (1954) made important observations on isolating anomalies, particularly about some of the mechanical methods for doing it. In general, structures must be separated from each other by a distance of more than twice their depth before their anomalies can be told apart. Examples of this will be shown later. It is sometimes quite difficult to estimate in advance whether the target structures on a prospect will be well enough separated that their anomalies will be resolved. This is especially true in the case of fault systems. Another difficulty comes up with the variable of isolation in applying the empirical method of gravity interpretation. A map of the observed gravity over known structures may very well have anomalies coinciding with these structures, but which are not valid evidence of them, because

there are similar anomalies on the map which do not coincide with structures. In this case the target structures are not well enough isolated from structures of a different nature which give similar anomalies.

The variable of *density contrast* is the one about which there is the most uncertainty in practice. In general, the density scale runs from light to heavy with salt, sandstones, shales (in proportion to depth), carbonates, granite, anhydrite, metamorphics, and basalt. In each class, however, the measured densities vary over a wide range, and in specific cases it is usually impossible to assign numerical density differences without large percentages of error. Even the algebraic sign of the density contrast is often uncertain, so it is not known in advance whether the target will give a positive or a negative anomaly.

The best way to measure density contrasts is by their observed effects, with known structures or outcrops, or from well cores when these are available. Density determinations from samples are good except for clastics, which is just where they are most important. It behooves a geophysicist who interprets gravity to be always conscious of the problems of density contrast and to be alert for all possible information on densities.

THE DIRECT PROBLEM

We have now taken the attack on the gravity problems as far as it can go by the method of analogy. This is to say that we have discussed how well we can answer the question: "Given a geologic structure, what gravity anomaly can it be expected to show?" Until now, everything has been straightforward; given the key variables of a structure, we can compute its anomaly. These variables are measurable so that in principle the problem has a solution. But this problem is really the inverse of the true problem of gravity interpretation. In practice, we always come face to face with the direct question: "Given a gravity anomaly, what structure can be said to cause it?"

This is, of course, the critical point in the whole interpretation process. There is an infinite number of possible answers to the question, which means that there is in practice no answer at all unless the possible answers are reduced to a very few. If the remaining few answers are such that gravity can be used to choose between them, then the question has been put into a form which has an answer, and the gravity problem can be solved. The point is that the only way to reduce the number of answers from infinity to a few in any particular case is to have some knowledge of the geology. The better the geology is known, the better the chances that gravity will be translatable into further knowledge. As a matter of practice, to reduce the possible answers to a number which can be handled is not as difficult as it sounds. While there are all sorts of geologic structures, their number is not infinite, and they can fortunately be classified into types in a way which simplifies exploration. Still, the step of making an assumption about the geology has to be taken before gravity can be used as a tool for getting geologic information. Whether such assumptions are made with

sound geologic feeling, plus an understanding of the physical relation between rock masses and gravity, determines whether or not gravity will be able to supply useful data to the geologist. Another way of saying this is that the possibility of solving the problem depends on how it is stated. If it is incorrectly stated from the standpoint of either geology or physics, it cannot be solved, no matter how accurate the observations or the computations.

If the petroleum geologist knows what class of questions the geophysicist can answer, he will be better able to ask them. Information about structures can be deduced from the key variables of gravity anomalies under the appropriate geologic assumptions. A list of the measurable variables in gravity anomalies, with examples, should help the geologist to know what questions he can ask that will have useful answers.

KEY VARIABLES OF GRAVITY ANOMALIES

List of Variables:

The key variables to look for on gravity maps are: *size*, *sharpness*, *perceptibility*, *resolution*, and *shape*. Size means magnitude or number of milligals. Shape, of course, is not a quantitative variable in an engineering sense. It is an attribute which includes many variables that must be considered in studying the relation between anomalies and structure.

Size:

The most important variable in gravity anomalies is, of course, the size or magnitude. The size (volume) of a structure is directly proportional to the size (magnitude) of its gravity anomaly and can be computed from it if the depth and density contrast are known. Even if the depth and density contrast are not known, the "anomalous mass" of a structure can be estimated from the "volume" of its gravity anomaly (Hammer, 1945). The size of an anomaly due to a concentrated structure is, of course, inversely proportional to the square of its depth, but it is interesting that this relation does not hold if the structure is not concentrated. Figure 1 shows how a *long* structure such as an extended ridge or fold gives an anomaly which decreases linearly with depth rather than with the square of depth. Moreover, the anomaly of a structure which is both *long and wide*, such as an idealized fault, does not decrease with depth at all, but remains constant. These relations hold only for idealized, infinite structures which do not exist in nature; but it is useful to know them because many folds and faults are found which are long enough, in proportion to their depth, so that the relation between size of anomaly and depth does not follow the regular inverse square law.

Sharpness:

The variable next in importance in gravity anomalies is the sharpness. This is because sharp anomalies are easy to identify, while broad anomalies tend to merge into the background and not be visible. It follows that sharpness must

be considered in deciding whether a given structure will give an identifiable anomaly. Figure 1 shows how the sharpness of anomalies from different structures decreases with depth. For a fault-type anomaly, sharpness decreases with depth. For a long anomaly, it decreases with the square of depth, and for a concentrated anomaly it decreases with the cube of depth. For each type of anomaly, the sharpness decreases with depth one power faster than the amplitude of the anomaly. In the case of simple anomalies this can be used as a way of estimating depth. (See Appendix.)

A convenient measure for sharpness is the magnitude or height divided by

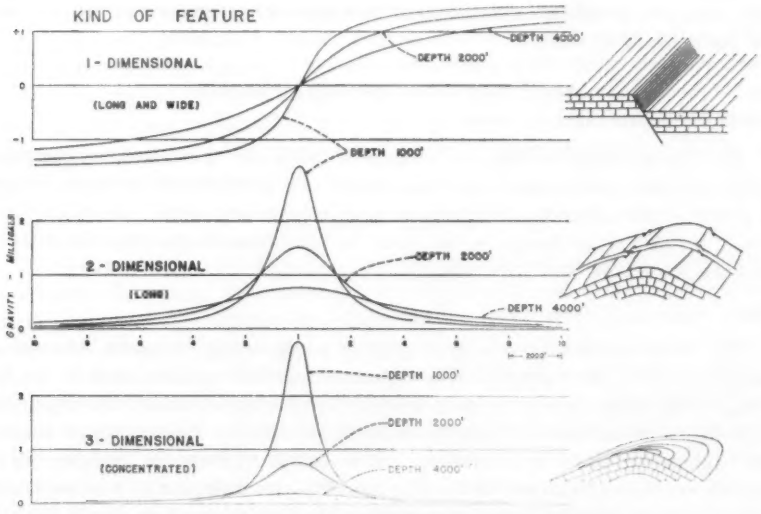

FIG. 1. Profiles of gravity anomalies of different types of structures showing variation in magnitude and sharpness with depth.

the width. The width is usually measured at half the total magnitude or height. For fault-type anomalies and long anomalies this width is twice the maximum possible depth, and for concentrated anomalies it is about one and one-half times the maximum depth. This gives a rough way of measuring the maximum depth of structures if they are not diffuse and if their density contrast is concentrated.

A well-known method of applying the idea of sharpness is to compute, for each station on a gravity map, the difference between the station gravity and the average gravity at an arbitrary distance. Nettleton (1954) calls this the center-point-and-one-ring residual method, and it produces in effect a map of the sharpness. Its dimensions will be in milligals divided by length, or the same

as those of the gravity gradient or first derivative. Residual anomalies decrease with the depth of the features causing them in the same way sharpness does. What this means is that the residual method emphasizes anomalies from shallow features, but it discriminates against those from deep features by reducing their size in proportion to their true magnitude.

Perceptibility:

Perceptibility is a variable which depends on the size, sharpness, and level of background noise of an anomaly. It is sufficiently hard to measure, so we shall not attempt to define it quantitatively. It is important, however, to know what makes an anomaly perceptible. If it can be easily separated from other anomalies, either smaller or larger, in its background, it is perceptible. If it is masked by other anomalies so that it cannot be isolated and identified then it is not perceptible.

The reason for considering perceptibility is that so much effort has gone into the art of making anomalies perceptible. The main purpose of all residual and derivative methods of interpretation is to make anomalies perceptible which were not perceptible on the map of the observed gravity anomaly, often called the map of the Bouguer anomaly.

Perceptibility and Second Derivatives:

Derivative methods (we shall speak here of the most popular one, which is the second vertical derivative) have both advantages and disadvantages. Their principal advantage is that they can pick out changes in a steep gravity slope which are difficult to see with graphic methods but which are quite important as evidence of gravity anomalies. Composite gravity anomalies which cannot be resolved on the Bouguer map may show up as separate components on a derivative map. They have the practical advantage that they can be made with automatic computing techniques, permitting the skilled interpreter to save much time by having maps fully prepared before he looks at them.

Second derivatives also have disadvantages. On the practical side, they mean little unless the stations are evenly and closely spaced; otherwise they tend to be an interpretation of the contours rather than of observed gravity. A derivative map of a single line of stations, for instance, or of any prospect where the lines are farther apart than the template radius (or differences in radii) is plainly meaningless. Furthermore, since second derivatives are computed from the differences between differences in gravity, they are affected by small errors. Observations have to be of high accuracy, with good terrain corrections applied wherever necessary, before they really permit the advantages of the method to appear.

There are also theoretical disadvantages to second derivatives. One is that the derivatives do not look like the anomalies or the geologic structures that caused them. It is reasonably easy for the interpreter to see the relation between

milligals of gravity and masses of rock. It is much harder to understand the relation between the rock masses and the second derivative, which is defined as the rate of change of the slope or gradient of gravity. Actually the size of an anomaly—its most important variable—cannot be deduced from the second derivative map. The reason for this is that, in taking derivatives, the constant terms in first the gravity and then the slope are discarded, so the operation cannot be reversed without resupplying these constants. Information is thus thrown away in the process of finding the second derivative.

Another theoretical disadvantage of the second derivative is its rate of decrease with depth. The second derivative of a fault-type anomaly decreases with

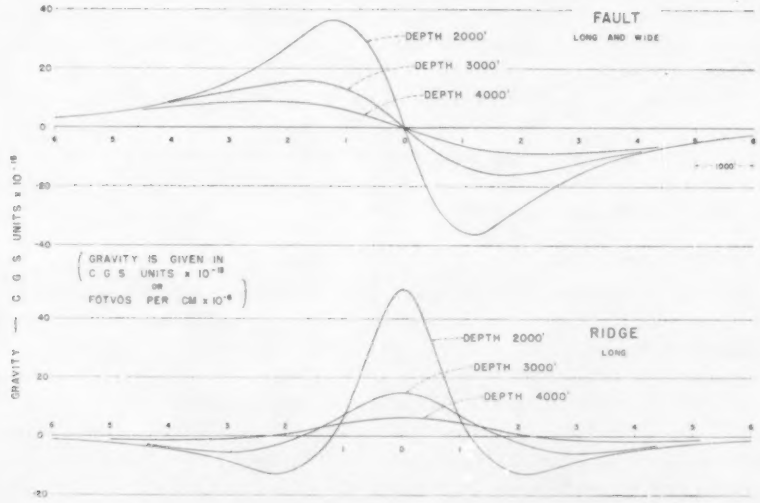

FIG. 2. Profiles of second derivatives of long and fault-type structures showing variation with depth.

the square of target depth. Second derivatives of long and concentrated anomalies decrease with the cube and fourth power, respectively, of the depth, or two powers faster than the gravity anomaly of the same type of structure. This is illustrated by Figure 2. It means that a concentrated structure twice as deep as another has an anomaly one-fourth as large, but a second derivative only one-sixteenth as large. The result is that a second derivative map is a map from which evidence of deep structure has been excluded.

A table of formulas for anomalies and derivatives appears in the Appendix to demonstrate the relations described above. It should be said that these relations are not strictly true for ordinary practice, as they would be if second derivatives were measured by a special instrument as gradients are measured with torsion balances. In practice, derivatives are measured by finding the differ-

ences between differences of gravity observations, and multiplying them by suitable coefficients. The two-power extra decrease with depth holds only to the extent that the practical methods approximate the true derivative.

Resolution:

The fourth variable important in gravity anomalies is resolution. Two anomalies are resolved if they can be recognized as belonging to separate structures. In the case of simple structures it is easy to demonstrate resolution. Figure 3 shows the gravity anomalies of two similar faults at a common depth, but

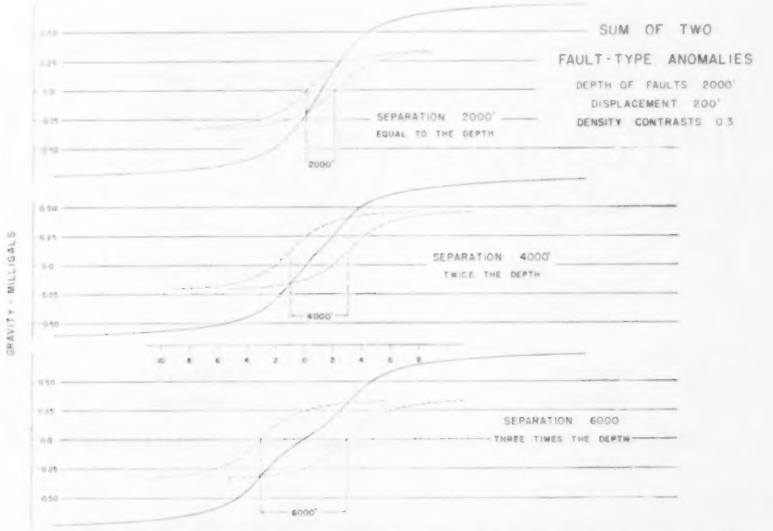

FIG. 3. Profile of the sum of the gravity anomalies of two faults for different separations.

separated by a varying distance. The sum of the two anomalies is of course what would be seen on a gravity map. Clearly, if the two faults are separated by a distance only equal to their depth, the sum of their anomalies looks like a single fault. The other graphs in the figure show that the two features must be separated by a distance between two and three times their depth to produce a total anomaly which can be identified as a double rather than a single anomaly. Resolution is a serious limitation in the study of fault systems with gravity.

This much is elementary. What is not understood is the extent to which, in practice, small density contrasts due to faults are found close to the surface thus giving very shallow evidences of faults from gravity data and permitting better resolution than would otherwise be expected.

Another example of resolution is the case of one or more salt domes that are

close together. The three salt domes at South Houston (Griffin, 1949; Nettleton, 1954) are a famous example of such a case. It turns out that concentrated anomalies like salt domes cannot be resolved by gravity unless they are a suitable distance apart with respect to their depths. Figure 4 shows the gravity anomalies of two salt domes whose centers are 12,000 and 24,000 ft apart. In the first case they could not be resolved by gravity because their resultant anomaly is no more eccentric than the average salt dome anomaly, usually because of a non-linear regional background. In the second case the anomalies can be clearly distinguished.

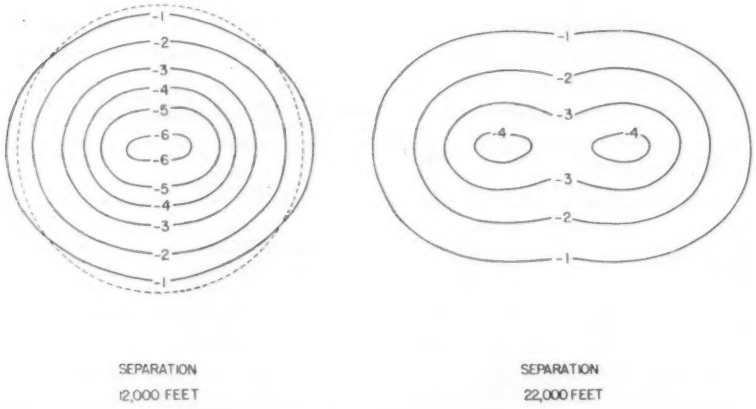

FIG. 4. Sum of the gravity anomalies of two salt domes for different separations.

Eccentricity:

An interesting aspect of resolution is eccentricity. A long, irregular, or eccentric geologic structure close to the surface gives an eccentric or elongated anomaly. The same structure at depth gives an anomaly so nearly circular that it is indistinguishable in practice from the anomaly which would be given by a round or a concentrated anomaly. Figure 5 shows the eccentricity of the gravity anomaly given by a long feature at various depths in proportion to its length. It can be seen that if the length is twice the depth, the anomaly is recognizably eccentric or elongated, but as the depth increases the resulting anomaly becomes almost circular.

The tendency of the gravity anomaly to hide the elongation or eccentricity of a structure is the most serious limitation to the study of the shape of deep salt domes. The portions of salt domes close to the surface may give elongated or eccentric anomalies if they are so shaped, but the deeper parts give round anomalies regardless of their shape. If the anomaly due to a salt dome has a

conspicuous eccentricity it is a safe bet that it is caused by more than one dome. In the case of deep structures, gravity is a poor guide to shape.

Shape:

The fifth variable to be considered, shape, is not a variable at all, but a set of attributes. As was hinted in the preceding paragraph, it is not often that precise information about the shape of a structure can be deduced from the shape of its gravity anomaly. Various examples will be given which show applications and limitations of the usefulness of considering shape in gravity interpretation.

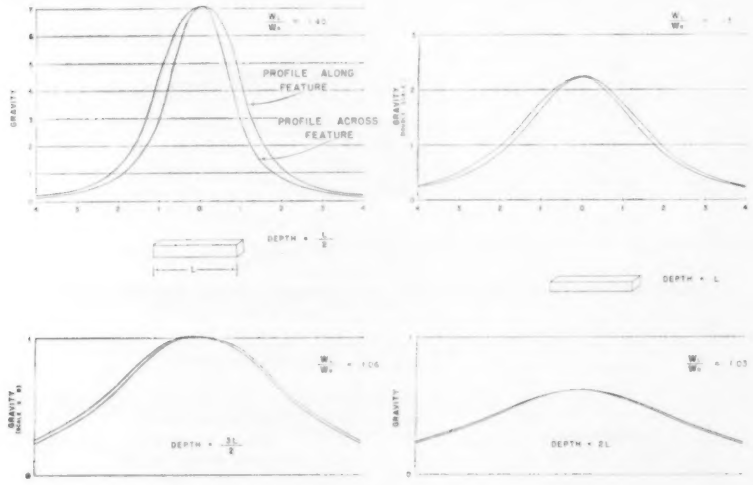

FIG. 5. Eccentricity of gravity anomaly of a long feature for varying depth.

1. *Salt Domes:* The first of these is the salt dome. Salt dome gravity anomalies are interpreted by assuming an upright cylinder of estimated size, with density contrast a function of depth, and computing its gravity anomaly. This anomaly will differ from the observed anomaly by a residual which resembles the anomaly of some segment of the dome, either deep or shallow (Figure 6). By adding (or subtracting) salt at this depth, the observed gravity of the model and an acceptable interpretation evolves. With certain simplifying conditions, this solution is unique (Allred, 1958).

2. *Large Faults:* Faults whose gravity displacement is a matter of one or two milligals can almost never be analyzed for anything except their sharpness because of the relatively large noise level. When, however, large mountain-range faults are being studied, with displacements of 10 milligals or more, their angle

can sometimes be deduced from their shape. This is illustrated by Figure 7. As the fault angle decreases—that is, as the fault comes to resemble a thrust fault—the "foot" of the anomaly becomes sharper and its "head" rounder.

3. *Shallow and Deep Density Contrasts:* Much work has been done (Hammer, 1950; Smith, 1950) on the value to exploration of knowing the distribution of density contrast up and down the geologic section. Tsuboi (1940) showed that if the density contrast were all at a given depth, the relation between gravity and structure could be computed directly. From this it is clear that by knowing the density contrast distribution we should probably be able to reduce the num-

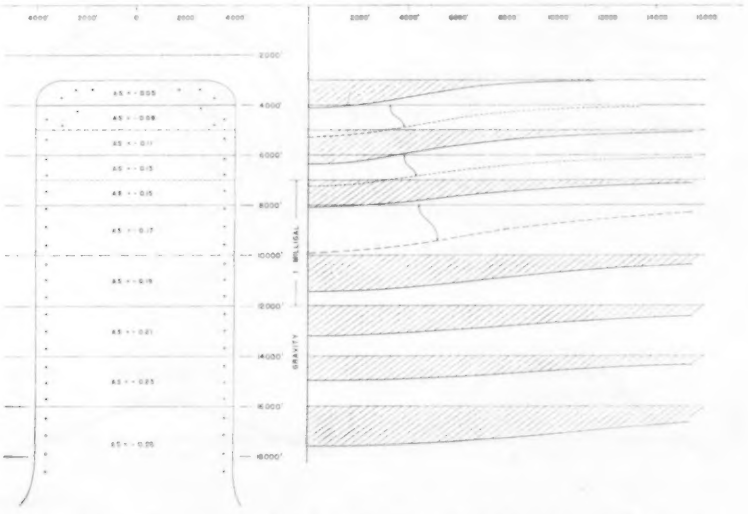

FIG. 6. Profiles of the anomalies of different segments of an idealized salt dome, convenient for varying the primitive cylinder model to fit observed gravity.

ber of possible solutions to the gravity problem drastically. For this reason it is interesting to show an example of problems worked backward, that is, to show the variation in anomaly shape due to different density contrasts.

Figure 8 shows the gravity anomaly of a concentrated structure compared with the anomaly of a structure which is horizontally concentrated but distributed vertically. This case is perhaps representative of a sharp fold in a thick shale section where the density difference is caused by displacement of material made dense by differential compaction. If the two anomalies are normalized to take care of the broad "foot" of the second anomaly (which would be diagnostic if it were visible, but is not), then the two anomalies resemble each other closely enough not to be distinguishable in an ordinary gravity picture.

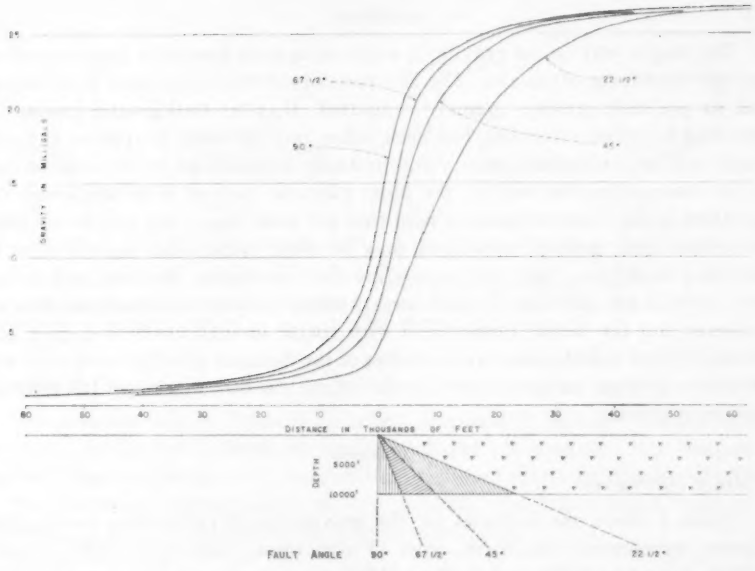

FIG. 7. Relation between shape and fault angle for a large mountain-front fault.

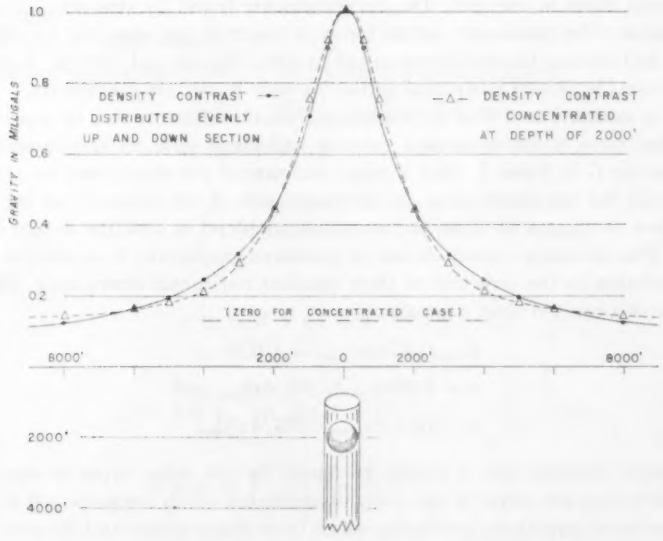

FIG. 8. Gravity anomaly of a concentrated structure compared with that of a structure with density contrast distributed up and down the geologic section.

SUMMARY

The proper way to use gravity in exploration is to assume a target based on geologic knowledge of the area. The key variables of this target must be estimated and its probable gravity anomaly computed. If, after background "noise" or crowding by other structures has been taken into account, it appears that the target will be perceptible, gravity will probably be useful as an exploration tool.

In interpreting the results, the most effective method is to single out the variables in the observed gravity map that are most important and to use them to deduce what geologic structures may be their cause. This is best done by assuming model structures and computing their anomalies. Residual and derivative methods are useful for shallow targets where stations are dense and data are accurate, but for deeper targets and with sparse or inaccurate data they contribute little. Critical quantitative studies of the Bouguer gravity, correlated with all known geologic and geophysical evidence, are the best way to get full information from gravity.

APPENDIX

Table of Derivatives:

Table I shows the formulas for the gravity, G, of elementary or simplified figures representing the three types of structures. Nettleton (1940), Dobrin (1952), Jakosky (1940), and Heiland (1946) have developed and expanded these formulas for many solid figures; they are given here merely as a verification for statements made in the text. The derivatives are found by straight partial differentiation. The maximum values for each function are obtained by differentiating and setting the derivative equal to zero. The second vertical derivative differs from the second horizontal derivative only by certain coefficients.

If it is assumed as a first approximation that a structure can be represented as a point-mass, a line-mass, or a sheet or half-plane mass, as illustrated by the formulas for G in Table I, then a rough estimate of the depth may be made by comparing the maximum slope to the magnitude of the anomaly, or the maximum rate of change of slope to the maximum slope in case the actual G is in doubt. The necessary quantities can be measured graphically from profiles across the anomalies in the direction of their smallest horizontal dimensions. Thus, in the case of a concentrated anomaly

$$G_{max}/(\partial G/\partial x)_{max} = z/0.86 \text{ or}$$

$$z = 0.86(G_{max})/(\partial G/\partial x)_{max} \text{ and}$$

$$z = (\partial G/\partial x)_{max}/(\partial^2 G/\partial x^2)_{max}$$

Similar relations can of course be found for the other types of structures. These relations are useful in the study of anomalies which are suspected to represent basement structures, anomalies which have sharp apexes and thus may have shallower components than their breadth indicates, and in other problems.

TABLE I

Function	Concentrated (point-mass)	Long (line-mass)	Fault-type (sheet-mass)
Multiplying Constant	kM	$2kM/l$	$2khs$
G	$z(x^2+z^2)^{-3/2}$	$z(x^2+z^2)^{-1}$	$\tan^{-1}(x/z)$
$\partial G/\partial x$	$-3xz(x^2+z^2)^{-5/2}$	$-2xz(x^2+z^2)^{-2}$	$z(x^2+z^2)^{-1}$
$\partial^2 G/\partial x^2$	$3z(4x^2-z^2)(x^2+z^2)^{-7/2}$	$2z(3x^2-z^2)(x^2+z^2)^{-3}$	$-2xz(x^2+z^2)^{-2}$
G_{max}	$1/z^2$	$1/z$	π
$(\partial G/\partial x)_{max}$	$0.86/z^3$	$0.65/z^2$	$1/z$
$(\partial^2 G/\partial x^2)_{max}$	$0.85/z^4$	$0.5/z^3$	$0.65/z^2$
$\partial^2 G/\partial z^2$	$3z(2z^2-3x^2)(x^2+z^2)^{-7/2}$	$2z(z^2-3x^2)(x^2+z^2)^{-3}$	$2xz(x^2+z^2)^{-2}$

$k = 6.67 \times 10^{-8}$
M = mass in grams
s = density (or density contrast)
l = length (cm)
h = height or displacement (cm)
x = horizontal distance (cm)
z = vertical distance (cm)

Distributed Density:

The simplest way to illustrate the effect of a density contrast distributed up and down the geologic column, as density contrasts are in nature, is to imagine a vertical column of elementary cross-section displaced upward a distance D. This is the elementary representation of, say, a small, closed anticline formed in a shale section by being pushed up from underneath. Let

s = density $= s(z)$
z = depth
A = area of the column
M = mass
D = upward displacement;

now the anomalous mass, ΔM, of part of the displaced column is

$$\Delta M = A[s(z) - s(z - D)]$$
$$\Delta G = kz\Delta M(x^2 + z^2)^{-3/2}$$

so that

$$G = kA \int_{z_1}^{z_2} z[s(z) - s(z - D)](x^2 + z^2)^{-3/2} Dz;$$

now let

$$s(z) = B + Cz \text{ and } Ds/Dz = C;$$

thus

$$G = kA \int_{z_1}^{z_2} (zCD)(x^2 + z^2)^{-3/2} Dz$$

$$= kACD \int_{z_1}^{z_2} z(x^2 + z^2)^{3/2} Dz$$

$$= kACD[(x^2 + z_2^2)^{-1/2} - (x^2 + z_1^2)^{-1/2}].$$

From this equation, G can be plotted. A number of examples of similar problems suggest themselves, but they are beyond the scope of this paper.

ACKNOWLEDGMENTS

The author wishes to acknowledge his debt to Dr. R. A. Geyer for his advice and discussions while the paper was being developed and for his criticism of the manuscript, to Mr. Lawrence McCarthy for assistance in computing the examples, and to Mr. Clint Fagg for the design and execution of the illustrations.

REFERENCES

Allred, J. R., 1958, Personal communication.

Dobrin, Milton B., 1952, Introduction to geophysical prospecting: New York, McGraw-Hill Book Company, Inc.

Griffin, W. Raymond, 1949, Residual gravity in theory and practice: Geophysics, v. 14, p. 39.

Hammer, Sigmund, 1945, Estimating ore masses in gravity prospecting: Geophysics, v. 10, p. 50.

———————, 1950, Density determinations by underground gravity measurements: Geophysics, v. 15, p. 637.

Heiland, C. A., 1946, Geophysical exploration: New York, Prentice-Hall, Inc.

Jakosky, J. J., 1940, Exploration geophysics: Los Angeles, Times-Mirror Press.

Nettleton, L. L., 1940, Geophysical prospecting for oil: New York, McGraw-Hill Book Company, Inc.

———————, 1954, Regionals, residuals, and structures: Geophysics, v. 22, p. 1.

Rosaire, E. E., 1938, Shallow stratigraphic variations over Gulf Coast structures: Geophysics, v. 3, p. 96.

Smith, Neil J., 1950, The case for gravity data from boreholes: Geophysics, v. 15, p. 605.

Tsuboi, Chuji, 1940, Relation between the gravity anomalies and the corresponding subterranean mass distribution. V. Isostatic anomalies and the undulation of the isostatic geoid in the United States of America: Bull., Earthquake Research Inst., Tokyo Imperial University, v. 18, p. 384

GEOPHYSICS, VOL. XXIII, NO. 4 (OCTOBER, 1958), PP. 701–711, 6 FIGS.

TERRAIN CORRECTIONS FOR AN INCLINED PLANE IN GRAVITY COMPUTATIONS*

C. H. SANDBERG†

ABSTRACT

In many instances an inclined-plane approximation represents more accurately the terrain near a gravity station than does the conventional block-cylinder approximation.

Combinations of the terrain effect of inclined planes through various terrain zones, as represented in the accompanying tables, can be used to approximate easily and quickly such familiar land forms as valleys, ridges, and hillsides.

INTRODUCTION

When making terrain corrections in gravity surveys, some geometric form readily amenable to mathematical computations is used as an approximation to the terrain. The Hayford-Bowie reduction tables used by the United States Coast and Geodetic Survey and the Hammer terrain correction tables for gravity are both based on the block-cylinder type of approximation. In many instances an inclined plane offers a better approximation to topographic features than does a series of cylindrical compartments. This is especially true of the area in the immediate vicinity of a station.

THE INCLINED PLANE

When Hammer (1939) presented his terrain correction table, he called attention to the possibility of using an inclined plane and gave the following formula for computing the correction:

$$T_R = 2\gamma\delta R[\pi - 2\cos\theta K(\sin\theta)].$$

T_R is the total terrain correction in gals for an inclined plane out to a distance of radius R in cm from the station (Figure 1); the slope angle is θ. The other symbols are δ, the density expressed as gm per cm^3; γ, the universal cgs gravitational constant, and $K(\sin\theta)$, the complete elliptic integral of the first kind.

TABLE FOR HAMMER ZONES

A table for corrections for radii (R) equal to the radii of Hammer Zones A through H for slope angles of 1° to 30° inclusive has been prepared (Table I). This table is intended to be used in conjunction with the Hammer Chart; consequently, a density (δ) of 2 gm per cm^3 was used in computations, and all values are in the same denominations and interchangeable with the Hammer Charts zone for zone.

Under each zone there are two columns; the first column is a height in feet,

* Publication authorized by the Director, United States Geological Survey. Manuscript received by the Editor March 13, 1958.

† United States Geological Survey, Menlo Park, California.

the second is a correction in milligals$\times 10^{-2}$. For each angle, there are two lines; the upper one labeled T is the total terrain correction for all zones in the cylindrical wedge, out to and including the zone indicated in the column. The lower line labeled $Z/2$ represents the contribution to the total of one-half the zone indicated at the head of the column. This half-zone contribution is that indicated in Figure 2 by the semiannular wedge $ABCDEFGH$ in which R_1 in the figure represents the inner radius of the zone and R_2 the outer radius. The h in the $Z/2$-line is

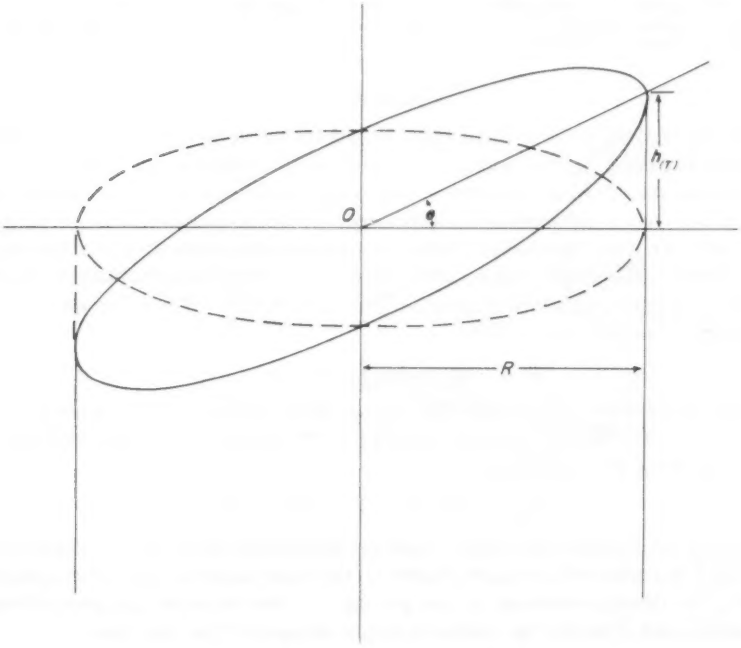

FIG. 1. An inclined plane through the station 0 intersecting a zonal cylinder. θ is the angle of inclination of the plane to the horizontal, and the cylinder includes all zones within radius R.

shown as $h_{(Z/2)}$ in Figure 2. The h in the T-line is the maximum elevation difference between the station and the outside radius of the zone in question and is shown as $h_{(T)}$ in both Figures 1 and 2.

The information in the Line $Z/2$ serves several purposes in estimating contributing effects and pointing out critical zones and slopes. It will be noted that, in general, the correction for one-half the D-zone $(Z/2)$ is greater than the entire correction through the C-zone for the same slope angle. This preponderant contribution by the D-zone to the total correction, within a radius of 558 ft of the

TABLE I

INCLINED-PLANE TERRAIN CORRECTIONS FOR HAMMER ZONES

Zone Compartments O.R. (ft) O.R. (cm)		A 1 6.56 200		B 4 54.6 1,664		C 6 175 5,334		D 6 558 17,008		E 8 1,280 39,014		F 8 2,936 89,489		G 12 5,018 152,949		H 12 8,578 261,457	
$\angle\theta^\circ$		h (ft)	mg $\times 10^{-2}$	h	mg $\times 10^{-2}$	h	mg $\times 10^{-2}$	h	mg $\times 10^{-2}$	h	mg $\times 10^{-2}$	h	mg $\times 10^{-2}$	h	mg $\times 10^{-2}$	h	mg $\times 10^{-2}$
1	T	0.1	0.0	1.0	0.0	3.1	0.0	9.7	0.1	22.3	0.3	51.3	0.5	87.6	1.2	149.8	2.1
	$Z/2$	0.1	—	0.9	—	2.1	—	6.6	—	12.6	0.1	29.0	0.2	36.3	0.3	62.2	0.5
2	T	0.2	0.0	1.9	0.0	6.1	0.1	19.5	0.5	44.7	1.0	102.5	2.4	175.2	4.1	299.5	7.0
	$Z/2$	0.2	—	1.7	—	4.2	—	13.4	0.2	25.2	0.3	57.8	0.7	72.7	0.8	124.3	1.5
3	T	0.3	0.0	2.9	0.1	9.2	0.3	29.2	1.0	67.1	2.3	153.9	5.3	263.0	9.0	449.6	15.3
	$Z/2$	0.3	—	2.6	—	6.3	0.1	20.0	0.3	37.9	0.6	86.8	1.5	109.1	1.9	186.6	3.2
4	T	0.5	0.0	3.8	0.2	12.2	0.5	39.0	1.7	89.5	4.0	205.3	9.1	350.9	15.5	599.9	26.5
	$Z/2$	0.5	—	3.3	0.1	8.4	0.2	26.8	0.6	50.5	1.1	115.8	2.6	145.6	3.2	249.0	5.5
5	T	0.6	0.0	4.8	0.3	15.3	0.9	48.8	2.7	112.0	6.3	256.9	14.3	439.0	24.5	750.5	41.9
	$Z/2$	0.6	—	4.2	0.1	10.5	0.3	33.5	0.9	63.2	1.8	144.9	4.0	182.1	5.1	311.5	8.7
6	T	0.7	0.0	5.7	0.4	18.4	1.2	58.6	3.9	134.5	9.0	308.6	20.5	527.4	35.1	901.5	60.0
	$Z/2$	0.7	—	5.0	0.2	12.7	0.4	40.2	1.3	75.9	2.5	174.1	5.8	218.8	7.3	374.1	12.5
7	T	0.8	0.1	6.7	0.5	21.5	1.7	68.5	5.3	157.2	12.1	360.5	27.7	616.1	47.3	1,053.2	80.9
	$Z/2$	0.8	—	5.9	0.2	14.8	0.6	47.0	1.8	88.7	3.4	203.3	7.8	255.6	9.8	437.1	16.8
8	T	0.9	0.1	7.7	0.7	24.6	2.2	78.4	7.0	180.0	16.0	412.6	36.8	705.2	62.8	1,205.6	107.4
	$Z/2$	0.9	—	6.8	0.3	16.9	0.8	53.8	2.4	101.6	4.5	232.6	10.4	292.6	13.0	500.4	22.3
9	T	1.0	0.1	8.7	0.9	27.7	2.8	88.4	8.9	202.7	20.4	465.0	46.8	794.8	80.0	1,358.6	136.7
	$Z/2$	1.0	—	7.6	0.4	19.1	1.0	60.7	3.1	114.3	5.8	262.3	13.2	329.8	16.6	563.8	28.4
10	T	1.2	0.1	9.6	1.1	30.9	3.4	98.4	11.0	225.7	25.0	517.7	57.3	884.8	97.9	1,512.6	167.4
	$Z/2$	1.2	—	8.5	0.5	21.3	1.2	67.5	3.8	127.3	7.0	292.0	16.2	367.1	20.3	627.8	34.7
11	T	1.3	0.2	10.6	1.3	34.0	4.1	108.5	13.2	248.8	30.2	570.7	69.2	975.4	118.4	1,667.4	202.3
	$Z/2$	1.3	—	9.3	0.6	23.4	1.4	74.5	4.5	140.3	8.5	321.9	19.5	404.7	24.6	692.0	42.0
12	T	1.4	0.2	11.6	1.5	37.2	4.9	118.6	15.7	272.1	36.0	624.1	82.6	1,066.6	141.2	1,823.3	241.4
	$Z/2$	1.4	—	10.2	0.7	25.6	1.7	81.4	5.4	153.5	10.2	352.0	23.3	442.5	29.3	756.7	50.1
13	T	1.5	0.2	12.6	1.8	40.4	5.8	128.8	18.4	295.5	42.3	677.8	96.9	1,158.5	165.7	1,980.4	283.2
	$Z/2$	1.5	—	11.1	0.8	27.8	2.0	88.4	6.3	166.7	11.9	382.3	27.3	480.7	34.4	821.9	58.8
14	T	1.6	0.3	13.6	2.1	43.6	6.7	139.1	21.4	319.1	49.1	732.0	112.7	1,251.1	192.6	2,138.8	329.3
	$Z/2$	1.6	—	12.0	0.9	30.0	2.3	95.5	7.4	180.0	13.9	412.9	31 8	519.1	40.0	887.7	68.3

TABLE I (*continued*)

Zone Compartments O.R. (ft) O.R. (cm)		A 1 6.56 200		B 4 54.6 1,664		C 6 175 5,334		D 6 558 17,008		E 8 1,280 39,014		F 8 2,936 89,489		G 12 5,018 152,949		H 12 8,578 261,457	
$\angle\theta^\circ$		h (ft)	mg $\times 10^{-2}$	h	mg $\times 10^{-2}$	h	mg $\times 10^{-2}$	h	mg $\times 10^{-2}$	h	mg $\times 10^{-2}$	h	mg $\times 10^{-2}$	h	mg $\times 10^{-2}$	h	mg $\times 10^{-2}$
15	T	1.8	0.3	14.6	2.4	46.9	7.7	149.5	24.6	343.0	56.4	786.7	129.4	1344.6	221.2	2298.5	378.1
	$Z/2$	1.8		12.9	1.0	32.3	2.7	102.6	8.4	193.5	15.9	443.7	36.5	557.9	45.9	953.9	78.5
16	T	1.9	0.3	15.7	2.7	50.2	8.8	160.0	28.0	367.0	64.3	841.9	147.6	1,438.9	252.2	2,459.7	431.1
	$Z/2$	1.9	0.1	13.8	1.2	34.5	3.0	109.8	9.6	207.0	18.2	474.9	41.7	597.0	52.3	1,020.8	89.5
17	T	2.0	0.4	16.7	3.1	53.5	9.9	170.6	31.7	391.3	72.7	897.6	166.7	1,534.2	284.8	2,622.6	486.9
	$Z/2$	2.0	0.2	14.7	1.4	36.8	3.4	117.1	10.9	220.7	20.5	506.3	47.0	636.6	59.6	1,088.4	101.0
18	T	2.1	0.4	17.7	3.5	56.9	11.1	181.3	35.5	415.9	81.4	954.0	186.7	1,630.4	319.1	2,787.2	545.5
	$Z/2$	2.1	0.2	15.6	1.6	39.2	3.8	124.4	12.2	234.6	22.9	538.1	52.7	676.4	66.2	1,156.8	113.2
19	T	2.3	0.5	18.8	3.9	60.3	12.4	192.1	39.7	440.7	91.0	1,011.0	208.7	1,727.8	356.7	2,953.7	609.7
	$Z/2$	2.3	0.2	16.5	1.7	41.5	4.3	131.8	13.7	248.6	25.7	570.3	58.9	716.8	74.0	1,225.9	126.5
20	T	2.4	0.5	19.9	4.3	63.7	13.8	203.1	44.0	465.9	101.0	1,068.6	231.6	1,826.4	395.8	3,122.1	676.6
	$Z/2$	2.4	0.2	17.5	1.9	43.8	4.8	139.4	15.1	262.8	28.5	602.7	65.3	757.8	82.1	1,295.7	140.4
21	T	2.5	0.6	21.0	4.8	67.2	15.2	214.2	48.6	491.3	111.4	1,127.0	255.5	1,926.2	436.6	3,292.8	746.4
	$Z/2$	2.5	0.3	18.5	2.1	46.2	5.2	147.0	16.7	277.1	31.4	635.7	72.1	799.2	90.6	1,366.6	154.9
22	T	2.7	0.6	22.1	5.2	70.7	16.7	225.4	53.4	517.2	122.4	1,186.2	280.8	2,027.4	480.0	3,465.8	820.3
	$Z/2$	2.7	0.3	19.4	2.3	48.6	5.8	154.7	18.4	291.8	34.5	669.0	79.2	841.2	99.6	1,438.4	170.2
23	T	2.8	0.7	23.2	5.7	74.3	18.3	236.9	58.5	543.3	134.1	1,246.2	307.5	2,130.0	525.6	3,641.1	898.5
	$Z/2$	2.8	0.3	20.4	2.5	51.1	6.3	162.6	20.1	306.4	37.8	702.9	86.7	883.8	109.1	1,511.1	186.4
24	T	2.9	0.7	24.3	6.2	77.9	20.0	248.4	63.7	569.9	146.1	1,307.2	335.2	2,234.2	572.9	3,819.2	979.4
	$Z/2$	2.9	0.4	21.4	2.8	53.6	6.9	170.5	21.9	321.5	41.2	737.3	94.6	927.0	118.9	1,585.0	203.3
25	T	3.1	0.8	25.5	6.8	81.6	21.7	260.2	69.3	596.9	158.8	1,369.1	364.3	2,339.9	622.7	4,000.0	1,064.5
	$Z/2$	3.1	0.4	22.4	3.0	56.1	7.5	178.6	23.8	336.7	44.8	772.2	102.8	970.8	129.2	1,660.1	220.9
26	T	3.2	0.9	26.6	7.3	85.4	23.5	272.2	75.1	624.3	172.2	1,432.0	394.9	2,447.4	674.9	4,183.7	1,153.8
	$Z/2$	3.2	0.4	23.4	3.2	58.8	8.1	186.8	25.8	352.1	48.6	807.7	111.4	1,015.4	140.0	1,736.3	239.5
27	T	3.3	1.0	27.8	7.9	89.2	25.4	284.3	81.0	652.2	185.9	1,496.0	426.4	2,556.8	728.8	4,370.7	1,245.9
	$Z/2$	3.3	0.5	24.5	3.5	61.4	8.8	195.1	27.8	367.9	52.5	843.8	120.3	1,060.8	151.2	1,813.9	258.6
28	T	3.5	1.0	29.0	8.5	93.0	27.4	296.7	87.3	680.6	200.3	1,561.1	459.4	2,668.1	785.1	4,561.0	1,342.1
	$Z/2$	3.5	0.5	25.5	3.8	64.0	9.5	203.7	29.9	383.9	56.5	880.5	129.6	1,107.0	162.8	1,892.9	278.5
29	T	3.6	1.1	30.3	9.2	97.0	29.5	309.3	93.9	709.5	215.5	1,627.5	494.2	2,781.5	844.7	4,754.9	1,444.0
	$Z/2$	3.6	0.5	26.7	4.0	66.7	10.2	212.3	32.2	400.2	60.8	918.0	139.4	1,154.0	175.3	1,973.4	299.7
30	T	3.8	1.2	31.5	9.8	101.0	31.5	322.2	100.6	739.0	230.7	1,695.1	529.1	2,897.1	904.3	4,952.5	1,545.8
	$Z/2$	3.8	0.6	27.7	4.3	69.5	10.8	221.2	34.6	416.8	65.0	956.1	149.2	1,202.0	187.6	2,055.4	320.8

T = total correction in milligals $\times 10^{-2}$ from station to the outer radius (O.R.) of the zone designated.
h = the maximum difference in elevation between the station and the outer radius of the zone.
Line $Z/2$ is the correction for one-half the zone in question. The h in the $Z/2$ line is the maximum difference in elevation between the inner and outer radius of the zone.

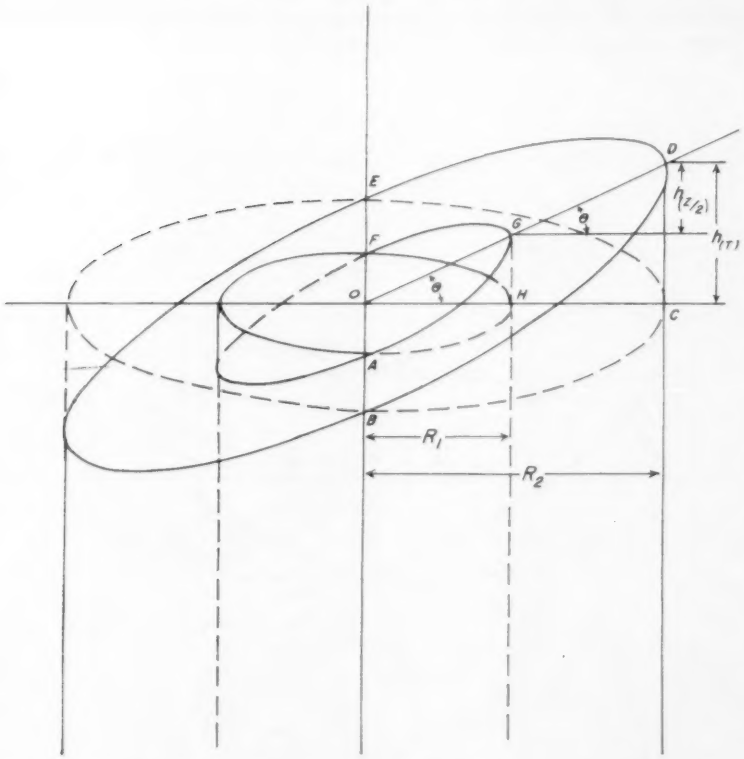

FIG. 2. An inclined plane through the station 0 intersecting the conventional cylindrical terrain-correction zone. R_1 is the inner radius and R_2 the outer radius of the zone. θ is the angle of inclination of the plane to the horizontal.

station, illustrates the critical nature of the D-zone. The sum of the $Z/2$ corrections—Zone A, through the zone in question—will be found to equal one-half the total correction (Line T) for the zone in question within rounding-off accuracy. Also, each $Z/2$ correction is equal to one-half of the increment in T from the next inner zone.

METHOD OF USING CHART

To use the inclined plane chart, a Hammer Chart template of proper map scale is centered over the station location on the topographic map. The elevation difference between the station and the outer radius of the zone for which an inclined plane is an acceptable terrain approximation is determined. Look in the h-column of the zone for the elevation in the T-line and read the correction.

FIG. 4. Two symmetrically-inclined planes intersecting a zonal cylinder through the station 0 approximating a symmetrical ridge for which the total correction is the same as that in Figure 1.

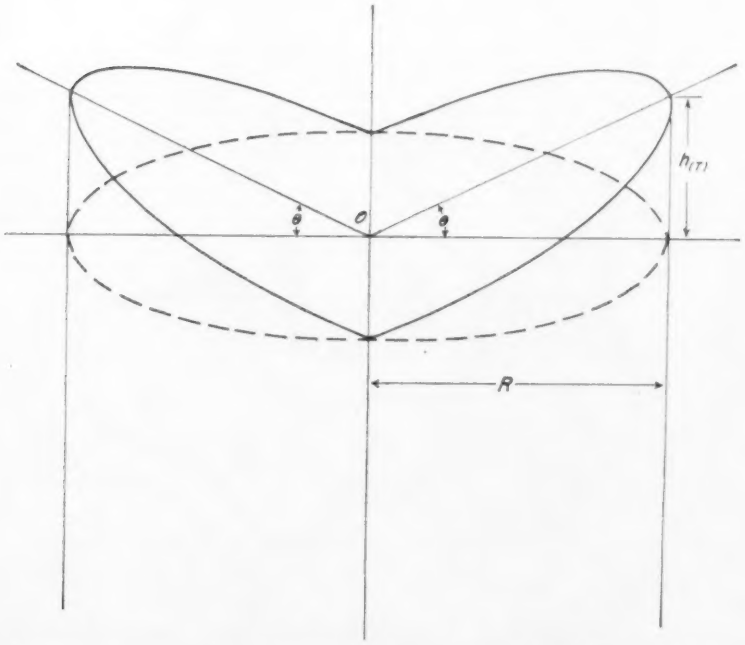

FIG. 3. Two symmetrically-inclined planes intersecting a zonal cylinder through the station 0, approximating a symmetrical valley for which the total correction is the same as that in Figure 1.

FIG. 5. Intersection of an inclined plane through the station 0 terminating on a horizontal line through the axis of the zonal cylinder for which the terrain correction is one-half the total correction illustrated in Figure 1. This is an approximation of a mountain slope intersecting a plain.

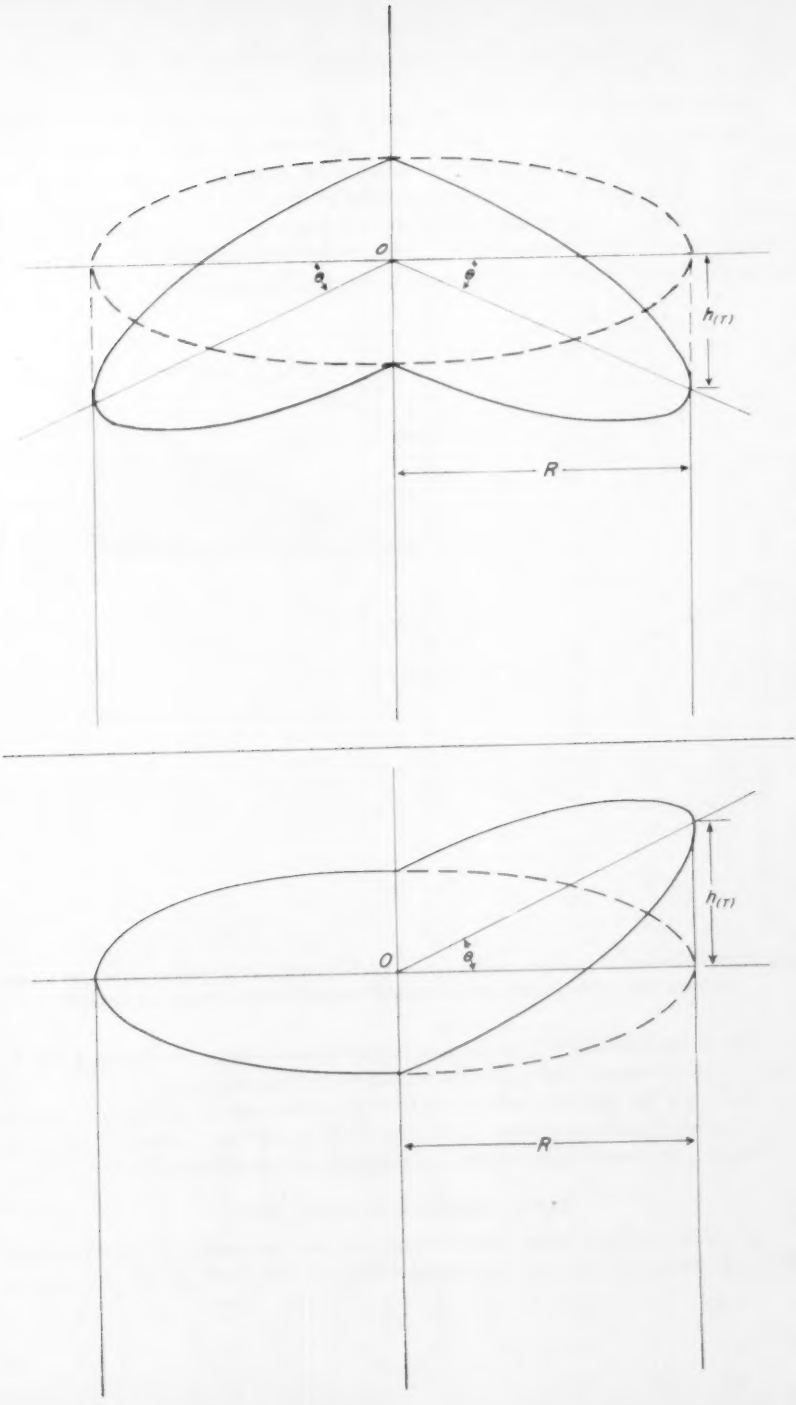
O
$\hat{e}_r$
$\hat{e}_\theta$
$h_{(T)}$
R
O
$\hat{e}_r$
$h_{(T)}$
R

As an illustration, we shall assume a hillside station such that Figure 1 applies and, further, that the dotted circle represents the outer boundary of the D-zone ($R=558$ ft). Now from the contours (or other means) we estimate the elevation difference h to be 150 ft. Referring to the chart in column h of Zone D we find $h=149.5$ ft for an angle of 15° for which the total correction for all the 17 compartments within the radius of 558 ft is 24.6×10^{-2} milligals. We then proceed to make the correction for the remaining zones in the usual way.

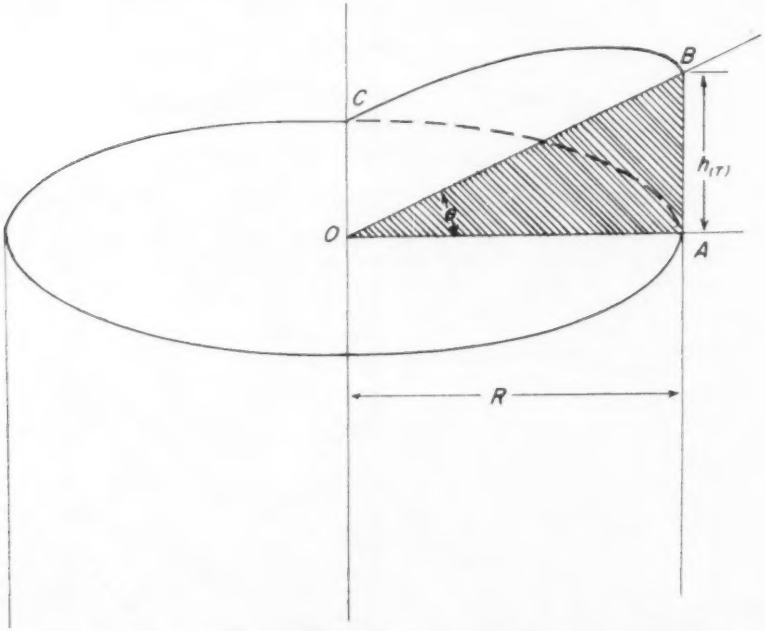

FIG. 6. One quadrant of the region resulting from the intersection of an inclined plane with a zonal cylinder. This is the smallest sector for which the inclined plane tables can be used.

The same total correction for land forms approximated by Figure 1 can be used for symmetrical land forms approximated by Figures 3 or 4.

The table can also be used for land forms approximated by Figures 5 and 6. For those forms approximated by Figure 5, the correction is one-half the total correction; for those approximated by Figure 6, one-quarter the total.

TABLES FOR HAYFORD-BOWIE ZONES

A similar inclined plane chart (Table II) for the modified Hayford-Bowie Zones A through G has also been prepared (Bowie, 1917). These are the zones in

Table II

Inclined-Plane Terrain Corrections for Hayford-Bowie Zones

Zone Compartments O.R. (ft)		A 1 6.56		B 4 223		C_1 4 427		C_2 4 755		D_1 6 1,247	
$\angle\theta°$		h'	mg×10⁻²	h'	mg×10⁻²	h'	mg×10⁻²	h'	mg×10⁻²	h'	mg×10⁻²
1	T	0.1	0.0	3.9	0.0	7.5	0.0	13.2	0.1	21.8	0.1
	$Z/2$	0.1	—	3.8	—	3.6	—	5.7	—	8.6	—
2	T	0.2	—	7.8	0.1	14.9	0.2	26.4	0.3	43.5	0.5
	$Z/2$	0.2	—	7.6	—	7.1	0.0	11.5	0.1	17.1	0.1
3	T	0.3	—	11.7	0.2	22.4	0.4	39.6	0.7	65.4	1.1
	$Z/2$	0.3	—	11.4	0.1	10.7	0.1	17.2	0.2	25.8	0.2
4	T	0.5	—	15.6	0.3	29.9	0.7	52.8	1.2	87.2	1.9
	$Z/2$	0.5	—	15.1	0.1	14.3	0.2	22.9	0.3	34.4	0.4
5	T	0.6	—	19.5	0.5	37.4	1.0	66.1	1.8	109.1	3.0
	$Z/2$	0.6	—	18.9	0.2	17.9	0.3	28.7	0.4	43.0	0.6
6	T	0.7	—	23.4	0.8	44.9	1.5	79.4	2.6	131.1	4.4
	$Z/2$	0.7	—	22.7	0.4	21.5	0.3	34.5	0.6	51.7	0.9
7	T	0.8	—	27.4	1.0	52.4	2.0	92.7	3.6	153.1	5.9
	$Z/2$	0.8	—	26.6	0.5	25.0	0.5	40.3	0.8	60.4	1.1
8	T	0.9	—	31.3	1.4	60.0	2.7	106.1	4.7	175.3	7.8
	$Z/2$	0.9	—	30.4	0.7	28.7	0.6	46.1	1.0	69.2	1.5
9	T	1.0	0.1	35.3	1.8	67.6	3.4	119.6	6.0	197.5	9.9
	$Z/2$	1.0	—	34.3	0.8	32.3	0.8	52.0	1.3	77.9	1.9
10	T	1.2	0.1	39.3	2.2	75.3	4.2	133.1	7.4	219.9	12.2
	$Z/2$	1.2	—	38.1	1.0	36.0	1.0	57.8	1.6	86.8	2.4
11	T	1.3	0.1	43.3	2.6	83.0	5.0	146.8	8.9	242.4	14.7
	$Z/2$	1.3	—	42.0	1.2	39.7	1.2	63.8	2.0	95.6	2.9
12	T	1.4	0.1	47.4	3.1	90.8	6.0	160.5	10.6	265.1	17.5
	$Z/2$	1.4	—	46.0	1.5	43.4	1.5	69.7	2.3	104.6	3.4
13	T	1.5	0.1	51.5	3.7	98.6	7.0	174.3	12.5	287.9	20.6
	$Z/2$	1.5	—	50.0	1.8	47.1	1.6	75.7	2.8	113.6	4.0
14	T	1.6	0.1	55.6	4.3	106.5	8.2	188.2	14.5	310.9	23.9
	$Z/2$	1.6	—	54.0	2.1	50.9	2.0	81.7	3.1	122.7	4.7
15	T	1.8	0.1	59.8	4.9	114.4	9.4	202.3	16.6	334.1	27.5
	$Z/2$	1.8	—	58.0	2.4	54.6	2.3	87.9	3.6	131.8	5.4
16	T	1.9	0.2	63.9	5.6	122.4	10.7	216.5	19.0	357.6	31.3
	$Z/2$	1.9	0.1	62.0	2.7	58.5	2.5	94.1	4.2	141.1	6.1
17	T	2.0	0.2	68.2	6.3	130.5	12.1	230.8	21.4	381.2	35.4
	$Z/2$	2.0	0.1	66.2	3.1	62.3	2.9	100.3	4.6	150.4	7.0
18	T	2.1	0.2	72.5	7.1	138.7	13.6	245.3	24.0	405.2	39.6
	$Z/2$	2.1	0.1	70.4	3.4	66.2	3.3	106.6	5.2	159.9	7.8
19	T	2.3	0.2	76.8	7.9	147.0	15.2	260.0	26.8	429.4	44.3
	$Z/2$	2.3	0.1	74.5	3.8	70.2	3.6	113.0	5.8	169.4	8.8
20	T	2.4	0.3	81.2	8.8	155.4	16.8	274.8	29.8	453.9	49.2
	$Z/2$	2.4	0.1	78.8	4.2	74.2	4.0	119.4	6.5	179.1	9.7
21	T	2.5	0.3	85.6	9.7	163.9	18.6	289.8	32.8	478.7	54.2
	$Z/2$	2.5	0.1	83.1	4.7	78.3	4.4	125.9	7.1	188.9	10.7
22	T	2.7	0.3	90.1	10.6	172.5	20.4	305.0	36.1	503.8	59.6
	$Z/2$	2.7	0.1	87.4	5.2	82.4	4.9	132.5	7.8	198.8	11.8
23	T	2.8	0.3	94.7	11.7	181.2	22.3	320.5	39.5	529.3	65.3
	$Z/2$	2.8	0.1	91.9	5.7	86.5	5.3	139.3	8.6	208.8	12.9
24	T	2.9	0.4	99.3	12.7	190.1	24.4	336.1	43.1	555.2	71.2
	$Z/2$	2.9	0.2	96.4	6.1	90.8	5.8	146.0	9.4	219.1	14.1
25	T	3.1	0.4	104.0	13.8	199.1	26.5	352.1	46.8	581.5	77.4
	$Z/2$	3.1	0.2	100.9	6.7	95.1	6.4	153.0	10.2	229.4	15.3
26	T	3.2	0.4	108.8	15.0	208.3	28.7	368.2	50.8	608.2	83.9
	$Z/2$	3.2	0.2	105.6	7.3	99.5	6.8	159.9	11.1	240.0	16.5
27	T	3.3	0.5	113.6	16.2	217.6	31.0	384.7	54.8	635.4	90.6
	$Z/2$	3.3	0.2	110.3	7.8	104.0	7.4	167.1	11.9	250.7	17.9
28	T	3.5	0.5	118.8	17.4	227.0	33.4	401.4	59.1	663.0	97.5
	$Z/2$	3.5	0.3	115.3	8.5	108.2	8.0	174.4	12.8	261.6	19.2
29	T	3.6	0.6	123.6	18.7	236.7	35.9	418.5	63.5	691.2	104.9
	$Z/2$	3.6	0.3	120.0	9.0	113.1	8.6	181.8	13.8	272.7	20.7
30	T	3.8	0.6	128.7	20.1	246.5	38.4	435.9	68.0	720.0	112.4
	$Z/2$	3.8	0.3	124.9	9.8	117.8	9.6	189.4	14.8	284.1	22.2

TABLE II.—(*Continued*)

D_2 6 1,936		E_1 8 2,854		E_2 8 4,200		F_1 10 5,512		F_2 10 7,513		G 12 11,549	
h'	mg$\times10^{-2}$	h'	mg$\times10^{-2}$	h'	mg$\times10^{-2}$	h'	mg$\times10^{-2}$	h'	mg$\times10^{-2}$	h'	mg$\times10^{-2}$
33.8	0.2	49.8	0.2	73.3	0.3	96.2	0.4	131.2	0.6	201.6	0.9
12.0	0.0	16.0	0.0	23.5	0.1	22.9	0.1	35.0	0.1	70.4	0.2
67.6	0.8	99.7	1.2	146.7	1.7	192.5	2.2	262.4	3.1	403.3	4.5
24.1	0.1	32.1	0.2	47.0	0.2	45.8	0.3	69.9	0.5	140.9	0.7
101.5	1.7	149.6	2.6	220.1	3.8	288.9	4.9	393.8	6.7	605.3	10.3
36.1	0.3	48.1	0.5	70.5	0.6	68.8	0.6	104.9	0.9	211.5	1.8
135.4	3.0	199.6	4.4	293.7	6.5	385.5	8.5	525.4	11.6	807.6	17.8
48.2	0.5	64.2	0.7	94.1	1.0	91.8	1.0	139.9	1.5	282.2	3.1
169.4	4.7	249.7	7.0	367.5	10.2	482.2	13.4	657.3	18.3	1,010.4	28.2
60.3	0.9	80.3	1.1	117.8	1.6	114.7	1.6	175.1	2.5	353.1	5.0
203.5	6.8	300.0	10.0	441.4	14.7	579.3	19.3	789.6	26.3	1,213.8	40.4
72.4	1.2	96.5	1.6	141.4	2.3	137.9	2.3	210.3	3.5	424.2	7.0
237.7	9.1	350.4	13.5	515.7	19.8	676.8	26.0	922.4	35.4	1,418.0	54.5
84.6	1.6	112.7	2.2	165.3	3.1	161.1	3.1	245.6	4.7	495.6	9.6
272.1	12.1	401.1	17.9	590.3	26.3	774.7	34.5	1,055.9	47.0	1,623.1	72.3
96.8	2.1	129.0	2.9	189.2	4.2	184.4	4.1	281.2	6.3	567.2	12.7
306.6	15.4	452.0	22.7	665.2	33.5	873.0	43.9	1,189.9	59.9	1,829.1	92.0
109.1	2.8	145.4	3.7	213.2	5.4	207.8	5.2	316.9	8.0	639.2	16.0
341.4	18.9	503.2	27.9	740.6	41.0	971.9	53.8	1,324.8	73.3	2,036.4	112.7
121.5	3.4	161.8	4.5	237.4	6.6	231.3	6.4	352.9	9.8	711.6	19.7
376.3	22.8	554.8	33.7	816.4	49.5	1,071.4	65.0	1,460.4	88.6	2,244.9	136.2
133.9	4.0	178.5	5.5	261.6	7.9	255.0	7.8	389.0	11.8	781.5	23.8
411.5	27.2	606.6	40.2	892.8	59.1	1,171.6	77.5	1,597.0	105.7	2,454.9	162.5
146.4	4.9	195.1	6.5	286.2	9.5	278.8	9.2	425.4	14.1	857.9	28.4
447.0	32.0	658.9	47.1	969.7	69.3	1,272.6	91.0	1,734.5	124.0	2,666.3	190.7
159.1	5.7	211.9	7.6	310.8	11.1	302.9	10.9	461.9	16.5	931.8	33.3
482.7	37.1	711.6	54.8	1,047.2	80.6	1,374.3	105.8	1,873.2	144.2	2,879.5	221.7
171.8	6.6	228.9	8.8	337.6	12.9	327.1	12.6	498.9	19.2	1,006.3	38.8
518.8	42.7	746.7	62.9	1,125.4	92.5	1,476.9	121.5	2,013.1	165.6	3,094.6	254.5
184.7	7.6	227.9	10.1	378.7	14.8	351.5	14.5	536.2	22.1	1,081.5	44.4
555.1	48.6	818.4	71.7	1,204.4	105.5	1,580.6	138.5	2,154.4	188.8	3,311.7	290.2
197.5	8.6	263.3	11.6	386.0	16.9	376.2	16.5	573.8	25.2	1,157.3	50.7
591.9	54.9	872.6	81.0	1,284.1	119.2	1,685.2	156.4	2,296.9	213.2	3,530.9	327.8
210.7	9.8	280.7	13.0	411.5	19.1	401.1	18.6	611.7	28.4	1,234.0	57.3
629.0	61.5	927.3	90.8	1,364.7	133.5	1,791.0	175.2	2,441.1	238.9	3,752.5	367.2
223.8	10.9	298.3	14.6	437.4	21.4	426.3	20.8	650.1	31.9	1,311.4	64.2
666.6	68.8	982.7	101.4	1,448.2	149.2	1,897.9	195.9	2,587.0	267.0	3,976.7	410.4
237.2	12.2	316.1	16.3	465.5	23.9	449.7	23.4	689.1	35.6	1,389.7	71.7
704.6	76.3	1,038.8	112.6	1,528.7	165.6	2,006.2	217.4	2,734.5	296.3	4,203.5	455.5
250.7	13.6	334.2	18.2	489.9	26.5	477.5	25.9	728.3	39.5	1,469.0	79.6
743.2	84.2	1,095.5	124.2	1,612.2	182.7	2,115.8	239.8	2,883.9	326.9	4,433.2	502.5
264.5	15.0	352.3	20.0	516.7	29.2	503.6	28.6	768.1	43.6	1,549.3	87.8
782.2	92.6	1,153.1	136.5	1,696.9	200.8	2,227.0	263.5	3,035.5	359.3	4,666.1	552.2
278.4	16.5	370.9	21.9	543.8	32.2	530.1	31.4	808.5	47.9	1,630.0	96.4
821.8	101.4	1,211.4	149.5	1,782.8	219.9	2,339.7	288.6	3,189.0	393.5	4,902.2	604.8
292.5	18.1	389.6	24.0	571.4	35.2	556.9	34.4	849.3	52.4	1,723.2	105.7
862.0	110.5	1,270.7	162.9	1,870.0	239.7	2,454.1	314.6	3,345.0	428.9	5,142.0	659.3
306.8	19.6	408.7	26.2	599.3	38.4	584.1	37.4	890.9	57.2	1,797.0	115.2
902.8	120.1	1,330.8	177.1	1,958.5	260.6	2,570.3	342.0	3,503.4	466.2	5,385.4	716.6
321.3	21.3	428.0	28.5	627.7	41.7	611.8	40.7	933.1	62.1	1,882.0	125.2
944.2	130.2	1,392.0	191.9	2,048.5	282.4	2,688.4	370.7	3,664.3	505.3	5,632.8	776.7
336.0	23.1	447.8	30.8	656.5	45.3	639.9	44.2	975.9	67.3	1,968.5	135.7
986.5	140.6	1,454.2	207.3	2,140.0	305.0	2,808.5	400.2	3,828.1	545.6	5,884.6	838.7
351.1	25.0	467.7	33.4	685.8	48.8	668.5	47.6	1,019.6	72.7	2,056.5	146.6
1,029.4	151.4	1,517.5	223.3	2,233.2	328.5	2,930.8	431.2	3,994.7	587.8	6,140.7	903.5
366.4	26.9	488.1	35.9	715.7	52.6	697.6	51.4	1,065.9	78.3	2,146.0	157.8
1,073.1	162.9	1,582.0	240.2	2,328.1	353.5	3,055.4	463.9	4,164.5	632.4	6,401.7	972.1
381.9	29.0	508.9	38.6	746.1	56.8	727.3	55.2	1,109.1	84.2	2,237.2	169.8
1,117.7	174.4	1,647.8	257.2	2,424.9	378.4	3,182.4	496.6	4,337.6	677.0	6,667.8	1,040.6
397.7	31.0	530.1	41.4	777.1	60.6	757.5	59.1	1,155.2	90.2	2,330.2	181.8

common use by the U. S. Coast and Geodetic Survey in their studies in geodesy and isostasy. No correction for the earth's curvature or isostasy is made in either table, and, where such correction is necessary, it can be done by the method outlined in U. S. Coast and Geodetic Survey Special Publication 232 (Swick, 1942).

In the Hayford-Bowie Chart, a density (δ) of one gm per cm^3 was used; hence any correction taken from this chart must be multiplied by the applicable density; both charts are otherwise used in the same way.

CONCLUSIONS

There are many ways in which an inclined plane can be used to increase the accuracy and speed up the work in making terrain corrections. A few of the more obvious applications have been presented with the hope that these may assist in relieving the strain and tedium.

REFERENCES

Bowie, William, 1917, Investigation of gravity and isostasy: U. S. Coast and Geodetic Survey Special Publication No. 40, p. 9.

Hammer, Sigmund, 1939, Terrain corrections for gravimeter stations: Geophysics, v. 4, p. 184–194.

Swick, Clarence H., 1942, Pendulum gravity measurements and isostatic reductions: U. S. Coast and Geodetic Survey Special Publication No. 232, p. 67.

GEOPHYSICS, VOL. XXIII, NO. 4 (OCTOBER, 1958), PP. 712—725, 2 FIGS.

PARA- AND DIAMAGNETIC SUSCEPTIBILITIES IN NON-FLUCTUATING WEAK FIELDS*

WILLIAM SCHRIEVER†

ABSTRACT

A Coulomb torsion balance apparatus was developed with which absolute measurements of para- and diamagnetic susceptibilities could be made in non-fluctuating field strengths of the order of 1 oersted. Solid specimens of the diamagnetic elements, bismuth, antimony, and cadmium, were measured in fields of 2.5, 5, and 10 oersteds, and the para-magnetic powders, $FeCl_3$, $FeSO_4+7H_2O$, and $Co_2(SO_4)_3+7H_2O$, in fields of 2, 3, and 5 oersteds. The susceptibilities decreased with increasing field strengths. A specimen of bismuth granules had lower susceptibilities than did the solid specimen made from the same supply of granules.

A semi-micro balance apparatus also was constructed for absolute measurements in fields ranging between 100 and 1,000 oersteds. The susceptibilities of the diamagnetic specimens and a water specimen were measured. The solid bismuth, antimony, and cadmium specimens and a water specimen exhibited constant susceptibilities. The susceptibility of the bismuth-granule specimen increased regularly from -4.67 to -7.87×10^{-6} C.G.S. when the field increased from 100 to 900 oersteds. The value found for water (-0.73×10^{-6}) agreed well with the International Critical Tables value (-0.72×10^{-6} C.G.S.).

INTRODUCTION

It is well known that the magnetic susceptibilities of ferro-magnetic rocks depend both on the field strength in which the measurements are made and on the grain-size of the powder or granule specimen. Recent results are reported by Nagato (1953) in his book on rock magnetism. Earlier results were reported by Slichter (1929).

Measurements on strictly para- and diamagnetic substances are commonly carried out in strong, steady fields or in alternating fields. Even the susceptibilities for relatively strongly magnetic rocks, reported by Nagato (1953) and by Sharpe (1953), were obtained in weak, alternating fields.

In magnetic prospecting we are interested in the values of the susceptibilities which apply when the solid substances are acted on by the weak, steady field of the earth. It apparently remains to be shown that the magnetic susceptibilities of para- and diamagnetic substances are the same when measured in weak (1 oersted) and strong (1,000 oersted) fields, and when measured in weak, steady and weak, alternating fields.

When we first considered this problem of measuring strictly para- and diamagnetic susceptibilities in weak fields, we expected to apply some standard method that had been employed in the study of pure elements and compounds to a large number of samples of rock specimens. We were astonished to find that (with one exception) the magnetic susceptibilities of pure diamagnetic and paramagnetic elements and compounds had never been measured in non-fluctuating fields as weak as a few oersteds.

* Paper read at the 11th Annual Midwestern Meeting at Tulsa on April 17, 1958. Manuscript received by the Editor April 1, 1958.

†University of Oklahoma, Norman, Oklahoma.

We decided, therefore, to devise a method and an apparatus that would yield the desired data and to make such susceptibility determinations on a few pure elements and compounds.

Steady-field methods for measuring para- and diamagnetic susceptibilities are based on the fact that a force acts on a specimen of the substance when it is placed in a non-uniform magnetic field; the force on a paramagnetic specimen urges it in the direction of the gradient of the field whereas the force on a diamagnetic specimen urges it in the opposite direction. The force on a spherical para- or diamagnetic specimen is given by Stoner (1926) as

$$F_x = KVH_x \frac{\partial H_x}{\partial x}, \tag{1}$$

where

F_x is the force in the x direction,

K is the volume magnetic susceptibility of the specimen,

V is the volume of the spherical specimen,

H_x is the component of the field strength in the x-direction at the center of the specimen, and $\partial H_x/\partial x$ is the gradient of the x-component of the field at center of the specimen.

This expression is a close approximation to the correct expression; it does not, of course, take into account any force caused by a permanent magnetization of the specimen.

It is to be noted that the magnetization induced in a para- or a diamagnetic specimen by the applied field is so very small that the values of H_x and $\partial H_x/\partial x$ can be taken as those of the applied field when the specimen is absent.

The force that acts on a specimen of practical size in a field of 1,000 oersteds is very small. Since, in a field caused by an electric current, $\partial H_x/\partial x$ is proportional to H_x, the force, F_x, is proportional to H_x^2. Thus, when a thousand-oersted field of a given form is reduced to one oersted, this small force is reduced by a factor of 10^{-6}.

McKeehan (1929), in his comprehensive survey of methods of magnetic measurements, indicates that the torsion-balance method of Shaw and Hayes (1916) is the most sensitive ever used. They found the volume susceptibility of a silver specimen in fields of 1 to 12 oersteds to be $+0.256\times10^{-6}$ C.G.S., whereas the International Critical Tables value is -2.1×10^{-6} C.G.S. No doubt the latter was determined in a relatively strong field. Most likely the positive value observed by Shaw and Hayes was caused by the presence of a very small amount of metallic iron on the silver specimen, such as that which would be left by a steel-cutting tool.

This work of Shaw and Hayes showed that the forces, that must be measured in order to determine para- and diamagnetic susceptibilities in fields of the order of one oersted, will require a Coulomb-type torsion balance. The design of a suitable balance requires a knowledge of the actual magnitude of the force, and this, in turn, depends on the value of $\partial H_x/\partial x$ for $H_x=1$ oersted.

We concluded that a magnetic field of the proper form could be provided most conveniently by an electric current in a suitable coil, since both H_x and $\partial H_x/\partial x$ could be calculated from the current and the geometry of the coil.

THE APPARATUS

The Magnetizing Coil

The investigation of the forms of the field generated by five different types of coils led to the conclusion that the best form of coil was the nearest equivalent to a single circular turn. The desired values of H_x and the product,

$$H_x \frac{\partial H_x}{\partial x}$$

could be obtained, the location of the point on the axis where the product, and, therefore, the force, was a maximum, and the range over which this product was nearly constant could all be regulated by a proper choice of the diameter of the coil.

The form of the coil is shown schematically in Figure 1. The actual section of the wire-filled space was 1.30 cm wide by 1.11 cm high, and the inside diameter was 19.93 cm. The coil contained 266 turns of double cotton-covered No. 24 gauge copper wire. The field caused by a current, i, through such a coil of N turns may be obtained in the following way.

The field, at a point $x=S$, due to a current filament $dy\,dx$ of radius y at a distance x from the center, is given by

$$dH_x = \frac{\pi N i y^2 dy dx}{C(B-A)\left[(S-x)^2+y^2\right]^{3/2}}. \tag{2}$$

When this expression is integrated from $x=C$ to $x=-C$ and from $y=A$ to $y=B$, one obtains for the field at point $x=S$

$$H_x = \frac{\pi N i}{C(B-A)}\left[(C-S)\ln\frac{B+\sqrt{(C-S)^2+B^2}}{A+\sqrt{(C-S)^2+A^2}} + (C+S)\ln\frac{B+\sqrt{(C+S)^2+B^2}}{A+\sqrt{(C+S)^2+A^2}}\right]. \tag{3}$$

The value of the gradient at $x=S$ is given by

$$\frac{\partial H_x}{\partial x}=\frac{\pi N i}{C(B-A)}\left[\ln\frac{(B+\sqrt{(C+S)^2+B^2})(A+\sqrt{(C-S)^2+A^2})}{(A+\sqrt{(C+S)^2+A^2})(B+\sqrt{(C-S)^2+B^2})} + \frac{B}{\sqrt{(C-S)^2+B^2}}-\frac{B}{\sqrt{(C+S)^2+B^2}}-\frac{A}{\sqrt{(C-S)^2+A^2}}+\frac{A}{+\sqrt{(C+S)^2+A^2}}\right]. \tag{4}$$

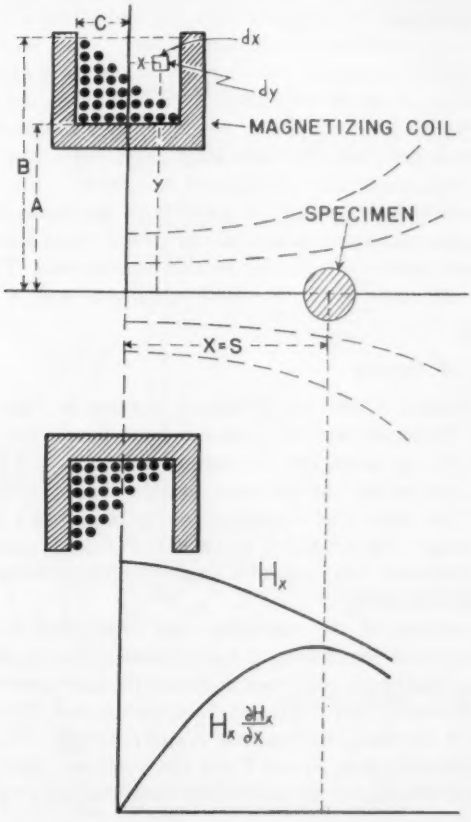

FIG. 1. The magnetizing coil. The spherical specimen was placed at the point where the force on the specimen was a maximum.

Calculations for this coil showed that the broad maximum of the product,

$$H_x \frac{\partial H_x}{\partial x}$$

occurred at the point $x=S=4$ cm. This value of S was sufficiently large to permit suspending the specimen in an evacuated case at the point where the maximum force acted on the specimen.

The curves showing H_x and

$$H_x \frac{\partial H_x}{\partial x}$$

as functions of x also appear in Figure 1.

Calculations were made with equations (1), (3), and (4) for a specimen having a volume of 1 cm^3 and a volume susceptibility of 10^{-6} C.G.S. unit. These showed that the force on such a specimen, when located at the point of maximum force in a field of 5 oersteds, would be only about 2.5×10^{-6} dynes. An appreciation of the magnitude of such a small force may be gained by a simple calculation. If a metal filament were so fine that a 620-mile length of it had a mass of 1 gm, then 1 mm of such a filament would have a weight of 10^{-6} dyne.

This force cannot be increased by the use of large specimens since the torsion constant of a suspension increases as the nth power of its breaking strength, where $n=2$ for a suspension of circular section for example. Thus, to achieve great sensitivity, one must resort to small specimens and a very fine, long suspension.

The Coulomb Torsion Balance

A schematic diagram of the torsion balance is shown in Figure 2. The beam, supported by the ribbon suspension, is shown in an evacuated brass case. The bulbs surrounding the specimen and the counter weight were of pyrex glass. The fine copper wires supporting the specimen and the counter weight were 15 cm from the center of the beam. The suspension for the beam was a phospher-bronze ribbon 101.5 cm long, 0.001 mm thick, and 0.40 mm wide. It could safely carry a load of 125 gm. The beam was made of a strip of heavy aluminum foil bent into the shape of a right-angled "U."

The torsion constant of the suspension was determined by measuring the period of torsional oscillation of each of two cylinders. The approximate mass of each cylinder was equal to the combined masses of the beam, specimen, and counter-weight. The diameters and lengths of the cylinders were different. If I is the rotational inertia of the clamp with mirror, I_1 and I_2 are the calculated rotational inertias of the added cylinders, T_1 and T_2 are the respective periods of oscillation, and k is the torsion constant of the suspension, then k is given by

$$k = 4\pi^2(I_1 - I_2)/(T_1^2 - T_2^2), \tag{5}$$

a well-known relation that is derived from the angular harmonic motion equation. The torsion constant of the suspension was found to be 0.0914 dyne cm/radian.

The upper end of the suspension was attached to a large brass torsion head which could be rotated in a vacuum-tight, greased ground cone joint. The rod to which the suspension was attached could be raised and lowered through a vacuum-tight packing by means of a screw. These two motions made it possible to take the beam off arrestment and to turn it into a central zero position.

The balance case was mounted in a large, triangular wooden frame that was assembled with brass screws. A $\frac{3}{4}$-inch diameter threaded brass leveling screw passed through the base of the frame near each of the three uprights. These screws passed through large holes in the floor of the room and rested on three concrete piers that stood on solid earth under the building. The balance was

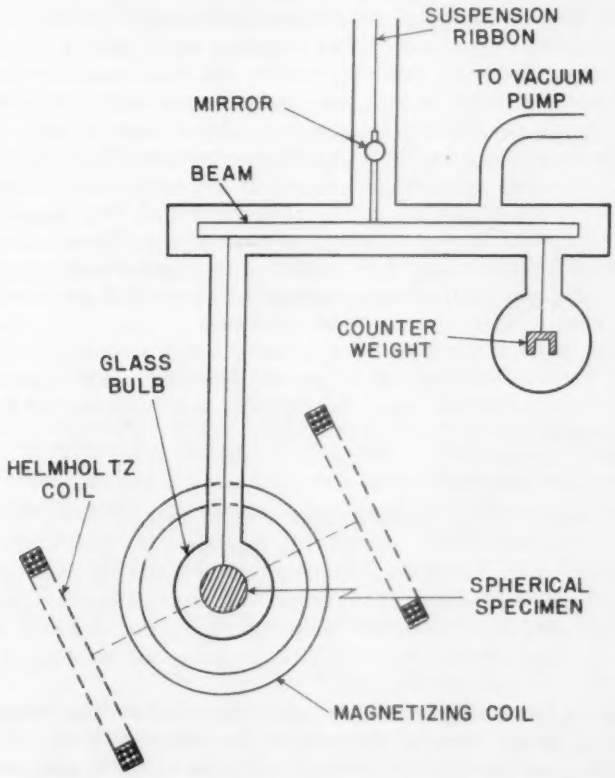

FIG. 2. The Coulomb torsion balance apparatus. The earth's field was neutralized with the Helmholtz coils.

found to be usable except when winds caused neighboring trees to shake the ground.

The Helmholtz Coils

The earth's magnetic field in the neighborhood of the specimen was neutralized by means of a set of Helmholtz coils, which are shown in Figure 2. The orientation of the coils, and the determination of the proper current for neutralizing the earth's field, was achieved by use of a dip-needle and a sensitive suspended set of compass needles mounted on the back of a galvanometer mirror.

Stabilizing the Suspension

A test of the balance revealed that the beam did not have a steady zero-posi-

tion. It continued to wander about in a random fashion. Preliminary tests on a copper suspension showed that proper annealing would remove this difficulty. There were two effects that needed correction. One was the continual drift, and the other was the change of zero position with temperature. If the annealing temperature were too high the second effect would not be corrected.

We also found that we could not handle a suspension sufficiently carefully to install a thoroughly stabilized suspension in the apparatus without causing further instability of the suspension. The phosphor-bronze suspension was annealed by passing an electric current through it while it was in place in the case under the operating load. A 0.5-ampere current was passed through it for 5 hours and this was then gradually reduced to zero over a period of 6 hours. This treatment resulted in a very stable suspension.

The deflections of the beam were determined with a conventional telescope and scale. The scale distance was 317 cm, and deflections could be determined to within 0.5 mm on the scale which corresponded to a beam rotation of approximately 17 sec of arc.

Extraneous Forces on the Specimen

Early work with this torsion balance revealed that the beam had a strong affinity for the sides of the case. Electric charges on the glass bulbs were suspected as the cause. A little uranium oxide powder inside the glass bulbs ionized the air and removed the charges on the inside. It was also necessary, however, to coat the outsides of the bulbs with a conducting layer of Aquadag (a colloidal graphite) and to connect this coating to the brass case in order to eliminate electrostatic effects completely.

When the magnetizing coil (no current) was set into position, or any metallic object was brought near the specimen or counter-weight flask, the beam deflected. This was corrected by connecting the brass coil-form of the magnetizing coil to the brass case and grounding them to a water-pipe.

After the current had passed through the magnetizing coil for a time, the beam would not return to its former zero-deflection when the current was reduced to zero. The coil and its form felt slightly warm to the hand. It was found that any warm object, like a can of warm water, would deflect the balance.

This "heat deflection" could not be eliminated, so it had to be measured. This was accomplished by winding the magnetizing coil with two parallel wires. These two independent windings were connected so that they produced the required magnetic field by passing the same current through both windings. After the coil had reached temperature equilibrium, the deflection was read. Then the current in one winding was reversed, so there was no net magnetic field, and the remaining deflection was that caused by the heat effect alone. The algebraic difference of these deflections was that caused by the magnetic field alone.

It was found that leaks in the vacuum system made it impossible to obtain satisfactory data. When the pressure in the case was reduced to a few millimeters

of mercury, a leak of 1 mm in 6 hours was just tolerable. The effect of a leak of 1 mm in 24 hours was not detectable. Most of the results were obtained when the leak was only 1 mm in 4 to 6 days.

Vibrations, caused by small motor trucks passing the building where the apparatus was set up, disturbed the balance. Fortunately, this seldom happened.

Temperature gradients in the room evidently caused temperature differences between different parts of the case that surrounded the beam of the balance, and these in turn caused the air in the case to convect and thus to disturb the balance. This effect was reduced to tolerable dimensions by caulking the windows of the room and by covering the balance case with a thick layer of hair felt. It was also found advantageous to work late at night while the outdoor temperatures were changing relatively slowly.

Mislocation Errors

The center of a specimen could be located at the point of maximum force with a precision of about ± 1 mm. To test the effect of such a mislocation, the bismuth specimen was moved along the axis 1 cm from the point of maximum force and also 1 cm perpendicular to the axis from that point. The force was measured in each of these positions. The results showed that a few millimeters off the axis would cause an entirely negligible effect, and that a one-millimeter displacement along the axis would cause an error of only about one percent. Thus the proper location of a specimen in the magnetizing field did not pose a serious problem.

THE SPECIMENS

Solid specimens of bismuth, antimony, and cadmium were prepared from granules of the pure metals. A spherical glass bulb having a volume of approximately 1.5 cm^3 was blown on the end of a pyrex tube of 3 mm bore. Sufficient granules of the metal were melted in the bulb to fill it and, in addition, a short length of stem. This was permitted to cool slowly so that the specimen would be solid. Then the glass was cracked off the specimen. The short stem on the specimen was removed with flint sandpaper.

Since molten cadmium oxidizes very rapidly in air, this specimen was prepared in vacuum. The metal was distilled from a small flask into the spherical bulb.

Specimens of powders (or granules) of bismuth, $FeCl_3$,$FeSO_4+7H_2O$, and $Co_2(SO_4)_3+7H_2O$ were made by filling spherical glass bulbs, having a volume of approximately 1.5 cm^3, with these materials.

Great care was taken not to touch any specimen with a steel tool, since a trace of metallic iron might be left on it. Even such a trace of iron can cause a much larger magnetic effect than the whole of the specimen. For example, the neck of one bismuth specimen was cut off with a pocket knife. The trace of iron rubbed off the knife blade caused this specimen to change from a diamagnetic body to one that acted paramagnetically.

PROCEDURE

The specimen and an appropriate counter-weight of wire solder were suspended from the balance beam, the glass bulbs were put into place on their greased ground joints, the case was evacuated until the manometer indicated a pressure of a few millimeters of mercury, the stopcock in the vacuum line was closed, and the pump was stopped. The torsion head was adjusted so that the balance beam oscillated about a central position in the case. The period of the balance was between 20 and 30 minutes; the period was determined by the mass of the specimen.

The magnetizing coil was moved into proper position and the appropriate currents were passed through both the Helmholtz and the magnetizing coils; the windings on the latter were connected non-inductively so that they produced no net magnetic field. The balance deflected because of the effect of the "heat radiation" from the magnetizing coil. In about an hour the deflection became steady and, after it had remained so for 10 to 15 minutes, this deflection was recorded as the heat deflection.

The windings of the magnetizing coil then were connected inductively, so they produced the desired field. A new steady deflection resulted and, after it had existed for 10 to 15 minutes, it was recorded as the deflection caused by magnetization of the specimen plus the heat deflection.

The windings were connected non-inductively again, and the heat deflection was redetermined to make certain that temperature equilibrium had actually existed.

The deflection due to the magnetization alone was the algebraic difference of the two deflections. For bismuth in a field of 10 oersteds for example, this was 0.0222 radian.

The data for the powder specimens were corrected for the forces that acted on the glass bulbs alone. These forces were measured before the bulbs were filled.

The force that acted on the specimen was computed from the experimentally-determined torsion constant, and then the volume magnetic susceptibility was calculated by use of equations (1), (3), and (4).

As was expected, no change in deflection was caused by reversing the magnetic field. This showed that no specimen had a permanent or residual magnetic moment. The solid specimens exhibited the same forces for different orientations of the specimens. This indicated that the specimens were isotropic.

RESULTS

The final results are shown in Table I. Also included in the table are the International Critical Tables values of the susceptibilities and the values obtained with another apparatus, described below, in fields ranging between 100 and 1,000 oersteds.

Some Comments

It is observed from Table I that the susceptibilities of five of the seven specimens decreased as the field-strength increased. For solid bismuth, the value at 5 oersteds was greatest, and that at 10 oesteds was least. For the cobalt salt, the lowest value occurred at two oersteds, and the highest at three oersteds. These peculiarities are not due to experimental errors; all data were checked several times to make certain that they were characteristic of the specimens.

TABLE I

OBSERVED MAGNETIC SUSCEPTIBILITIES

Substance	Vol. (cm^3)	Mass (gm)	Vol. Suscept. K in 10^{-6} pole/cm^2 oersteds				
			2.5 oers.	5.0 oers.	10 oers.	I.C.T.	100 to 1,000 oers.
Bismuth (solid)	1.32	12.87	−10.90	−11.20	−10.66	−13.78	−12.37
Antimony (solid)	1.55	9.61	− 4.45	− 3.89	− 3.10	− 5.75	− 4.71
Cadmium (solid)	1.59	13.78	—	− 0.90	− 0.63	− 1.56	− 1.15
Bismuth (granules)	0.99	9.70	− 9.78	− 7.65	− 7.13	—	− 4.67 to − 7.87
Water	2.28	2.28	—	—	—	− 0.72	− 0.73
Powder			2.0 oers.	3.0 oers.	5.0 oers.		
$FeCl_3$	0.43	1.20	153.	148.	140.	240.	—
$FeSO_4+7H_2O$	0.51	0.96	78.5	77.7	75.0	79.0	—
$Co_2(SO_4)_3+7H_2O$	0.44	0.85	69.5	79.8	75.0	72.5	—

Under "I.C.T." are listed the values given in the International Critical Tables. Under "100 to 1,000 oers." are listed values obtained with the semi-micro balance apparatus. At 1 oersted $FeCl_3$ had a susceptibility of 159×10^{-6} C.G.S.

The observed decreases in susceptibilities with increase in field strength are far greater than the experimental errors; the variations are real. For the larger susceptibilities at the higher field strengths the data were reproducible to within 1 percent, and for the smaller susceptibilities in low fields to within 6 percent.

SUSCEPTIBILITIES IN FIELDS OF 100 TO 1,000 OERSTEDS

The Apparatus

In order to ascertain what the susceptibilities for the four diamagnetic specimens would be in relatively strong fields, comparable to those usually employed in such measurements, an apparatus was designed and constructed with which absolute measurements could be made in fields ranging between 100 and 1,000 oersteds.

The general principle of the method was the same as that employed with the torsion balance. After much cut-and-try investigation, an air-core coil was designed which would produce a field of 1,000 oersteds at the point where the maximum force acted on the specimen.

The dimensions of the coil, in terms of the notation used in Figure 1, were: $A=3.175$ cm, $B=8.696$ cm, and $C=6.05$ cm. The coil was wound with two parallel heavy Formax No. 16 copper wires; each winding consisted of 1,887 turns. The form was made of quarter-inch-thick brass.

Inside the central tube of this form was a second thin-wall brass tube separated 3/16 inch from the form tube by a stretched-out helix of 3/16-inch-diameter copper wire. There was thus formed a helical path through which cooling water passed continously. The cooling was necessary in order to reduce greatly the convection air-currents that disturbed the specimen, and it also served to remove heat from the inner part of the winding.

The coil stood on three legs so that its axis was vertical. It stood on a brass base which was provided with three leveling screws. These served both to plumb the coil and to raise it to the proper level so that the specimen was at the point on the axis where the force due to the field was a maximum. This point was (Figure 1) at $S=5.10$ cm.

The values of H_x and

$$H_x \frac{\partial H_x}{\partial x}$$

were calculated by use of equations (3) and (4).

The force measurements were made with a new Christian Becker semi-microbalance. The specimen was hung from a hook on the underside of the left scale pan through a hole in the case of the balance; the suspension was a No. 40 copper wire. A $1\frac{1}{2}$-inch-diameter glass tube, closed at the lower end, surrounded the specimen and its suspension. The balance was operated with a reproducibility of about ± 4 micrograms.

Test of the Apparatus

The apparatus was tested by making measurements on a specimen (2.2830 gm) of pure water in a small Pyrex glass bulb. Each force measurement involved reading the balance deflection four times; first, with the two windings connected non-inductively so as to obtain a value of the heat deflection; second, with the field upward; third, with the field downward; and fourth, with the non-inductive connection again. The force due to magnetization was the algebraic difference of the force with the field and that due to heat deflection only.

Five force measurements were made at each of seven field strengths ranging from 985 down to 245 oersteds. When the observed force was plotted as a function of the square of the magnetizing current, the points fell accurately along a straight line that passed through the origin. This showed that the susceptibility was constant over that range of fields.

The slope of the line was corrected by subtracting the small forces that acted on the empty glass bulb. Then the susceptibility of the water was calculated by use of equations (1), (3), and (4). Estimates were made of the errors in the measurements of the current, the force, and the balance sensitivity; these totaled

1.4 percent. The calculated value of the volume susceptibility of water was $-0.73\pm0.01\times10^{-6}$ pole/cm² oersted. The value listed in the International Critical Tables is -0.72×10^{-6}.

The fact that our value agrees well with that in the Tables indicates that our apparatus should yield correct results on other specimens.

Susceptibilities of the Four Diamagnetic Specimens

Exactly similar measurements were made on the solid specimens. With the bismuth specimen, measurements were made at eight different field strengths ranging between 985 and 122 oersteds. Again the curve of the force plotted as a function of the square of the current was a straight line passing through the origin. The constant value of the volume magnetic susceptibility was $-12.37\pm0.07\times10^{-6}$ pole/cm² oersted.

The solid antimony specimen over the same range of fields also yielded a straight line through the origin. The resulting volume susceptibility was $-4.71\pm0.04\times10^{-6}$pole/cm² oersted.

Measurements on the solid cadmium specimen yielded a straight line over the range 985 down to 245 oersteds. This straight line, however, did not pass through the origin; it intercepted the i^2-axis quite near the origin. The slope of the line indicates that the value of the susceptibility is a constant, $-1.15\pm0.02\times10^{-6}$ pole/cm² oersted, over the range of the fields that were employed. The intercept indicates that the susceptibilities at fields below 245 oersteds must have been less, since the straight-line curve must bend so as to pass through the origin.

Measurements on the bismuth powder specimen were made over the range of 985 down to 122 oersteds. The curve in this case passed through the origin, but the slope of the curve increased regularly with i^2. All eight points fell on this smooth curve after the observed forces were corrected for the force on the empty bulb. Calculations of the susceptibilities near the origin and at the high field strengths were made from the slopes of the curve at these points. They were -4.67×10^{-6} pole/cm² oersted at the origin and -7.87×10^{-6} pole/cm² oersted at 900 oersteds.

These values of the diamagnetic susceptibilities that were observed between 100 and 1,000 oersteds are also listed in Table I so that comparisons can readily be made.

DISCUSSION OF RESULTS

It appears that the torsion balance apparatus which has been developed, can be used for measuring the susceptibilities of all sorts of solid and liquid para- and diamagnetic specimens in weak fields. Any torque that arises because of a permanent magnetization of the specimen will be reversed when the field is reversed and can therefore be subtracted out.

We have no explanation for the decrease in susceptibilities of both the dia- and the paramagnetic specimens with increasing field strengths in weak fields.

One may guess that a small amount of ferromagnetic impurity would account for the behavior of the diamagnetic specimens, but there exists no comparable magnetic substance that would serve as an impurity and reduce the magnetizations of the paramagnetic specimens.

The solid bismuth specimen was prepared from granules out of the same sealed bottle from which came the bismuth for the bulb-of-granules specimen; yet the granules exhibited a much lower susceptibility, in both weak and strong fields, than did the solid specimen. This effect may be characteristic of granules and powders. It is remarkable that the susceptibility of the granules increased by 60 percent for an increase in field from 100 to 1,000 oersteds. It is possible that a small amount of ferromagnetic impurity in the granule-specimen might account for this.

It appears that measurements on specimens of spectroscopically pure elements must be made in order to determine that the changes of susceptibility with field strength, and with the size of the granules, are really characteristic of certain elements.

Even if the susceptibility of a substance in the powder or granule form is the same as that of a solid specimen of that substance, such powders or granules must not be prepared with steel cutters or grinders. The contact of the substance with a steel cutter, in all probability, will contaminate the specimen with so much metallic iron that its susceptibility, in a field of the order of an oersted, will be quite different from that of an uncontaminated specimen. In fact, a diamagnetic specimen may be rendered quite paramagnetic by such contamination.

ACKNOWLEDGEMENTS

It is a pleasure to acknowledge the many hours of study and of laboratory work that each of the following dedicated students contributed to this project while he was doing the research for his master's degree: John M. Nordquist (1931), John A. Gillin (1932), Everett B. Miller (1933), R. Ellis Smith (1935), William J. Leas (1940), and Russell L. Collins (1950).

REFERENCES

Collins, Russell L., 1950, Para- and diamagnetic susceptibilities in fields of 100 to 1,000 oersteds: Thesis, University of Oklahoma.

Gillin, John A., 1932, Magnetic susceptibilities in weak fields: Thesis, University of Oklahoma.

Leas, William J., 1940, Magnetic susceptibilities in fields of 100 to 500 oersteds: Thesis, University of Oklahoma.

McKeehan, L. W., 1929, The measurement of magnetic quantities: Jour. Optical Society of America, v. 19, p. 213–242.

Miller, Everett B., 1933, Magnetic susceptibilities in weak fields II: Thesis, University of Oklahoma.

Nagata, T., 1953, Rock-magnetism: Tokyo, Maruzen Company Ltd., p. 20, 87, 88, 95.

Nordquist, John M., 1931, A method of measuring magnetic susceptibilities of rocks: Thesis, University of Oklahoma.

Sharpe, J. A., 1953, The magnetic susceptibility of rocks: Proc. Geophysical Society of Tulsa, v. 1, p. 23–44.

Shaw, R. E., and Hayes, C., 1916, A sensitive magnetometer: Proc. Physical Society of London, v. 28, p. 293–300.

Slichter, L. B., 1929, Geophysical prospecting: New York, American Institute of Mining Engineers, p. 244, 245, 247.

Smith, R. Ellis, 1935, Magnetic susceptibilities in weak fields III: Thesis, University of Oklahoma.

Stoner, E. L., 1926, Magnetism and atomic structure: London, Methuen and Company Ltd., p. 39.

GEOPHYSICS, VOL. XXIII, NO. 4 (OCTOBER, 1958), PP. 726–737, 4 FIGS.

RESULTS OF AIRBORNE MAGNETOMETER PROFILE FROM BROWNSVILLE, TEXAS, TO GUATEMALA CITY*

W. B. AGOCS†

ABSTRACT

An airborne magnetometer profile was obtained in the course of ferrying an aircraft from Brownsville, Texas, to Guatemala City, Guatemala, via Tampico, Tuxpan, Veracruz, Tuxtla, Tapachula and Tequisate, a distance of slightly over 1,000 miles.

The profile indicates that the basement depth is on the order of −20,000 ft along the eastern coast of Mexico, except for the Tamualipas uplift. In southern Mexico and Guatemala the basement level rises to approximately −10,000 ft, and it is exposed in the extreme southern part of Mexico. Several major fault systems and intra-sedimentary volcanic horizons are indicated by the profile.

Bouguer anomaly data, supplied by Dr. G. P. Woollard, show surprisingly good agreement with the sub-surface structure as determined from the magnetics.

Gross errors in the depth determinations from the single profile may arise due to simplifying assumptions that the trends are transverse to the direction of the profile and that they are elongate. The excellent correlation between the structures determined from the magnetics and the Bouguer gravity anomalies lends confidence to conclusions drawn from these indications, and this should permit further analysis of the gravity.

INTRODUCTION

An airborne magnetometer profile was obtained early in 1957 in the course of ferrying an aircraft from the United States to Guatemala. The course of this profile from Brownsville, Texas, to Guatemala City is shown on Figure 1.

The magnetometer used to obtain this data was a Gulf Research and Development Corporation Model MK III saturable core, continuously recording instrument mounted "inboard" on the aircraft. The recording sensitivity was maintained at 300 gamma for a full-scale deflection of 10 inches, with 250 gamma "steps" provided to remain on scale.

The course of the profile was recorded on 1:1,000,000 World Aeronautical Charts, and the ground positions were recorded on the magnetometer tape so that the magnetic data could be correlated with the ground positions.

The flight level was maintained at barometric levels ranging from 1,000 to to 7,000 ft, and the level of flight was noted on the magnetometer tape for final recovery.

The Bouguer gravity anomaly profile which is shown with the magnetic profile was kindly supplied by Dr. G. P. Woollard of the University of Wisconsin.

Figures 2, 3, and 4 illustrate the magnetic profile and its attendant data, divided into three sections for the sake of convenience. Figure 2 is the northernmost portion of the profile, from Brownsville to Tuxpan; Figure 3 is the central portion, from Tuxpan to Rio Grijalva; and Figure 4 is the southern portion, from Rio Grijalva to Guatemala City.

* Paper read at the 27th Annual Meeting of the Society at Dallas on November 17, 1957. Manuscript received by the Editor January 23, 1958.

† Aero Service Corporation, Philadelphia, Pa., Canadian Aero Service, Limited.

FIG. 1. Index map showing course of aeromagnetic profile.

The uppermost portions of Figures 2, 3, and 4 show the observed total magnetic field intensity. The normal regional gradient is shown in relation to the observed record. The position of the observed record with respect to the normal regional gradient is arbitrary.

Immediately below the observed total magnetic intensity record is the same record after the normal regional gradient has been subtracted, to illustrate the anomalous total magnetic intensity. The zero line has been arbitrarily chosen.

Below this, the Bouguer gravity information supplied by Dr. Woollard is shown.

At the bottom of each figure is a cross-section showing the structural condi-

tions inferred from the geophysical data at hand, and the flight level. The small circles on the cross-sections mark individual depths calculated from the magnetometer record. The basement and the volcanic horizons recognized are delineated by mean lines through these circles.

The entire flight was about 1,000 miles long. Reference marks 50 miles apart

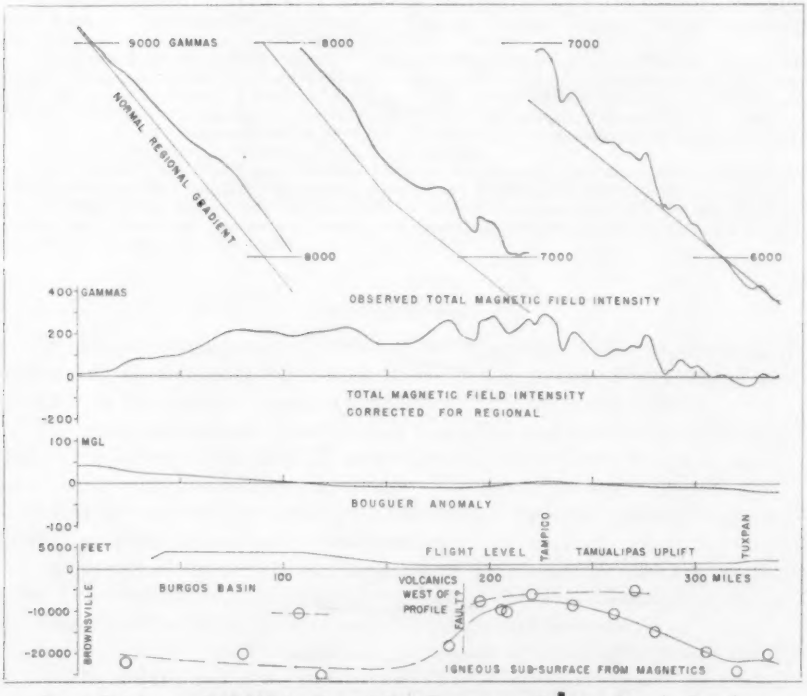

FIG. 2. Total magnetic field intensity variation, Bouguer gravity anomaly and sub-surface structure for aeromagnetics from Brownsville, Texas, to Tuxpan, Mexico.

have been placed on the corrected total magnetic intensity profiles, the Bouguer gravity profiles, and the structure sections.

GEOLOGY

The major geological features from north to south along the length of the profile are: The Burgos basin, Mile 0–175; the Tamaulipas uplift, Mile 175–300; the volcanics west of Nautla, Mile 400–450; the Veracruz basin, Mile 450–525; the volcanics of the San Andres mountains, Mile 525–575; the Salinas basin, Mile

600–775; the Paleozoic intrusives on the approach to the Sierra Madre, Mile 700–770; the Jurassic sedimentary re-entrant at Jaltenango, Mile 775–800; and, finally, the volcanic zone with its core of intrusive rocks on the approach to Guatemala City, at Mile 1,000.

The major structural trend along the line of the profile is northwest-southeast to about the latitude of Minatitlan, but to the southeast of this point, on the

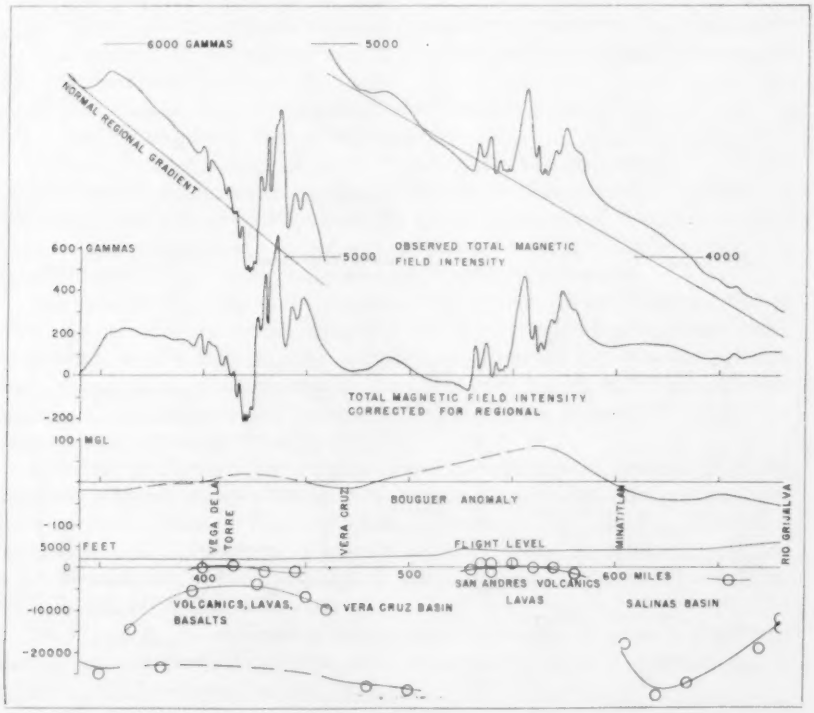

FIG. 3. Total magnetic field intensity variation, Bouguer gravity anomaly and sub-surface structure for aeromagnetics from Tuxpan to Rio Grijalva, Mexico.

entrance to the Salinas basin, the structural trends become more complex as a result of the dual transverse and vertical movement in this area. Continuing on southeastward, the general northeast-southeast trend is resumed.

MAGNETICS

The intensity of the earth's total magnetic field at the northern end of the profile is approximately 49,000 gamma, and the inclination of the total magnetic field vector is 54½°; at the termination of the profile at Guatemala City, the

magnitude of the total magnetic field intensity is 42,500 gamma, and the inclination of the total magnetic field vector is 43½°.

The depths of basement cited in the following analysis are considered to be equal to the horizontal projection of the essentially straight portion of the gradient of the magnetic anomaly in question. This is an approximation, based on the theoretically calculated and empirically observed proportionality between

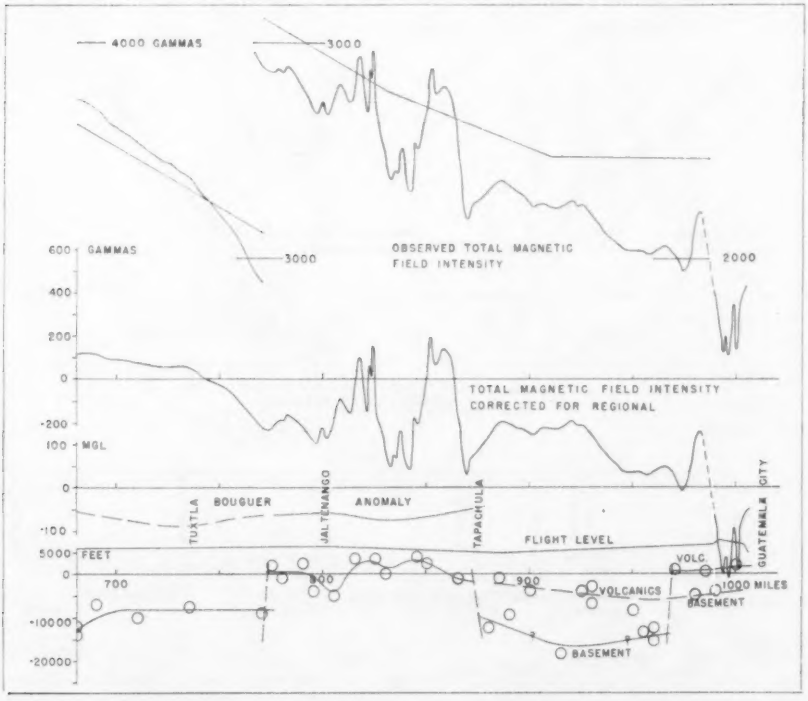

FIG. 4. Total magnetic field intensity variation, Bouguer gravity anomaly and sub-surface structure for aeromagnetics from Rio Grijalva, Mexico, to Guatemala City, Guatemala.

the horizontal width of a magnetic anomaly and the distance separating the causative body and the plane of observation.

Methods of utilizing this relationship, in terms of horizontal gradient length, or horizontal distance between maximum and half-maximum points on an anomaly, have been advanced by various authors (Henderson and Zeitz, 1948; Peters, 1949; Vacquier, Steenland, et al., 1951; Smellie, 1956). The refinements and corrections offered by these methods are dependent on the size, shape, and orientation of the body as well as its magnetic latitude. Such treatment is not

applicable in the case of a single profile. However, the simple equivalence of horizontal slope length and depth to anomaly cause is considered sufficient to yield the magitude of the depth.

The depth determinations from single profiles are subject to gross errors as a result of the simplifying assumptions which must be made. The following are the usual assumptions for the depth determinations from a single profile.

1. The magnetic trends are at right angles to the direction of the profile.
2. The magnetic trends are elongate transverse to the direction of the profile.
3. The magnetic anomalies are caused by sharp discontinuities in the magnetite content of the igneous rocks.
4. The sides of the rock masses at the contacts between different zones of varying magnetite content are vertical.

Greater confidence may be placed in the depth determinations if drill hole depth values to basement are available and if igneous exposures are available to check the depth indices used to obtain the quantitative values. Even under these conditions, however, local to regional deviations from the above simplifying assumptions will yield gross errors over which there is no control.

The relative intensity of the magnetometer profile can be considered a very rough indication of the overall composition of the corresponding basement rocks. In general, areas of high magnetic intensity are underlain by a basement with a high concentration of the mineral magnetite and are, by inference, of basic composition. Conversely, areas of low magnetic intensity are presumably deficient in magnetite and are of acidic composition.

Referring to Figure 2, comparison of the normal regional gradient with the observed gradient shows a 200 gamma high in the first 300-mile section from Brownsville to Tuxpan. This high rises to its level from Mile 0 to 70, and it remains generally 200 gamma above the normal regional level for the next 150 miles; and thereafter, from Mile 220 to 310, it drops to the normal level. It remains at this level until Mile 340.

On Figure 3, the observed magnetic level increases 200 gamma above the normal regional gradient between Mile 340 and 360, south of Tuxpan; and it maintains this level over the next 50 miles.

To the southeast of the previous high, marked local deviations from the normal regional gradient are observed. These are attributed to the volcanics in these sections.

Referring to Figures 3 and 4, from Vega dela Torre to Tuxtla, Mile 400 to 740, the observed gradient is in general parallel to the normal regional gradient, but it has strong local magnetic deviations to the northwest of Veracruz and northwest of Minatitlan. These latter features may be correlated with the volcanics in these zones. The maximum local magnetic anomaly found in these zones is over 800 gamma.

To the southeast of Tuxtla, and continuing on to the end of the profile, the observed magnetic level in general lies 200 gamma below the normal regional

gradient level, and it drops abruptly to about 600 gamma below the normal regional gradient level at the approach to Guatemala City.

The general conclusions could be drawn that the igneous basement in the first section from Brownsville to Tuxpan represents a possible igneous phase intermediate between acidic and basic as does the block southeast of Tuxpan. These blocks may be separated by a granitic zone at Tuxpan.

The 100-gamma high zone extending for about 200 miles south of the San Andres mountains to Tuxtla would be a more acidic igneous phase than the zones previously mentioned.

The section from Tuxtla to the end of the profile, with its level ranging from 200 to over 400 gamma below the general magnetic level, could represent the most acidic phase of basement encountered along the profile or a reversal in polarization either in the basement rocks or in the near-surface volcanics.

Hence, within the length of the profile, the basement igneous material changes from a basement intermediate in composition, possibly with acidic intrusives, to a basement which may be strongly acidic or reversely polarized. This is exclusive of the violent, local magnetic anomalies in zones of known volcanics.

The study of the location of the zones of volcanics shows that they occur at the contacts between the broad susceptibility contrast zones. The violent magnetic anomalies between Tuxtla and Tapachula are not in this classification, since they are associated with exposed or shallow basements.

BOUGUER GRAVITY ANOMALY

The Bouguer gravity anomaly from Brownsville, Texas, to Tapachula, Mexico, was obtained from Dr. G. P. Woollard of the University of Wisconsin.

The gravity gradient is to the south from Brownsville from Mile 0 to 150. The maximum level at Brownsville is +40 mg and at its lowest point it is −10 mg. Over this section the magnetic level rises about 200 gamma, but superimposed on this generally high magnetic zone are minor magnetic anomalies of 30 to 100 gamma.

A +5 mg anomaly is located at Tampico, at Mile 225, and proceeding southward the gravity level drops to −20 mg between Tuxpan and Vega dela Torre at Mile 350. The magnetic level in this section decreases approximately 200 gamma.

The Bouguer gravity anomaly rises to +20 mg at Vega dela Torre, then decreases to −15 mg at Veracruz, and rises to about +80 mg over the San Andres mountains, Mile 560. The magnetics at Vega dela Torre show an intense anomaly of approximately 800 gamma, with gentle, low-level magnetic anomalies at Veracruz, and then they show a series of violent anomalies rising over 400 gamma over the San Andres volcanics and lavas.

The level of the Bouguer gravity anomaly drops to about −45 mg at Mile 630, southeast of Minatitlan, from its high of +80 mg over the San Andres mountains. The gravity level rises to a small high of −30 mg at Mile 650, and it continues to decrease to Tuxtla, where the gravity anomaly is −90 mg. The magnet-

ics in this section are relatively quiet, except for a very local 20 gamma high (which may have some relationship to the aforementioned local gravity high) at a general level of about 100 gamma. The magnetic level starts to decrease at the low point of the gravity at Tuxtla.

From Tuxtla to Tapachula, the Bouguer anomaly is at a generally common level of about −65 mg, but in this section relatively violent magnetic anomalies of up to 400 gamma are observed due to the intrusive igneous outcrop zone of the Sierra Madre area.

In conclusion, it is noteworthy that there is general correspondence between the Bouguer gravity anomalies and the magnetic anomalies.

IGNEOUS HORIZON DEPTHS AND STRUCTURE FROM AEROMAGNETICS

The aeromagnetic control data obtained on this profile have been analyzed for depth to determine the possible cause of the anomalies. In a region such as that covered by this profile, relatively complex structural conditions may be expected. However, the availability of gravity data along this section permits some checking of the quantitative determinations and the interpretations.

The magnetic anomalies, from the origin of the profile at Brownsville to about Mile 170, 35 miles south of Pesca, are relatively gentle. The lack of magnetic features and the width and low amplitude of the magnetic anomalies indicate a relatively uniform igneous basement at relatively great depth. Depth determinations show that the basement ranges from 22,000 to about 25,000 ft sub-sea with a possible dip to the south along this segment of the profile. A local, erratic depth determination is located at Mile 105, which is at about 11,000 ft sub-sea. This erratic may be due either to the lack of isolation of the anomaly from which the depth determination was made or a local zone of intrusive material. The magnetics are not diagnostic relative to the latter, and the former must therefore be accepted.

The magnetic anomalies increase in amplitude from Mile 150 to Tuxpan at Mile 325, rising to over 100 gamma. A study of these anomalies indicates that there may be two frequencies of magnetic anomalies showing the possibility of a dual igneous level cause for the magnetic deviations. This section of the profile is on the approach to and crossing of the Tamualipas Uplift. Depth determinations show that the level of the igneous horizon rises from a depth of over 20,000 ft at Mile 150 to about 7,000 ft at Tampico. From there it drops gradually, within a distance of about 100 miles, to over 20,000 ft at Tuxpan. A few points in this section yielded shallower depths, and they are indicated as a possible level of volcanics. This may be likely in view of the presence of volcanic outcrops to the west of the profile.

The Bouguer gravity anomaly over the section from Mile 150 to Tuxpan shows a 15 mg rise. It is of interest to note that the apex of this gravity high lies at Tampico, coincident with the apex of the basement high located from the aeromagnetic depth study. The gravity high shown here is on the eastern flank of an

elongate gravity axis whose apex lies to the west of Tampico. In view of flank location of this gravity high, and the indicated basement uplift, it is doubtful whether a true density contrast value would be obtained from this profile. However, based on the section determined from the magnetics, and assuming a tabular mass having a thickness of 15,000 ft, a density contrast of 0.073 cgs units[1] is found between the sediments and the igneous uplift.

The depth determinations in the vicinity of Tuxpan show that the depth to the igneous horizon is over 20,000 ft. A possible erratic depth determination shows a depth of 20,000 ft which may be indicative of a possible, local basement high, but due to depth, the lack of areal magnetic control, etc., it is considered a weak feature.

The character of the magnetic anomalies from Mile 380 to Veracruz shows a changing characteristic of high frequency, 30 to 60 gamma anomalies superimposed on a broad gradient, and then a marked negative-positive anomaly association on which the amplitude of the super-imposed magnetic anomalies increases to as much as 500 gamma. This dual nature of the anomalies could be due to shallow igneous causes, and the strong, broad positive-negative feature could possibly be due to a single pole feature. Volcanics outcrop in the general section from Vega dela Torre to Veracruz.

The depth determinations in the section from Mile 380 to Veracruz show three possible levels for the causes of the magnetic anomalies. A series of depth determinations shows values of from sea level to about 1,000 ft sub-sea, with the shallowest zone being in the vicinity of Vega dela Torre. The second zone is at a depth of 5,000 ft sub-sea with depths increasing to 10,000 ft to the south on the approach to Veracruz, and possibly increasing to almost 15,000 ft on the north flank. This latter depth value, on the north flank, is in considerable question due to lack of depth control points. Finally, a depth value of 23,000 ft on the north flank of the Vega dela Torre "high" could possibly indicate a continuation of the deep basement under the "high." No deep determinations were obtained in the vicinity of Vega dela Torre, but to the south of Veracruz, in the Veracruz basin, only deep values over 25,000 ft were obtained. Hence, on the basis of the known volanics in the vicinity of Vega dela Torre, and the deep value observed on the approach, the basement depth was continued to the south. Otherwise, it would be necessary to show the Vega dela Torre "high" as a horst.

The Bouguer gravity anomaly over the Vega dela Torre "high," shows about a +40 mg maximum. Assuming that this is a basement structure and that it approaches a horizontal slab in section, the density contrast required would be 0.214 cgs units. This value is considerably higher than for the Tampico "high," but this probably is due to the fact that the approximation of a tabular body is more correct for the Vega dela Torre "high" than for the profile at Tampico. This density value indicates the probability that the feature is a basement horst on

[1] Approximate calculations of this kind may be valid but are subject to gross errors on account of possible isostatic effects. Editor.

the basis of the gravity. However, in view of the interpretation from the magnetics, no final conclusion can be drawn.

The magnetic anomalies from about Mile 500 to Minatitlan, over the San Andres volcanics and lavas, show a relatively high frequency and a maximum central anomaly of almost 500 gamma. The depth determinations in this zone show a horizon ranging from sea level to about 2,000 ft. No depth values were obtained for features below this level. This zone also corresponds to a roughly circular gravity high of over 90 mg. For a slab-like mass, with a thickness of 30,000 ft, the density contrast would be 0.236 cgs units.[2] This value compares quite favorably with that obtained for the Vega dela Torre "high" of 0.214 cgs units.

The magnetic anomalies from Mile 590, at about Minatitlan, to about Mile 770, almost 30 miles southeast of Tuxtla, are relatively low amplitude, broad features, except for a single relatively sharp magnetic anomaly at Mile 655. This zone would characterize a relatively uniform, deep igneous horizon across the Salinas basin. Depth determinations show the deepest values in the Salinas basin of over −25,000 ft, southeast of Minatitlan, whence the basement rises to about −8,000 ft in a distance of 80 miles. This depth of −8,000 ft is maintained for a distance of 80 miles to Mile 770, southeast of Tuxtla. The gravity anomaly in this section decreased uniformly to about Tuxtla, and it then begins to rise slowly. The depth of the Salinas basin is not indicated by the gravity, and the basement platform zone is found to be a gravity low.

The minor magnetic anomaly located at Mile 655 which correlates with a minor gravity high may be the sole magnetic expression of local intrusives. The depth to its cause is determined to be about −3,000 ft, but there is an insufficient amount of data to outline the mass or for use to determine the density contrast for the associated gravity anomaly. In addition, the magnetic anomaly appears to be considerably more local in character than the gravity feature, and the correspondence between the two may be misleading.

The magnetic anomalies from Mile 770, northwest of Jaltenango, to Tapachula are relatively intense and of high frequency. This is the area of the intrusive outcrops of the Sierra Madre mountains. The basement surface is found to oscillate above sea-level with faults to the north at Mile 770 and south at Mile 870. These fault traces are shown since the igneous horizon depths suddenly change from about 8,000 ft to surface. It is interesting to note that the 4,000-ft low zone at Jaltenango coincides roughly with the Jurassic re-entrant in this area. The general level of the Bouguer anomaly in this zone remains relatively constant.

From Tapachula to Mile 980, the magnetic anomalies are composed of a combination of broad, 40 to 50 gamma amplitude features, and narrow, minor 20 to 30 gamma anomalies. Depth determinations show the possible presence of two magnetic horizons, of which one is at a depth of about −5,000 ft and the other at depths ranging from −10,000 to over −15,000 ft. The former horizon is interpreted as being a possible volcanic zone and the latter as the basement. This

[2] See Editor's Note *supra*.

section is terminated to the southwest by a possible fault at about Mile 970. This latter fault trace may be the southeastward continuation of the fault trace at Mile 870, the Sierra Madre fault trace.

The magnetic level decreases abruptly on the approach to Guatemala City by about 500 gamma. Again, from Mile 970 to the end of the profile, two possible depth levels are indicated, and they are interpreted as being due to the shallow volcanics which outcrop in this zone and the basement at a depth of about 5,000 ft, respectively.

CONCLUSIONS

The combination of quantitative determinations from magnetic profiles with gravity surveys aids considerably in deciding the possible cause of the anomalies. The study of this profile showed that there is an almost one-to-one correspondence between the igneous "highs" as determined from magnetics and the Bouguer gravity highs.

These regional magnetic surveys will aid in outlining basin zones, shallow outcrop areas, and intrusive areas. However, the presence of volcanics does not necessarily mean that no information on deeper horizons can be obtained with the magnetometer, since in some areas it is possible to obtain indications of the deep basement, provided the magnetic effects of the deep basement structural features can be seen through the magnetic effects due to the volcanics.

ACKNOWLEDGEMENTS

The writer wishes to thank the crew of the aircraft, composed of Messrs. H. J. Moore, pilot; E. L. McLendon, co-pilot; R. Coombes mechanic; and R. Pate, magnetometer operator, for obtaining this profile. Without the cooperation of these men it would have been impossible to prepare this paper. Permission to publish these findings was granted by Mr. Virgil Kauffman, President of Aero Service Corporation.

Thanks are due to M. S. Reford, Manager of the Magnetometer Division of Canadian Aero Service, Limited, for his critical reading of this paper.

The author also wishes to express his gratitude to Dr. G. P. Woollard for permission to publish his gravity data.

REFERENCES

Barnatche, A., and Illing, L. V., 1957, Water-gas injection saves Poza Rica field: Petroleo Interamericano, p. 88–92.

Benevides, G. Luis, 1956, Notas sobre la geologia petrolera de Mexico: Symposium Sobre Yacimientos de Petroleo y Gas, XX Congreso Geologico Internacional.

Henderson, R. G., and Zeitz, I., 1948, Analysis of total magnetic intensity anomalies produced by point and line sources: Geophysics, v. 13, p. 428–436.

Martinez, R. M., 1957, San Andres strike may revive entire Golden Lane trend: Petroleo Interamericano, p. 72–77.

Peters, L. J., 1949, The direct approach to magnetic interpretation and its practical application: Geophysics, v. 14, p. 290–320.

Roberts, Ralph J., and Irving, Earl M., 1957, Mineral deposits of Central America: Geological Survey Bulletin 1034.

Smellie, D. W., 1956, Elementary approximations in aeromagnetic interpretation: Geophysics, v. 21, p. 1021–1040.

Vacquier, V., Steenland, N. C., Henderson, R. G., and Zeitz, I., 1951, Interpretation of aeromagnetic maps: Memoir 47, G.S.A.

XX Congreso Geologico Internacional, 1956, Carta geologica de la Republica Mexicana.

GEOPHYSICS, VOL. XXIII, NO. 4 (OCTOBER, 1958), PP. 738–748

INTERRELATIONSHIPS BETWEEN MAGNETIC ANOMALY COMPONENTS*

JAMES AFFLECK†

ABSTRACT

The relationships between the various magnetic anomaly components are developed from fundamental theory. A symbolism is introduced which permits expression of the relationships in algebraic form. These techniques have been found useful in predicting anomaly shapes for any magnetic latitude and in simplifying calculations of aeromagnetic or other component intensity anomalies for rock masses. Two examples of the application are shown.

INTRODUCTION

The magnetic anomaly for a particular rock mass depends upon the parameters of geometric shape, depth, and magnetization. Analytical formulas have been deduced for many of the simpler geometric bodies and magnetizations. Because of well-known inherent difficulties, the more complex shapes and magnetizations do not lend themselves to simple analytical solutions, and the anomalies are usually calculated by means of graphical or other approximations.

The normal procedure in calculating the total intensity anomaly for a given rock mass with an assumed direction and strength of magnetization is to calculate each of the three components of magnetic intensity for each of the three components of magnetization. The nine components are added vector-fashion, and this resultant is the true total intensity anomaly. This vector total will change very appreciably both in magnitude and direction over the extent of the anomaly. The airborne magnetometer records only the magnitude of the earth's field relative to some arbitrary datum. Directions of the field cannot be measured with adequate precision partly because of a lack of a satisfactory geodetic reference in an airplane. Local anomalies modify the earth's field both in magnitude and direction, and the minor changes in direction cannot be measured. When one deals with the small anomalies encountered in oil survey work, it is generally agreed that the vector sum of the nine components projected on the average direction of the earth's field is a very satisfactory approximation of the total intensity anomaly. In mineral survey work, very strong anomalies may make this approximation unacceptable.

One of the parameters which determines the configuration of an anomaly is the total magnetization. It consists of the vector sum of induced and remanent magnetizations. The first is in the direction of the earth's field, while the second may have any direction and magnitude. Some rocks have large induced magnetizations and practically zero remanence. Others have the two factors roughly equal. In others, the remanence can be ten times as large as the induced effect.

* Manuscript received by the Editor May 12, 1958.

† Gulf Research and Development Company, Pittsburgh, Pennsylvania.

It is, therefore, improper to assume that remanence is negligible although this is a common assumption in much of the literature on magnetic interpretation. In the mathematical development which follows, the magnetization is considered as an unknown vector.

Obviously, the calculation of total intensity anomalies is tedious and expensive. Vertical or horizontal anomalies are less difficult, but three component calculations, one for each of the three component magnetizations, are still necessary.

The purpose of this paper is to develop relationships between the nine components of intensity in the form of special algebraic processes. Some of the material which follows is available in other forms in the literature. Some of it appears to be new.

MATHEMATICAL DEVELOPMENT

Consider an element of volume $d\alpha d\beta d\gamma$ within the magnetized mass. The components of its total magnetization are I_α, I_β, and I_γ respectively. The magnetic potential (ϕ) at a point at coordinate locations (x, y, z) in space beyond the magnetized mass is[1]

$$\phi = \iiint_v \left[I_\alpha \frac{\partial}{\partial \alpha} + I_\beta \frac{\partial}{\partial \beta} + I_\gamma \frac{\partial}{\partial \gamma} \right] \left(\frac{1}{r} \right) d\alpha d\beta d\gamma \tag{1}$$

where

$$r = \left\{ (x - \alpha)^2 + (y - \beta)^2 + (z - \gamma)^2 \right\}^{1/2}. \tag{2}$$

The x-component of intensity H_x is

$$H_x = -\frac{\partial \phi}{\partial x} = \frac{-\partial}{\partial x} \iiint_v \left[I_\alpha \frac{\partial}{\partial \alpha} + I_\beta \frac{\partial}{\partial \beta} + I_\gamma \frac{\partial}{\partial \gamma} \right] \left(\frac{1}{r} \right) d\alpha d\beta d\gamma, \tag{3}$$

and similar equations can be written for H_y and H_z. By simple application to $1/r$ as defined by equation (2), it can be demonstrated that

$$-\frac{\partial}{\partial x}\left(\frac{1}{r}\right) = \frac{\partial}{\partial \alpha}\left(\frac{1}{r}\right); \quad -\frac{\partial}{\partial y}\left(\frac{1}{r}\right) = \frac{\partial}{\partial \beta}\left(\frac{1}{r}\right); \quad -\frac{\partial}{\partial z}\left(\frac{1}{r}\right) = \frac{\partial}{\partial \gamma}\left(\frac{1}{r}\right). \tag{4}$$

Therefore,

$$H_x = \iiint_v \left[I_\alpha \frac{\partial^2}{\partial \alpha^2} + I_\beta \frac{\partial^2}{\partial \alpha \partial \beta} + I_\gamma \frac{\partial^2}{\partial \alpha \partial \gamma} \right] \left(\frac{1}{r} \right) d\alpha d\beta d\gamma, \tag{5}$$

$$H_y = \iiint_v \left[I_\alpha \frac{\partial^2}{\partial \alpha \partial \beta} + I_\beta \frac{\partial^2}{\partial \beta^2} + I_\gamma \frac{\partial^2}{\partial \beta \partial \gamma} \right] \left(\frac{1}{r} \right) d\alpha d\beta d\gamma, \tag{6}$$

[1] For development of this equation, see J. Jeans, *Electricity and Magnetism*, p. 373, or other texts on potential theory.

and

$$H_z = \iiint_v \left[I_\alpha \frac{\partial^2}{\partial\alpha\partial\gamma} + I_\beta \frac{\partial^2}{\partial\beta\partial\gamma} + I_\gamma \frac{\partial^2}{\partial\gamma^2} \right] \left(\frac{1}{r}\right) d\alpha d\beta d\gamma. \tag{7}$$

Consider a special case in which the magnetized mass has only one component of magnetization (I_α). Then,

$$H_{z,x} = \iiint_v I_\alpha \frac{\partial^2}{\partial\alpha^2} \left(\frac{1}{r}\right) d\alpha d\beta d\gamma. \tag{8}$$

Note that a new symbol ($H_{z,x}$) has been introduced. In general, the symbol $H_{m,n}$ represents the m-direction component of intensity caused by the n-direction component of magnetization only.

Similarly

$$H_{z,y} = \iiint_v I_\beta \frac{\partial^2}{\partial\alpha\partial\beta} \left(\frac{1}{r}\right) d\alpha d\beta d\gamma \tag{9}$$

$$H_{z,z} = \iiint_v I_\gamma \frac{\partial^2}{\partial\alpha\partial\gamma} \left(\frac{1}{r}\right) d\alpha d\beta d\gamma \tag{10}$$

$$H_{y,x} = \iiint_v I_\alpha \frac{\partial^2}{\partial\alpha\partial\beta} \left(\frac{1}{r}\right) d\alpha d\lambda d\gamma \tag{11}$$

$$H_{y,y} = \iiint_v I_\beta \frac{\partial^2}{\partial\beta^2} \left(\frac{1}{r}\right) d\alpha d\beta d\gamma \tag{12}$$

$$H_{y,z} = \iiint_v I_\gamma \frac{\partial^2}{\partial\beta\partial\gamma} \left(\frac{1}{r}\right) d\alpha d\beta d\gamma \tag{13}$$

$$H_{x,x} = \iiint_v I_\alpha \frac{\partial^2}{\partial\alpha\partial\gamma} \left(\frac{1}{r}\right) d\alpha d\beta d\gamma \tag{14}$$

$$H_{x,y} = \iiint_v I_\beta \frac{\partial^2}{\partial\beta\partial\gamma} \left(\frac{1}{r}\right) d\alpha d\beta d\gamma \tag{15}$$

$$H_{z,z} = \iiint_v I_\gamma \frac{\partial^2}{\partial\gamma^2} \left(\frac{1}{r}\right) d\alpha d\beta d\gamma. \tag{16}$$

Equations (8) through (16) are the nine components of intensity referred to in the introduction.

The first assumption is now introduced. We shall assume that the mass is uniformly magnetized. It is now legitimate to place the magnetization components in front of the integrals and replace I_α by I_x, I_β by I_y, and I_γ by I_z. Equations (8) through (16) can be written, by simple algebra,

$$\frac{H_{x,x}}{I_x} = \iiint_v \frac{\partial}{\partial \alpha^2}\left(\frac{1}{r}\right) d\alpha d\beta d\gamma \tag{17}$$

$$\frac{H_{x,y}}{I_y} = \iiint_v \frac{\partial^2}{\partial \alpha \partial \beta}\left(\frac{1}{r}\right) d\alpha d\beta d\gamma \tag{18}$$

$$\frac{H_{x,z}}{I_z} = \iiint_v \frac{\partial^2}{\partial \alpha \partial \gamma}\left(\frac{1}{r}\right) d\alpha d\beta d\gamma \tag{19}$$

$$\frac{H_{y,x}}{I_x} = \iiint_v \frac{\partial^2}{\partial \alpha \partial \beta}\left(\frac{1}{r}\right) d\alpha d\beta d\gamma \tag{20}$$

$$\frac{H_{y,y}}{I_y} = \iiint_v \frac{\partial^2}{\partial \beta^2}\left(\frac{1}{r}\right) d\alpha d\beta d\gamma \tag{21}$$

$$\frac{H_{y,z}}{I_z} = \iiint_v \frac{\partial^2}{\partial \beta \partial \gamma}\left(\frac{1}{r}\right) d\alpha d\beta d\gamma \tag{22}$$

$$\frac{H_{z,x}}{I_x} = \iiint_v \frac{\partial^2}{\partial \alpha \partial \gamma}\left(\frac{1}{r}\right) d\alpha d\beta d\gamma \tag{23}$$

$$\frac{H_{z,y}}{I_y} = \iiint_v \frac{\partial^2}{\partial \beta \partial \gamma}\left(\frac{1}{r}\right) d\alpha d\beta d\gamma \tag{24}$$

$$\frac{H_{z,z}}{I_z} = \iiint_v \frac{\partial^2}{\partial \gamma^2}\left(\frac{1}{r}\right) d\alpha d\beta d\gamma. \tag{25}$$

The following relationships are deduced by equating the proper equations (17) through (25).

$$\frac{H_{x,y}}{I_y} = \frac{H_{y,x}}{I_x} \tag{26}$$

$$\frac{H_{x,z}}{I_z} = \frac{H_{z,x}}{I_x} \tag{27}$$

$$\frac{H_{y,z}}{I_z} = \frac{H_{z,y}}{I_y} \tag{28}$$

or, in general,

$$\frac{H_{m,n}}{I_n} = \frac{H_{n,m}}{I_m}. \tag{29}$$

Equations (26), (27), (28), and (29) describe one of the special algebraic theorems, limited in that it pertains to masses with uniform magnetization. It is important to recognize that the equalities refer to scalar values of the intensities and magneti-

zations. In the vector sense, the intensities on the two sides of each of these equations are normal to each other.

Addition of equations (17), (21), and (25) gives

$$\frac{H_{x,x}}{I_x}+\frac{H_{y,y}}{I_y}+\frac{H_{z,z}}{I_z}=\iiint_v\left(\frac{\partial^2}{\partial\alpha^2}+\frac{\partial^2}{\partial\beta^2}+\frac{\partial^2}{\partial\gamma^2}\right)\frac{1}{r}\,d\alpha d\beta d\gamma. \tag{30}$$

By performing the derivative operation on $1/r$, as defined in equation (2), the integral in equation (30) is found to be zero.

Therefore,

$$\frac{H_{x,x}}{I_x}+\frac{H_{y,y}}{I_y}+\frac{H_{z,z}}{I_z}=0, \tag{31}$$

and this is a second algebraic theorem, with application only in the scalar sense and limited to masses with uniform magnetization.

Consider now equation (17) which can be reduced to

$$\frac{H_{x,x}}{I_x}=\iiint_v\frac{\partial}{\partial\alpha}\,\frac{(x-\alpha)}{\{(x-\alpha)^2+(y-\beta)^2+(z-\gamma)^2\}^{3/2}}\,d\alpha d\beta d\gamma \tag{32}$$

and

$$\frac{H_{x,x}}{I_x}=\iint\frac{(x-\alpha)}{\{(x-\alpha)^2+(y-\beta)^2+(z-\gamma)^2\}^{3/2}}\Bigg|_{\alpha_1}^{\alpha_2}d\beta d\gamma, \tag{33}$$

where α_1, and α_2 are the limits of integration for α.

In the special case of a slab of uniform thickness in the β and γ dimensions, and extending from $-\infty$ to $+\infty$ in the α dimension, equation (33) reduces to

$$\frac{H_{x,x}}{I_x}=0 \quad \text{or} \quad H_{x,x}=0. \tag{34}$$

Note that the integral with infinite limits becomes zero regardless of the value of I_x which can be any value including zero. Therefore, $H_{x,x}/I_x=0$ and not an indeterminate when $I_x=0$.

By symmetry, it is apparent that with infinite limits for β in one case and for γ in another,

$$\frac{H_{y,y}}{I_y}=0, \qquad \frac{H_{z,z}}{I_z}=0. \tag{35}$$

Equation (18) can be reduced to

$$\frac{H_{x,y}}{I_y}=\iiint_v\frac{\partial}{\partial\alpha}\,\frac{(y-\beta)}{\{(x-\alpha)^2+(y-\beta)^2+(z-\gamma)^2\}^{3/2}}\,d\alpha d\beta d\gamma \tag{36}$$

and

$$\frac{H_{z,y}}{I_y} = \iint \frac{(y-\beta)}{\left\{(x-\alpha)^2+(y-\beta)^2+(z-\gamma)^2\right\}^{3/2}}\Bigg|_{\alpha_1}^{\alpha_2} d\beta d\gamma \tag{37}$$

which, with infinite limits, yields

$$\frac{H_{z,y}}{I_y} = 0. \tag{38}$$

Equation (18) can also be reduced to

$$\frac{H_{z,y}}{I_y} = \iiint_v \frac{\partial}{\partial\beta}\frac{(x-\alpha)}{\left\{(x-\alpha)^2+(y-\beta)^2+(z-\gamma)^2\right\}^{3/2}} d\alpha d\beta d\gamma \tag{39}$$

and

$$\frac{H_{x,y}}{I_y} = \iint \frac{(x-\alpha)}{\left\{(x-\alpha)^2+(y-\beta)^2+(z-\gamma)^2\right\}^{3/2}}\Bigg|_{\beta_1}^{\beta_2} d\alpha d\gamma \tag{40}$$

which yields, with infinite limits for β,

$$\frac{H_{x,y}}{I_y} = 0. \tag{41}$$

By symmetry, it is apparent from these procedures that, in general,

$$\frac{H_{m,n}}{I_n} = 0, \qquad \frac{H_{m,m}}{I_m} = 0 \tag{42}$$

when the limits for integration for m or n in either of the subscript positions are $-\infty$ and $+\infty$. The two equalities in equation (42) form a third algebraic theorem, again limited to masses with uniform magnetization. This can be expressed as follows. A component of intensity is zero if a slab mass has infinite extent in either the direction of the intensity component or the direction of magnetization. In addition, the ratio of the component of intensity to the magnetization is equal to zero even when the magnetization has a value of zero.

Consider a magnetized mass with one component of magnetization (I_{-x}). This represents magnetization in the negative x direction. Obviously, since the magnetization has been reversed,

$$\frac{H_{z,-x}}{I_{-x}} = \frac{-H_{z,x}}{I_x} \tag{43}$$

and, in general,

$$\frac{H_{m,-n}}{I_{-n}} = \frac{-H_{m,n}}{I_n} \tag{44}$$

which includes,

$$\frac{H_{m,-m}}{I_{-m}} = \frac{-H_{m,m}}{I_m}. \tag{45}$$

Similarly, it is obvious that

$$\frac{H_{-m,n}}{I_n} = \frac{-H_{m,n}}{I_n} \tag{46}$$

and

$$\frac{H_{-m,m}}{I_m} = \frac{-H_{m,m}}{I_m}, \tag{47}$$

since, in these, only the directions of intensity measurement have been reversed. From the pairs of equations, (44) and (46), (45) and (47),

$$\frac{H_{m,-n}}{I_{-n}} = \frac{H_{-m,n}}{I_n}, \tag{48}$$

and

$$\frac{H_{m,-m}}{I_{-m}} = \frac{H_{-m,m}}{I_m}. \tag{49}$$

Consider now cases in which both the direction of intensity measurements and magnetizations are reversed. By substituting $-m$ for m in the first subscript position in equations (48) and (49),

$$\frac{H_{-m,-n}}{I_{-n}} = \frac{H_{m,n}}{I_n} \tag{50}$$

and

$$\frac{H_{-m,-m}}{I_{-m}} = \frac{H_{m,m}}{I_m}. \tag{51}$$

These complete the necessary interrelationships. In summary, then, the following special algebraic relationships have been established, subject only to the limitations of uniform magnetization. The values of I are absolute values.

(1) $$\frac{H_{m,n}}{I_n} = \frac{H_{n,m}}{I_m}$$

(2) $$\frac{H_{m,-n}}{I_{-n}} = \frac{-H_{m,n}}{I_n} = \frac{H_{-m,n}}{I_n}$$

$$\frac{H_{m,-m}}{I_{-m}} = \frac{-H_{m,m}}{I_m} = \frac{H_{-m,m}}{I_m} \tag{3}$$

$$\frac{H_{-m,-n}}{I_{-n}} = \frac{H_{m,n}}{I_n} \tag{4}$$

$$\frac{H_{-m,-m}}{I_{-m}} = \frac{H_{m,m}}{I_m} \tag{5}$$

in each of which m and n can be any one of three directions x, y or z.

$$\frac{H_{x,x}}{I_x} + \frac{H_{y,y}}{I_y} + \frac{H_{z,z}}{I_z} = 0. \tag{6}$$

When a slab mass extends from negative to positive infinity in either the direction of intensity measurement or the direction of magnetization,

$$H_{m,n} = 0 \tag{7}$$

$$H_{m,m} = 0 \tag{8}$$

and, even when I_m or I_n equals zero,

$$\frac{H_{m,n}}{I_n} = 0 \tag{9}$$

$$\frac{H_{m,m}}{I_m} = 0. \tag{10}$$

Note, however, that $H_{m,m} \neq 0$ for a mass extending downward to infinity since here the integration limits are only from zero to infinity.

EXAMPLES OF APPLICATION

In the development, x, y, and z have been used as general Cartesian co-ordinates. In the examples, x is positive northward, y is positive eastward, and z is positive downward. These are geodetic directions. The direction of the earth's magnetic field will be represented by I, and H_t is the airborne magnetometer anomaly. The magnetic inclination angle is θ, positive downward, and the declination angle is ψ, positive eastward.

Example 1

Compare the airborne magnetometer anomalies for a mass at a) the north magnetic pole, b) the south magnetic pole, and c) the magnetic equator. The mass has infinite extent in the east-west direction, the declination is zero, and the magnetization is that induced by the earth's field. This is a special case in which the remanent magnetization is zero.

In condition a), the north magnetic pole, $H_t = H_z$, $I_t = I_z$, and

$$H_z = H_{z,z} + H_{z,y} + H_{z,x}$$

by definition of the symbols. But $H_{z,x} = 0$, by relationship 7, and $H_{z,y} = 0$, since $I_y = 0$. Therefore, $H_t = H_{z,z}$ at the north magnetic pole.

In condition b) the south magnetic pole, $H_t = H_{-z,-z}$ only, and $I_t = I_{-z}$. By relationship 5,

$$\frac{H_{z,z}}{I_z} = \frac{H_{-z,-z}}{I_{-z}} .$$

Since I always represents an absolute value, this shows that for equal magnitudes of magnetization, the aeromagnetic anomalies will be identical at the north and south magnetic poles.

In condition c), the magnetic equator, $H_t = H_{z,z}$ only, and $I_t = I_z$. By relationship 6,

$$\frac{H_{z,z}}{I_z} + \frac{H_{z,x}}{I_z} + \frac{H_{y,y}}{I_y} = 0.$$

By the special case relationship 10, $H_{y,y}/I_y = 0$. Therefore,

$$\frac{H_{z,z}}{I_z} = \frac{-H_{z,x}}{I_z}$$

This proves that under the specified conditions with I_z numerically equal to I_z, the airborne anomaly at the magnetic equator is the negative of what it should be at either of the two magnetic poles. One should therefore expect that certain igneous uplifts in low magnetic latitudes will be associated with magnetic lows, and certain igneous faults near the magnetic equator will show magnetic highs over the downthrown side. Note, however, that the complete reversal of anomalies at the magnetic equator holds only for rock masses elongated in the east-west direction. For other types of rock mass, the ratio $H_{y,y}/I_y$ is not equal to zero even if I_y is zero.

Example 2

Consider a uniformly magnetized rock mass with vertical sides extending downward to infinity, from $-a$ to $+a$ in the east direction, and from $-\infty$ to $+\infty$ in the north direction. The rock mass is magnetized in some direction not necessarily that of the earth's field. Calculate the airborne anomaly for this mass.

The two well-known equations apply,

$$H_{z,z} = 2I_z\left[\tan^{-1}\frac{y+a}{h} - \tan^{-1}\frac{y-a}{h}\right]$$

and

$$H_{z,y} = -I_y \ln \frac{(y+a)^2 + h^2}{(y-a)^2 + h^2},$$

where h is the vertical height of the airplane above the rock mass. By relationships 7, 8, 9, and 10,

$$H_{z,z},\ H_{z,z},\ H_{z,y},\ H_{y,z},\ H_{z,z}, \quad \text{and} \quad \frac{H_{z,x}}{I_x}$$

are each zero. Therefore,

$$\frac{H_{z,z}}{I_z} = \frac{-H_{y,y}}{I_y}.$$

Also,

$$\frac{H_{z,y}}{I_y} = \frac{H_{y,z}}{I_z} \text{ by relationship 1,}$$

and, therefore,

$$H_{y,y} = -2I_y\left[\tan^{-1}\frac{y+a}{h} - \tan^{-1}\frac{y-a}{h}\right],$$

and

$$H_{y,z} = -I_z \ln \frac{(y+a)^2 + h^2}{(y-a)^2 + h^2}.$$

Therefore,

$$H_z = H_{z,z} + H_{z,y} = 2I_z\left[\tan^{-1}\frac{y+a}{h} - \tan^{-1}\frac{y-a}{h}\right] - I_y \ln \frac{(y+a)^2 + h^2}{(y-a)^2 + h^2},$$

and

$$H_y = H_{y,y} + H_{y,z} = -2I_y\left(\tan^{-1}\frac{y+a}{h} - \tan^{-1}\frac{y-a}{h}\right) - I_z \ln \frac{(y+a)^2 + h^2}{(y-a)^2 + h^2}.$$

$$H_t = H_z \sin\theta + H_y \sin\psi \cos\theta$$

$$= 2(I_z \sin\theta - I_y \sin\psi \cos\theta)\left[\tan^{-1}\frac{y+a}{h} - \tan^{-1}\frac{y-a}{h}\right]$$

$$- (I_y \sin\theta + I_z \sin\psi \cos\theta) \ln \frac{(y+a)^2 + h^2}{(y-a)^2 + h^2}$$

and this is the airborne anomaly.

Note, that for a magnetization unknown both in magnitude and direction, we can write

$$H_t = 2C\left(\tan^{-1}\frac{y-a}{h} - \tan^{-1}\frac{y-a}{h}\right) - K \ln \frac{(y+a)^2 + h^2}{(y-a)^2 + h^2},$$

where

$$C = I_z \sin\theta - I_y \sin\psi \cos\theta \quad \text{and} \quad K = I_y \sin\theta + I_z \sin\psi \cos\theta.$$

Since I_z and I_y are each unknowns, C and K are also unknowns. If the rock magnetizations were C instead of I_z and K instead of I_y, the new equation for H_z would be identical to the original equation for H_t. Substitution of $-C$ for I_y and K for I_z makes the new H_y equation identical to the original H_t equation. This can be generalized to the extent that for bodies in which the mass extends from $-\infty$ to $+\infty$ in one horizontal direction, the airborne anomaly can be treated as if it were either the vertical or the horizontal intensity anomaly for the same rock mass by replacing the true magnetization by a pseudo-magnetization. The same pseudo-magnetization could not be used for both the horizontal and vertical components of intensity, however. It is also apparent that, under the same limitation, horizontal intensity anomalies can be treated as vertical intensity anomalies by the substitution of a pseudo-magnetization.

These algebraic processes have proven convenient for many of the special problems of magnetic interpretation. They are particularly valuable for the prediction of anomaly shapes at any given inclination, declination, and attitude of the rock masses with respect to the magnetic meridian.

ACKNOWLEDGEMENTS

The writer wishes to express his appreciation to the officials of the Gulf Research and Development Company for permission to publish this paper.

GEOPHYSICS, VOL. XXIII, NO. 4 (OCTOBER, 1958), PP. 749-769, 4 FIGS.

MAGNETIC ANALYSIS BY LOGARITHMIC CURVES*

RALPH D. HUTCHISON†

ABSTRACT

The standard expression for the anomaly of a magnetized dyke consists of two elementary functions which in practice are easily separable. Under certain conditions, these functions have a simple symmetry which makes them plottable as families of logarithmic master-curves; and in each family there is a systematic change of shape corresponding to a depth/breadth parameter of the dyke. On this basis the problem of analysis can be made as simple and direct as the method commonly used for depth determinations by electrical resistivity. In addition to the dyke model, two other closely related classes are developed which thus provide master curves that can be used for a large variety of two-dimensional anomalies.

INTRODUCTION

The anomaly of a magnetized dyke has been used as the basis for perhaps the majority of analytical methods published during the last twenty or thirty years. Some of these methods are sound in theory but unsuitable for general use. Others, although not really sound in theory, often give satisfactory results. There does not seem to have been published any really sound, complete, and directly analytical method. Yet the mathematical expression of the dyke anomaly is quite simple—one of the simplest among the various geometrical models that are used for representing geological structures.

By an analytical method, we mean one in which we can start with an observed anomaly and proceed step by step to a solution. We need not expect a unique solution or a complete solution. Potential theory rules against the one, and the degree to which variables are separable limits the other. Nevertheless, a strictly analytical process can establish certain parameters, which may not give all the information required, but which can at least confine it within limits and show what those limits are. For example, the depth of cover is often required; and it will be shown that depth is a secondary determination and sometimes a very uncertain one. For another example, the structural dip and direction of magnetization are combined in a single parameter, and they cannot be separated unless one of them is determined by some other means than a magnetic survey.

Although the present paper deals only with magnetic anomalies, the basis of dyke analysis can be applied as well to gravity and self-potential cases, the mathematical functions being closely related. The writer, in his experience to date, has had more useful results (perhaps through luck) from non-magnetic cases.

* Manuscript received by the Editor March 24, 1958.

† Consulting geophysicist, Toronto, Ontario, Canada.

STATEMENT OF CASE

If a magnetized body has a very great strike length, a uniform cross-section, and uniform magnetization, its anomaly will consist of two elementary functions. These two functions will have odd and even symmetry with respect to a central axis. In the general case it is not difficult to find the axis and resolve the anomaly into its odd and even components.

The above statement requires some qualifying restrictions; but, passing these over for the moment, we can express the anomaly as

$$T = A\lambda + B\phi,$$

where λ and ϕ are geometrical functions, and A and B are coefficients of amplitude.

Considered as a profile across strike, the anomaly has shape and dimensions. The main purpose of this paper is to show that, by abstracting shape from dimensions, we can reduce the problem to a very simple form and be able to analyze an entire anomaly curve rather than having to deal with specific points or features.

Logarithmic plotting is the key. This has been used for some twenty years in resistivity analysis. The method is credited initially to Roman (1934); its significance is fully explained by Watson and Johnson (1938) and by Wetzel and McMurry (1937).

The primary requirement is a set of master curves covering the range of possibilities within a given class of anomaly. The curves are plotted on double logarithmic paper. A field curve is plotted on tracing paper of the same pattern; in this state the dimensions do not affect the shape of the curve but fix its position on the plotting sheet. By sliding the field curve over master curves, it can be established whether the field curve belongs to the given class of anomaly, and, if so, where it belongs within that class, and finally whether it fits to a satisfactory degree of accuracy.

Master curves are related to two normal axes. The field curve when matched will show direct readings of an amplitude and a length corresponding to the two axes. These two values and a parameter of shape represent complete analysis. The process of finding them is like using a slide rule in two dimensions instead of one.

MATHEMATICAL DEVELOPMENT

The dyke anomaly can be expressed as follows, in horizontal and vertical components.

$$\left.\begin{aligned} X &= 2I \sin M[\lambda \cos (M - \psi) - \phi \sin (M - \psi)] \\ Z &= 2I \sin M[\lambda \sin (M - \psi) + \phi \cos (M - \psi)] \end{aligned}\right\}, \qquad (1)$$

where λ stands for the function $\ln r_1/r_2$, and other symbols are identified in footnote 1 and Figures 1 and 2.

This is often called Haalck's formula, although several writers have pointed out that what Haalck actually published (in 1927) was wrong. Koulomzine and Massé (1947) have given a complete development of the case in terms of complex variables. The present writer used their work some years ago for developing a more versatile model—the dyke whose upper surface is tilted from the horizontal.

This more general case can be expressed,

$$\left.\begin{aligned} X &= 2I \sin (M - N)[\lambda \cos (M + N - \psi) - \phi \sin (M + N - \psi)] \\ Z &= 2I \sin (M - N)[\lambda \sin (M + N - \psi) + \phi \cos (M + N - \psi)] \end{aligned}\right\}. \qquad (2)$$

Any of these expressions can be condensed to the elementary form,

$$T = A\lambda + B\phi.$$

So can the total-force anomaly if it is considered as nothing more than the projection of X and Z on an axis of fixed orientation.

One reason for introducing the general expression at this stage is that the character of λ and ϕ can be examined without unnecessary restrictions. The anomaly of a scarp, for example, is expressed by calling M the regional slope of bedrock surface (zero or otherwise) and N the slope of the scarp face. The occasion for developing the general case happened to be a ground survey in mountainous country, where survey surface and bedrock surface could often be equated

[1] *Symbols not defined in text*

X, Z—horizontal and vertical components of anomaly as departures from normal field.

T—general symbol for unspecified anomaly.

I, ψ—Strictly speaking, the anomalous magnetization is a vector difference between the directed values of specific volume intensity inside and outside the anomalous body. The component along strike contributes nothing to the anomaly so that the significant quantities, I, an intensity, and ψ, a dip angle, represent the anomalous vector projected into the xz-plane. For cases of induced magnetism the anomalous intensity is kF_0, or the product of susceptibility-difference and regional total field; and this with the geomagnetic dip must be projected into the xz-plane.

M, N—structural dip of the boundaries of the general model; M for the parallel walls extending to infinity, and N for the base (mathematically, the top of dyke or face of scarp can be called a base for the figure of the model, and a base for the character of anomaly). M, N, and ψ are all directed angles, considered positive when measured downwards from the x-axis; and M must lie in the range $N < M < N + \pi$.

r_1, r_2—distances from the point of observation to the two edges of base; r_1 refers to the northerly edge in a sense of rotation. Specifically, if the body is viewed in cross-section normal to the strike axis, and viewed towards the more westerly direction of strike (as in Figures 1 and 2), the boundary of the body can be traced in a clockwise sense and this can be called northerly; because this boundary contour represents the limiting traverse along which we can proceed northerly, around and over, but not through, the body. In Figure 1, whatever the direction of the x-axis, r_1 and r_2 would remain as shown.

ϕ—angle between the lines r_1 and r_2; becomes negative if the base is viewed from the inner side (from the right of center for the scarps in Figure 2).

to extensive planes of marked slope, and where dykes and horizontal beds were the usual cause of anomalies.

Now, taking the general expression, consider the co-ordinates a, h as a rotation from x, z through the angle N (see Figure 1). Then a represents traverse-distance along a line parallel to the top of the dyke. Let d be the half-breadth of the top of the dyke, and h be the height of observation (perpendicular distance between top of dyke and traverse).

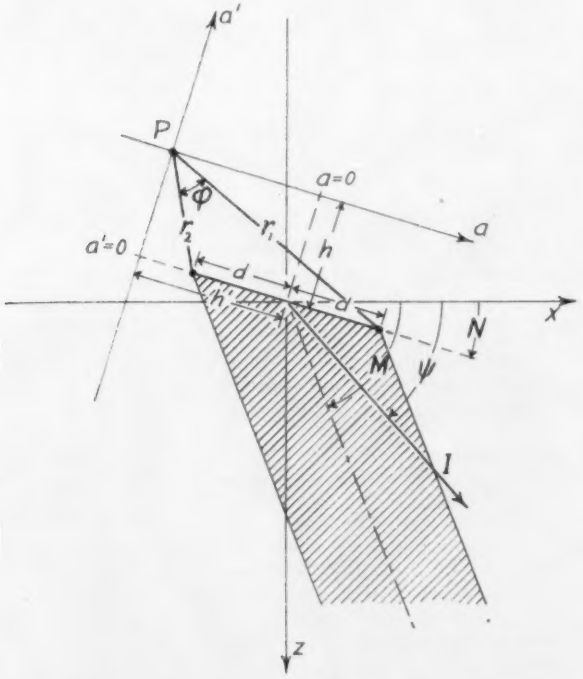

FIG. 1. Cross-section through the general dyke model, to illustrate symbols used in text. The x-axis is horizontally across strike, preferably towards the north; the z-axis is vertically downwards; the y-axis (not shown) is along strike, and all properties are considered uniform with respect to y. The boundaries of the dyke are defined by a length and two angles: d is the half-breadth of the top, N the slope of the top, and M the dip of the dyke walls, the walls being assumed parallel and extending to infinite depth.

P is a general point of observation, and through P there are two directions, a and a', along which the anomaly in profile can have analytical symmetry. The two directions give two classes of anomaly, and these are distinguished by the terms "dyke" and "scarp." Height of observation (or depth to anomalous body) is represented by h or h', according to class. The "thin bed" model can be regarded as a slice off the top of the dyke, having infinitesimal thickness t in the direction of h.

The anomalous magnetization is projected into the xz-plane as a vector of magnitude I and dip ψ.

Then

$$r_1 = \sqrt{(a-d)^2 + h^2} \quad \text{and} \quad r_2 = \sqrt{(a+d)^2 + h^2},$$

whence

$$\left.\begin{aligned} \lambda &= \ln \sqrt{\frac{a^2 + d^2 + h^2 - 2ad}{a^2 + d^2 + h^2 + 2ad}} = -\tanh^{-1} \frac{2ad}{a^2 + d^2 + h^2} \\ \text{and} \qquad \phi &= \tan^{-1} \frac{h}{a-d} - \tan^{-1} \frac{h}{a+d} = \tan^{-1} \frac{2hd}{a^2 - d^2 + h^2} \end{aligned}\right\}. \tag{3}$$

It is easy to show that the extremes of λ and the points of half-amplitude of ϕ occur at $a^2 = d^2 + h^2$. This indicates an obvious normalizing factor for length, if we wish to examine λ and ϕ as functions of a. Thus we can put (see Figure 2)

$$h = R \cos\theta, \qquad d = R \sin\theta, \quad \text{and} \quad a = \alpha R.$$

Then

$$\left.\begin{aligned} \lambda &= -\tanh^{-1} \frac{2\alpha \sin\theta}{1 + \alpha^2} \\ \phi &= \tan^{-1} \frac{\sin 2\theta}{\cos 2\theta + \alpha^2} \end{aligned}\right\}. \tag{4}$$

Finally, dividing by 2θ, we can normalize for amplitude, so that for all θ, when

$$\alpha = 0, \qquad \phi_n = 1 \text{ and } \lambda_n = 0;$$

and when

$$\alpha^2 = 1, \qquad \phi_n = 1/2 \text{ and } \pm\lambda_n = \text{extreme} = 1/2 \text{ or more.}$$

The normalized functions, $\lambda_n(\alpha)$ and $\phi_n(\alpha)$ are tabulated and plotted for $\theta = 0°$, 45°, 60°, 75°, and 90°.

Equations (4) express λ and ϕ as functions of traverse distance for a special case in which the top of the dyke is parallel to the line of traverse. There is a second special case, with functions of corresponding symmetry, which for convenience may be called the scarp case, the face of scarp being perpendicular to traverse.

These functions are derived in the same manner, with h measured from the center of the scarp face, and d having the same direction as h. In this case we put

$$h = R \cosh\omega, \qquad d = R \sinh\omega, \quad \text{and} \quad a = \alpha R.$$

Then[2]

$$\left.\begin{aligned}\lambda &= \tanh^{-1}\frac{\sinh 2\omega}{\cosh 2\omega + \alpha^2}\\ \phi &= \tan^{-1}\frac{2\alpha \sinh \omega}{1+\alpha^2}\end{aligned}\right\}. \tag{5}$$

It is equally valid to write

$$\left.\begin{aligned}\lambda &= \tanh^{-1}\frac{2\sin\theta}{1+\sin^2\theta+\alpha^2\cos^2\theta}\\ \phi &= \tan^{-1}\frac{2\alpha\tan\theta}{1+\alpha^2}\end{aligned}\right\}. \tag{5a}$$

These functions are normalized for amplitude by the divisor 2ω. The relation between the two forms (5 and 5a) can be expressed

$$\tan\theta = \sinh\omega, \quad \text{or} \quad \sin\theta = \tanh\omega.$$

On the basis of symmetry λ(scarp) belongs to the family ϕ(dyke) and ϕ(scarp) to the family λ(dyke). In particular, when θ or ω equals zero,

$$\lambda(\text{scarp}) = \phi(\text{dyke})$$
$$-\phi(\text{scarp}) = \lambda(\text{dyke}).$$

The normalized scarp functions are tabulated and plotted for $\omega = 0.881$, 1.315, and 2.03, which correspond to

$$\theta = 45°, \ 60°, \quad \text{and} \quad 75°.$$

This completes the family of dyke and scarp curves.

[2] The elementary scarp functions are given without plus or minus sign, because they can have either with equal probability. The proper sign—to be consistent with the general expression of anomaly—is determined from the specific definitions of r_1, r_2, and ϕ in footnote 1. Note also, in Figure 1, that the xz-plane is divided quadrantally by the base plane (in projection the axis of dip N) and its normal; and, with this frame of reference, λ and ϕ change sign according to quadrant in a manner resembling the sine and cosine of an angle. Thus for traverse a' in Figure 1, λ(scarp) is always positive, ϕ(scarp) is positive with respect to a'. To the right of the body a corresponding scarp traverse would have to run downwards (antiparallel to a') to be northerly in rotation; this condition is exactly reproduced by the scarps in Figure 2, and both scarp functions would now have negative sign. The dyke case is simpler. λ(dyke) is always negative with respect to a. ϕ(dyke) is positive for all a with this exception: A composite traverse (in Figure 1) could include a segment having the direction of a but lying below the base plane, and the anomaly for this segment would contain ϕ (dyke) locally negative. The sign of coefficients is another matter, having nothing to do with the sign proper to an elementary function.

Finally, a third special case is required. This may be called the thin-bed anomaly. It is defined as the negative h-derivative of the dyke anomaly multiplied by a thickness factor Δh or t, and with modified coefficients (equations (2)) such that $M-N=90°$. When fully normalized these functions can be expressed

$$\left.\begin{aligned}\frac{R}{2\tan\theta}\lambda' &= \frac{-2\alpha\cos^2\theta}{(1+\alpha^2)^2-4\alpha^2\sin^2\theta}\\ \frac{R}{2\tan\theta}\phi' &= \frac{(1-\alpha^2)\cos\theta}{(1+\alpha^2)^2-4\alpha^2\sin^2\theta}\end{aligned}\right\}. \tag{6}$$

These are tabulated and plotted as for the dyke.

Two other simple cases may be mentioned, though not considered part of

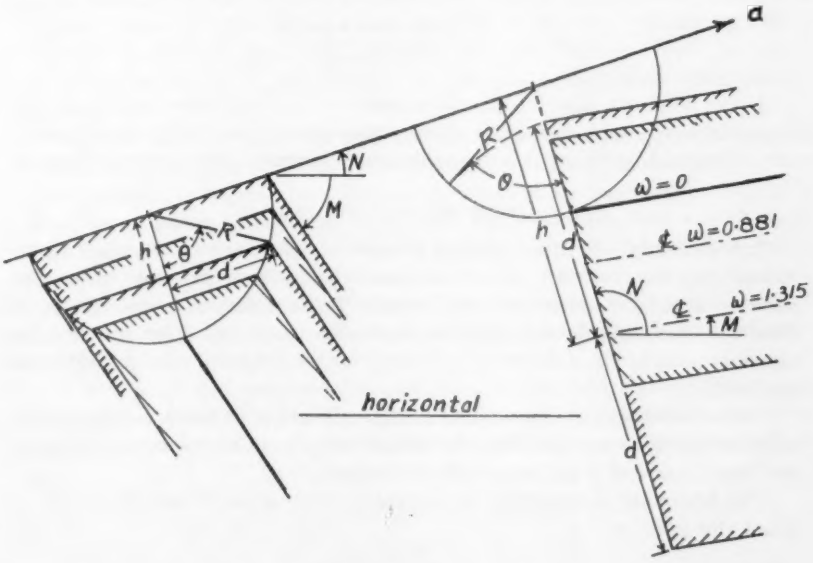

FIG. 2. Family of dykes (left) and family of scarps (right) satisfying the conditions for analytical symmetry with respect to a common traverse-line a. In each family the radius R is a common parameter, so that the anomaly for each member of the family will have the same basic points of symmetry. The dimensions h, d, and θ are shown for one member of each family. A choice in expressing the scarp anomaly is given by the relation: $d/R=\tan\theta=\sinh\omega$.

In the dyke family are shown five members covering the full range of possibilities. In the scarp family only three members are shown. With larger values of θ, or ω, we approach a particular case of another class—the plane contact extending to infinite depth; and the anomaly is then one of simple analytical symmetry requiring no restriction on structural dip.

In this illustration it may be noted that M is positive for the dykes, negative for the scarps, and N is negative for both. The value of M, however, has no bearing on the question of symmetry.

this paper. One can be called the thin-vein anomaly (counterpart of the thin bed, derived from the scarp). The other is the anomaly of a plane contact:

$$T = -A \ln r + B \tan^{-1} a/h.$$

One way of dealing with the plane contact is to take its a-derivative, which consists of the functions for a thin dyke (λ and ϕ, with $\theta=0$).

To conclude this section we record general expressions for λ and ϕ (dyke or scarp) as functions of x and z. The x-axis need not be considered horizontal so long as it is understood to be the reference axis for the angles M, N, and ψ (equations (2) and Figure 1). Then,

$$\left.\begin{aligned} \lambda &= -\tanh^{-1}\frac{2d(x\cos N + z\sin N)}{x^2+z^2+d^2} \\ \phi &= \tan^{-1}\frac{2d(x\sin N - z\cos N)}{x^2+z^2-d^2} \end{aligned}\right\}. \tag{7}$$

It can be shown that the general expression $T(x)=A\lambda+B\phi$, and its derivatives, can have simple symmetry about some center x_0 and radius points $x_0 \pm x_1$ only when $\sin 2N=0$; and it is upon this simple symmetry that analysis depends.

SYMMETRY OF FUNCTIONS

It is probably safe to say that all systems of dyke analysis are based fundamentally on the symmetry of the functions λ and ϕ. It is quite safe to say that some systems have limited validity because they are derived from only one of these functions and do not apply to anomalies where the other function has significant amplitude. A review of symmetry for the dyke and related cases seems justified.

The symmetry of the elementary functions λ and ϕ, as listed, is valid specifically for the dyke case; but what is said of λ applies in all respects to ϕ(scarp), and what is said of ϕ applies equally to λ(scarp).

The first point of symmetry is the center, $a=0$, or $\alpha=0$; and the symmetry about this point is

$$\left.\begin{aligned} \lambda(-\alpha) &= -\lambda(+\alpha) \\ \phi(-\alpha) &= \phi(+\alpha) \end{aligned}\right\}. \tag{8}$$

The second point of symmetry is at radius-distance from center, $a^2=R^2$, or $\alpha^2=1$; and the symmetry about this point is

$$\left.\begin{aligned} \lambda(1/\alpha) &= \lambda(\alpha) \\ \phi(1/\alpha) &= \phi(0) - \phi(\alpha) \end{aligned}\right\}. \tag{9}$$

For the thin-bed functions λ' and ϕ', the central symmetry is expressed by equations (8); and symmetry about the radius point is

$$\left.\begin{aligned}\lambda'(1/\alpha) &= \alpha^2\lambda'(\alpha)\\ \phi'(1/\alpha) &= -\alpha^2\phi'(\alpha)\end{aligned}\right\}. \tag{10}$$

Equations (9) and (10) express characteristic symmetry of the functions which is well suited to logarithmic plotting. It is obvious that this symmetry is helpful in constructing master curves, because basic computation need only be done in the range $0 \leq \alpha \leq 1$.

There is a definite practical use for the symmetry of ϕ in equation (9). It is this.

The component of even symmetry derived from a field anomaly cannot be logarithmically plotted without first choosing a datum or zero-level. Background magnetic level is not always an easy thing to determine from survey results. Varying the choice of datum will vary the shape of the plotted curve. This affects the determination of R, although θ is less affected, being usually determined in the range $\alpha < 1$.

The even component of the field anomaly, however, can be plotted as peak-less-anomaly, giving a curve that rises rapidly from center and levels off more or less (according to magnetic roughness of the area) at a value equal to amplitude. Thus the magnetic background is plottable logarithmically over a large range. This upside-down anomaly can then be matched against the ϕ master-curves reversed; because logarithmically these are curves of $\phi(1/\alpha)$, and this, by equation (9), is peak-less-anomaly. Thus one stage of plotting does the job, and the uncertainty of R appropriate to the uncertainty of background can be directly determined.

A final point that may be called symmetry is that the thin-bed functions are basically the h-derivatives of the dyke functions and are therefore also the a-derivatives, with the following relation (λ' and ϕ' being as expressed in equations (6)):

$$\lambda' = -\partial\lambda/\partial h = +\partial\phi/\partial a$$
$$\phi' = -\partial\phi/\partial h = -\partial\lambda/\partial a.$$

Thus, in the thin-bed functions we have a set of master curves suitable for any first-derivative treatment of dyke anomalies.

By a closely related argument, it can be said also that λ and ϕ for the magnetic dyke or scarp constitute the first derivatives of the gravity anomaly for dyke or scarp, apart from coefficients. The magnetic master curves for the dyke or scarp can be used directly for gravity analysis of bodies in the thin-bed or thin-vein classes, as defined in connection with equations (6).

COEFFICIENTS—AMPLITUDE

In the system of complex variables, as used by Koulomzine and Massé (1947) the dyke (or scarp) anomaly can be completely expressed

$$\boldsymbol{T} = \boldsymbol{K}(\lambda + i\phi),$$

where $\boldsymbol{K}$ is a complex coefficient of amplitude. Then for any orthogonal components, U and V, in the xz-plane,

$$\text{if } U = A\lambda + B\phi, \qquad \boldsymbol{K} = A - iB \quad \text{or} \quad iA + B,$$

whence

$$V = \pm (B\lambda - A\phi).$$

It follows that a knowledge of one component of the anomaly is sufficient to give all the obtainable information, λ and ϕ being equally suitable for analysis.

There will be a reduction of amplitude, however, if the anomaly is read on some axis not in the xz-plane, as may happen in total-force or horizontal-force surveys. When practical, therefore, the measurement of vertical component is to be preferred.

The nature of the coefficients implies that the anomaly, no matter how it is surveyed, can provide only two equations in the four possible unknowns, I, M, N, and ψ—equations (2). In practice, however, N must be known or assumed so as to satisfy the conditions for symmetry given with equations (7).

The form of coefficients A and B for a particular case can always be determined from the general expression, equations (2). This is merely trigonometry and need not be elaborated here; but a few points are worth mentioning.

In dealing with the logarithmic master curves, one must realize that they are all normalized for geometric amplitude, the normalizing factors being $1/2\theta$, $1/2\omega$, and $R/2 \tan \theta$, for the three classes presented. The dyke anomaly $(A\lambda + B\phi)$ can be equally well expressed as $2\theta(A\lambda_n + B\phi_n)$. In curve-matching the amplitude of a field curve is read off as a value in gammas corresponding to the horizontal axis $\lambda_n = 1$ or $\phi_n = 1$. The magnetic amplitudes, A and B, will be these values divided by 2θ, or by the normalizing factor appropriate to the class. For this purpose θ must be in radians, not degrees.

It can be seen from equations (2) that the general anomaly has a true amplitude,

$$\sqrt{A^2 + B^2} = 2I \sin (M - N),$$

and that A and B are related by a phase-angle $(M + N - \psi)$. The true thickness of parallelepiped (dyke or scarp) can always be expressed as $t = 2d \sin (M - N)$ so that true amplitude can be written as It/d.

For a thin dyke (θ less than 45°), θ and, therefore, d may not be determinable at all; but we have the approximate relation $d = R\theta$, whence the true amplitude is

$It/R\theta$. Since the master curves give direct readings of $2\theta A$, $2\theta B$, and R, it is possible to determine It, the product of thickness and intensity of magnetization. In the thin-bed class the true amplitude is $2It$, by the conditions for equations (6); and for small θ the determinable value will be Is, or magnetization times cross-sectional area; the limiting case in this class is the anomaly of a horizontal cylinder.

For a sample of reduced amplitude, consider the total-force anomaly represented by equations (1) projected on the total-field axis:

$$F = Z \sin J + X \cos Az \cos J$$
$$= A\lambda + B\phi.$$

Then

$$A = 2I \sin M(\cos J \cos Az/\cos j) \cos (j + \psi - M)$$
$$B = 2I \sin M(\cos J \cos Az/\cos j) \sin (j + \psi - M),$$

where J is the geomagnetic dip, j is its projection in the xz-plane, and Az is the difference in azimuth between the xz-plane and the plane of the magnetic meridian.

The apparent amplitude of this anomaly is the true amplitude ($2I \sin M$) multiplied by the reduction factor ($\cos J \cos Az/\cos j$). If $Az = 0$ (east-west strike), there is no reduction of amplitude. If $Az = 90°$, the reduction factor becomes $\sin J$. Or if $J = 0$ (magnetic equator, or a horizontal-force survey), the reduction factor is $\cos Az$.

Thus for an airborne survey in low magnetic latitudes there may be a two-dimensional body with a healthy anomaly in X and Z, of which little or nothing will be observed if strike is northerly. With most present-day equipment the observed anomaly, whether vertical, horizontal, or total force, is always measured in the plane of the magnetic meridian. In the case just cited a vertical-force survey would be the only practical method of detecting the anomaly at full strength.

In a case of induced magnetism only, $\psi = j$; and a body striking north at the magnetic equator will produce no anomaly at all, because magnetization is entirely along strike; pole effects can appear only where strike continuity is interrupted.

Finally, there is the question of what useful information can be derived from the magnetic amplitudes. Geomagnetic values are well enough established in most parts of the world that J, Az, and, therefore, j can be considered as known quantities; so there is no increase in the number of unknowns in the total-force anomaly. Induced magnetism is often assumed as a basis for analysis; this implies that ψ is known and, therefore, M and I can be determined. But there are numerous cases where M is known within reasonable limits from geological data, and the consequent determinations of I and ψ may show that magnetization is completely independent of the geomagnetic field. This is not surprising in view of what has been published on such subjects as processes of magnetization, remanence and structural deformation, and the history of the earth's magnetic field.

Thus for analysis it must be a matter of judgment based on local geological knowledge as to whether M (the structural dip known or probable) or ψ (assumption of induced magnetism) is the better starting point from which to determine the other quantities.

The value of determining I may often be a matter of elimination. For example, a large and strong anomaly may be found to involve a degree of magnetization not at all uncommon to rock types of the region and to have no particular significance in connection with the survey. In iron surveys, on the other hand, the question of converting a high magnetization or susceptibility into percentage of magnetite is very uncertain, although a rough figure may be helpful. And in some cases, already cited, I is not separable from t.

RESTRICTIONS OF FORM

Two basic restrictions in the present paper are that the anomalous body has the form of a parallelepiped and that it has infinite strike length.

The assumption of infinite strike length simplifies the case mathematically. (The anomaly of a short dyke, for example, contains nine elementary functions instead of two.) The meaning of a "two-dimensional" anomaly may be explained as follows. Let strike direction be y in an xyz co-ordinate system. Without specific proof, it should be obvious that if all the properties of the body are uniform with respect to y, then potential will be independent of y, and there can be no y-component of the anomalous field—even if there is a y-component of magnetization within the body. The anomaly is two-dimensional in the sense that its components are confined to the xz-plane; and the vector equations expressing the basic laws of potential field theory are accordingly simplified.

With this condition of strike uniformity, the parallelepiped can be treated simply as a parallelogram in the xz-plane. The general anomaly has been presented for the case where one side of the parallelogram is at infinity; and it is shown that the anomaly depends basically on the geometry of the near side, as defined by the vector $\boldsymbol{d}$.

For the elementary functions to be have simple analytical symmetry, the vector $\boldsymbol{d}$ must be either parallel or perpendicular to the line of traverse. And for the elementary functions to be two in number (rather than four) the side opposite $\boldsymbol{d}$ must be at either infinite or zero distance from $\boldsymbol{d}$.

These are the restrictions mentioned in the statement of the case. Uniformity of cross-section is not enough; the type of cross-section must be specified.

Other than uniformity, there need be no restriction on the nature of magnetization. It may be induced or permanent, in the sense of being dependent or not on the surrounding field. This point affects the coefficients but not the elementary functions.

TWO-DIMENSIONAL CRITERIA

To qualify for this case, a body must have great strike length, and its properties must be reasonably uniform along the strike.

In airborne surveys, a common sort of anomaly is one that runs for miles and appears to represent a single, continuous structure. It is less common to find an anomaly that is strictly two-dimensional in the sense of being invariable along the strike. But any variation of anomaly in the y-direction necessarily implies the presence of a y-component; and clearly if marked y-variations exist, two-dimensional analysis will not be valid.

A basic criterion for a two-dimensional case is that the contours of the anomaly (whatever the observed component) must run parallel for a distance at least equal to the length of profile required for analysis. For reasonable results, this length must obviously exceed the diameter ($2R$) of the anomaly.

From a study of the magnetic anomalies of short dykes, it is found that, if magnetization is entirely down-dip, the anomaly on a central profile across strike will be reasonably similar to the infinite-dyke profile. Such a case, if analyzed by the infinite-dyke process, gives a value of R that is less than the true value but with a limiting error of about 20 percent. The effect of other components of magnetization is too large a subject for the present paper.

ANALYTICAL PROCEDURE

Some distinction must be made between the general subject of interpretation and the more specific subject of analysis. In any geophysical survey there is information to be read from the character of results, chiefly from contour patterns, as to what sort of rock types or structures occur and where the features are that may have a direct bearing on the exploration problem. These are questions of interpretation; finding the answers is largely a matter of skill in geophysical map-reading.

Analysis, in the sense used throughout this paper, means the measurement of a particular anomaly to establish the position, dimensions, and attitude of the anomalous body, as well as its magnetization or other physical property, so far as these things can be determined. This is distinct from synthesis, the converse problem of computing an anomaly from a known set of conditions.

In any case, the first requirement is a contour map. Interpretation, both geophysical and geological, precedes analysis; and this should establish which anomalies can legitimately be treated as dykes, thin beds, or other elementary forms. For examples, see Smellie (1956) and Vacquier et al. (1951). The true meaning of an analytical solution will always depend on this stage of interpretation, because, for example, it is possible to have a "dyke" anomaly from a distribution of magnetic matter that does not in any respect constitute a structural dyke.

Since we are dealing here only with the two-dimensional anomaly, the logical basis for analysis is a profile at right angles to the strike axis. The nature of the survey may suggest whether it is more sensible to treat several profiles individually or to use an average profile.

The competent geophysicist should have no difficulty in spotting the approximate center of a dyke anomaly. If the profile is first drawn on thin cross-section

TABLE 1A—DYKE AND SCARP—ODD FUNCTION

$\frac{1}{2\theta}\lambda$ (dyke) $\qquad$ $\frac{1}{2\omega}\phi$ (scarp)

α	$\theta=90°$ $\omega=$	75°	60°	45°	0 0	0.881	1.315	2.03
0	0.000	0.000	0.000	0.000	0.000	0.000	0.000	0.000
0.1	0.064	0.074	0.083	0.090	0.099	0.111	0.125	0.157
1/7	0.092	0.106	0.118	0.128	0.140	0.155	0.172	0.199
0.2	0.129	0.149	0.165	0.177	0.192	0.208	0.223	0.237
0.3	0.197	0.226	0.248	0.261	0.275	0.285	0.289	0.276
0.4	0.270	0.306	0.329	0.339	0.345	0.342	0.332	0.296
0.5	0.350	0.390	0.407	0.407	0.400	0.383	0.359	0.308
0.6	0.440	0.483	0.480	0.465	0.441	0.410	0.376	0.314
0.7	0.554	0.580	0.544	0.509	0.470	0.428	0.387	0.318
0.8	0.695	0.670	0.591	0.539	0.488	0.438	0.394	0.321
0.9	0.952	0.749	0.620	0.556	0.497	0.444	0.397	0.322
1.0	∞	0.775	0.628	0.560	0.500	0.446	0.398	0.322

TABLE 1B—DYKE AND SCARP—EVEN FUNCTION

$\frac{1}{2\theta}\phi$ (dyke) $\qquad$ $\frac{1}{2\omega}\lambda$ (scarp)

α	$\theta=90°$ $\omega=$	75°	60°	45°	0 0	0.881	1.315	2.03
0	1.000	1.000	1.000	1.000	1.000	1.000	1.000	1.000
0.1	1.000	0.9981	0.9958	0.9936	0.9901	0.9844	0.9753	0.944
1/7	1.000	0.9960	0.9916	0.9870	0.9800	0.9691	0.9527	0.904
0.2	1.000	0.9921	0.9832	0.9746	0.9615	0.942	0.916	0.852
0.3	1.000	0.9814	0.9612	0.943	0.918	0.885	0.847	0.775
0.4	1.000	0.9646	0.929	0.899	0.861	0.821	0.780	0.714
0.5	1.000	0.940	0.885	0.845	0.800	0.756	0.719	0.662
0.6	1.000	0.903	0.826	0.780	0.735	0.696	0.664	0.621
0.7	1.000	0.846	0.756	0.710	0.671	0.640	0.616	0.585
0.8	1.000	0.762	0.674	0.639	0.610	0.588	0.572	0.554
0.9	1.000	0.643	0.586	0.567	0.552	0.542	0.533	0.525
1.0	1.000 0.500 0.000	0.500	0.500	0.500	0.500	0.500	0.500	0.500

TABLE II—THIN BED—ODD AND EVEN FUNCTIONS

$\frac{R}{2\tan\theta}\lambda'$ $\qquad$ $\frac{R}{2\tan\theta}\phi'$

α	$\theta=0$	45°	60°	75°	0	45°	60°	75°
0	0.000	0.000	0.000	0.000	1.000	0.707	0.500	0.259
0.1	0.196	0.100	0.0505	0.0136	0.970	0.699	0.500	0.261
1/7	0.274	0.143	0.0729	0.0198	0.940	0.693	0.500	0.263
0.2	0.370	0.200	0.1038	0.0288	0.888	0.677	0.499	0.267
0.3	0.505	0.298	0.163	0.0472	0.766	0.639	0.495	0.275
0.4	0.595	0.390	0.231	0.0717	0.624	0.579	0.485	0.291
0.5	0.640	0.470	0.308	0.106	0.480	0.499	0.461	0.308
0.6	0.649	0.531	0.390	0.159	0.346	0.400	0.415	0.330
0.7	0.630	0.565	0.466	0.240	0.230	0.291	0.340	0.338
0.8	0.595	0.568	0.519	0.357	0.134	0.181	0.234	0.310
0.9	0.549	0.544	0.532	0.474	0.058	0.081	0.112	0.194
1.0	0.500	0.500	0.500	0.500	0.000	0.000	0.000	0.000

When $\theta=90°$ both functions are zero except at $\alpha^2=1$.

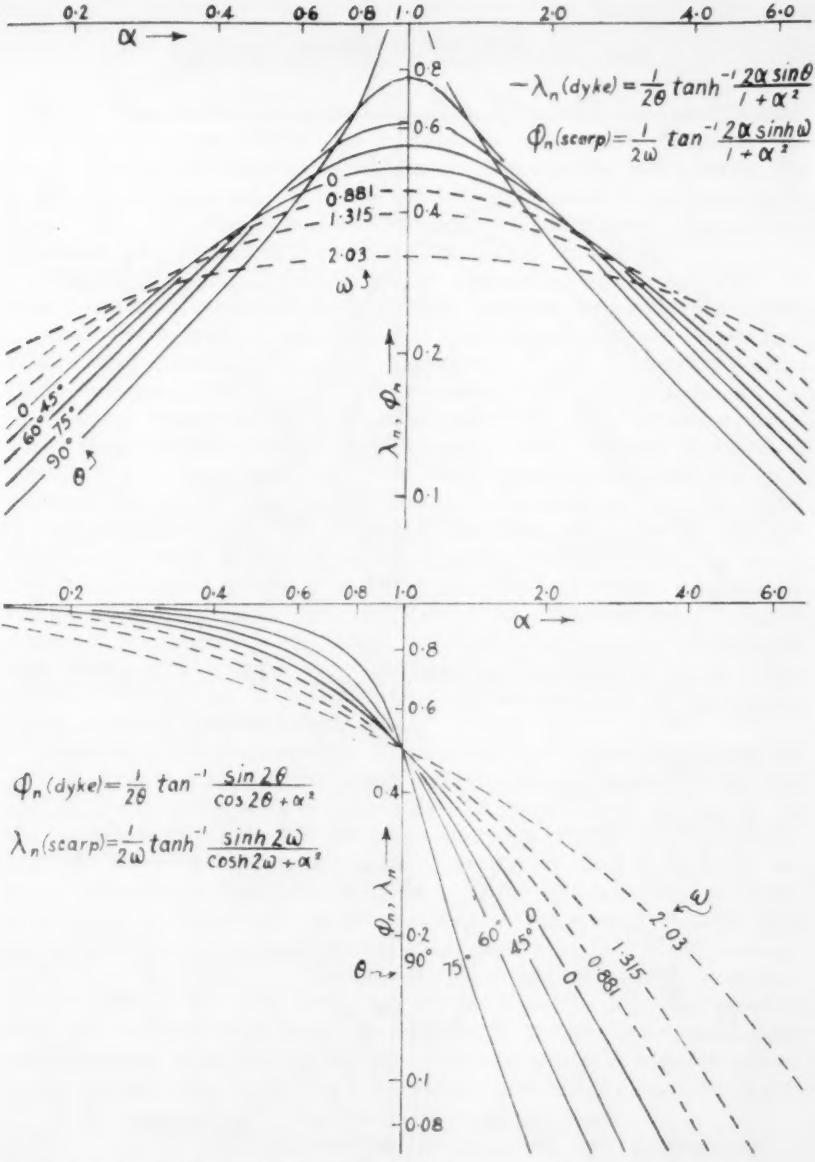

FIG. 3. Normalized elementary functions of dyke anomaly (solid lines) and scarp anomaly (broken lines), plotted logarithmically and showing change of shape with respect to the parameters θ and ω. Upper set are functions of odd symmetry, lower set functions of even symmetry, about the center of the anomaly ($\alpha=0$). Traverse distance, α, is in units of radius-of-anomaly, measured from center. Apart from the sign of coefficients in the general expression of anomaly, the elementary functions have their own proper sign. λ (dyke) is always negative for positive α; ϕ (dyke) is usually positive for all α, but certain exceptions are possible. The scarp functions can be positive or negative with equal probability. Particulars are given in footnote 2. Tables IA and IB show the computed values for these master curves.

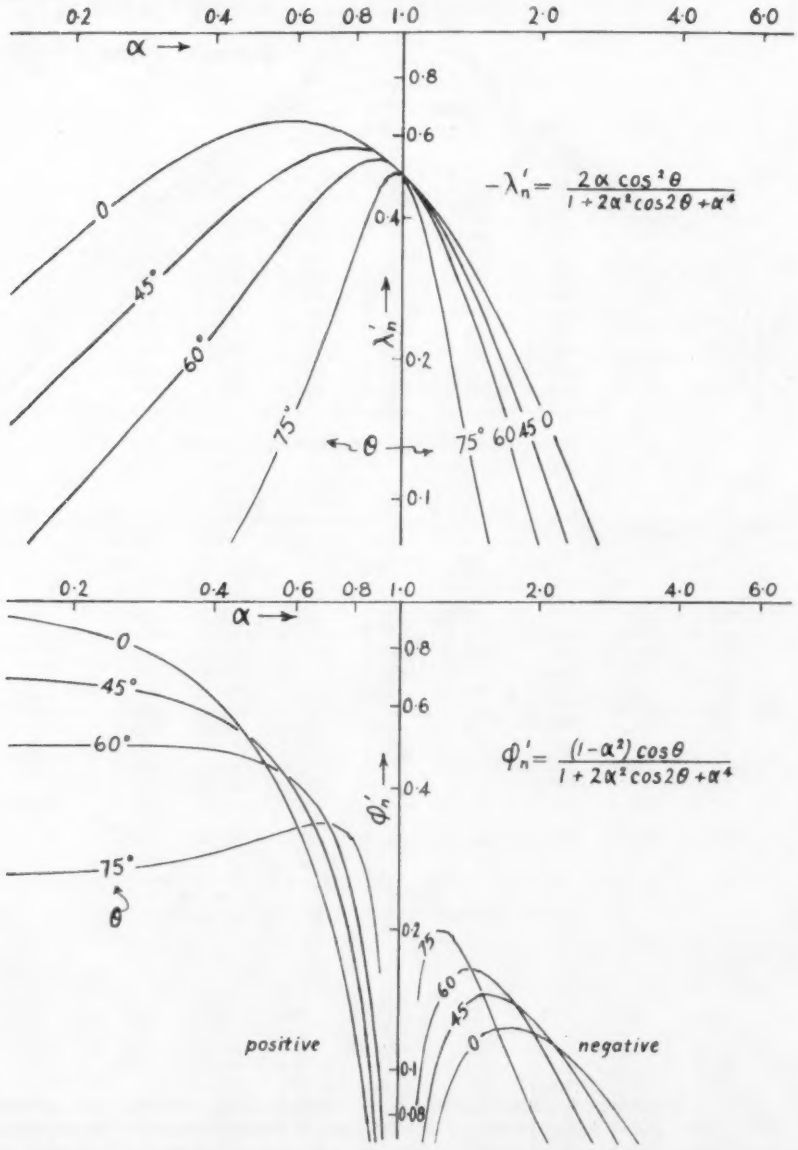

FIG. 4. Normalized elementary functions of the thin-bed anomaly, plotted in the same manner as in Figure 3, but without the functions derivable from the scarp anomaly. Note that the even function ϕ' changes sign at $\alpha = 1$. λ' represents both the vertical derivative of λ (dyke) and the horizontal derivative of ϕ (dyke). Similarly, ϕ' represents the vertical derivative of ϕ (dyke) and the horizontal derivative of λ (dyke). Computed values for these master curves are given in Table II.

paper, it can be folded at the approximate center, and the right and left halves can be compared by eye; their average represents an even function of traverse distance, and the half-difference represents the corresponding odd function; the position of fold can be adjusted so that the half-amplitude of one function and the peak of the other coincide in distance from the fold. This gives at least an approximate determination of center and radius (R) of the anomaly.

The odd function can now be directly replotted on logarithmic paper (to match the scale of master curves) in whatever field units are used for the survey: gammas against feet, meters, miles, etc. The even function can be similarly plotted after deduction of magnetic base-level, or it can be inversely plotted (peak-less-anomaly) as suggested in the discussion of the symmetry of functions.

Obviously when these field curves are matched with the two families of master curves (Figure 3) they must both give the same values of R and θ. R is read off directly as the length (feet, meters, etc.) on the field plotting sheet that corresponds with the vertical axis ($\alpha = 1$) of the master curves; and θ is read off (by interpolation, if necessary) from the particular master curve that fits the field curve in each family. Sometimes the fit can be improved by adjusting the choice of center and replotting. Sometimes it is obvious that only a rough fit is possible; and in such a case it is often found that R is reasonably well established though θ remains uncertain. Sometimes it is clear that the field curves do not belong to the dyke class at all. They may—with a readjustment of center or datum—be found to belong to the thin-bed class, or to lie between the two classes; and this signifies a body of minor or moderate depth extent.

In one respect, a weakness of fit is to be expected in the dyke anomaly. It may be noted that the functions λ fade out gradually with increasing traverse distance, being calculated for a model dyke with truly infinite depth extent. It can also be seen that the functions λ' are the same sort of curves with a much more rapid fade-out. In actual dyke anomalies a truly infinite depth extent is not expected. The writer has not yet found one in which the odd function did not begin to fall below the master curve at distances greater than a few R, although this can be due to failure of strike infinity as well as depth extent.

Background gradient, background curvature, and neighboring anomalies are complications that often arise. They can sometimes be eliminated satisfactorily; this is a matter for ingenuity. If, however, the anomaly under examination cannot be cleared of other anomalies, one can at least determine from the master curves the possible limits of R and θ. The method of inverting ϕ (as stated in the section on the symmetry of functions) is useful in this respect.

The question of amplitudes has already been discussed, and it has been pointed out that an amplitude read from the horizontal axis of master curves is not simply the type of coefficient indicated by equations (2). There is a large variety of problems in which the elementary functions can be directly analyzed for shape and dimensions, but the particular form of coefficients may be complicated. In practice there are many cases where the location and outline of anomalous bodies are all that matters, and further specific properties are not required; in such cases the resolution of coefficients may be passed over.

Another matter is the relative amplitude of the two functions, and this involves the direction of magnetization relative to the boundary planes of the dyke or other model. It may happen that only one function appears for analysis, the other being insignificant.

Depth determination depends, in the first place, on how well R can be determined and, secondly, on whether the field curve is sufficiently pure to give a reliable value of θ. It can be seen from the grouping of master curves that shape is more or less directly sensitive to $\cos\theta$; and $h = R\cos\theta$. This would suggest that h ought to be directly readable. But it is not unusual in an airborne survey to find a dyke anomaly or group of anomalies giving a consistent value of R, say half a mile, and values of θ ranging apparently between 0° and 60°. It is difficult to argue that the large values of θ in such a case are really due to reduced depth rather than to distortion of anomaly from some other cause. If flying height is 1,000 ft, the conclusion in this case is that basement surface (top of dykes) is, in round figures, anywhere between ground surface and 1,500 ft down. The purpose of this illustration is not to belittle the idea of depth determination but to show that, by complete analysis, anomalies may be found incapable of giving usefully accurate depths.

SAMPLE CASES

A few cases from the writer's experience are outlined here as examples of what can be done with analysis. They are chosen more as curiosities than as routine cases.

Case 1—Ground magnetic

This was a strong anomaly answering closely to dyke characteristics, near the magnetic equator, and found in a ground survey on a slope of 30°–40°. Determinations of h and d were fairly definite and with consistency along the strike. Magnetization was too strong to be ascribed to susceptibility; and I, as determined from the anomaly, agreed reasonably with direct measurements of I on samples of basalt float. If the direction of magnetization were horizontally north (in alignment with the geomagnetic field) the structural dip would have to be steep; but a more probable solution, from limited drilling and other geological information, would be a nearly horizontal structural dip and, therefore, magnetization steeply downwards.

Case 2—Aeromagnetic

This was a system of dykes striking about east-west (magnetic) in high magnetic latitude. Strong and consistent end-effects occurred where the dykes were offset by cross-faults, and there was negligible anomaly near mid-section of dykes. General structural trends had been established by ground examination of the outcrop. The most obvious geophysical solution was a direction of magnetization horizontally along strike, towards the west.

Case 3—Aeromagnetic

Here there were magnetite sands in present and ancient river channels, with

a low-level airborne survey to distinguish these deposits from possible bedrock anomalies. Simplified dyke rules, when applied, showed that a few of the anomalies, if really due to dykes, must represent dykes projecting well above the ground. In these cases it was easy to say that the causes were not dykes and might, therefore, be sand deposits. Other anomalies could not be classed by this method. Analysis of shape gave a much clearer picture by showing that a large proportion of the anomalies belonged definitely to the thin-bed class. And thus, even where the depth to target was not well established, the nature of the target could be classed as either overburden or some feature of bedrock surface. Contour trends and amplitudes then showed which of the anomalies were most probably due to magnetic sands.

Case 4—Self-potential

A healthy anomaly was established, but trenching revealed no trace of mineralization at bedrock surface. An estimate of radius (based on gravity dyke formulas) was about 50 ft, and therefore the cause of anomaly must be within that depth, but it need not come anywhere near the bedrock surface. Concentrated sulphides (not ore) were found beneath 40–50 ft of barren rock, when drilled.

Case 5—Gravity

In a survey for Palaeozoic structure (gas and oil prospects) the strongest feature could be explained only as a basement dyke. After a simple solution and elimination of this anomaly, the residual showed an interesting minor anomaly at a distance of several R from the dyke. In a previous reduction by a grid process, the dyke anomaly remained the strongest feature of the residual, and the minor anomaly failed to appear. The argument here is that a background or "regional" field can sometimes be treated as one or more simple geophysical functions, and this should be more effective than a computational process that has no physical meaning.

REVIEW OF DEPTH RULES

Numerous simple rules have been put forward for the direct determination of depth or some other dimension. In most cases these rules are derived from some property of λ or ϕ and are valid only for a limited range of the general anomaly $A\lambda+B\phi$. A few of these rules are listed below, with comments on their validity for determining h, d, or R. Most of the rules involve distance of some critical point from the center of the anomaly, or the distance between a pair of points. They apply basically to dyke anomalies, and the significance of comments can be seen from the master curves (Figure 3). Matters of slope or curvature are best illustrated by the thin-bed functions (Figure 4), as these are the first derivatives of the dyke functions, with the relation given in the discussion of the symmetry of functions.

1. Points of inflection (extreme slope, or zero curvature)

For ϕ, these occur at distances less than R but greater than d; they approach d for large θ; they are not at all related to h.

For λ, they occur between R and $R+h$, approaching the latter value for large θ; they occur also at center for θ less than 60°, and roughly at $R-h$ for θ greater than 60°; they have no apparent relation with d.

2. Separation between points of half-maximum slope on flank of anomaly

For large θ and for ϕ only, this separation is close to $2h$; otherwise there is no reasonably constant relation to R, h, or d.

3. Points of extreme curvature

For ϕ, these occur at the center and slightly beyond R if θ is small; with large θ they occur no longer at the center but roughly at $R-h$ and $R+h$.

For λ, the principal extrema approach d for large θ, and secondary extrema occur.

4. Length of section of "uniform" slope

This is nonsense mathematically; but it depends on optical illusion, with steepness of slope obscuring the curvature, allowing for which it is roughly proportional to h: for ϕ in the region less than R, and for λ in the region greater than R.

5. Points of half-amplitude

For ϕ, these occur at R; the rule is meaningless for λ.

6. Positive and negative extrema

For λ, these occur at R; a single extremum for ϕ occurs at the center.

A basic criticism of rules such as the above is that none of them apply equally and similarly to the two elementary functions, and, therefore, it cannot be said that they are satisfactory for the general compound function. Clearly a choice of rule can be made if one of the functions has minor amplitude; but also the range of θ must be considered.

The first three rules suggest that broad dykes (large θ) may be treated more satisfactorily if each wall is considered as an isolated plane contact. This is sensible in practice because it relaxes some of the analytical restrictions on the dyke model. The form of λ(contact) and its relation to λ(dyke), etc., have been given in the mathematical development. Thus Rules 1, 2, and 3, for the contact anomaly, can be stated:

1. Points of extreme slope

occur at h for λ and at the center for ϕ.

2. Points of half-maximum slope

occur at h for ϕ, and, therefore, $2h$ apart; $2\sqrt{3}h$ apart on each flank of λ, but probably not determinable.

3. Points of extreme curvature

occur at the center and $\sqrt{3}h$ for λ, at $h/\sqrt{3}$ for ϕ.

In the case of thin-bed anomalies, it can be seen that a rule such as 5 or 6 may give a value of only $R/2$, and the other rules would have to be restated to have any meaning at all.

Thus there is a reasonably strong case against the indiscriminate use of these rules of thumb. It may be argued that they all give some dimension of the order of R, and, therefore, an approximate figure for limiting depth; but that much can usually be estimated from a contour map.

GENERAL CONCLUSIONS

These statements are confined to points of practical interest and points that might be considered in future geophysical developments.

1. Complete analysis is not always required and is not always possible. Unless R, as the primary parameter, can be found, there is no point in trying to go further. R alone, however, may be useful. For the dyke, it defines a semicircle as the locus of top of dyke; and an angled drill-hole set tangent to this semicircle must penetrate the dyke walls, for any depth or thickness—unless structural dip has been miscalled.

2. Development of equipment may lead to such things as gradient-measuring apparatus and stabilized orientation for airborne instruments. In the section on coefficients and amplitudes, it is argued that vertical measurements are best where practicable. This argument applies equally to both field intensity and its derivatives. Every anomaly has a vertical component of field and a vertical derivative to any field component that occurs; it must also have horizontal equivalents of the same amplitude though different form; but for the two-dimensional anomaly there can be no field or derivatives in strike direction; this is the "blind spot" in horizontal measurements.

3. Criticisms in the review of depth rules are not intended as an argument against the derivative methods proposed by Vacquier et al. (1951). The problem of the short dyke is complicated, and general rules are largely out of the question; but a field anomaly identified with a specific model can be handled with specific rules. In two-dimensional cases, however, specific classes and class characteristics cover the problem so well that there is no advantage to computing derivatives; there is only the disadvantage of computational errors—not to mention the extra work.

4. Apart from analysis, a common problem is to compute the anomaly of a known structural or topographic system, sometimes for use as a "regional" reduction to observations. The general expressions given in the mathematical development, equations (2) and (7), are useful for this purpose, because a given system can often be represented by a combination of parallelepipeds. Contacts and changes of surface slope (N) must both be considered as boundaries in the mathematical model.

REFERENCES

Koulomzine, T., and Massé, L., 1947, On the magnetic anomaly of an inclined vein of infinite length: A.I.M.E. Technical Publication No. 2260.

Roman, I., 1934, Some interpretations of earth-resistivity data: A.I.M.E. Transactions, v. 110, p. 183–197.

Smellie, D. W., 1956, Elementary approximations in aeromagnetic interpretation: Geophysics, v. 21, p. 1021–1040.

Vacquier, V., Steenland, N. C., Henderson, R. G., and Zeitz, I., 1951, Interpretation of aeromagnetic maps: G.S.A. Memoir 47.

Watson, R. J., and Johnson, J. F., 1938, On the extension of two-layer methods of interpretation of earth resistivity data to three or more layers: Geophysics, v. 3, p. 7–21.

Wetzel, W. W., and McMurry, H. V., 1937, A set of curves to assist in the interpretation of the three-layer resistivity problem: Geophysics, v. 2, p. 329–341.

GEOPHYSICS, VOL. XXIII, NO. 4 (OCTOBER, 1958), PP. 770–794, 10 FIGS.

SOME EFFECTS OF FORMATION ANISOTROPY ON RESISTIVITY MEASUREMENTS IN BOREHOLES*

K. S. KUNZ† AND J. H. MORAN†

ABSTRACT

It is shown that a wide class of potential problems involving anisotropic media can be transformed into equivalent problems involving only isotropic media. By means of such transformations it is possible, in a large number of cases, to determine the apparent resistivities which would be observed in anisotropic formations, using electrode-type resistivity logging devices. Discussion is given of an infinite, anisotropic medium with and without borehole, of two semi-infinite anisotropic beds (without borehole), and of a thin isotropic bed bounded by anisotropic adjacent formations (without borehole). An interpretation chart for the normal device is presented for thick, non-invaded, anisotropic beds penetrated by a borehole.

INTRODUCTION

In many sedimentary strata, electric current flows more easily in a direction parallel to the bedding planes than transversely to them. The reason for this anisotropy is that a great number of mineral crystals possess a flat or elongated shape (e.g., mica and kaolin). At the time they were laid down, they naturally took an orientation parallel to the plane of sedimentation. The interstices in the formations are, therefore, parallel to the bedding plane, and the current is able to travel with greater facility along these interstices which generally contain mineralized water. Such electrical anisotropy is observed mostly in shales.

If a cylindrical sample is cut from a formation, parallel to the bedding planes, the resistivity of this sample measured with a current flowing along its axis is called the longitudinal resistivity R_H. If a similar cylinder is cut perpendicular to the bedding, the resistivity measured with a current flowing along its axis is called the transversal resistivity R_V. The anisotropy coefficient λ, by definition, is equal to $\sqrt{R_V/R_H}$. Laboratory measurements have shown that λ may range from 1 to about 2.5 in different shales.

Furthermore, the formations are often made up of a series of relatively thin beds having different lithologic characteristics and, therefore, different resitivities (as, for example, sequences of thin shales and hard streaks). In electrode systems used for electrical prospecting and for electrical logging, the distances between the electrodes are great enough that the volume involved in a measurement may include several such thin beds. Since, in this situation, the current flows more easily along the more conductive streaks than transversely to the series of beds, there is effective anisotropy. The effects on resistivity measurements of this "macroscopic" anisotropy are added to the effects of the anisotropy due to the microscopic structure of the sediments which was described above.

The electrical anisotropy of sedimentary formations was recognized by

* Manuscript received by the Editor January 28, 1958.

† Schlumberger Well Surveying Corporation, Ridgefield, Connecticut.

C. Schlumberger (1920) early in the history of electrical prospecting. Later, in 1932, a method of computing the electric field in anisotropic media was presented by R. Maillet and H. G. Doll. Practical use has also been made of the anisotropic properites of sediments for the determination of the directions of the strike and the dip, both in surface prospecting and in well logging (Schlumberger and Schlumberger, 1930; Schlumberger, Schlumberger, and Leonardon, 1934; Schlumberger, Schlumberger, and Doll, 1933).

One important result brought to light in the papers by Schlumberger, Schlumberger, and Leonardon (1934) and by Maillet and Doll (1932) is that the resistivity measured with a system of electrodes aligned perpendicularly to the bedding planes is equal to the longitudinal resistivity (paradox of anisotropy). In the particular case of electrical logging in boreholes, the measuring device is generally vertical, and, whenever the formation dip is small or nil, the measured resistivity accordingly is equal to the longitudinal resistivity, provided the electrode spacing is large enough for the effect of the borehole to be negligible.

Recently, some features observed on resistivity logs have called attention to the need for a more complete investigation of the effect of anisotropy. One of these phenomena is the difference in readings between the Induction Log[1] and the 16-inch Normal[2] at the level of certain shales (the former being systematically lower than the latter). Another phenomenon is the abnormally low values read with the lateral device[2] at the level of certain sands bounded by shales.

A mathematical study has accordingly been made of the effect of anisotropy on resistivity logs made with electrode devices, with special attention to the following cases:

a) Homogeneous, infinitely thick, anisotropic formations, traversed by a borehole;

b) Sequences of horizontal, homogeneous, anisotropic beds, borehole effect neglected.

It will be shown that the evaluation of the anisotropy effect is possible by substituting for each anisotropic formation an appropriate isotropic medium. Using such equivalences, the responses of normal and lateral devices in anisotropic media can often be determined.

Departure curves, giving the apparent resistivity read by a normal device in a thick anisotropic bed as a function of the electrode spacing, are presented for several values of the anisotropy coefficient. These curves take into account

[1] As explained in detail in Doll (1949), in measurements of resistivity by Induction Logging, current loops encircling the axis of the hole are induced in the earth. Since, for a vertical drill hole, in the absence of formation dip, these currents circulate horizontally, their flow is affected only by the longitudinal resistivity; and the reading so found is a measure of R_H.

[2] For the arrangement of the current and measuring electrodes in normal and lateral resistivity logging devices, see Figure 1. For a more detailed explanation, see Chapter I, Section 2, of the Schlumberger Corporation's *Interpretation Hand-Book for Resistivity Logs*. A 16-inch Normal is a normal device with an AM spacing of 16 inches.

the presence of a borehole and have been numerically computed using an IBM 701 Data Processing Machine.

The behavior of the normal and lateral curves is discussed for the case of two semi-infinite media with a common boundary, and for the case of a thin bed.

GENERAL EQUATIONS FOR CYLINDRICAL SYMMETRY

On the assumption that all the beds are horizontal and the borehole is vertical, one may speak of a horizontal (longitudinal) resistivity R_H parallel to the bedding

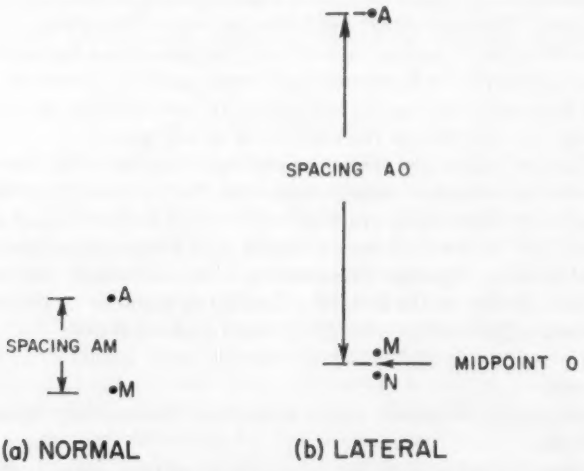

FIG. 1. Electrode designations for the simplified normal and lateral devices referred to in this paper. A designates a current electrode, whereas M and N designate measure electrodes. A current return electrode, B, is located at a great distance from the hole device proper. In the idealized lateral, assumed in the computations, measure electrodes M and N are very close together.

To simplify the discussion, the electrodes are treated as points. No consideration is made of the size of the electrodes or the presence of the insulating mandrel on which they are mounted. The effects of these, however, are minor.

planes and of a vertical (transversal) resistivity R_V perpendicular to these planes. If the current sources lie on the axis of the borehole, the potential surfaces and the lines of current flow possess a cylindrical symmetry.

In a cylindrical co-ordinate system (ρ, z, θ), Ohm's law may be generalized to state that the current density J is given in terms of the potential V by the equation

$$-J = \left[\frac{1}{R_H}\frac{\partial V}{\partial \rho}\rho_1 + \frac{1}{R_V}\frac{\partial V}{\partial z}z_1\right] \tag{1}$$

where z_1 is a unit vector parallel to the axis of the borehole (z-axis) and ϱ_1 a unit vector perpendicular to z_1 and directed away from the borehole axis.

The normals to the equipotential surfaces, $V(\rho, z) = \text{constant}$, are parallel to the gradient of V, given by

$$\nabla V = \frac{\partial V}{\partial \rho} \varrho_1 + \frac{\partial V}{\partial z} z_1. \tag{2}$$

Thus, in general, the current flow in an anisotropic formation ($R_V \neq R_H$) will not be normal to the potential surfaces.

The absence of current sources or sinks, everywhere except on the borehole axis, is expressed by requiring that the divergence of the current density vanishes for $\rho \neq 0$. This leads to the differential equation

$$\nabla \cdot J = \frac{1}{\rho} \frac{\partial}{\partial \rho}\left(\frac{\rho}{R_H} \frac{\partial V}{\partial \rho}\right) + \frac{\partial}{\partial z}\left(\frac{1}{R_V} \frac{\partial V}{\partial z}\right) = 0. \tag{3}$$

For a homogeneous, isotropic medium, in which $R_H = R_V = \text{constant}$, this equation reduces to the Laplace equation in cylindrical co-ordinates.

It is convenient to introduce the *mean* resistivity R and the *coefficient of anisotropy* λ, defined by setting

$$\begin{aligned} R &= \sqrt{R_H \cdot R_V} \\ \lambda &= \sqrt{R_V / R_H} \end{aligned} . \tag{4}$$

Then

$$R_H = \frac{R}{\lambda}, \qquad R_V = \lambda R. \tag{5}$$

If it is assumed that the variation of the coefficient of anisotropy with ρ and z is expressible in the form

$$\lambda = f(\rho) \cdot g(z), \tag{6}$$

then, by (3)

$$\frac{f}{\rho} \frac{\partial}{\partial \rho}\left(\frac{f\rho}{R} \frac{\partial V}{\partial \rho}\right) + \frac{1}{g} \frac{\partial}{\partial z}\left(\frac{1}{gR} \frac{\partial V}{\partial z}\right) = 0. \tag{7}$$

By introducing the new variables

$$\rho' = \int_0^{\rho} \frac{d\rho}{f(\rho)} \quad \text{and} \quad z' = \int_0^{z} g(z) dz \tag{8}$$

and letting

$$V(\rho, z) = V'(\rho', z'), \tag{9}$$

one finds that

$$\frac{\partial V}{\partial \rho} = \frac{1}{f} \frac{\partial V'}{\partial \rho'} \tag{10}$$

and

$$\frac{\partial V}{\partial z} = g \frac{\partial V'}{\partial z'} . \tag{11}$$

With these transformations, (7) becomes

$$\frac{\partial}{\partial \rho'}\left(\frac{\rho}{R} \frac{\partial V'}{\partial \rho'}\right) + \frac{\partial}{\partial z'}\left(\frac{\rho}{R} \frac{\partial V'}{\partial z'}\right) = 0. \tag{12}$$

Finally, by introducing a new value of resistivity at each point, given by

$$R' = \frac{\rho'}{\rho} R, \tag{13}$$

one may replace (12) by

$$\frac{1}{\rho'} \frac{\partial}{\partial \rho'}\left(\frac{\rho'}{R'} \frac{\partial V'}{\partial \rho'}\right) + \frac{\partial}{\partial z'}\left(\frac{1}{R'} \frac{\partial V'}{\partial z'}\right) = 0. \tag{14}$$

A comparison of equation (14) with (3) shows that in terms of the primed co-ordinates (ρ', z') the differential equation for the potential V' is that required for an isotropic medium of resistivity R'. Therefore, *within the conditions imposed by* (6), *any medium involving anisotropic formations may be replaced by an equivalent isotropic one.* This is done by mapping each point (ρ, z) in the original space into a corresponding point (ρ', z') of a new space. In this mapping the potential remains the same at corresponding points (see equation (9)), but the mean resistivity changes from R to R' $(=\rho' R/\rho)$. It remains necessary only to investigate how the boundary conditions are to be transformed.

TRANSFORMATION OF BOUNDARY CONDITIONS

The boundary conditions of importance here are those involving the continuity of potential and of the normal component of current across various boundaries. The continuity of potential in the primed system is insured immediately by (9), and thus we need only to consider the transformation of the current across equivalent sections of a given boundary.

The current flowing out through the sides of any cylinder of radius ρ, whose axis is that of the borehole, is given by

$$I_H = -2\pi\rho \int_{z_1}^{z_2} \frac{1}{R_H} \frac{\partial V}{\partial \rho} dz, \tag{15a}$$

where z_1 and z_2 are the z co-ordinates of top and bottom of the cylinder. The current I' flowing out of the corresponding cylinder of radius ρ' in the transformed space is given by

$$I'_H = -2\pi\rho' \int_{z_1'}^{z_2'} \frac{1}{R'} \frac{\partial V'}{\partial \rho'} dz'. \tag{15b}$$

Direct substitution from equations (5), (6), (8), (10), and (13) proves that $I_H = I'_H$.

The current flowing in the positive z-direction through any plane horizontal annular surface, bounded by circles of radii ρ_1 and ρ_2, is given by

$$I_V = -2\pi \int_{\rho_1}^{\rho_2} \frac{\rho}{R_V} \frac{\partial V}{\partial z} d\rho \tag{16}$$

which again can be shown to be equal to the current I'_V through the corresponding annular surface in the primed system. Using these results, it is easy to show that the transformation described by equations (8), (9), and (13) leaves unchanged the current flowing through corresponding surfaces. In particular, this means that the strength of any current source or sink will not be changed.

AN INFINITE, HOMOGENEOUS, ANISOTROPIC MEDIUM

For such a medium, $\lambda =$ constant, and one can, by (6), make one of the following choices:

$$f(\rho) = 1, \qquad g(z) = \lambda \tag{17a}$$

or

$$f(\rho) = \lambda, \qquad g(z) = 1. \tag{17b}$$

By equations (8) and (13) the first choice leads to an expansion in the z-direction given by $z' = \lambda z$ and a resistivity R' of the equivalent medium equal to the mean resistivity R; whereas the second choice corresponds to a radial compression given by $\rho' = \rho/\lambda$ and an equivalent homogeneous resistivity given by $R' = R/\lambda = R_H$.

The transformation to an isotropic medium represented by the second choice, since it involves no change in the electrode spacings, shows at once that theoretically, *if the borehole could be neglected*, a normal or lateral device would measure R_H, the horizontal resistivity (paradox of anisotropy).

For the first choice, which corresponds to a transformation to an isotropic medium having a resistivity equal to the mean resistivity R, it is necessary only to take into account the increase by a factor λ in the equivalent electrode spacing. This increase in the spacing will mean that the potential measured by a normal sonde, and hence the apparent resistivity measured by it, will be reduced by the factor $1/\lambda$, and thus one again measures $R_H = R/\lambda$. For the lateral sonde

the increase in the spacing AO reduced the signal by $1/\lambda^2$, but the increase in the measure electrode span MN increases the potential difference between them by λ, and the horizontal resistivity R_H is again measured.

EFFECT OF THE BOREHOLE

Subsurface resistivity measurements with an electrode device are generally made by lowering the device into a drilled hole filled with drilling mud. The presence of the electrically conductive (and isotropic) column of drilling mud containing the device can be taken into account in equation (6) by noting that

$$\lambda = \begin{cases} 1 & \text{for} \quad \rho < a \\ \lambda_0 & \text{for} \quad \rho > a, \end{cases} \tag{18}$$

where a is the radius of the borehole. Also, since λ is a function of ρ, one sets $f(\rho) = \lambda$ and $g(z) = 1$; thus, from (8),

$$z' = z \tag{19a}$$

and

$$\rho' = \begin{cases} \rho & \text{for } \rho < a \\ a + (\rho - a)/\lambda_0 & \text{for } \rho > a \end{cases}. \tag{19b}$$

The equivalent isotropic resistivity after the transformation is, from equation (13),

$$R' = \begin{cases} R_m & \text{for } \rho < a \\ \dfrac{R\rho'}{\lambda_0\rho' - (\lambda_0 - 1)a} & \text{for } \rho > a, \end{cases} \tag{20}$$

where R_m is the resistivity of the mud filling the hole, and R is the mean resistivity of the anisotropic formation. The radial resistivity profile as given by (20) is shown in Figure 2. Note that, as $\rho' \to \infty$, the resistivity R' of the equivalent isotropic formation approaches asymptotically $R_H = R/\lambda_0$, the horizontal resistivity. At the edge of the borehole ($\rho' = a$), as seen from (20), R' is equal to R; but at

$$\rho' = \left(1 + \frac{1}{\lambda_0}\right)a,$$

which is less than twice the borehole radius, $R' = \frac{1}{2}(R + R_H)$. At this distance R' has returned halfway to its asymptotic value R_H.

From this analysis the departure curves for normal and lateral devices should lie above the isotropic curves for a formation of resistivity R_H and below those for a formation of resistivity $R = \lambda_0 R_H$, and they should approach the former for large spacings. This problem is treated quantitatively in the next section, and, as seen in Figure 3, these characteristic features are indeed borne out. One is led,

therefore, to believe that the transformation to an equivalent isotropic formation will often serve to gain a qualitative prediction of the apparent resistivity to be expected.

QUANTITATIVE STUDY OF THE BOREHOLE

It has been shown above that a normal or lateral sonde in an infinite, homogeneous, anisotropic medium will measure R_H and that the effect of the borehole through such a medium is to increase the observed apparent resistivity

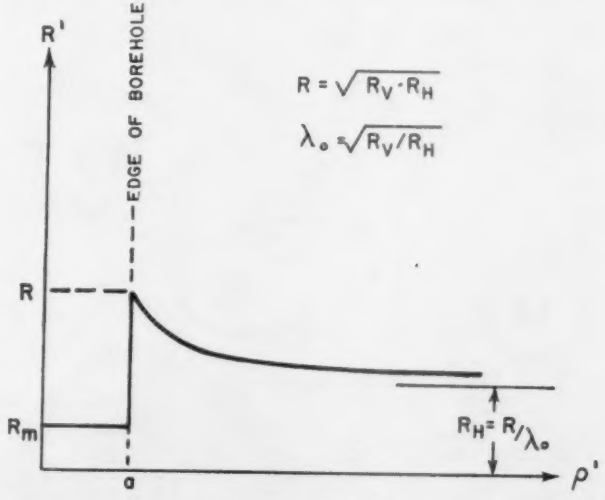

FIG. 2. Radial plot of the resistivity R' of an isotropic medium equivalent to a homogeneous anisotropic medium pierced by an isotropic homogeneous mud column of resistivity R_m. (Plotted for $\lambda_0 = 2$.)

as compared to a homogeneous, isotropic formation of resistivity R_H. In fact, the formation will appear as an isotropic medium with a resistivity lying between R_H and λR_H, depending on the spacing.

This problem will now be formulated quantitatively and some numerical results given. Let the potential in the borehole be V_m while that in the formation is V_f. Then a solution of (3) must be found subject to the boundary conditions:

$$\text{(a)} \qquad V_m \to \frac{I R_m}{4\pi r} \qquad \text{as } r \to 0,$$

$$\text{(b)} \qquad V_m,\ V_f \to 0 \qquad \text{as } r \to \infty, \qquad (21)$$

$$\text{(c)} \qquad \frac{1}{R_m}\frac{\partial V_m}{\partial \rho} = \frac{1}{R_H}\frac{\partial V_f}{\partial \rho} \qquad \text{at } \rho = a,$$

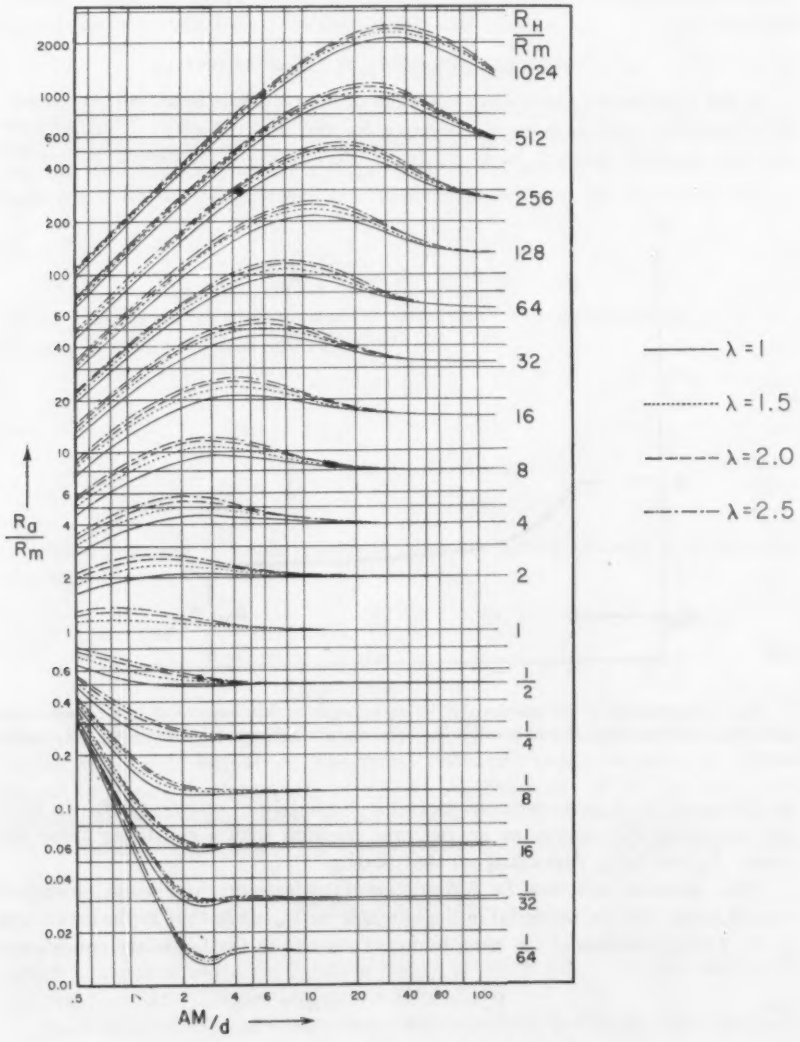

FIG. 3. Normal device (no invasion).

(d) $$V_m = V_f \qquad \text{at } \rho = a,$$

where

$r = \sqrt{\rho^2 + z^2}$ and a is the borehole radius.

Condition (a) specifies the source as an isotropic current emitter located at the center of the borehole. Condition (b) simply fixes the potential at infinity. Condition (c) is the statement of continuity of the normal component of current density across the cylinder $\rho = a$, representing the wall of the borehole. Condition (d) is a statement of the continuity of potential across the cylinder $\rho = a$ and is equivalent to the statement that there is no charge double layer on this surface.

A formal solution of this problem can be constructed in a fashion entirely analogous to the treatment given in the Appendix of the Schlumberger Corporation's *Interpretation Hand-Book for Resistivity Logs*. The notation adopted is that in the previous section, but now the origin is at the current electrode, and thus z is the spacing of the normal device. The potential in the borehole, expressed in terms of the modified Bessel functions K_0, K_1, I_0, and I_1, is found to be

$$V_m(\rho, z) = \frac{IR_m}{4\pi}\left[\frac{1}{r} + \frac{2}{\pi}\int_0^\infty A(x) I_0(x\rho/a) \cos(xz/a)\frac{dx}{a}\right], \tag{22}$$

where

$$A(x) = \frac{K_0(x/\lambda)K_1(x) - \dfrac{R_m}{\lambda R} K_0(x)K_1(x/\lambda)}{K_0(x/\lambda)I_1(x) + \dfrac{R_m}{\lambda R} I_0(x)K_1(x/\lambda)}.$$

The "apparent" resistivity for the normal device is given by the formula[3]

$$R_a = \frac{4\pi z}{I} V(0, z). \tag{23}$$

The essential step in the computation of (23) is the evaluation of the Fourier cosine integral which appears in (23) when $V(0, z)$ is inserted from (22), namely:

$$F\left(\lambda, \frac{R}{R_m}, \frac{z}{a}\right) = \frac{2}{\pi}\int_0^\infty A(x) \cos(xz/a)\, dx. \tag{24}$$

An effective technique for the numerical evaluation of such an integral for large values of z/a and a slowly varying function $A(x)$ has been described by L. N. G. Filon (1928–1929).

Filon's suggestion amounts to fitting $A(x)$ with a set of parabolic arcs. The

[3] The factor $4\pi z$ is the K of the normal device. See equation (26) and associated discussion.

resulting formula has the same form as Simpson's formula except that the weights to be assigned to the ordinates depend on the magnitude of zh/a and reduce to Simpson's weights only when zh/a is small compared to one, h being the width of the x-intervals in the numerical integration.

This method of evaluating the integral in (24) was programmed for the IBM 701 Data Processing Machine and was found to give satisfactory results even for a highly oscillatory integrand corresponding to $z/a = 256$.

The results of these computations are shown in Figure 3 as a set of departure curves for the normal device. Curves are plotted for various values of R_H/R_m (ratio of horizontal formation resistivity to mud resistivity) for four degrees of anisotropy ($\lambda = 1, 1.5, 2$, and 2.5). Each curve shows the variation of R_a/R_m (ratio of apparent resistivity to mud resistivity) versus AM/d (ratio of normal spacing to hole diameter).

The comments on an infinite, homogeneous, anisotropic medium are seen to describe the qualitative features of the curves quite accurately. For a given R_H/R_m, increased anisotropy (increased λ) corresponds in general to an increased R_a/R_m. (This explains why the 16-inch Normal reading at the level of shales may be higher than the Induction Log reading, as mentioned in the Introduction.) For spacings large in comparison with the hole diameter (AM/d large), the apparent resistivity R_a approaches R_H.

It was possible to use this same approach to compute the effect of anisotropy when the formation has been invaded with mud filtrate. The formation close to the borehole will have a different resistivity from the uncontaminated part of the formation further back from the borehole. The formulas are then, of course, more complicated, particularly if the coefficient of anisotropy in the invaded zone is not assumed to be the same as in the uncontaminated zone.

GENERAL CASE NEGLECTING THE BOREHOLE AND INVASION

If the influence of the borehole is neglected, the transformation to an isotropic medium can be made by setting

$$f(\rho) = 1 \quad \text{and} \quad g(z) = \lambda \tag{25}$$

in equation (6). The transformation of equations (8) and (13) then involves only a stretching in the z-direction and no change in the radial distance or the mean resistivity. Each anisotropic bed will be replaced by an isotropic bed having the same mean resistivity, but the thickness of the bed will be multiplied by the anisotropy coefficient λ. Also, of course, after such a transformation, one must take for the new spacings between the electrodes of a sonde the differences in their z'-coordinates, as given by (8).

The above transformation makes it possible to reduce the problem of finding the potentials, or potential differences, to be observed on the measuring electrodes in the anisotropic case to that of finding the corresponding potentials in an equivalent isotropic case. To express the results in terms of the apparent resistivity R_a recorded on a log, however, use is made of the linear relation

$$R_a = KV/I \tag{26}$$

between R_a and the measured[4] potential difference, V. The proportionality constant K is so chosen that R_a is equal to the true resistivity for an infinite, homogeneous, isotropic medium. For the normal sonde, K is proportional to the spacing AM, whereas for the lateral it is proportional to $(AM)\cdot(AN)/(MN)$. Thus, if one computes directly the potential difference to be expected in any given case, by solving the equivalent isotropic problem above, this potential difference may be substituted for V in equation (23) to obtain R_a.

In some cases the equivalent isotropic problem may have already been solved, as on existing interpretation charts (from resistor network measurements, experiments, or computations), giving the effect of electrode spacing, bed thickness, etc. Such data will ordinarily be presented in terms of an apparent resistivity

$$R_a' = K'V/I, \tag{27}$$

where the coefficient K' depends on the spacings used *in the equivalent isotropic problem*.

It is necessary, in using such data, to know whether the K' of the equivalent problem is the same as the K in the original problem or whether a transformation of the K is involved. In the present case (in which the z-co-ordinates, and hence the electrode spacings, are transformed) there has indeed been a transformation of the K.

The apparent resistivity data of the equivalent case can be used to obtain the potential difference V needed in (22) if care is taken that at each depth the K' must correspond to the transformed spacings. Substituting this V into (22), it is seen that the apparent resistivity R_a (for the given anisotropic problem) is related to the apparent resistivity R_a' (for the equivalent isotropic problem) through the equation

$$R_a = \frac{K}{K'} R_a'. \tag{28}$$

Note that K is determined by the actual sonde spacings in the original problem, whereas K' is determined by the transformed spacings in terms of the z'-co-ordinates.

In particular, for the normal sonde, in the case being discussed of no borehole and no invasion,

$$\frac{K}{K'} = \frac{z_M - z_A}{\int_{z_A}^{z_M} g(z)dz} = \frac{1}{\bar{\lambda}}, \tag{29}$$

where $\bar{\lambda}$ is the average of λ between the current electrode A at $z=z_A$ and the measure electrode M at $z=z_M$.

[4] For the normal sonde the potential difference referred to is that between the electrode M and a reference electrode N at the surface. See the Schlumberger Corporation's *Interpretation Hand-Book for Resistivity Logs*, p. 8–11.

For a lateral sonde having a short MN span, the K' coefficient is very nearly proportional to $(AO)^2/MN$, as measured in the equivalent isotropic medium, and, therefore,

$$\frac{K}{K'} = \left[\frac{z_O - z_A}{\int_{z_A}^{z_O} g(z)dz}\right]^2 g(z_O) = \frac{\lambda}{\bar{\lambda}^2}, \tag{30}$$

where $\lambda = g(z_O)$ is the value of the anisotropy coefficient at O, and $\bar{\lambda}$ is its average value between A and O.

QUANTITATIVE STUDY OF THE TWO-MEDIA PROBLEM WITHOUT BOREHOLE

The problem considered here belongs to the class treated in the above section. It is assumed that two thick anisotropic beds have a common boundary, and it is desired to evaluate the response of the normal and lateral devices near this boundary. In the first bed the horizontal and vertical resistivities are R_{H_1} and R_{V_1}, respectively. The mean resistivity, $R_1(=\sqrt{R_{V_1} \cdot R_{H_1}})$ and the anisotropy coefficient $\lambda_1(=\sqrt{R_{V_1}/R_{H_1}})$ are defined in agreement with equation (4). With similar definitions for the second bed, the original problem can be replaced by an equivalent isotropic problem, in the manner indicated in the previous section (equation (25)).

The current electrode A and a point of measurement M are assumed to be located on the same normal to the boundary between the two media. The upper half of Figure 4 shows three different versions of the problem: (a) Electrodes A and M are in medium no. 1; (b) electrode A is in medium no. 1, and electrode M is in medium no. 2; or (c) both electrodes are in medium no. 2. (In each case shown, A is above M. However, the same end result is found for the potential if A and M are simply interchanged in position.) The equivalent isotropic cases are pictured in the lower half of Figure 4.

Using L as the distance from electrode A to the boundary and z as the vertical co-ordinate of M with reference to A (positive downward), the potential in the two beds can be found from the equivalent isotropic cases, by the method of images.

$$\left.\begin{aligned}
V &= \frac{IR_1}{4\pi\lambda_1}\left[\frac{1}{|z|} + \frac{R_2 - R_1}{R_2 + R_1}\left(\frac{1}{|2L - z|}\right)\right] && \text{for } A \text{ and } M \text{ in medium no. 1} \\
V &= \frac{I}{4\pi} \cdot \frac{2R_1R_2}{R_1 + R_2} \cdot \frac{1}{|\lambda_1 L + \lambda_2(z - L)|} && \begin{matrix}\text{for } A \text{ in medium no. 1} \\ M \text{ in medium no. 2}\end{matrix} \\
V &= \frac{IR_2}{4\pi\lambda_2}\left[\frac{1}{|z|} + \frac{R_1 - R_2}{R_1 + R_2}\left(\frac{1}{|2L + z|}\right)\right] && \text{for } A \text{ and } M \text{ in medium no. 2}
\end{aligned}\right\} \tag{31}$$

Using these relations, the apparent resistivities which would be given by the

normal and lateral devices may be found.[5] For this determination, the coordinate z is set equal to the spacing of the appropriate normal device.

Special Case $R_2 = R_1$

This is a case of special interest because the equivalent isotropic problem corresponds to a homogeneous medium. The apparent resistivity profiles versus depth for such a case are illustrated by the solid curves, in Figure 5 for the normal device, and in Figure 6 for the lateral. In each figure the upper anisotropic bed

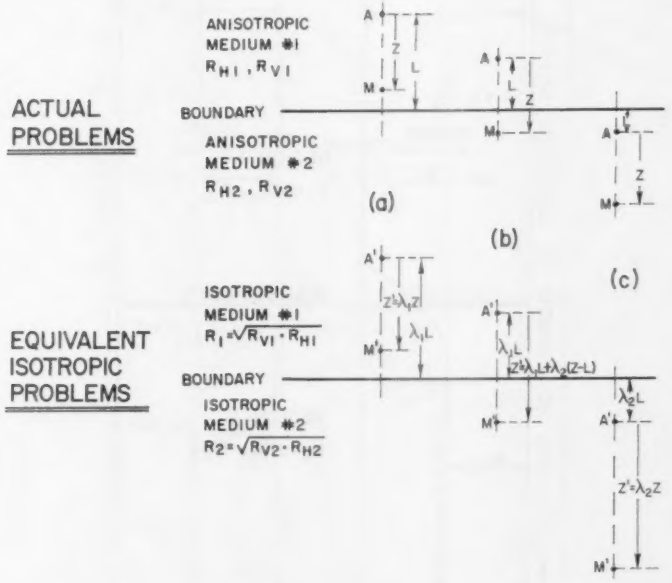

FIG. 4. Two semi-infinite anisotropic media, borehole effect neglected. (Drawn for $\lambda_1 = 1.25$, $\lambda_2 = 2$.)

(region 1) has a horizontal resistivity R_{H_1} of 2, and the lower anisotropic bed (region 2) has R_{H_2} equal to 1. (Note that the reference points for depths have been shifted to the midpoint of AM for the normal, and to point O for the lateral.)

[5] The normal apparent resistivity is computed from equation (23) (or equivalently equation (26)). In the present and following sections, the lateral apparent resistivity is computed from the relation

$$(R_a)\ \text{lateral} = \frac{-4\pi z^2}{I}\frac{\partial V}{\partial z}$$

where z is set equal to the spacing AO. This relation is a good approximation when MN is negligible in comparison with AO.

Also shown for comparison in Figures 5 and 6, in dashed line, are the apparent resistivity profiles for two isotropic beds whose resistivities R_1^* (upper bed) and R_2^* (lower bed) are equal to the *horizontal* resistivities of the corresponding anisotropic beds; i.e., $R_1^* = R_{H_1}$ and $R_2^* = R_{H_2}$. (R_1^* and R_2^* are not equivalent isotropic resistivities.)

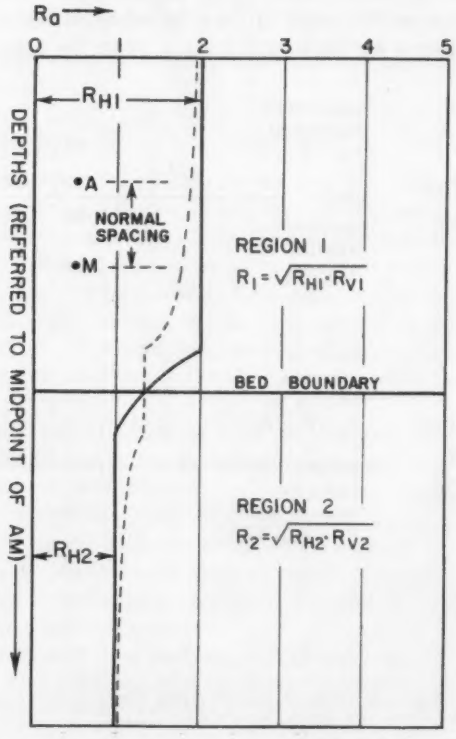

FIG. 5. Normal sonde, borehole effect neglected.

Both normal and lateral curves for the anisotropic case show values of R_a which are constant and equal to $R_{H_1}(=R_1/\lambda_1)$, until the measure electrodes cross the boundary. Then, for the normal, while the A electrode is in one medium and the measure electrode in the other, the value of the potential makes a smooth transition from $IR_{H_1}/4\pi z$ to $IR_{H_2}/4\pi z$. This transition from an apparent resistivity R_{H_1} to one of R_{H_2} is completed in the distance $z(=AM)$, which is one sonde spacing.

For the lateral, when the measure electrodes cross the bed boundary, the apparent resistivity makes a jump such that the readings on the two sides of the boundary are in the ratio λ_1/λ_2 (equal in this case to R_{H_2}/R_{H_1}). This sudden

jump is followed by a smooth transition to the value $R_{H_2}(=R_2/\lambda_2)$, which takes place in the distance of one sonde spacing AO.

This example illustrates some of the novelty due to anisotropy. If we attempted to interpret the apparent resistivity curve in this case as though the media were isotropic, we would have to assign resistivities R_{H_1} and R_{H_2} to match

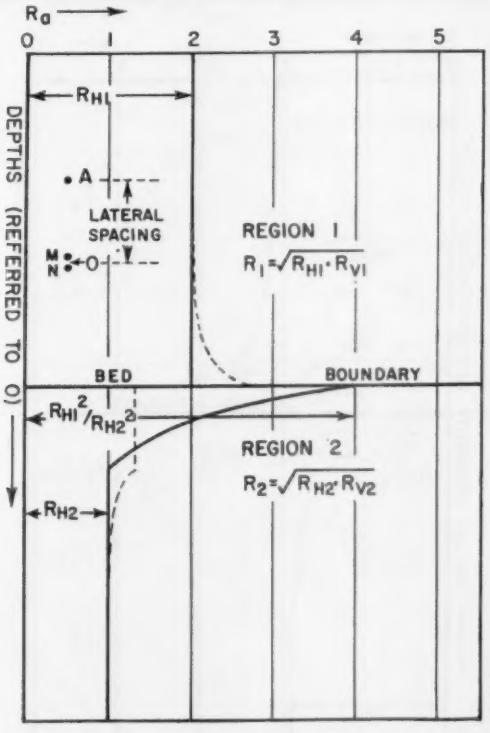

FIG. 6. Lateral sonde, borehole effect neglected.

the curve at a distance from the boundary. Then the behavior at the boundary would be misleading. (Compare dashed and solid curves in Figures 5 and 6.)

Special Case $R_{H_1}=R_{H_2}$, *but* $R_1 \neq R_2$

The apparent resistivity R_a will be the same in both media except in the immediate neighborhood of the boundary. Let us suppose that $\lambda_2>\lambda_1$. Then, as indicated in Figure 7, the reading of the normal device will increase as the boundary is approached from above, reaching a value

$$\frac{2\lambda_2}{\lambda_1+\lambda_2}R_H$$

when the measure electrode arrives at the boundary. After the measure electrode crosses the boundary, the apparent resistivity decreases smoothly, becoming equal to $2\lambda_1 R_H/(\lambda_1+\lambda_2)$ when the current electrode reaches the boundary. The reading then increases to the value R_H as the normal device continues to move downward.

The lateral device under the same circumstances will show a decreasing read-

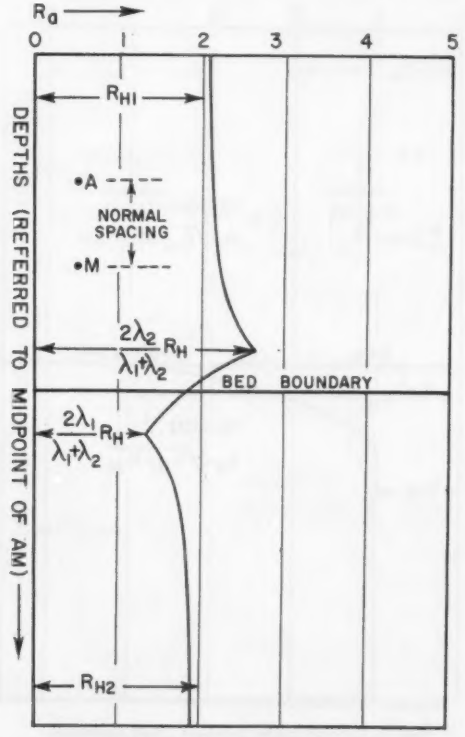

FIG. 7. Normal sonde, borehole effect neglected. Special case of $R_{H_1}=R_{H_2}=R_H$. (Plotted for $\lambda_1=1$, $\lambda_2=2$, $R_H=2$.)

ing, as shown in Figure 8, arriving at a value $2\lambda_1 R_H/(\lambda_1+\lambda_2)$ when the measure electrodes are just above the boundary. When the measure electrodes cross the boundary, the apparent resistivity jumps up by a factor of $(\lambda_2/\lambda_1)^2$. It then decreases, reaching a second minimum when the current electrode passes the boundary. (The minima have the same value as the one for the normal device.) Thereafter the apparent resistivity increases toward its final value of R_H.

For both of the special cases illustrated in Figures 5 to 8 inclusive, it has been

assumed that $\lambda_2 > \lambda_1$. In a case where $\lambda_1 < \lambda_2$, the character of the features would be reversed. For example, in Figure 8 the dip in the lateral just above the upper bed boundary would become a peak. The peak just below the upper bed boundary would become a dip. The dip at one sonde spacing below the bed boundary would become a peak.

The resistivity profiles of Figures 5 to 8 furthermore indicate that the response

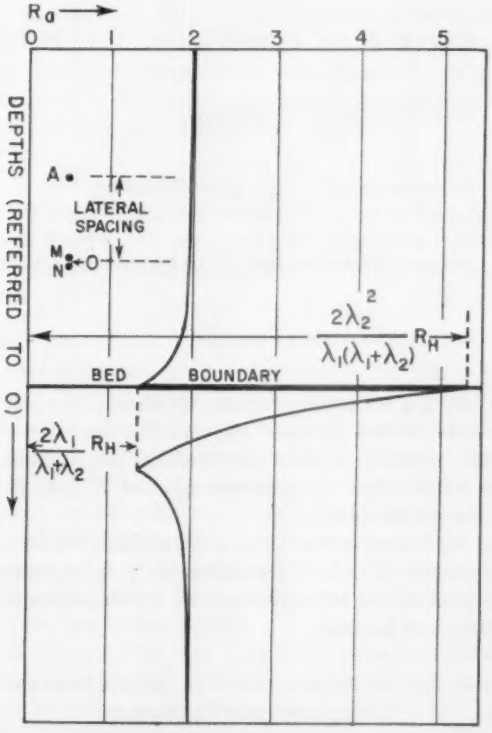

FIG. 8. Lateral sonde, borehole effect neglected. Special case of R_{H_1} R_{H_2} R_H. (plotted for $\lambda_1 = 1$, $\lambda_2 = 2$, $R_H = 2$.)

of the lateral device is more strikingly affected by the presence of anisotropy than the response of the normal.

General Case

The most interesting features on the apparent resistivity curve are those observed when the measure electrodes are near the boundary and when the current electrode penetrates the boundary. These values are listed below in terms of the

"mean" resistivity $\overline{R}$, defined by

$$\frac{1}{\overline{R}} = \frac{1}{2}\left(\frac{1}{R_1} + \frac{1}{R_2}\right).$$

$$\left.\begin{aligned} R_a &= \frac{\overline{R}}{\lambda_1} && \text{measure electrode at boundary} \\ &= \frac{2\overline{R}}{\lambda_1 + \lambda_2} && \text{midpoint of } AM \text{ at boundary} \\ &= \frac{\overline{R}}{\lambda_2} && \text{current electrode at boundary} \end{aligned}\right\} \text{NORMAL DEVICE}$$

$$\left.\begin{aligned} R_a &= \frac{\overline{R}}{\lambda_1}\left(\frac{R_1}{R_2}\right) && \text{measure electrodes just above boundary} \\ &= \frac{\overline{R}}{\lambda_1}\left(\frac{\lambda_2}{\lambda_1}\right) && \text{measure electrodes just below boundary} \\ &= \frac{\overline{R}}{\lambda_2} && \text{current electrode at boundary} \end{aligned}\right\} \text{LATERAL DEVICE} \qquad (32)$$

With these key values, a response curve may be sketched for any case of interest. If medium 2 is isotropic and we know R_{H_1} and R_2 from the readings above and below the boundary, then it is clear that readings corresponding to the lateral device response would allow the determination of $R_{V_1}(=\lambda_1 R_1)$ from the discontinuity in R_a at the boundary.

The fact that the lateral device shows a discontinuity upon crossing a boundary in the ratio R_{V_2}/R_{V_1} is quite a general result. It is, of course, dependent on the assumed smallness of the MN-span between the measuring electrodes and the absence of borehole and invasion.

THIN ISOTROPIC BED BETWEEN ANISOTROPIC ADJACENT FORMATIONS (SAND BED BOUNDED BY SHALES)

Using the technique of reducing the anisotropic problem to an equivalent isotropic problem, apparent resistivity profiles can be computed for the normal and lateral devices passing through isotropic beds, such as sands, bounded by anisotropic adjacent formations, such as shales. From these results, interpretation charts can be prepared. Only the lateral device will be considered here, because it seems clear that this device will be influenced more significantly by anisotropy.

That anisotropy in the adjacent formations may cause some ambiguity in determining the resistivity of a thin bed is apparent from the fact that at either boundary the lateral reading R_{aB}, in the bed *just inside* the boundary, is related

to the reading R_{aS}, in the adjacent formation *just outside* the same boundary, by the relation

$$\frac{R_{aB}}{R_{aS}} = \frac{R_B}{R_V} = \frac{R_B}{\lambda^2 R_H} = \beta, \tag{33}$$

where R_V and R_H are the vertical and horizontal resistivities in the adjacent formations, λ is the coefficient of anisotropy in the adjacent formations, and R_B is the resistivity of the isotropic bed. At points well above or below the bed the apparent resistivity is $R_a = R_H$. If $R_B < \lambda^2 R_H$, equation (33) shows that R_a will decrease upon entering the bed, and this can occur even though $R_B > R_H$. Thus it is quite conceivable that a drop in R_a will correlate with an increase in actual (horizontal) resistivity. From (33) this can be expected to happen for

$$1/\lambda^2 < \beta < 1.$$

One might hope that this difficulty could be overcome by using other information from the resistivity curve, along with interpretation charts, to arrive at a better estimate of R_B than the one deduced directly from the log. This possibility will be considered.

Special Case $\lambda R_H = R_B$

Before considering the general case, however, let us take a look at a special problem that can be solved very simply by using the scaling technique of the sections which covered the general case (neglecting the borehole and invasion) and the quantitative study of the two-media problem without borehole. This special problem corresponds to the assumption that the mean resistivity of the anisotropic adjacent formation $R_s (= \sqrt{R_V \cdot R_H} = \lambda R_H)$ is equal to the bed resistivity R_B. The scaled problem then leads to a homogeneous medium of resistivity R_B, and, therefore, it can be solved easily. This approach leads to an apparent resistivity profile for the lateral sonde as sketched in Figure 9. In this figure, z is taken equal to the lateral spacing AO.

It is interesting to note that this curve could have been drawn directly from (28) and (30), since in this case $R_a' = R_B = R_S$ and the character of the curve is due completely to the variation of K'. The curve obtained in this case is typical of the result when $\beta < 1$, which is the case most likely to cause difficulty in log interpretation. If $\beta > 1$ the discontinuities are executed in the opposite directions.

General Case $\lambda R_H \neq R_B$

In generalizing to the case $R_S \neq R_B$, it is important to decide what data from the R_a curve should be used to determine R_B. It seems that for thin beds the best measurements would be:

(1) a measurement at the upper or lower boundary of the ratio β defined in (33);

(2) a measurement of R_a in the plateau when the sonde spans the bed. This value will be given the symbol R_P;

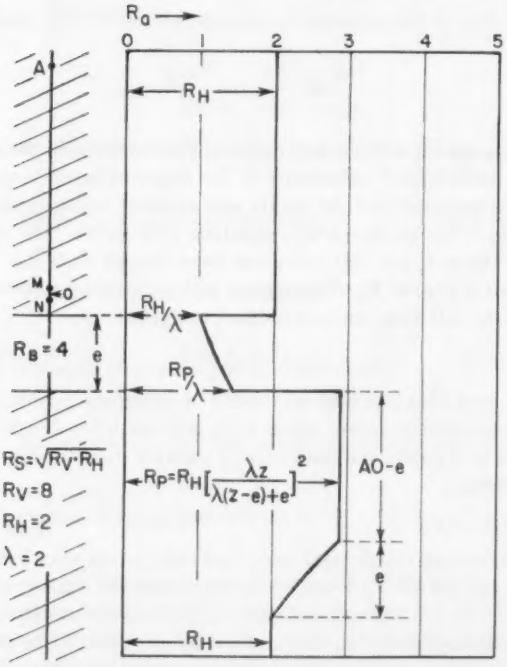

FIG. 9. Lateral sonde, borehole effect neglected. Thin isotropic bed between anisotropic shoulder formations for special case of $R_B=R_S$. ($R_B=R_S=4$, $\lambda=2$.)

(3) a measurement of R_H in the adjacent formations;

(4) a measurement of e, the bed thickness.

By (33), $R_B/R_H=\lambda^2\beta$, where β is known from measurement (1) above. Since in practice $1<\lambda<2.5$, it is known that $\beta<R_B/R_H<6.25\beta$. For more precise knowledge of R_B, measurement (2) must be interpreted using the following theoretical expression, derivable by means of the theory of images:

$$\frac{R_P}{R_H}=\left(\frac{\lambda z}{2e}\right)W\left(\alpha^2,\frac{\lambda z}{2e}-\frac{\lambda-1}{2}\right), \tag{34}$$

where

$$W(x,y)=(1-x)\int_0^\infty \frac{ue^{-yu}du}{1-xe^{-u}},$$

z = the lateral spacing AO,

and

$$\alpha = \frac{R_B - R_S}{R_B + R_S} = \frac{\dfrac{R_B}{R_H} - \lambda}{\dfrac{R_B}{R_H} + \lambda}.$$

Using (33) and the definition of α to eliminate λ and α, in (34), it is possible to find an expression for R_P/R_H which is a function of z/e, β, and R_B/R_H. Such a relation may be used to determine R_B/R_H, since the other quantities are known from the four measurements above.

The nature of the above solution is shown in the plots of R_B/R_H vs R_P/R_H in Figure 10a for $z/e=2$ and in Figure 10b for $z/e=5$. Curves are plotted for several values of β (heavy curves). Also shown are curves of constant λ (thin curves).

Inspection of these curves shows that, particularly for the thin-bed case ($z/e=5$) for a given value of β, a small error in R_P/R_H can cause a large error in R_B/R_H. This means that for thin beds the method does not have much resolution for the determination of R_B. For bed thicknesses approaching the lateral spacing the resolution is somewhat better (compare case of $z/e=2$).

The above discussion cannot, of course, be taken to apply unmodified to the practical case where there is a borehole. It does point up the conclusion that there is no highly satisfactory way of correcting the lateral reading by itself to give the true resistivity of a *thin* isotropic bed between anisotropic adjacent formations.

CONCLUSION

A method of analysis has been described whereby a potential problem involving anisotropic media can be transformed into an equivalent problem involving isotropic media only. The method is subject to the limitation of equation (6) which requires that the coefficient of anisotropy λ be expressible as a product of a function of the radial co-ordinate only by a function of the axial co-ordinate only.

The potentials found by the solution of the equivalent isotropic problem, transformed back into the coordinates of the original problem, are sufficient to determine the apparent resistivities which would be observed by electrode-type logging devices in anisotropic formations.

By means of the above transformations, one can predict, qualitatively, that a short-spacing measuring device in a borehole filled with isotropic mud will read higher than for an isotropic formation of resistivity R_H (the horizontal anisotropic resistivity). This is confirmed in the case of the normal device by the accurately computed departure curves of Figure 3.

In *the case where the borehole is neglected* some conclusions related to log interpretation have been noted.

1. Both normal and lateral devices measure R_H when the sonde is completely within the bed, and not too close to a bed boundary.

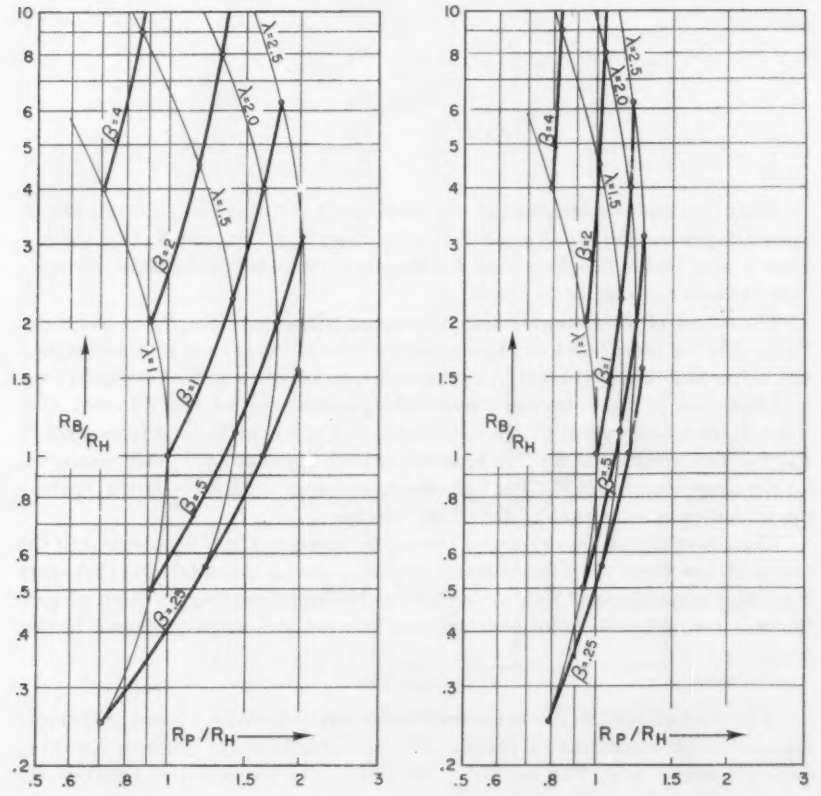

FIG. 10. Lateral sonde, borehole effect neglected, relation between R_B/R_H and R_P/R_H as a function of β (heavy curves) and λ (light curves).

2. Some anomalies occur when the electrode system is crossing a boundary between beds. In general these anomalies tend to be more striking for the lateral device.

3. The apparent resistivity shown by the lateral device shows a discontinuity when the measure electrodes cross the bed boundary. The apparent resistivities just above and just below the boundary are in proportion to the *vertical resistivities* at these points (equations (32) and (33)).

4. It is thus possible in some cases, for the sense of the discontinuity in the

lateral curve to be in the opposite direction to the change in horizontal resistivity. As a result, a direct interpretation of the log may sometimes be misleading, particularly in the case of a thin isotropic bed between thick anisotropic shoulder formations. An attempt to interpret such a case from the readings of the lateral alone indicated poor resolution in the determination of R_B, particularly for smaller bed thicknesses.

In case there is a borehole, the above conclusions can apply approximately if the sonde spacing is large in comparison with the borehole diameter.

ACKNOWLEDGMENT

The authors are indebted to Messrs. M. Martin and F. Segesman for their substantial contributions to the preparation of this paper.

LIST OF SYMBOLS

R_H Formation resistivity measured by passing current parallel to bedding planes (horizontal or longitudinal resistivity).

R_V Formation resistivity measured by passing current in a direction perpendicular to bedding planes (vertical or transversal resistivity).

R Mean resistivity ($R=\sqrt{R_H \cdot R_V}$).

λ Coefficient of anisotropy ($\lambda=\sqrt{R_V/R_H}$).

ρ Radial coordinate of a cylindrical system of coordinates.

z Axial coordinate of a cylindrical system of coordinates. In the discussion, z is set equal to the spacing of a normal or lateral resistivity logging device.

ρ' Radial coordinate in equivalent isotropic problem.

z' Axial coordinate in equivalent isotropic problem.

R' The formation resistivity in the equivalent isotropic problem.

R_m The resistivity of the isotropic mud column filling the borehole.

R_a The apparent resistivity indicated by a given resistivity logging device.

R_a' The apparent resistivity which would be seen by the equivalent resistivity logging device in the equivalent isotropic problem.

$\overline{R}$ A reference resistivity for the two-media case, ($\overline{R}=2R_1R_2/(R_1+R_2)$), where R_1 is the mean resistivity of the upper bed and R_2 is the mean resistivity of the lower bed.

R_B Resistivity of an isotropic bed.

R_S Mean resistivity of anisotropic adjacent formations on either side of isotropic bed.

R_{aB} Apparent resistivity observed in a bed just within bed boundary.

R_{aS} Apparent resistivity observed in anisotropic adjacent formation just outside bed boundary.

β Equal to R_{aB}/R_{aS} at either bed boundary in the no-borehole case.

REFERENCES

Doll, H. G., 1949, Introduction to induction logging and application to logging of wells drilled with oil base mud: Jour. of Petroleum Technology, v. 1, p. 148.

Filon, L. N. G., 1928–1929, On a quadrature formula for trigonometric integrals: Proc. of the Royal Society of Edinburgh, v. 49, p. 38.

Maillet, R., and Doll, H. G., 1932, Sur un théorème relatif aux milieux électriquement anisotropes et ses applications à la prospection électrique en courant continu: Ergänzungshefte für angewandte Geophysik, v. 3, p. 109.

Schlumberger, C., 1920, Etude sur la prospection électrique du sous-sol: Paris, Gauthier-Villars, p. 40.

Schlumberger, C., and Schlumberger, M., 1930, Sur la détermination électromagnétique du pendage des couches sédimentaires: Comptes Rendus, Académie des Sciences (Paris).

Schlumberger, C., Schlumberger, M., and Doll, H. G., 1933, The electromagnetic teleclinometer and dipmeter: London, World Petroleum Congress.

Schlumberger, C., Schlumberger, M., and Leonardon, E. G., 1934, Some observations concerning electrical measurements in anisotropic media and their interpretation: Trans. American Institute of Mining Engineers, v. 110, p. 159.

Schlumberger Well Surveying Corporation, 1950, Interpretation hand-book for resistivity logs.

GEOPHYSICS, VOL. XXIII, NO. 4 (OCTOBER, 1958), PP. 795–822, 20 FIGS.

GETTING THE MOST OUT OF PRESENT SEISMIC INSTRUMENTS*

JOSEPH W. HAMMOND† AND JAMES E. HAWKINS†

ABSTRACT

Much of the present seismic work is being carried out in areas where results are difficult to obtain. The paper outlines the requirements for seismic instruments for these operations. The particular characteristics desired for specific problems are illustrated, and the instrument factors that affect these characteristics are outlined. Examples of the effect of instrument adjustment are shown. The attainment of optimum results with present equipment under diversified field conditions may require modifications according to area, in shooting techniques, geophones, amplifiers, galvanometers, recording, and record presentation. The discussion of the advantages of magnetic recording assumes that the best field techniques have been applied.

INTRODUCTION

Much of the present seismic work throughout the world is being carried out in areas where results are difficult to obtain. In the past 25 years seismic operations have moved into more and more difficult areas. In general, it might be stated that no two of these areas present the same problem, and each area must be analyzed and the characteristics of the seismic instruments adapted to the problem at hand. New instrumental characteristics and shooting techniques continually push back the NR (no reflection) areas. The shooting techniques are inseparable from the instrument characteristics. As an example, continuous profiling is impossible in most areas without a certain amount of high-pass filtering. Before amplifiers had been designed with sufficient filtering, it was necessary to separate the geophone spread some critical distance from the shot, and this prevented the use of continuous profiling as we know it today. With the design of the instruments to handle the high-amplitude ground roll close to the shot, continuous profiling became a practical method. Thus, the shooting or recording technique was determined by the instrument design.

FUNDAMENTALS

The type of energy obtained from a normal seismic shot, as recorded on the lower record with wide-frequency-response recording equipment and on the upper record with conventional seismic instruments, is shown in Figure 1. Reflections are not recognizable until sufficient filtering is done by means of geophones and amplifier filters as shown by the top record. Had the spread been placed so that the ground roll was not present during the arrival of the reflections, the reflections on the wide-frequency-response record would probably have been better than on the filtered record.

The first problem in an area is, of course, to obtain recognizable reflections.

* Presented at the Ninth Annual Midwestern Meeting at Fort Worth on March 8, 1956. Manuscript received by the Editor September 16, 1957.

† Seismograph Service Corporation, Tulsa, Oklahoma.

Having obtained recognizable reflections, every effort is then made to adjust the instrument characteristics and the field techniques to provide information which may be handled with some desired interpretational procedure. Sometimes the instrument characteristics, the shooting technique, or the interpretational procedure are modified to provide a practical or an economic solution. Without reflections, the interpretational procedure is of no value. On the other hand, almost any record obtained with reflections on it can yield an interpretation. In some cases it may not be economical to spend the time and effort in the instrument adjustment or the field technique necessary to obtain consistent re-

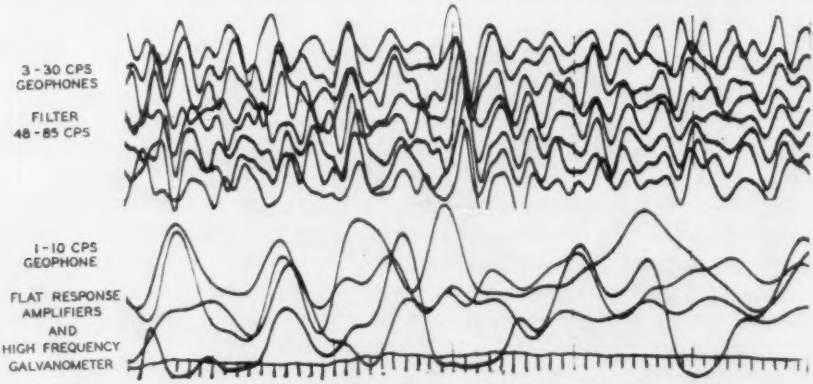

FIG. 1. Illustration of the type of energy from a typical seismic shot. The upper traces are a conventional filtered seismic record, and the lower traces are a wide frequency response seismic record.

flections. It may even be desirable from an economic standpoint to obtain something less than the optimum individual record quality in the interest of getting more records of a somewhat lower grade of quality. These factors affect the requirements for seismic instruments.

A typical seismic channel consists of a geophone, an amplifier, and a recording galvanometer. For convenience in operations, most of the adjustments and controls are placed in the amplifier, and the geophone and galvanometer are selected to be compatible with the amplifier. A geophone normally attenuates or cuts the frequencies somewhat below the natural frequency of the geophone. A galvanometer will attenuate or cut the frequencies somewhat above its natural frequency. The response of both depend not only on their natural frequency, but upon their damping. The damping is generally kept somewhere in the range of 0.5 to 0.7 critical; this prevents too much overshoot on impulses. The amplifier without filters will normally pass frequencies over the entire range passed by the geophone and the galvanometer. Thus, the basic seismic channel will pass frequencies from somewhat below the lowest desired reflection frequency of some

20 cps to somewhat above the highest desired reflection frequency, which may be some 80 cps in normal reflection work, to several hundred cps in high-frequency recording.

Present interpretational techniques make continuous profiling the field procedure in greatest demand. Continuous profiling sets a rigorous performance qualification on the seismic channel. It must be capable of recording reflections in the presence of very high-level interference energy.

The results of one method of determining the type of interfering energy that may be present is illustrated in Figure 2. An interference determination spread

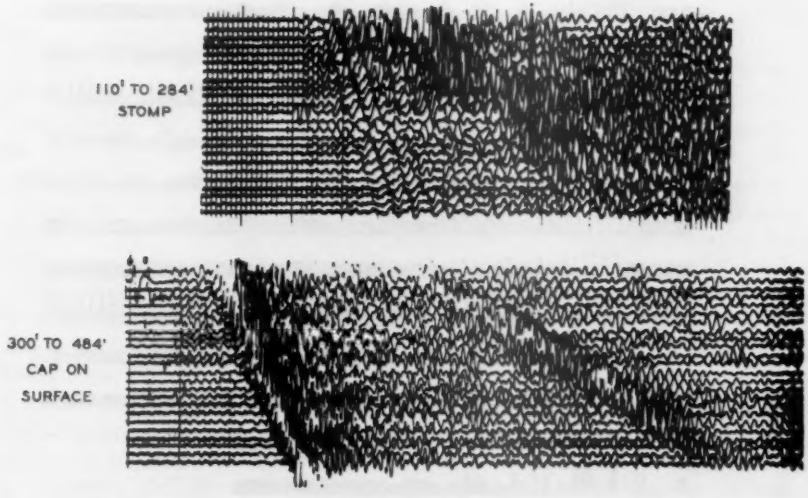

FIG. 2. This shows the use of an interference spread for the analysis of interfering energy. The top record shows the energy resulting from a man jumping from the recording unit fender to the ground. The bottom record shows the energy resulting from firing a cap on the surface.

is laid out, consisting of a single geophone per trace placed at short intervals in the line of profile, with the first geophone being placed some distance from the energy source. Small charges are then fired and the resultant bands of interference noted.

The most common form that interference energy takes, although not by any means the only form, is that of low-frequency ground roll. In continuous profiling this ground roll or other refraction interference is generally present on some portion of the reflection record, and the instrument must be capable of eliminating it. Other undesired energy may take the form of high-frequency chatter, due to near-surface high-velocity layers, hole blow, wind noise, high

line interference, ghost reflections, etc. Dip shooting likewise requires faithful duplication in the seismic channels if the dips are to be accurate.

In some prospects, shots of similar size and depth produce great variations in the amount and character of the resultant energy. This is illustrated in Figure 3. The top record has high-frequency reflection energy with low-frequency ground roll. The middle record has medium-frequency reflection energy with

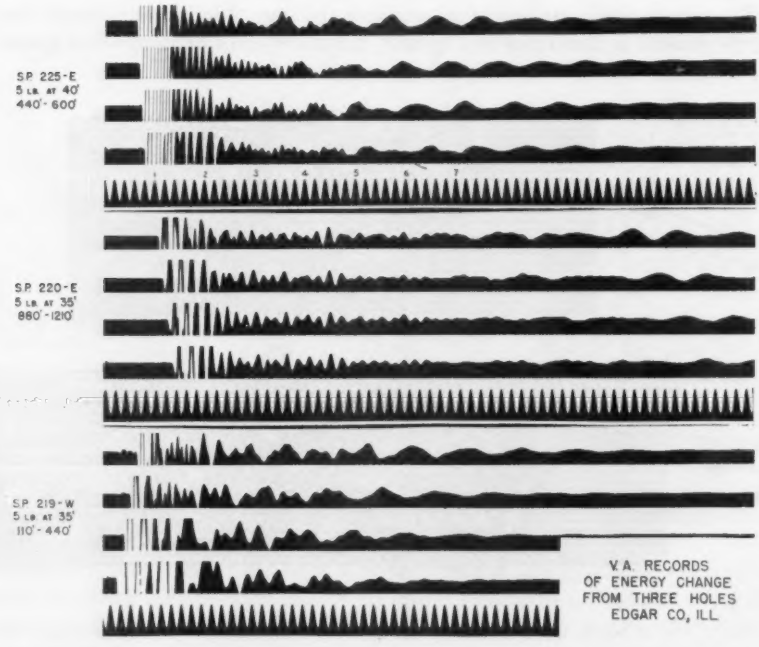

FIG. 3. The three variable area records illustrate the great variation in energy resulting from equal charges shot in the same area. Note that approximately equal amounts of ground roll are present on all records, but that the reflection energy on the three records varies considerably in frequency.

low-frequency ground roll. The bottom record has low-frequency reflection energy and low-frequency ground roll. The frequency and the amount of energy produced from a charge of explosives is a function of the medium in which the explosive is detonated. In general, hard formations produce high frequencies with an overall low-energy level, while the soft formations produce low frequencies with an overall high-energy level.

DIVISION OF THE PROBLEM

In considering the seismic energy and its conversion and representation

from shot initiation to presentation, there are five general areas wherein changes can be made to improve the results. These include shot hole and shooting techniques, geophones, amplifiers, galvanometers, and recording and record presentation.

Shot Hole and Shooting Techniques

The shot hole has an important bearing on the quality of reflections obtained. The statement has often been made that as much change can be made by varying the shot conditions as can be obtained by varying the instrument characteristics. Shooting techniques involve the following main variables: hole depth, charge size, number of holes (single or directional), type of charges (normal or directional), and spread distance to shot.

An illustration of the importance of shooting at the correct depth is shown in Figure 4. The top record has the appearance of an insufficient amount of explosive being used. No energy is present after the initial first-breaks. The second record, which was made at a depth 20 ft shallower than the top record, has more overall energy, but little or no reflected energy is present. The bottom record, which was made at a depth of 16 ft below the surface and 14 ft above that of the second record, has several usable reflections. Correct placement of the charge is one of the recording techniques that cannot be overemphasized.

Overshooting has a detrimental effect upon reflection quality and timing accuracy. An example of overshooting is shown in Figure 5. The bottom record has much better reflection separation than that of the records obtained with heavier charges; the three separate and well-defined reflections present between 0.6 and 0.7 sec on the bottom record have very little definition on the top record. The first-trough times of the reflection at a record time of 580 milliseconds are the same on all three records, while the next and succeeding troughs have a maximum of 8 milliseconds difference in time. The first-trough times of the later reflection under study cannot be picked accurately on the upper records due to the fact that extra legs follow the earlier reflection of the heavier charge.

Closely related to hole depth and charge size is the problem of ghost reflections (Van Melle and Weatherburn, 1953). The ghost energy reflects from a velocity interface located above the point at which the charge was detonated; it then follows a path downward to the velocity interface below the shot. The velocity interface above the charge may be either the bottom of the weathered layer or the ground interface. Figure 6 illustrates the paths followed by a true reflection and a ghost reflection. An illustration showing a series of six shots recorded from the same shot hole at various depths, ranging from 75 to 208 ft, on which ghost reflections are present, is shown in Figure 7. The ghosts, which converge on the true reflections as the shot depth becomes shallower, may be seen following the true reflections. The ghost energy was reflected from the base of the weathering, thence to the reflecting horizon, and back to the surface. This illustrates the effect of ghost energy on record character and the interpretational hazards resulting from shooting at improper depths. It is the authors' belief that ghost reflec-

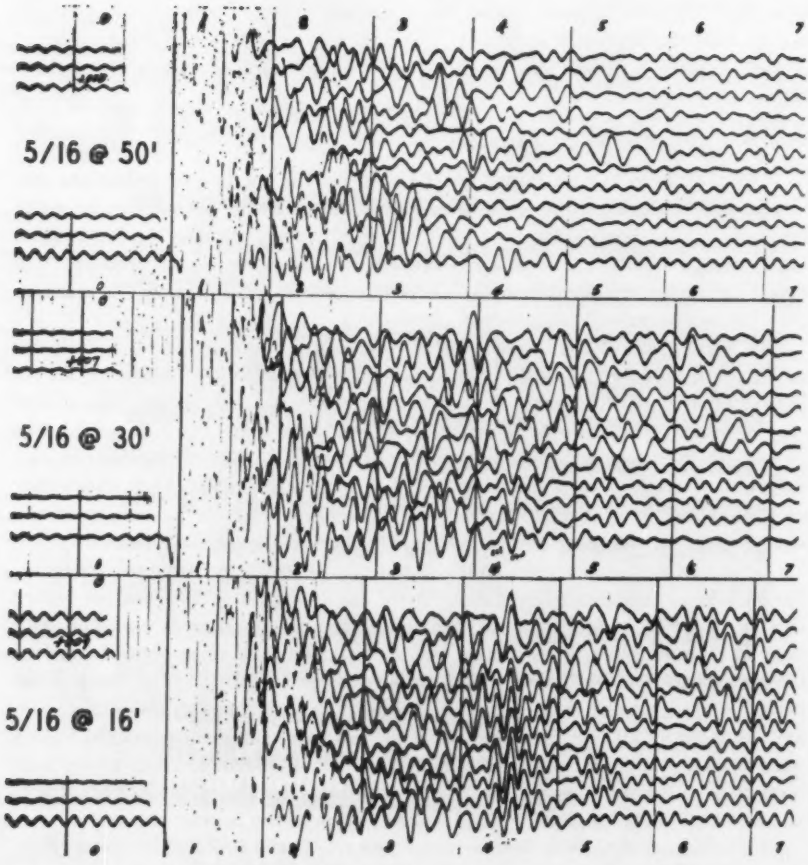

FIG. 4. This illustrates the importance of shooting at the correct hole depth. The deep shot has the appearance of insufficient energy. The medium depth shot shows sufficient overall energy but little or no reflected energy. The shallow depth shows usable reflections.

tions cause more variation in record character between successive shots and between successive holes than any other factor.

Theoretically and experimentally, directional charges offer good possibilities of improving results by reducing undesired energy (Musgrave, Ehlert, and Nash, 1958). The chief deterrent to the use is the cost of material and the difficulty and time consumed in handling directional charges. At the present time, they are not being extensively used.

The use of a favorable spread distance to the shot, so as to record the reflection at a time when interfering energy has either not arrived or has passed, is one

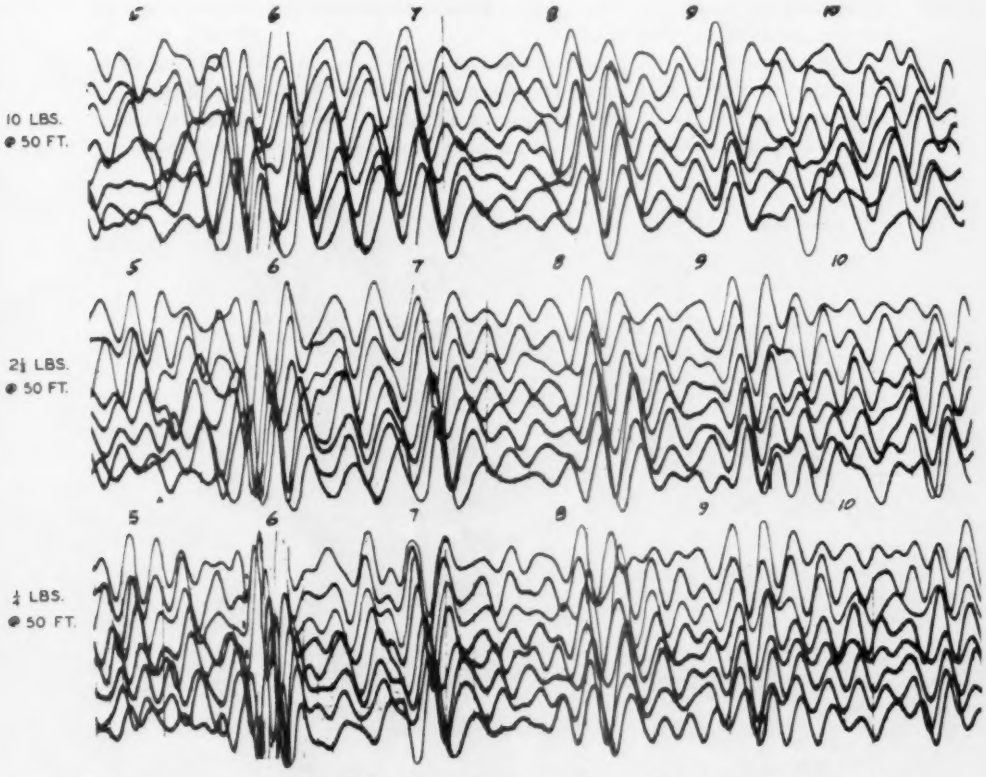

FIG. 5. This shows the effect of overshooting upon reflection quality and timing accuracy. The well defined reflections obtained with the small charge run together with those of the larger charges.

of the oldest practices in the reflection seismic technique. Unfortunately, it is not easy to do this and use a continuous profiling technique.

Geophones

Geophones are designed in a wide variety of types with respect both to electrical characteristics and to mechanical form. Emphasis in recent years on size and weight may have de-emphasized, to some extent, the electrical characteristics. The electrical characteristics of the geophone should be considered along with those of the amplifier and galvanometers as an integral part of the complete seismic channel. The main factors with which we are concerned in connection with geophones are frequency response, damping, plants, and the number of geophones.

The importance of good geophone plants is well known, although the use

of multiple geophones has resulted in a general decrease in the attention paid to getting good individual plants.

The effect of multiple geophones and multiple holes on reflection quality is illustrated in Figure 8. A small improvement is shown by the use of multiple holes over the results obtained by using a single hole. Additional improvement is shown by using 30 geophones and a single hole over that obtained with the

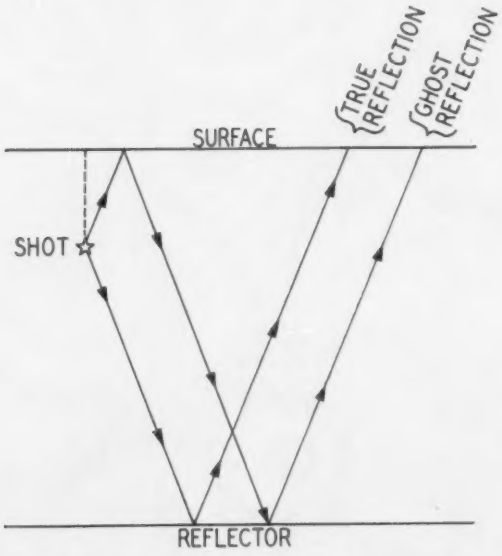

FIG. 6. Diagram of true reflection and ghost reflection paths.

three geophones and multiple holes. The bottom record shows the results of using multiple geophones and multiple holes. Thus, from the top record to the bottom one, the evolution from an NR to a very good record was accomplished by using the proper combination of multiple geophones and multiple holes.

Amplifiers

The amplifier is the heart of the seismic instruments. Upon its operation depend the entire results of the seismic survey. Proper knowledge of its capabilities and limitations is a necessity for obtaining optimum performance. A considerable number of independent elements constitute the amplifier. Of these, the main ones can be enumerated and subdivided as follows:

1. High pass filters
2. Low pass filters

3. Sensitivity controls
   a. Manual
   b. Time (suppression and expansion)
   c. Automatic (AGC or AVC)
4. Amplitude trim or recording level
5. Mixers

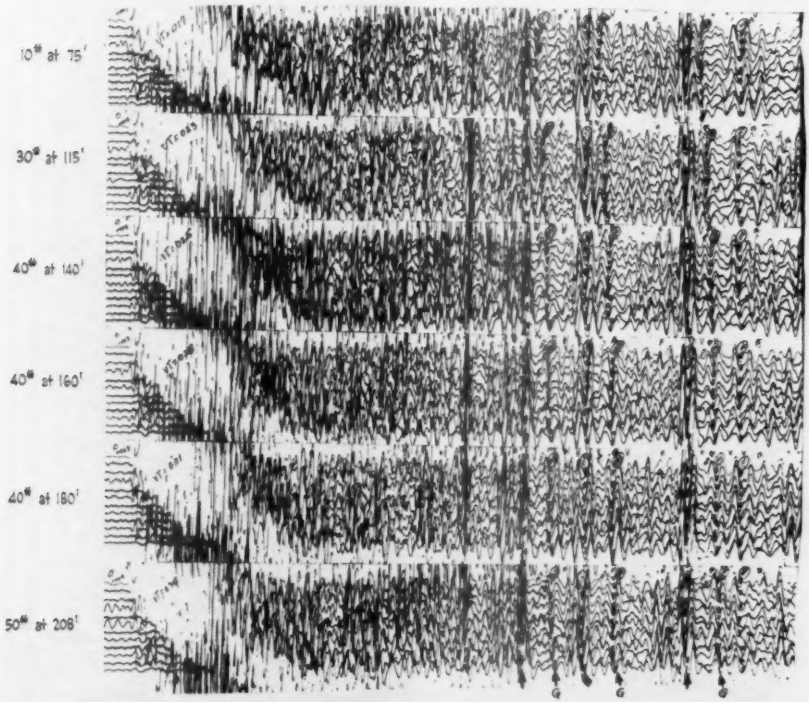

FIG. 7. Six records made from the same shot hole at depths ranging from 75 to 208 ft. Ghost reflections which converge on the true reflections as the shot depth becomes shallow may be seen following the true reflections.

The effect of filtering in an area where there is little ground roll and the reflections are of relatively high frequency is demonstrated by Figure 9. The reflected energy recorded on the top record may be seen on the other recordings, but it has better definition on the first record which, in this case, represents the optimum filter setting for the energy present.

The effect of a low-frequency versus a medium-frequency pass band upon

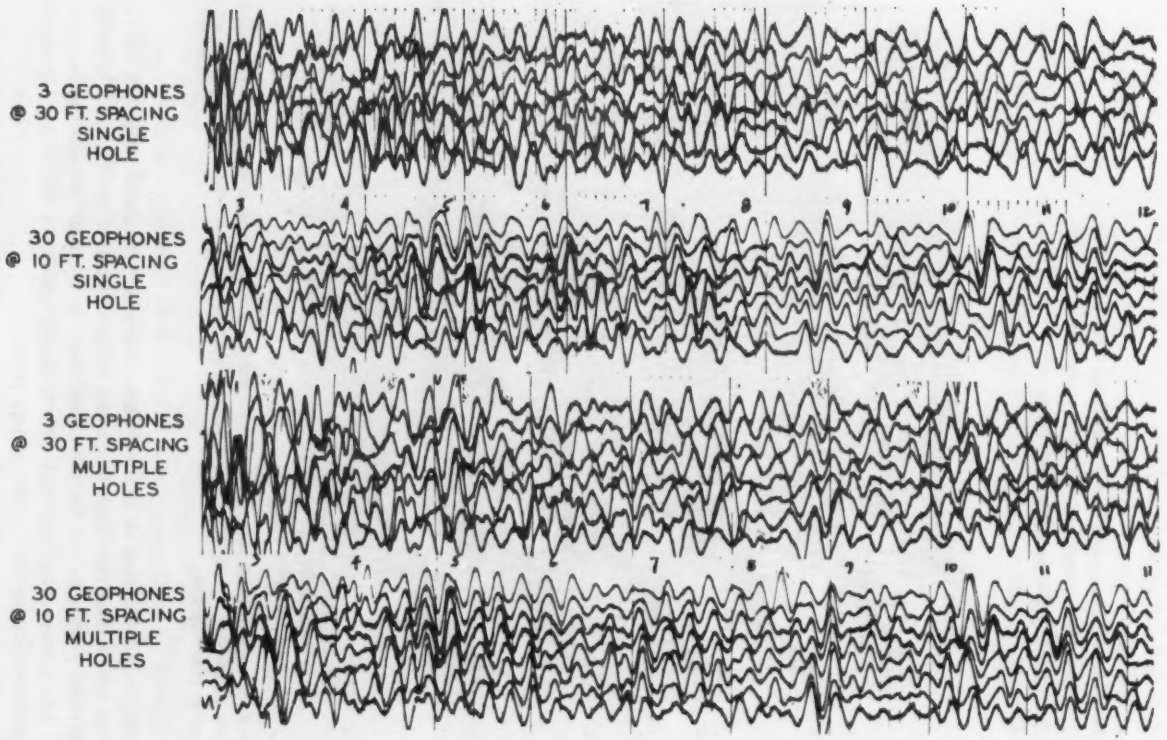

FIG. 8. Illustration of the effect of multiple holes and multiple geophones on reflection quality. Top record to bottom record shows the improvement from an NR to a good record through the use of multiple geophones and multiple holes.

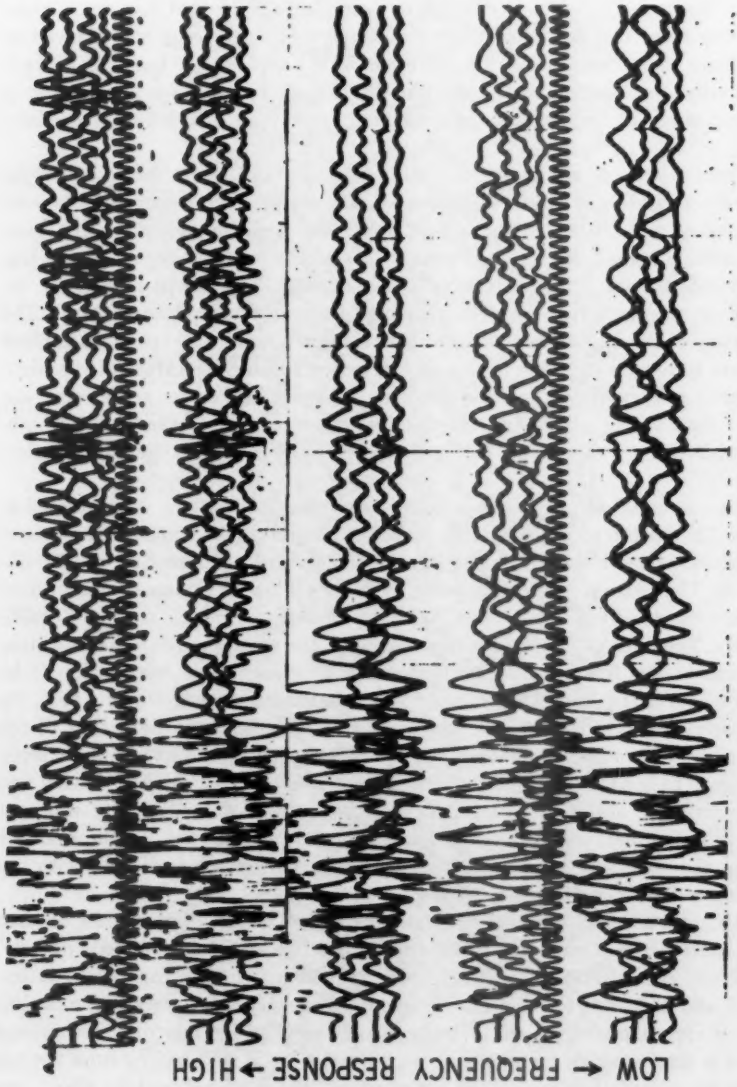

FIG. 9. This group of records illustrates the use of an optimum filter for relatively high frequency reflections.

reflection quality when the reflections are low-frequency is demonstrated in Figure 10. In the top record, the filters were adjusted so that too much high-frequency noise and not enough low-frequency reflected energy was allowed to pass. Note that reflected energy is present in the top record, but it is of very low quality. For the bottom record, the filters were adjusted for low-frequency response only. The signal-to-noise ratio was more than doubled on the reflections.

A pair of records made with a combination of standard recording and high-frequency recording is shown in Figure 11. The standard reflection records were made using a 1,320-0-1,320-ft spread, while the high-frequency records were made using a spread having an interval of 10 ft between adjacent geophone stations located from 50 to 90 ft from the shotpoint. The 35-cps reflections, recorded on the standard record, have a high-frequency component as well. The frequency of the high-frequency reflection is approximately 80 cps. This is often the case to depths of a few thousand feet below the surface. Most of the high-frequency energy traveling from horizons below those depths are filtered out due to the filtering effect of the earth. Here is an example of the need for high-natural-frequency galvanometers in the recording of the higher-frequency reflections.

The choice of AVC time constants is very important. This is illustrated in Figure 12. The top record was made by using a Normal-AVC time constant, having an approximate clamp time of 40 milliseconds and a release time of 90 milliseconds. The bottom record was made by using a Fast-AVC time constant, having an approximate clamp time of 20 milliseconds and a release time of 40 milliseconds. The no-AVC amplitude relationship of the strong to the weak reflection was 8 to 1. The Normal-AVC permitted the same amplitude relationship to be recorded while the Fast-AVC reduced this relationship to a factor of 3 to 1. By purposely changing the relative amplitudes of the reflections by means of the AVC action, the weaker reflection was brought up in amplitude to a usable level.

Figure 13 is an illustration showing a comparison of Normal-AVC action and Expander-AVC action. Expander-AVC action is used to reduce the wipe-out time in order that very shallow information may be recorded. In the example shown, the wipe-out time with Normal-AVC is 150 milliseconds, and with the Expander-AVC it is 50 milliseconds.

Mixing is a useful function in improving record quality, but it must be used with caution. In Figure 14, two forms of mixing are demonstrated, namely, uni-directional adjacent trace and bi-directional taper. The top record is unmixed, and it shows stepout across the record from the fourth trace to the twelfth trace of approximately 12 milliseconds at a record time of 0.6 second. The second record is that resulting from 50-percent adjacent trace mix, mixing from the top to the bottom of the record. The trace stepout has been reduced by about one millisecond. The third record is that resulting from a 60 percent bi-directional mix. This record is considerably cleaner than the previous ones. A single trace is

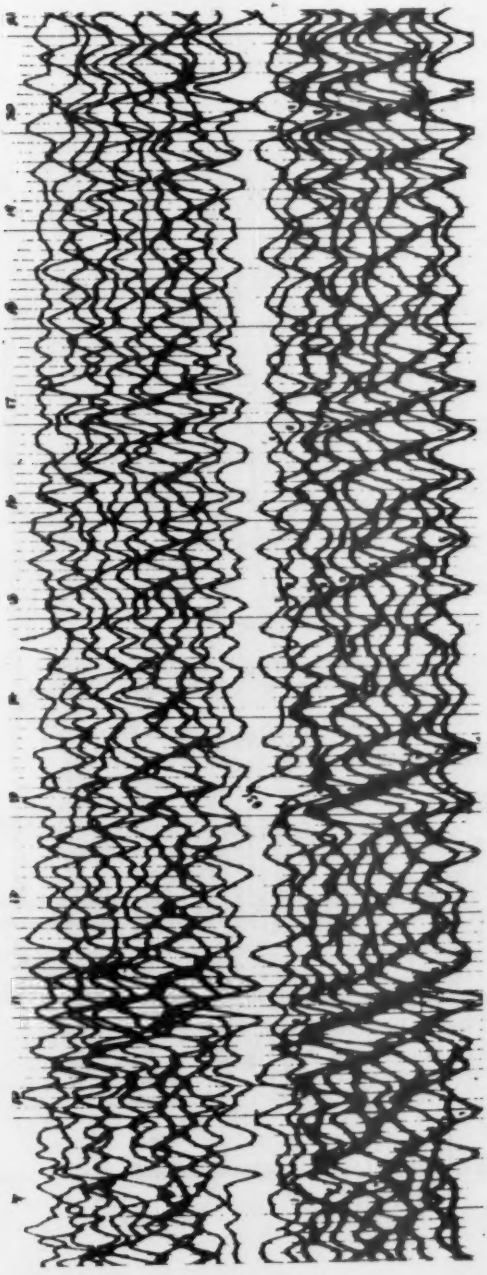

FIG. 10. An illustration showing the improvement by using filters of low frequency response (bottom record) when the reflections are low frequency.

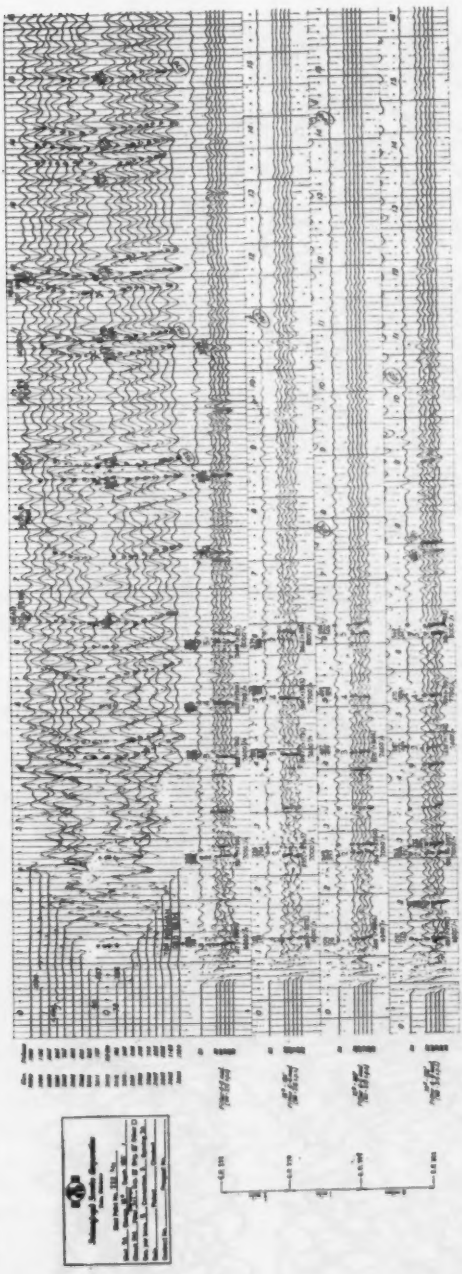

FIG. 11. An illustration of records made with standard and high frequency recording.

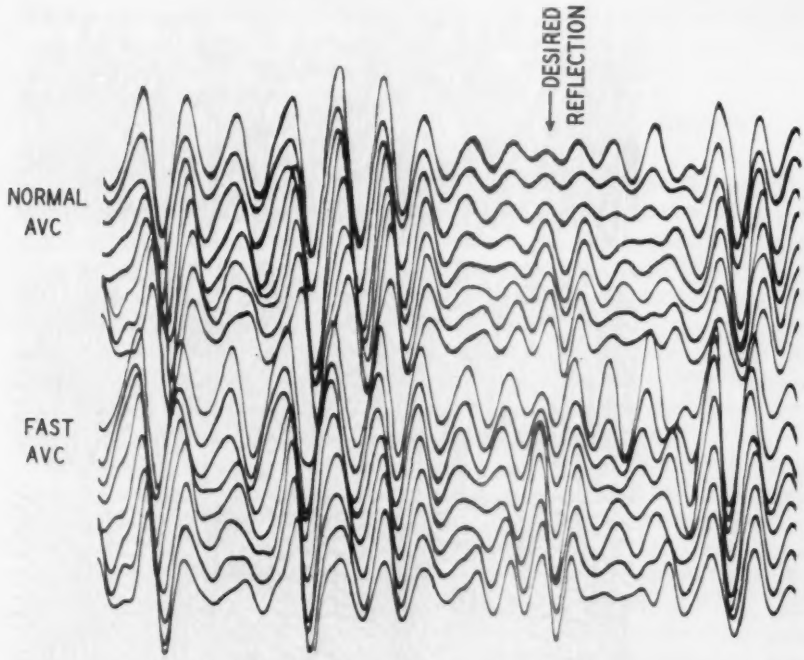

FIG. 12. Illustration showing the effect of AVC time constants. The top record has a "normal" AVC time constant, while the bottom record has a "fast" AVC time constant.

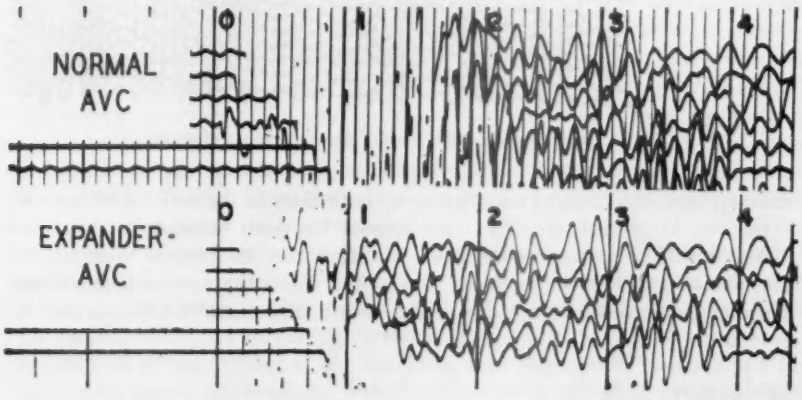

FIG. 13. A comparison of signal-controlled AVC and time-controlled plus signal-controlled AVC.

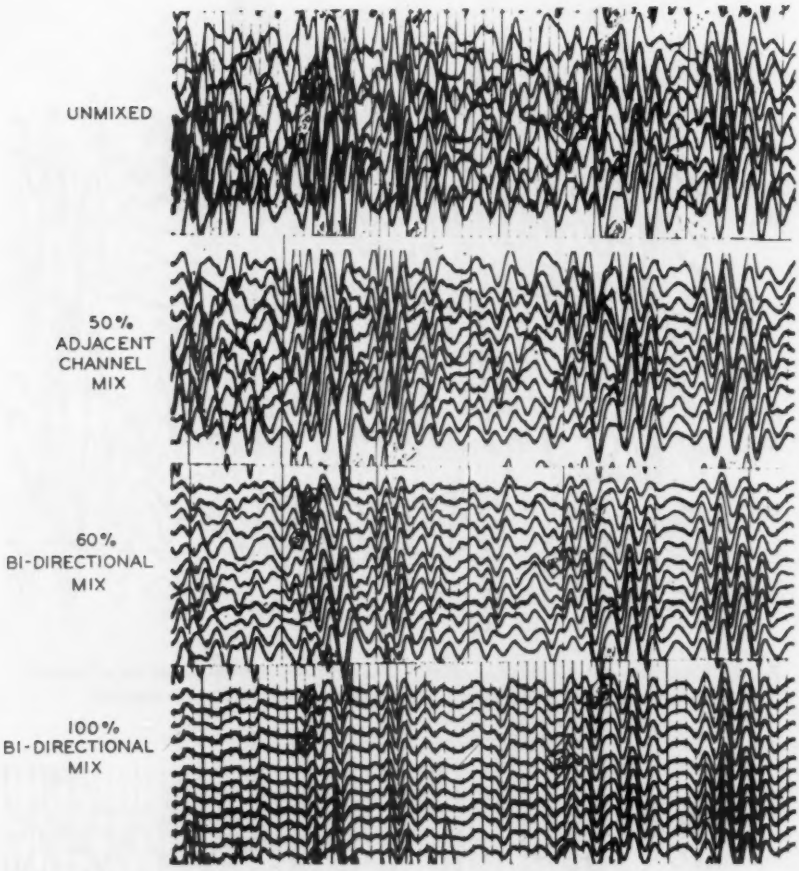

FIG. 14. An illustration of the effect of various amounts of mixing.

made up of energy coming from traces on both sides in the ratio of 60 percent, 30 percent, 15 percent, etc. The trace stepout has been reduced by about two milliseconds. The bottom record is that resulting from 100 percent bi-directional mix. The stepout has been reduced to zero; this shows that, somewhere between the unmixed record and the overmixed record, dips would be completely destroyed.

Galvanometers

The galvanometers which are normally used are those which have natural frequencies high enough to record the highest reflection frequencies of interest.

This usually means that natural frequencies of 80 to 150 cps are satisfactory. However, when high-frequency recording is desirable, the natural frequencies of the galvanometers should be increased to some 300 to 500 cps to extend their recording capabilities.

Recording and Record Presentation

Since records are visually analyzed, considerable attention should be paid to the amplitude and clarity of the traces, the relative trim, the trace spacing, and the density ratio of the traces to the time lines. Otherwise, what may be in actuality a very good record may be, from superficial study, considered of low grade or having poor signal-to-noise ratio. Even though a reflection meets all the required qualifications of a good reflection (essential copy, elevation, and envelope), as set forth by Phil Gaby (1947), if the relative trim is poor or the traces are out of focus, if the time lines are too heavy, or if there is other evidence of poor recording, the processing of the record would be tiring to the interpreter, and the normal reaction would be that the record was of low quality.

One of the difficulties of improving records in difficult areas when an NR is first obtained is the problem of knowing just where to start and how much improvement is required. This problem again goes back to the fact that the records are visually analyzed. Karl Dyk and J. D. Eisler (1951) have shown that if the signal-to-noise ratio is 6 db, that is, the signal amplitude twice the noise amplitude, 100 percent of the reflection picks will be made correctly; that at a signal-to-noise ratio of 0 db, that is, the signal just equaling the noise, some 63-percent-correct picks could be made; that if the signal-to-noise ratio were −6 db, less than 20-percent-correct picks would be made. Extrapolating the curve obtained by Dyk and Eisler, we might expect that at some −10 db of signal-to-noise ratio, no correct picks could be made. J. L. Lawson and G. E. Uhlenbeck (1948), in general, confirm this observation. The important point is this: Within a 3-to-1 or, at most, a 6-to-1 signal-to-noise ratio variation, the reflections can change from unrecognizable to satisfactory and reliable. When an NR record is obtained, there is no way of knowing whether the signal is buried in the noise or interference by a factor of 3-to-1 or 100-to-1. If it is the former, a slight change in the instrument characteristics will probably produce satisfactory records. If, on the other hand, it is the latter, the operator may be hard pressed, with all the potential improvements shown in the previous examples, to bring a usable signal out of the interference.

Usually, the greatest return for the effort with any one of the above list of variables will be apparent from the first modifications made. The point of diminishing returns is reached rather quickly. For example, in the use of multiple geophones the statistical improvement is generally considered equal to the square root of the number of phones. Thus, four phones will give a 2-to-1 improvement over a single phone, but 16 phones are required to obtain a 4-to-1 improvement and 100 phones to obtain a 10-to-1 improvement. It is generally wise, therefore, having investigated one means of record improvement to a

reasonable degree, to determine whether or not another approach may be a valuable supplement to the first one.

With the most recent of present instruments it is possible to perform some operations that were previously impossible to do directly from the shots; that is, through the use of reproducible recording, of which magnetic recording is the most popular, it is now possible 1) to have composite shots taken at different times; 2) to mix traces after weathering, elevation, and normal move-out corrections have been made; and 3) to display the corrected traces in cross-section form for interpretational purposes. These operations are in addition to the more common ones of obtaining records of different filter settings, different AGC action, etc.

A seismic cross-section having $4\frac{3}{4}$ miles of surface coverage is shown in Figure 15. This cross-section takes the place of a time-depth cross section normally drawn up on cross-section paper. Each trace on the cross-section contains information originating from a depth point located midway between shotpoints. The distance between depth points is 660 ft. Multitrace recordings were made for each shotpoint, but only the trace information representing the midpoint was transferred to the cross-section. A total of 21 9-trace records were recorded over the $4\frac{3}{4}$-mile traverse with 38 traces being used to make up the cross-section. This is an example of a selective-trace-type cross-section. In areas of good records and of low relief, it is not necessary to use all traces obtained during the field recording to make up a cross-section. The Oread (OR) and Woodford (Wd.) reflections, on the seismic cross-section, show the true relationship of the horizons to sea level datum, since all corrections, including spread, have been removed prior to the re-recording from magnetic medium to paper through the use of a cross-section camera.

The amplitude relationship and phasing of reflections generally associated with reflection shooting are retained on this type of cross-section. In general, these are beneficial in making the final interpretation.

RECENT TRENDS

Some of the recent trends that have been apparent in seismic instruments and shooting techniques are:

1. Multiple geophones (patterns and spaced)
2. Increased number of traces
3. Increased dynamic range
4. Increased frequency response
5. Multiple shot holes (patterns and spaced)
6. Multiple section filters
7. Lower distortion characteristics
8. Air shooting
9. Weight dropping
10. Magnetic recording

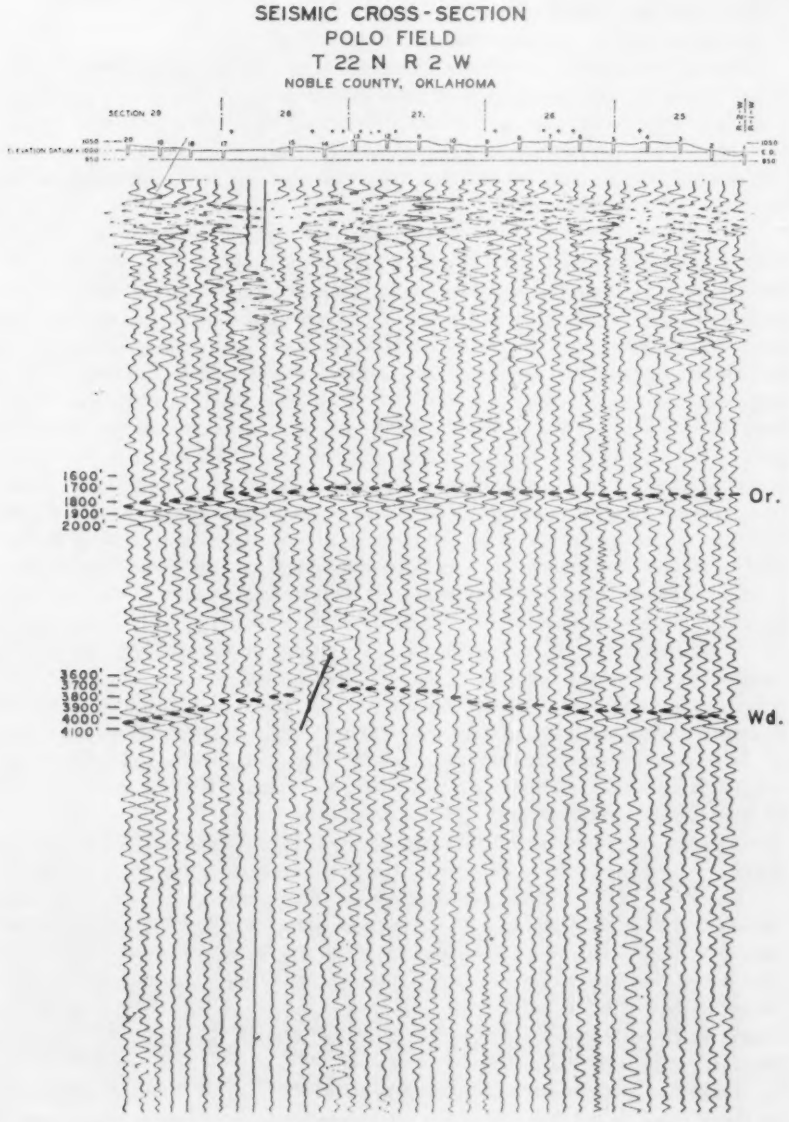

FIG. 15. A seismic cross-section of 4¾ miles of surface coverage. Corrections for weathering, elevation, and normal stepout have been made.

11. Corrected cross-sections
12. New types of cross-sections

These trends may not be entirely independent but are sometimes interrelated. As an example, the use of cross-sections is enhanced by the use of magnetic recording, since corrected sections can be made easily. Variable-area cross-sections, variable-density cross-sections, and Reynolds Sections are being used for presentation of data. In addition, the cross-sections are being displayed in depth as well as in time.

A comparison of the conventional galvanometer cross-section versus the variable-density cross-section is shown in Figure 16. In comparison, the reflection troughs on the conventional galvanometer cross-section appear as white spaces on the variable-density cross-section, and conversely the black spaces represent the signal peaks. The gray portions of the variable-density traces prior to the first breaks represent the no-signal light level. High-signal levels are indicated by large variations in the density of the trace, going from black to white in extreme cases. With low-signal or noise levels, the density approaches the no-signal density prior to the first break. Reflection character appears as shades of gray. Reflection or signal frequency is represented by the width of the white and black spaces. One cycle of energy is composed of one white and one black space. Note the fault evidence on Shotpoint 3 at a record time of 1.05 sec. The fault is more readily seen on the variable-density than on the conventional galvanometer cross-section.

A variable-density cross-section containing information from 17 shotpoints of 24 traces each, and representing 4 miles of surface coverage is shown in Figure 17. At Shotpoint 3, good fault evidence is shown on the 1.05-sec reflection, being uplifted to the south. Good evidence of a "pinch-out" is shown on the 1.0-sec reflection from Shotpoint 8 to Shotpoint 10. The "pinch-out" is indicated by the disappearance of the first black space and first white space of the 1.0-sec reflection.

In recent years greater emphasis has been placed on the distortion characteristics of amplifiers, on handling a wider range of signals, both at low levels and at high levels, and handling a wider frequency range. This has come about through the use of increased filtering, the use of multiple geophones, and the requirement of working areas which have large amounts of interference energy.

The use of multiple geophones has become the common practice rather than the exception. It is estimated that "a single manufacturer has produced more geophones in the past 10 years than were in use by the entire industry 10 years ago." The use of multiple geophones may not always have merit. In many cases, it is believed that a set of indifferently planted geophones is taking the place of a single well planted geophone, as would have been done by the old-time "jug hustler."

There has likewise been increasing demand for more and more traces. This, in many cases, is not justified if the interpretational procedure is considered. It is often found that little or no use is being made of these traces beyond the doubtful one of reflection identification. Yet these additional traces place a heavy

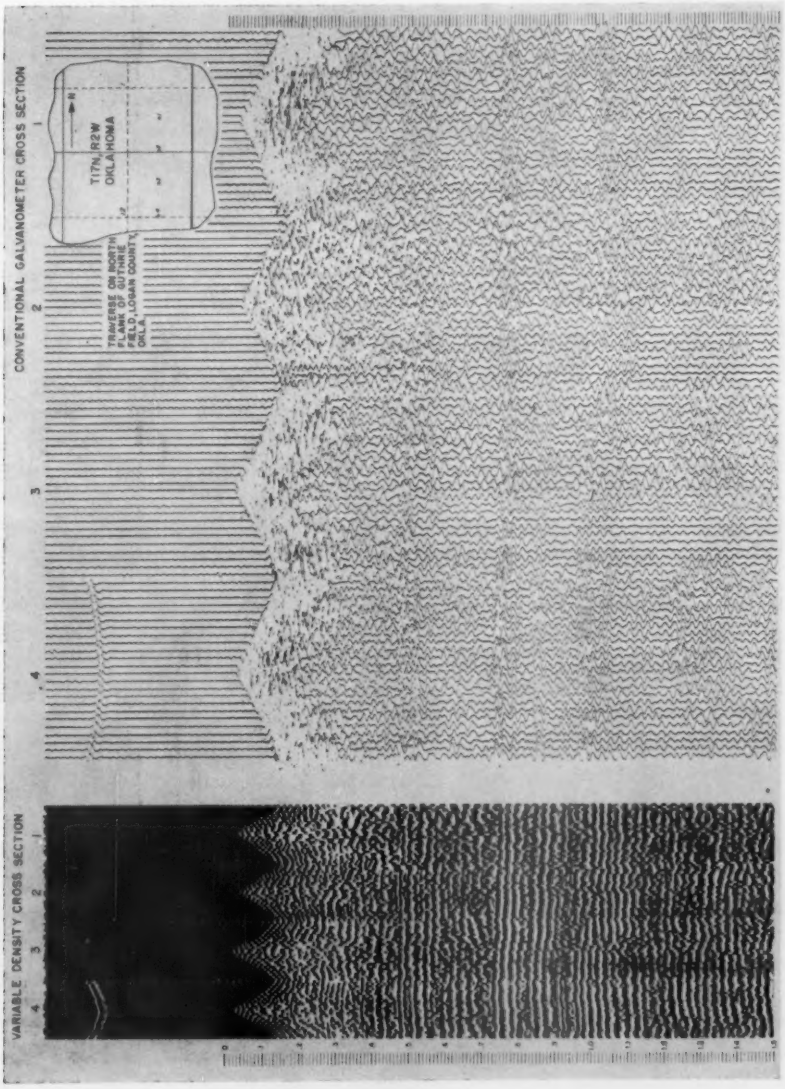
CONVENTIONAL GALVANOMETER CROSS SECTION
VARIABLE DENSITY CROSS SECTION
T17N, R2W
OKLAHOMA
TRAVERSE ON NORTH FLANK OF GUTHRIE FIELD, LOGAN COUNTY, OKLA.

FIG. 16. A comparison of a conventional galvanometer cross-section with a variable-density cross-section.

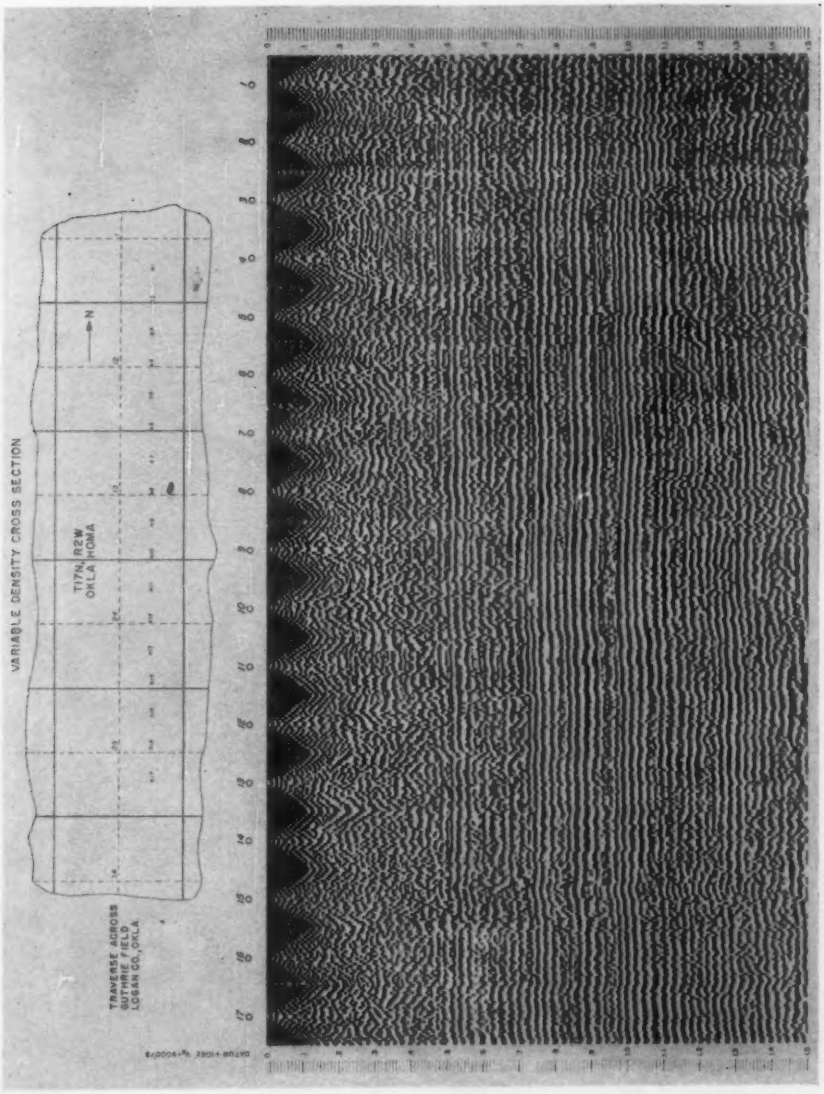

FIG. 17. A variable-density cross-section composed of 17 shotpoints (408 traces) and representing 4 miles of surface coverage.

operating and economic burden on the field crew. It might be wise to require that the interpretational group justify every trace used in the equipment on a value received basis in the interest of obtaining more information from the traces in use; for multiplicity of traces themselves adds very little to the basic improvement of the reflection records.

The use of increased filtering when compatibly designed with the distortion characteristics of the amplifiers is of appreciable value in a number of difficult areas.

As Andrew Gilmour (1950) has pointed out, instruments should be matched with care and precision and field operations carried out in such a way that data of the highest possible quality and of the greatest accuracy are obtained. Otherwise, the small time differences obtained from small structures will not be dependable. Time breaks, up-hole time, and good refraction breaks are an absolute necessity for the interpretation to be reliable.

Trained personnel are essential to the proper operation of seismic instruments with the complex and varying problems which are continually being presented. The features that are incorporated in the instruments for the solution of the problems that have been mentioned make them so complex that considerable skill is required to get the highest performance from the instruments. Modern instruments, with possibly 600 geophones to keep in working order, as many as 1,380 filter combinations available, and a wide selection of AGC, pre-suppression, and mixing combinations, and with 24 or more channels, represent a formidable piece of apparatus to a young observer. Is it any wonder that there is a problem in getting adequately trained personnel? Furthermore, it should be kept in mind that the observer has a matter of a few minutes at most to decide whether a record is adequate or not. In a quick look at the record he has to decide whether to change the charge, the hole depth, the instrument settings, or to move on to a new hole. After a day's shooting has taken place, the interpreter has all of the next day or more to analyze the records and reach the conclusion that the observer had not made very good decisions in some of the cases. The emphasis that has been placed on production should be kept in mind when one considers the quality of the records obtained and the decisions that the observer had to make together with the pressure of the entire field production probably dependent on him. As George E. Wagoner (1951) said, "Many reflections have been left behind with speed in mind."

THE FUTURE

An answer to this dilemma may lie in the use of magnetic recording. Utilizing wide-frequency-band equipment with a wide dynamic range and with adequate monitoring of the shots so that the best hole shooting conditions have been utilized, the information may be stored for replay under conditions considerably

more conducive to good records than those of the field. Furthermore, the previously mentioned additional advantage of the reproducible recording may be brought into play. We have, then, the possibility of a reversal in the trend of more and more complex instruments being required in the field; these more complex instruments may now be replaced with simpler field instruments and the complex instrumentation put in what more nearly resembles laboratory conditions. This may result in a further overall improvement of the record quality and ability to work more and more difficult areas.

Use of variable-density cross-sections gives promise of being of great value for interpretation. This form of recording, while not new, is of much greater value in cross-section use than in individual records. When combined with magnetic recording, which permits corrected cross-sections to be made, it becomes a very powerful form of information display.

A variable-density cross-section obtained near the Mexican border in the vicinity of Laredo is shown in Figure 18. The cross-section, representing a 6-mile traverse, contains 24 24-trace spreads of 1,320 ft each. The section was recorded by using a filter having a frequency response of 32 to 50 cps.

A variable-density cross-section of the same traverse as that of Figure 18, except that a filter response of 43 to 100 cps was used, is shown in Figure 19. The comparison of the two filter settings shows that deeper reflections were better recorded with the lower frequency response, and the shallower reflections were better with the higher frequency response. This points out one of the useful features of replaying from magnetic tape in that interpretations may be made more easily and more accurately through the use of selective filtering. The strong reflection at a record time of 1.8 sec is the top of the Middle Cretaceous. Note the convergence of the Upper Cretaceous reflections and the Middle Cretaceous reflection, particularly from the fourth shotpoint onward, reading from left to right. Fault evidence is also recorded at the seventh and eighteenth shotpoints from the left-hand border. The converging reflections at a time of 1.6 sec were not readily recognizable on the standard trace field records.

The central office magnetic replay equipment used by the authors for making standard records, galvanometers and variable-density cross-sections, and composite recordings from magnetic tapes is shown in Figure 20. The unit on the left is the visual display on which a playback may be viewed without taking and processing a paper type record. The unit is used for viewing the effect of filtering, of AVC time constants, and of mixing, and to check time-break alignments. The center unit is the seismic replay console, which contains 24 seismic amplifiers (full range frequency response from 4 to 520 cps), a recorder-reproducer with both static and dynamic correctors, a 10-inch 50-trace camera, and associated power supplies. The unit on the right is the cross-section camera from which galvanometer type and variable density type cross-sections are photographically made on paper or film. The size of the cross-sections may be up to 24 inches wide and 43

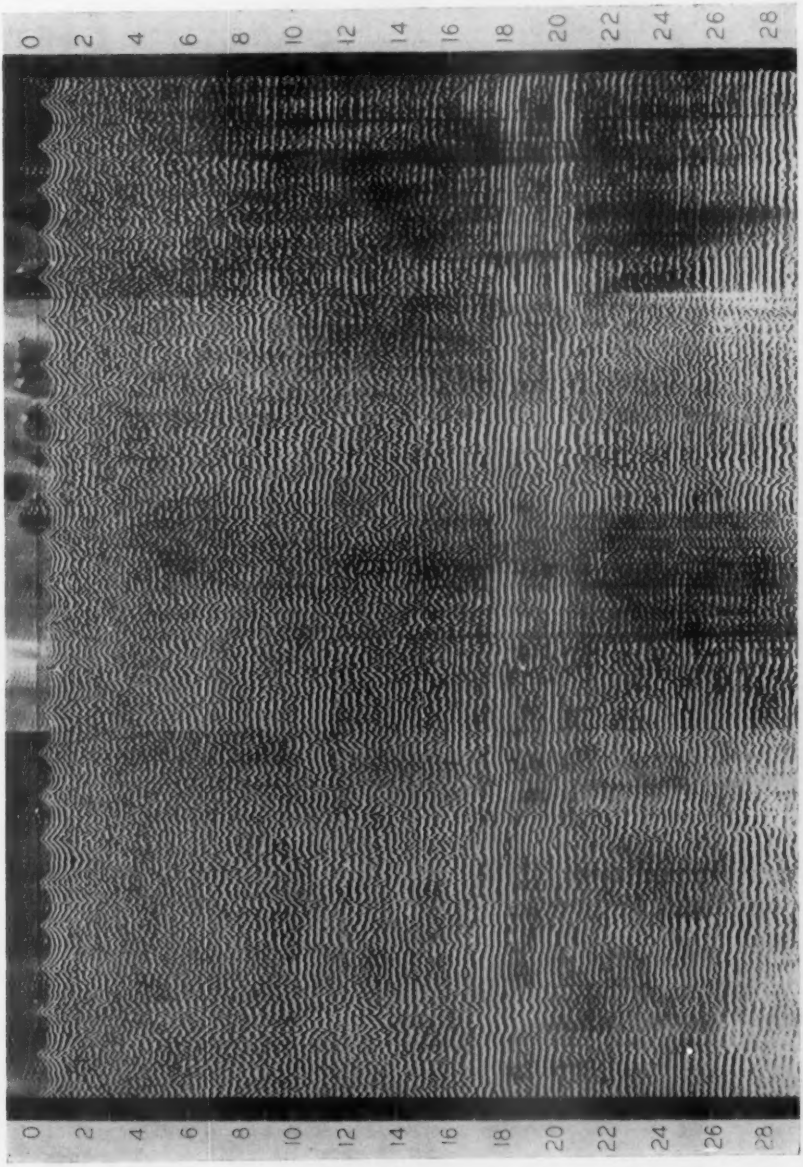

FIG. 18. A variable-density cross-section composed of 24 shotpoints (576 traces) and representing 6 miles of subsurface coverage. Filter response was 32 to 50 cps.

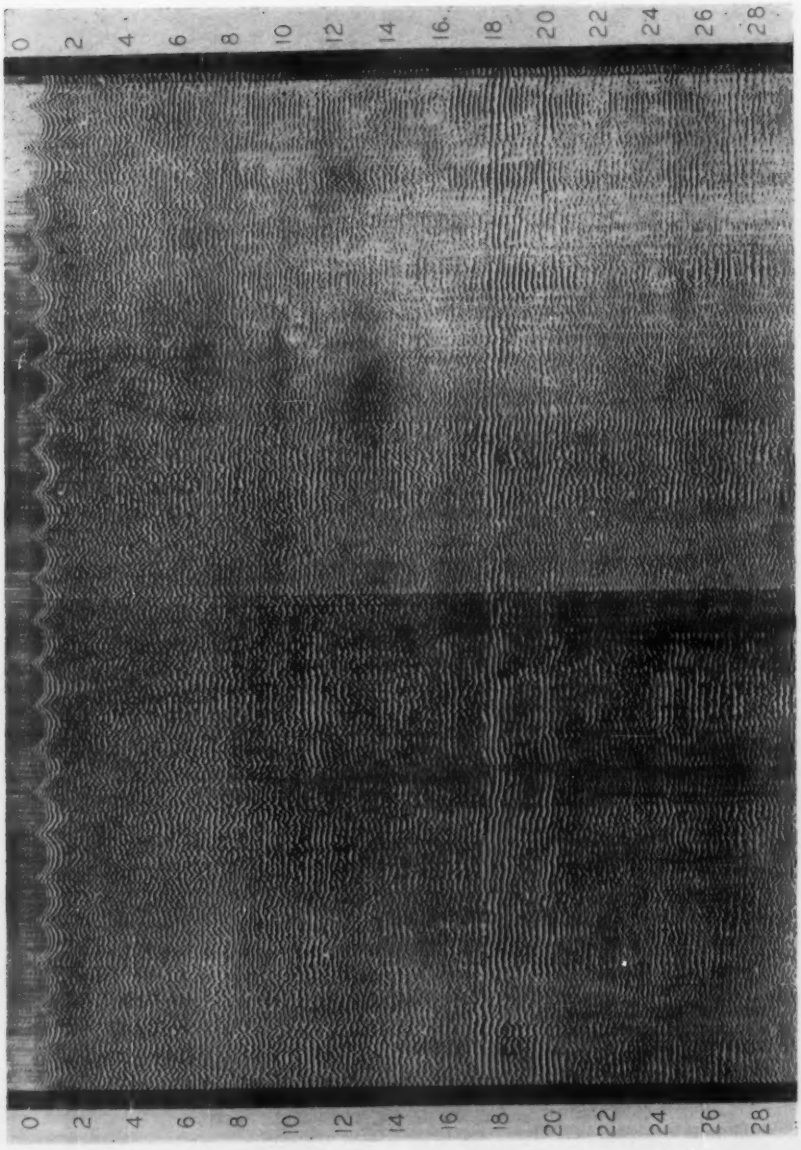

FIG. 19. A variable-density cross-section composed of 24 shotpoints (576 traces) and representing 6 miles of subsurface coverage. Filter response was 43 to 100 cps.

inches long containing 100 variable-amplitude traces or 400 variable-density traces.

Finally, we have held out before us the lure of automatic computing and the dream of automatic record interpretation. Developments in the seismic industry for the automatic handling of seismic data are anything but clear. If by computing we mean applying the routine corrections to the raw data, then machines can do this work. The exercise of geophysical and geological judgment in the picking and correlation of reflections will probably remain in the hands of the geophysicist

FIG. 20. A central office magnetic replay center.

for some time to come as will the final conversion of the geophysical data into maps depicting the geology.

Thus, wide-band magnetic recording and replay, using the most versatile of instrumentation, combined with automatic computing for handling the routine corrections and increased use of cross-sections for interpretation and data presentation, offer the greatest promise for the future in furthering our goal of improved results.

REFERENCES

Dyk, Karl, and Eisler, J. D., 1951, A study of the influence of background noise on reflection picking: Geophysics, v. 16, p. 450–455.

Gaby, Phil P., 1947, Grading system for seismic reflections and correlations: Geophysics, v. 12, p. 590–617.

Gilmour, Andrew, 1950, The state of seismic prospecting: Geophysics, v. 15, p. 395–399.

Lawson, James L., and Uhlenbeck, George E., 1950, Threshold signals: M.I.T. Radiation Laboratory Series, v. 24, p. 185–193.

Musgrave, A. W., Ehlert, G. W., and Nash, D. M., Jr., 1958, Directivity effect of elongated charges: Geophysics, v. 23, p. 81–96.

Van Melle, F. A., and Weatherburn, K. R., 1953, Ghost reflections caused by energy initiated above the level of the shot: Geophysics, v. 18, p. 793–804.

Wagoner, George E., 1951, Geophysical frontiers: Geophysics, v. 16, p. 385–390.

GEOPHYSICS, VOL. XXIII, NO. 4 (OCTOBER, 1958), PP. 823–837, 11 FIGS.

AN EMPIRICAL VELOCITY DETERMINATION IN SOUTHERN OKLAHOMA*

DONALD R. OKSA†

ABSTRACT

Lack of adequate velocity data can sometimes be overcome by the proper co-ordination of seismic and geologic factors. The basic assumption that seismic and geologic data are directly correlatable must be utilized to its fullest extent. Upon this basis reliable basic seismic data of time and delta t values are computed with variations in the other parameters to make the computed seismic data closely match the known geologic conditions by one of several standard computing methods. The empirical fitting of the seismic data to match geologic conditions establishes the velocity gradient which can be then be extrapolated into immediately adjacent areas. An iso-velocity section can also be prepared, if desired. Generally, it appears that iso-velocity contours parallel formational strikes. The application of such empirically derived velocity data will result in seismic structural maps and cross-sections which are compatible with actual geologic conditions. The value of the oftentimes neglected true dip section is shown and is actually an integral part of the analysis. The application of electronic computing techniques makes such determinations much more rapid and makes the method entirely feasible.

INTRODUCTION

The introduction of velocity factors into a seismic interpretation makes the results more readily understood by the geologists. Sometimes when inadequate velocity data is available, the results are presented in terms of reflection times only. The factor of velocity simply cannot be avoided when steep dips are to be computed. In such cases, the best velocity data available are used.

An erroneous velocity function can distort the seismic results to such an extent that the presentation is of very questionable quality and yet the actual interpretation of the records may be perfectly satisfactory. The checking of the seismic results against the known geologic factors should be a most important part of a seismic survey. If the geologic factors are not adequately verified then additional checks are necessary to determine whether the basic interpretation is correct or whether an erroneous velocity function has been used.

In an area of southern Oklahoma the seismic results were in great disagreement with the known geologic conditions. It was obvious that the reason for disagreement was probably due entirely to inadequate velocity information. Since the velocity data being used was the best data available, it became necessary to resort to an empirical approach to determine a better velocity function.

ASSUMPTIONS

1. "The assumption is made that there is a direct correlation between velocity discontinuities and geologic strata. This assumption is universal in all seismic

* Paper read at the 11th Annual Midwestern Meeting at Tulsa on April 18, 1958. Manuscript received by the Editor April 14, 1958.

† Sinclair Research Laboratories, Inc., Tulsa, Oklahoma.

work, since without it seismic data would have no value in geologic interpretation of the subsurface. There may be special cases where this assumption breaks down; however, practical experience has shown that in general it is valid." Alcock (1943).

2. The assumption is made that the velocity distribution type is the same over a relatively localized area. It is possible that the crossing of major faulting may change the velocity distribution and probably would cause a variation in the horizontal distribution of velocities. Musgrave (1952) states that a number of vertical velocity assumptions which have been made in the past are:

a. Linear increase of velocity with depth, i.e., the curved path method,
b. Linear increase of velocity with vertical time, i.e., parabolic increase of velocity with depth,
c. Hyperbolic increase of velocity with depth,
d. Exponential increase of velocity with depth, and
e. Complex variation of velocity with depth.

A linear increase of velocity with depth function was used in this area as indicated by past experience and the closest available velocity surveys. The choice of a velocity assumption, of course, should be that most appropriate in consideration of available velocity information in the general vicinity and past experience in the area.

3. The assumption is made that the iso-velocity contours, i.e., the horizontal distribution of the velocity function, will parallel the formational strikes. This assumption permits the extrapolation of the velocity distribution areally.

4. The possible origin of the reflections should be considered. The assumption that one or more prominent reflections would originate at or within a limestone member rather than in a shale section, for example, would be most helpful in the selection of the final velocity. At the critical point of the velocity determination slight variations in the initial velocity or the acceleration factor do not change dip values appreciably but will change the vertical and horizontal location of the subsurface coverage to a better match with the geologic lithology and probable velocity discontinuities.

PREREQUISITES FOR THE EMPIRICAL VELOCITY DETERMINATION

Before a satisfactory empirical velocity determination can be made, the following seismic-geologic criteria must be available:

1. Sufficient geologic data for control purposes. Two or more wells, subcrop or outcrop data, well dip meter readings, etc., must be available and suitably located.
2. Reliable seismic data between the geologic control points. The continuity of reflections, reflection quality, time, delta t values and their resolution all contribute to the reliability of the final velocity determination.
3. Parallelism of the seismic strikes is a factor that permits the construction of a good "synthetic" or true dip section. A probable variation of ten de-

grees in strike direction would be permissible without seriously affecting the accuracy of such a true dip section.

4. No faulting of consequence indicated by the seismic data between the control points.

The foregoing prerequisites were satisfied in a steep dip seismic prospect in southern Oklahoma.

GEOLOGIC FACTORS

The published geologic data available in this area are of a general nature. The same type of data are available in many areas. The data available are:

1. Surface geologic maps showing outcrop data in the general vicinity. These maps also provide a basic description of the formations in the area and give a general idea of the geology. The general geologic column for this area is:

PERIOD	GROUP OR FORMATION	REMARKS
Cretaceous	Undifferentiated	Overlies most of the area
Major Unconformity		
Pennsylvanian	Springer Fm.	
Mississippian	Caney Fm. Sycamore Fm. Woodford Fm.	Shale Limestone Shale
Devonian Silurian	Hunton Group	Limestones
Upper Ordovician	Sylvan Viola Fm.	Shale Limestone
Middle Ordovician	Simpson Group	Upper Simpson Bromide usually logged. Primarily sandstones and limestones, some shales.
Lower Ordovician Cambrian	Arbuckle Group	Primarily dolomitic and limestone members, some sandstones

2. Several dry holes in the area, mostly shallow wells, and a few deep holes into the Bromide member of the Simpson group.

3. Two dry holes about one-half mile apart. One well was bottomed in the Sycamore shale and the other in the Viola.
4. Sufficient regional geologic data to indicate that the formations in this area could be safely considered conformable beneath the unconformity represented by the basal Cretaceous contact.
5. Subcrop and surface contact location of the several formations.

The available geologic data gave no indications whether faulting would or would not be present in the immediate area of the survey.

PROCEDURE

Figure 1, Seismic and Geologic Control Data, shows the relationship of the shotpoints, the geologic control points, consisting of two dry holes, and the subcrop and outcrop positions of the various formations. Also shown in this figure are the strike-dip symbols for several seismic horizons as determined by the computation of the data with the velocity function "A" being $V = 8{,}850$ ft/sec $+0.63Z$, a linear increase with depth function. A second line of control points is indicated, with the strike-dip symbols, which shows the general uniformity of seismic formational strikes.

Figure 2 is a record section of the seismic control of Line 1, less cross spread data. The continuity of the reflections plotted in Figure 1 is indicated. No faulting is indicated by this line of control between the geologic control points.

Figure 3 is a true dip or "synthetic" section AA′ made perpendicular to the average strike of the seismic data, and shows the geologic data and the key seismic data plotted as dip segments for velocity function "A." Figure 4 is the same section, AA′, except that the control points are taken from the contoured map. This latter figure shows more clearly several relationships to be discussed. The essential parallelism of the seismic strikes permits the construction of this type of section with a good degree of accuracy. Since the seismic data do not indicate faulting the attitude of the formations can be shown by the joining of the appropriate geologic control points, as has been done with the Sycamore, the Hunton, the Viola, and the Simpson-Bromide formations. Although the latter two formations are estimated for three of the four points, the acceptance of the geologic premise of uniform formational thicknesses makes this permissible.

Section AA′, Figure 4, immediately shows the excessive seismic dip rate obtained with velocity function "A." However, this is a true dip section, which is not too frequently employed because its construction is both tedious and time consuming. The more ordinary displays of seismic data by apparent dip sections, record sections with or without velocity information, or a multiplicity of dip vectors, as in Figure 1, may fail to show this excessive seismic dip as clearly because the direct comparison of geologic control to the seismic control is absent or, at least, obscured. Regardless of the method of presentation of data the reflection "A" may very well be considered as being of Viola origin from its relationship to the well control and the fact that it is a prominent reflection. The choice that

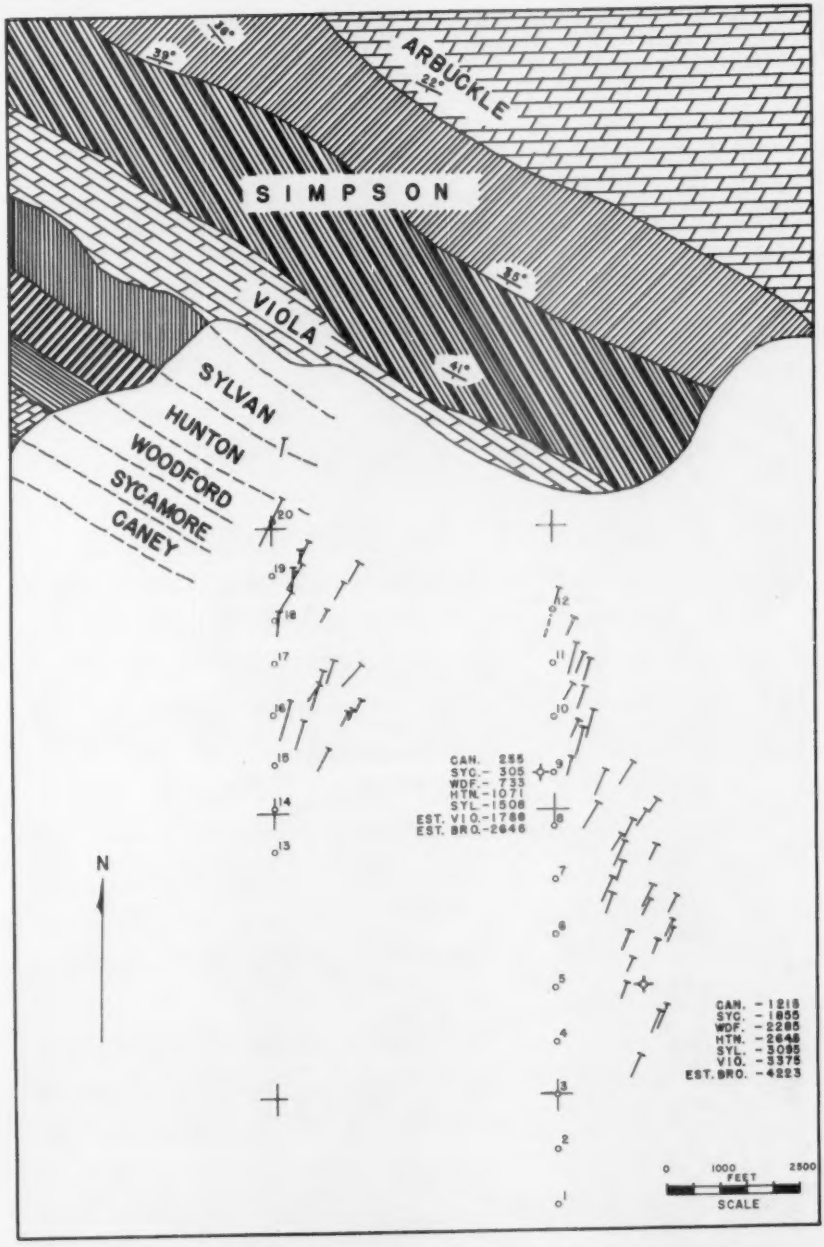

FIG. 1. Seismic and geologic control data.

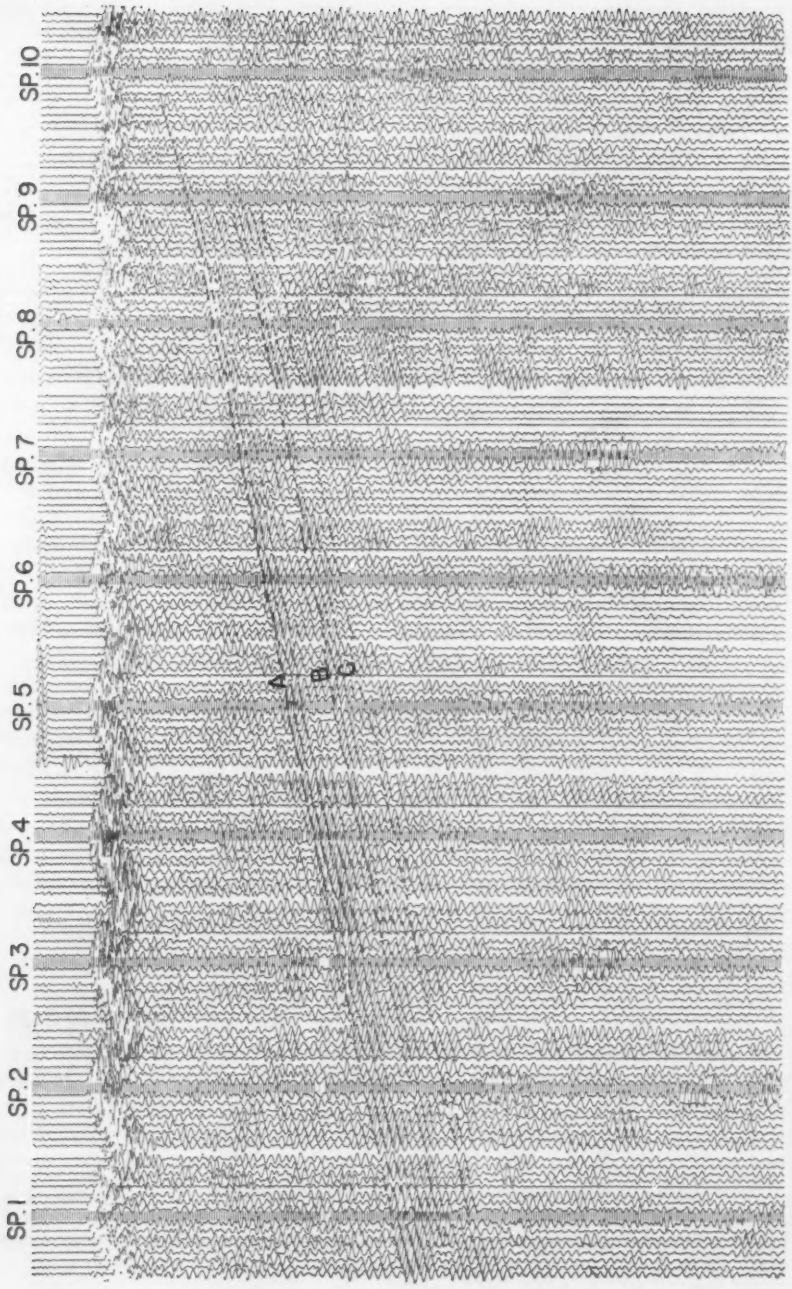

FIG. 2. Record section of velocity determination line.

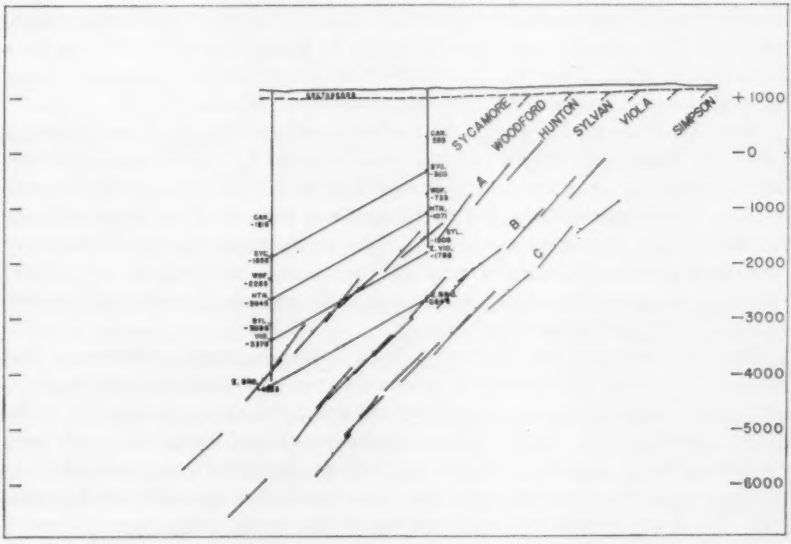

FIG. 3. Seismic—geologic cross-section AA′. V_0 and a constant.

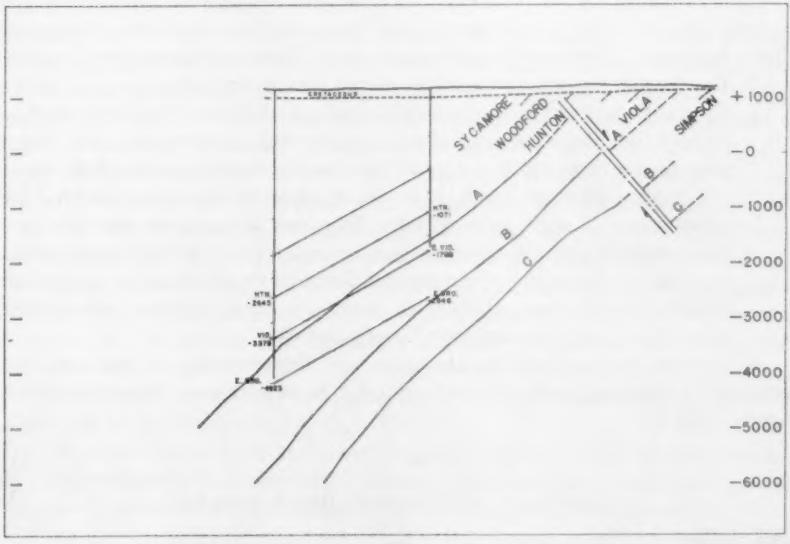

FIG. 4. Seismic—geologic cross-section AA′. V_0 and a constant.

the reflection "A" represents the Viola then suggests that a fault of approximately 1,000 ft of displacement is necessary as shown in Figure 4, to fit the seismic data to the subcrop data. This fault would be downthrown to the northeast. Similar conclusions would be reached concerning reflections "B" and "C."

This particular section should be studied in relation to the general geology of the area. First, it can readily be noted that Horizons A, B, and C do not exhibit the conformibility that the scattered well data and other geologic data would lead one to suspect exists. Secondly, the profile of the reflections cross from one geologic horizon to another as they go up-dip as shown in Figure 4. While only three check points exist, the two wells and the subcrop positions, the suspicion of a possible erroneous velocity function should be apparent, especially since the seismic data do not indicate faulting.

The introduction of this "velocity" fault in the structural presentation thus leads directly to the presentation of erroneous maps and cross-sections. The location of the "velocity" fault occurs where the seismic data are lacking due to the extreme shallowness of the formations being mapped and the fact that the areas of outcrop and/or subcrop locations occur where the Cretaceous cover is thin to lacking and thereby creating conditions unfavorable to the recording of seismic data. This is an unfortunate condition, but it may easily be by-passed if an inadequate presentation of the data by true dip cross-sections exists.

The foregoing conditions are correctable with an empirical velocity function. The determination of this function requires that the seismic data match the geologic data. In order to get a good match of seismic to geologic data it appears that a minimum of two conditions must be met. These conditions are:

1. The seismic dip must reasonably match the geologic dip.
2. The best match of the seismic and geologic dip should occur in such a manner that the occurrence of good seismic reflections should be at those geologic positions which one would assume would give rise to reflections of this quality. In other words, it would be expected that reflection "A," for example, would occur at or within a limestone or sandstone member, perhaps preferably at a shale-limestone contact, but not within a shale member. Further adjusting of the selected function should likewise bring other prominent reflections, those with continuity, into positions where their occurrence would be considered more plausible.

With these factors held in abeyance, the determination of an empirical velocity function can begin. The following formulas were used (Kaufman, 1953; Agocs, 1950):

$$V = V_0 + aZ \tag{1}$$

$$\text{Depth } Z = [(V_0)/(a \sin \theta_0)][\sin \theta - \sin \theta_0] \tag{2}$$

when $\Delta t \neq 0$

$$\text{Offset } X = [(V_0)/(a \sin \theta_0)][\cos \theta_0 - \cos \theta] \tag{3}$$

when $\Delta t \neq 0$

$$\sin \theta_0 = [V_0 \Delta t]/[\Delta X] \tag{4}$$

$$\cos \theta_0 = [1 - \sin^2 \theta_0]^{1/2} \tag{5}$$

$$\tan (\theta_0/2) = [\sin \theta_0]/[1 + \cos \theta_0] \tag{6}$$

$$\tan (\theta/2) = [\tan (\theta_0/2)][e^{aT/2}] \tag{7}$$

$$\cos \theta = [1 - \tan^2 (\theta/2)]/[1 + \tan^2 (\theta/2)] \tag{8}$$

$$\sin \theta = [1 + \cos \theta][\tan (\theta/2)] \tag{9}$$

Formulas (4) through (9) are listed because they show how curved path computations can be made with only two table lookups, the first being an exponential, $e^{aT/2}$, and the second the determination of the angle $\theta/2$ which is then doubled to give the angle of dip.

In the above formulas, V_0 is the initial velocity, θ_0 is the emergent angle, Δt is the difference in the corrected reflection times between symmetrically placed geophones separated by a distance ΔX, the "split" spread distance, and T is the reflection time. With the formulas set up, work can begin on the determination of the empirical functions.

One can determine by inspection the desired direction of movement of the vectors; in this particular case, the desired movement is to decrease the angle of dip, offset distance, and depth. Once this decision is reached, the best approach is to avoid trying to guess the correct function but deliberately to choose a function which would exceed the requirements of matching data. The reason for this is that an extreme change in the velocity function will then bracket the desired function between two values. A study of the change thus produced will permit a better estimate of further functions to try for matching of the data. During the trial period of determining the new velocity function, it is better to work on only two or three shotpoints for one reflection. In this case, the shallow reflection "A" was used with the shotpoints chosen to get data near each well and about midway between the walls. As each set of computations is completed, the data are plotted in the true dip section. When the seismic data are essentially coincident with the geologic data, an empirical function has been established for that specific shotpoint. As the seismic data dip values approach the geologic dip values, one will note that changes in V_0 and a do not produce much change in the dip value, but they do produce changes in offset and depth which can be utilized to good advantage for matching purposes.

With a reasonable fit of the seismic-geologic data for one reflection, checks are then performed on other good reflection data. Each reflection is plotted on the true dip section and its relationship to reflecting conditions noted.

Since the function is now in a condition where changes in offset and depth are more controllable without materially affecting the dip value, adjustment can probably be made for the most suitable location of the reflections in relationship

to physical factors. It is best to use continuous reflected data. Reflection "A" in this example was empirically matched to the Hunton geologic position. This is a shale to limestone contact and could easily give rise to a reflection of this quality. The various segments of information plot very closely to the geologic control. Figure 5 shows Section AA′, derived from a contoured map, after the velocity function variables were adjusted.

Reflection "B," using the above determined function, occurs several hundred feet below the top of the Viola, but in a location where the occurrence of a reflection is plausible. Likewise, Reflection "C" occurs near the top of the Simpson Group in the Bromide section, a likely position of origin for this reflection.

It was found in this case that the best velocity function for the three control points was different. This difference was then extrapolated, up and down dip, at a linear rate for both the initial velocity, V_0, and the acceleration value, a. The data for each shotpoint were then computed by the extrapolated function determined. The function thus established is good for Line 1 but it must be extrapolated into the adjacent seismic locations to be of any value. The obvious solution seemed to be the extrapolation of the velocity data parallel to the strike of the formations. This actually proved to be the case. In this particular case, a check was available for this assumption, since outcrop and subcrop data were available at the termination of control for each line. It is apparent that the geologic attitude is essentially homoclinal. The plotting of the data in cross-section form shows that extrapolation of the seismic data to the surface position, in a straight line, brought each horizon to the proper geologic position on known control points. This fact makes the assumption of the velocity extrapolation paralleling the formational strike apparently correct.

Figure 6 shows the true dip Section BB′ for constant initial velocity, V_0, and acceleration, a, values. It was again necessary to have a "velocity" fault in the interpretation to satisfy outcrop data. This section, however, shows more clearly the variation in formational thickness which was previously mentioned. Notice that the thickness between "A" and "B" increases markedly with depth. Figure 7 is the same true dip section BB′, but the data have been computed using the variable velocity function established on Line 1 and extrapolated to this line of control. The formations exhibit uniform thicknesses and the data extrapolate well into the subcrop positions.

Figure 8 is a composite of Figures 6 and 7 and shows more clearly the effect of the constant velocity function. The excessive rate of dip of the constant velocity function is readily apparent. The thickening down dip versus the more uniform formational thickness of the empirical function is also easy to see.

Figure 9 shows the true dip section CC′ for constant initial velocity, V_0, and acceleration, a, values. This section is included since it illustrates the excessive dip rate outstandingly. Again a "velocity" fault was necessary in order to satisfy geologic subcrop data. By comparison, Figure 10 is the same basic data computed with the variable velocity function of Line 1. Note that the data at the (−)6,000-

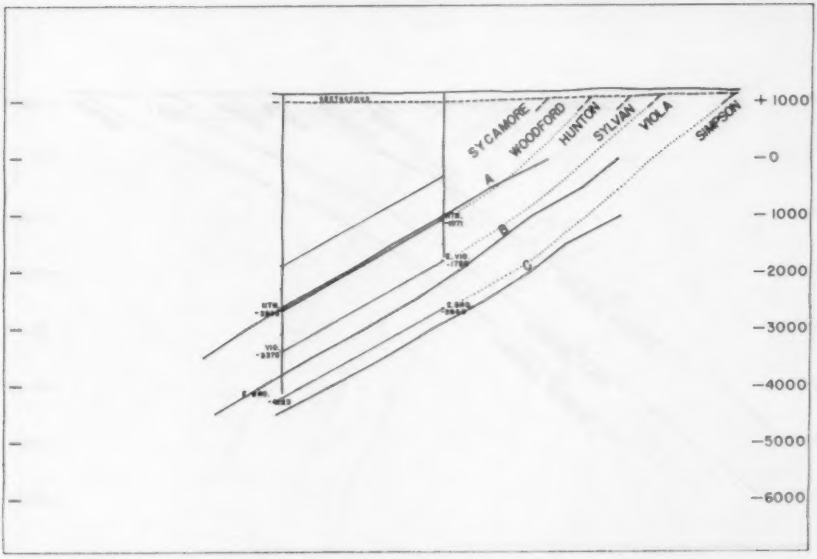

FIG. 5. Seismic—geologic cross-section AA′. V_0 and a vary,

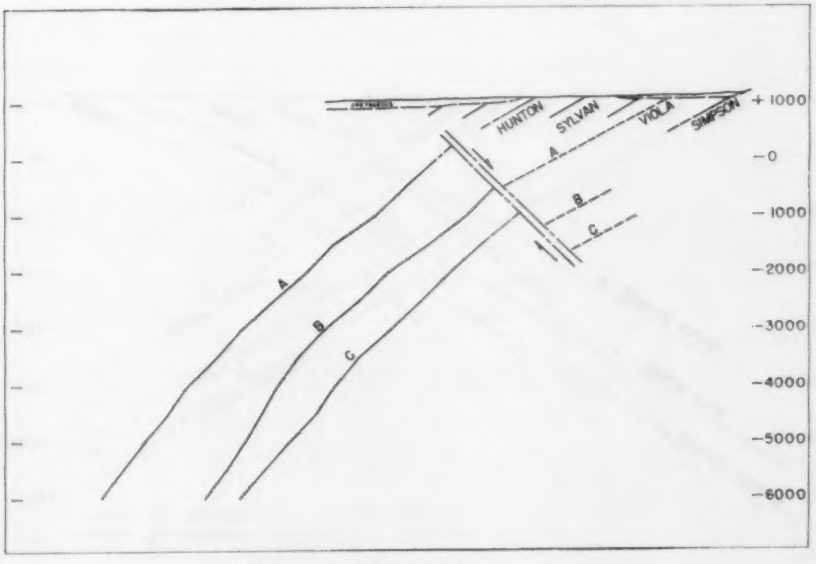

FIG. 6. Seismic—geologic cross-section BB′. V_0 and a constant.

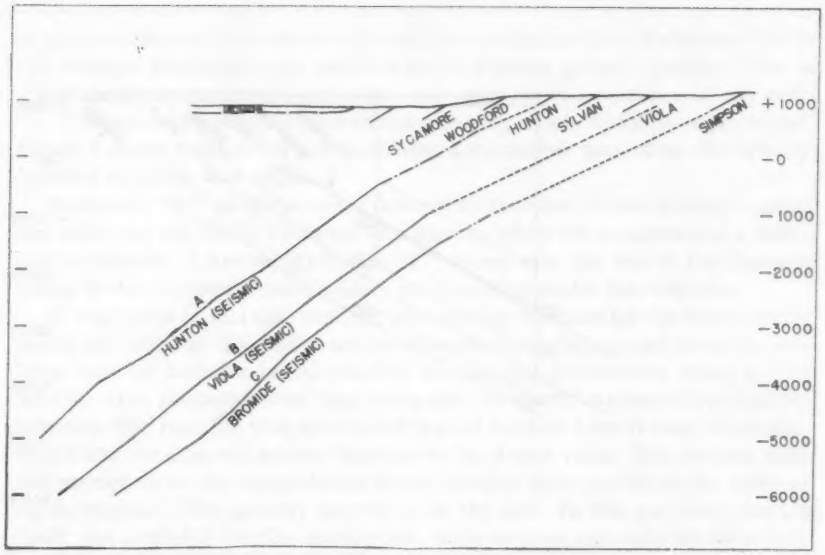

FIG. 7. Seismic—geologic cross-section BB′. V_0 and a vary.

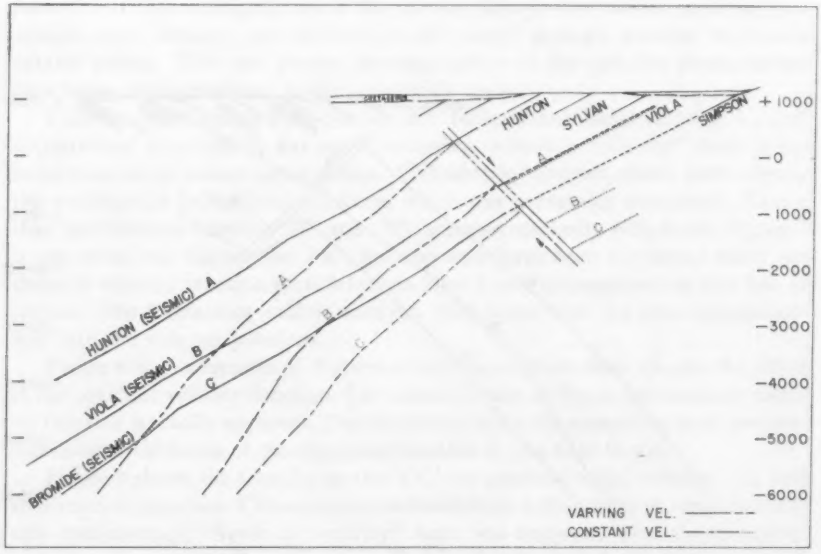

FIG. 8. Seismic—geologic cross-section BB′: Composite.

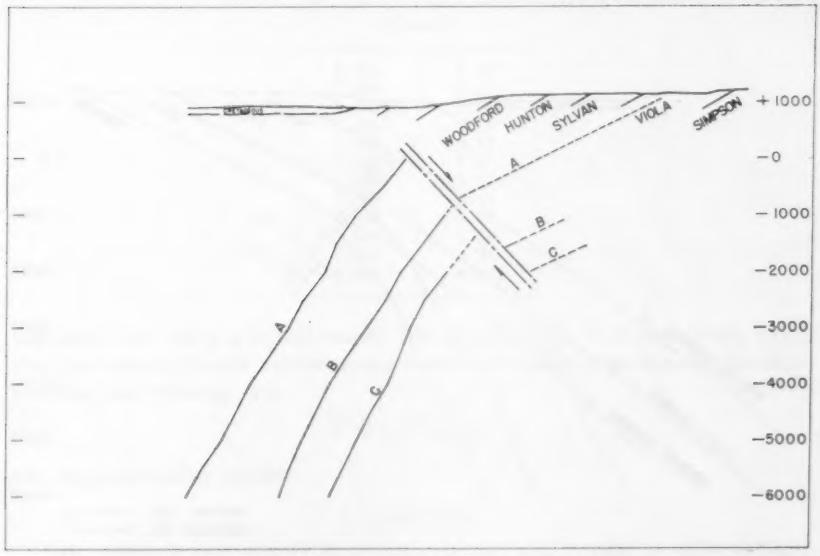

FIG. 9. Seismic—geologic cross-section CC′. V_0 and a constant.

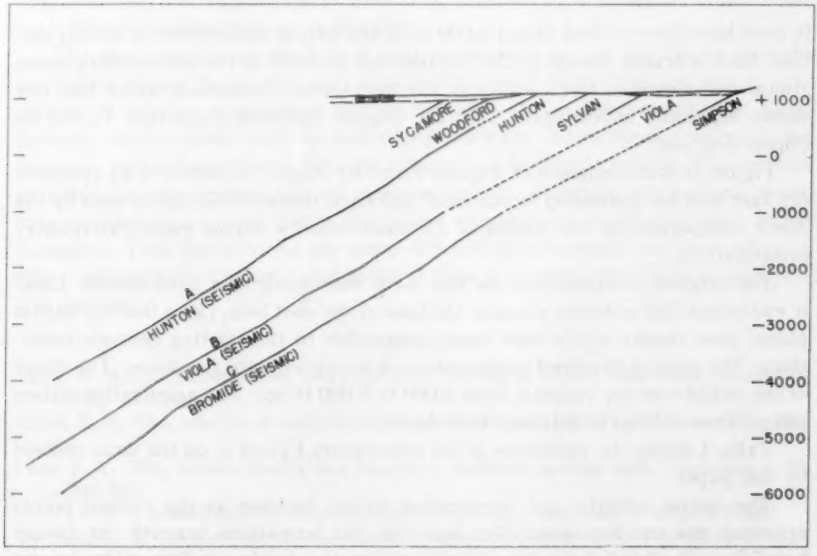

FIG. 10. Seismic—geologic cross-section CC′. V_0 and a vary.

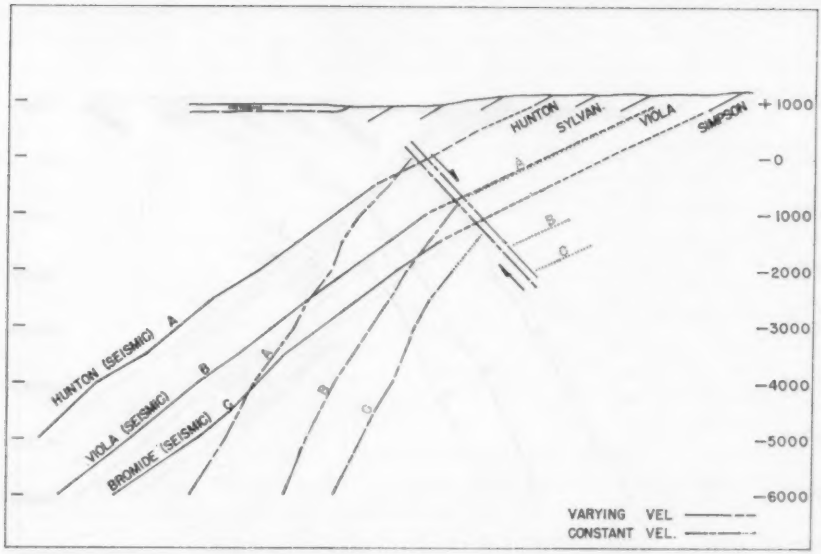

FIG. 11. Seismic—geologic cross-section CC′. Composite.

ft level have been shifted about 4,000 ft to the left, or southwesterly in this section. Such a drastic change in the location and attitude of the seismic data seems almost unbelievable, but a study of the near-surface conditions along this line shows, especially in retrospect, that the original choice of a constant V_0 was an impractical one.

Figure 11 is a composite of Figures 9 and 10. Again, the effect of an excessive dip rate and an increasing formational thickness down dip is readily seen by the direct comparison of the results of constant velocity versus empirical velocity computations.

The original computations for this work were made to a fixed datum. Later it was found that a datum plane at the base of the shot hole, i.e., a floating datum plane, gave results which were more compatible to the existing geologic conditions. The project involved computation of many velocity functions. The range of the initial velocity values is from 6,000 to 8,000 ft/sec. The acceleration values ranged from 0.50 to 0.60 ft/sec/ft of depth.

Table I shows the variations in the parameters, V_0 and a, on the data covered by this paper.

The initial velocity and acceleration values increase as the control points approach the outcrop areas. The fact that the formations beneath the unconformity at the base of the Cretaceous are steeply dipping and are older up dip

TABLE I

7,200	0.50
7,300	0.50
7,400	0.51
7,500	0.52
7,600	0.52
7,600	0.54
7,700	0.54
7,700	0.56
7,700	0.58
7,800	0.58
7,900	0.59
8,000	0.60

indicates that this is a logical result. The premise of L. Y. Faust (1951, 1953) that the velocity can be expressed as a function of depth, time elapsed since deposition, and lithology, viz.,

$$V = f(Z, T, L),$$

also suggests similar results.

CONCLUSIONS

The foregoing case history establishes the fact that empirical velocity functions can be established. The determination can be made with desk model calculations, but the application of electronic computing techniques would make such determinations even more feasible.

The main conclusion reached is that an examination of the known geologic conditions versus the seismic data obtained may lead to definite conclusions concerning a velocity relationship compatible with the geologic conditions. Valid geologic assumptions, such as essentially constant formational thickness, for example, provide additional data for comparison to seismic results. The method of displaying the seismic data is most important. Apparent dip sections, while easy to prepare, are most misleading unless extreme care is taken in their interpretation. True dip sections are more difficult to construct, but they afford a direct comparison of seismic and geologic data in perhaps the simplest interpretive scheme.

REFERENCES

Agocs, W. B., 1950, Computation charts for linear increase of velocity with depth: Geophysics, v. 15, p. 227–236.

Alcock, E. D., 1943, Selection of computational methods for seismic paths: Geophysics, v. 8, p. 297–307.

Faust, L. Y., 1951, Seismic velocity as a function of depth and geologic time: Geophysics, v. 16, p. 192–206.

———, 1953, A velocity function including lithologic variation: Geophysics, v. 18, p. 271–288.

Kaufman, H., 1953, Velocity functions in seismic prospecting: Geophysics, v. 18, p. 289–297.

Musgrave, A. W., 1952, Wave front charts and raypath plotters: Quarterly Bulletin, Colorado School of Mines, v. 47, n. 4.

REVISED DATE OF ISSUE FOR GEOPHYSICS

The first issue of GEOPHYSICS for 1959, Volume 24, Number 1, will appear in February, 1959, instead of January as has been the custom. The purpose of this change is to permit more time between the issuance of the Yearbook, Volume 23, Number 5, December, 1958, and the appearance of the first copy of GEOPHYSICS for 1959. The rescheduling is calculated to allow for the sequential processing of these two numbers. Subsequent copies of GEOPHYSICS for 1959 are planned for April, July, October, and December.

It is the present expectation of the Executive Committee of the Society of Exploration Geophysicists that the 25th Anniversary of GEOPHYSICS will be celebrated by the addition of a sixth number to that volume and to subsequent volumes. The six numbers of Volume 25 are scheduled to appear bimonthly. Volume 25, Number 1, February, 1960, is being planned as a special Silver Anniversary Issue. The Editor would welcome any suggestions concerning material appropriate for inclusion.

THE EDITOR

DEPARTMENTS

PATENTS

O. F. RITZMANN*

ELECTRICAL PROSPECTING

U. S. No. 2,830,263. L. Shipiro. Iss. 4/8/58. App. 1/26/55. Assign. Radio Corp. of America.

Metal Detector. A noise suppressor for a tramp metal detector in which part of the picked-up signal is fed into a pulse-shaping circuit that generates a blocking pulse in response to noise pulses having a rapid rise time and the blocking pulse deenergizes the alarm circuit.

Re. 24,464 (Original No. 2,685,058). W. J. Yost. Iss. 4/22/58. App. 8/27/49, 7/27/54 and 7/23/56. Assign. Socony Mobil Oil Co., Inc.

Geophysical Exploration by Electric Pulses. An electrical prospecting system using two current electrodes in contact with the ground energized by rectangular pulses at least 100 milli-second in duration and two pick-up electrodes whose potential difference is momentarily measured during the interval 50 to 100 microseconds following initiation of the current pulse.

MAGNETIC PROSPECTING

U. S. No. 2,825,977. A. A. Fayers and B. G. Gates. Iss. 3/11/58. App. 2/11/53. Assign. Minister of Supply (Great Britain).

Magnetometer Compass. A flux-gate compass having quadrature cores with coils excited by oscillators whose frequencies vary with the flux in the core, the cores being rotated by a motor and the frequency modulation detected, orientation being obtained by comparison of the modulation with a signal from a contactor.

U. S. No. 2,832,041. M. Trachtenberg. Iss. 4/22/58. App. 12/31/52.

Automatic System for Degaussing Control. A degaussing system in which the signal from a distant reference magnetometer on the vessel is fed to a monitoring magnetometer affected by the degaussing coil and the resultant signal at the monitor used to control the current in the coil.

U. S. No. 2,834,939. W. E. Tolles. Iss. 5/13/58. App. 7/31/44. Assign. U.S.A.

Compensation of Induced Magnetic Fields. A system for compensating induced field in an aircraft using two magnetic detectors controlling currents in neutralizing coils whose axes are parallel to the axes of the detectors and with the controls algebraically combined so as to effect compensation for induced field in the aircraft structure.

U. S. No. 2,836,791. C. H. Kaplan. Iss. 5/27/58. App. 7/31/52 and 7/29/53. Assign. Compagnie pour la Fabrication des Compteurs et Materiel d'Usines á Gaz.

Magnetometers. A compensated flux valve whose output is detected by a galvanometer which mechanically adjusts plates of a variable condenser in series with an oscillator and a detector-amplifier whose current is fed to a compensating coil surrounding the flux-valve and indicated.

RADIOACTIVITY PROSPECTING

U. S. No. 2,828,423. S. A. Scherbatskoy. Iss. 3/25/58. App. 7/22/50. Assign. PGAC Development Co.

Radiation Detector Device. A radioactivity detector having a photomultiplier tube and scintillating

* Gulf Oil Corporation, Patent Department.

crystals immersed in a liquid of the same refractive index as the crystals so as to attain high technical efficiency.

U. S. No. 2,829,264. A. D. Garrison. Iss. 4/1/58. App. 9/4/51 and 10/8/56. Assign. Texaco Development Corp.

Detection and Measurement of Penetrative Radiation. A radioactivity detector having a material which absorbs high energy radiation and gives off less penetrative radiation and a luminophor positioned to intercept the latter and activating a scintillation detector, the absorbing material and the luminophor being arranged in the form of a cellular disk.

U. S. No. 2,829,270. W. C. Davidon. Iss. 4/1/58. App. 12/1/54. Assign. Nuclear-Chicago Corp.

Apparatus for Indicating Percentage Ratios of Radioactivity and Analogous Properties. A radioactivity measuring device in which the detector is connected to a scaler, register switch and timer, with a time-delay switch controlling the scaler and register, so that the time-delay switch can be set to the time for 100 counts of a first sample and made to cut off the count at the same time for the second sample.

U. S. No. 2,830,189. S. A. Scherbatskoy. Iss. 4/8/58. App. 12/18/53.

Neutron Detector. A neutron detector having a detector sensitive to neutrons and gamma rays surrounded by a detector sensitive only to gamma rays and an anticoincidence circuit connected to the detectors.

U. S. No. 2,833,932. J. M. Constable and G. J. Achtellik. Iss. 5/6/58. App. 1/25/56. Assign. Electronic Products Co.

Portable High-Sensitivity Radiation Measuring Circuit. A Geiger-Muller tube circuit in which voltage is supplied to the G-M tube through two series resistors whose junction is connected to a cold-cathode gas discharge tube arranged to break down for each current pulse in the G-M tube so as to give a larger current pulse in the indicating meter.

U. S. No. 2,835,839. J. J. Borzin. Iss. 5/20/58. App. 5/31/55. Assign. U.S.A.

Wide Range Proportional Counter Tube. A radioactivity detector for use over a wide range of energy levels having a short wire anode and also a longer and thinner wire anode.

U. S. No. 2,836,726. T. A. Rich. Iss. 5/27/58. App. 9/2/54. Assign. U.S.A.

Radiation Survey System. An airborne system for measuring ground radioactivity using two shielded detectors, one detector shield having a conical opening flaring upward and the other having a similar conical opening flaring downward, and subtracting the outputs of the detectors.

SEISMIC PROSPECTING

U. S. No. 2,825,621. W. A. Alexander. Iss. 3/4/58. App. 9/19/56. Assign. Esso Research and Engineering Co.

Seismic Recording Apparatus. A recorder using electrosensitive paper and having an aperatured disk with circumferential electrodes that wipe across the paper at right angles to the trace, the galvanometer beam passing through the aperatures onto a photocell whose output is amplified and applied to the electrode to mark the paper.

U. S. No. 2,825,885. V. T. Reynolds. Iss. 3/4/58. App. 6/14/54. Assign. Southwestern Industrial Electronics Co.

Vibration Record Interpreter. A reproducing apparatus for seismograms in which the traces are scanned by a light source and a projected reproduction made on a recorder that is moved with respect to the scanner so as to apply time-varying corrections.

U. S. No. 2,826,750. W. W. Grannemann. Iss. 3/11/58. App. 11/29/55. Assign. California Research Corp.

Method of Removing Noise from Seismic Signals. A system for analyzing seismic signals in which the seismogram is played back through a narrow band-pass filter and losser network that passes only the first 1½ cycles of increasing signal amplitude.

U. S. No. 2,827,622. G. K. Guttwein. Iss. 3/18/58. App. 5/28/52.

Recording Vibration Meter Using Angular Modulation. A vibrometer having a magnetic recording head mounted on the outer end of a cantilever beam fastened to the vibrometer case and recording on a magnetic tape whose direction of motion is parallel to the motion of the head.

U. S. No. 2,829,361. R. B. Crandell, H. C. Maulshagen and R. W. Samsel. Iss. 4/1/58. App. 10/1/45. Assign. General Electric Co.

Electroacoustic Transducer. A hydrophone having a focusing device and array of piezoelectric crystals that are scanned radially in successive azimuths and their signals reproduced on a c-r tube screen with synchronized scanning.

U. S. No. 2,829,556. D. O. Carter. Iss. 4/8/58. App. 3/22/57.

Apparatus for Producing a Stereoscopic Photograph from Seismic Data. A device having a stereoscopic camera which photographs the interior of a black box with a light that is moved by mechanical connections to a tracing point which is manually traced over subsurface contour lines of a seismic map, the photograph later being viewed through a stereoscopic viewer.

U. S. No. 2,830,202. L. Feinstein. Iss. 4/8/58. App. 9/22/55. Assign. Sylvania Electric Products Inc.

Uni-Directional Accelerometer. A piezoelectric accelerometer having a mass wedged between the crystal and the case with remaining space in the case filled with an insulating plastic.

U. S. No. 2,831,177. L. D. Palmer. Iss. 4/15/58. App. 10/1/56. Assign. Gulf Research & Development Co.

Delay Line for Hydrophones. A hydrophone having an internal liquid in pressure equilibrium with the ambient fluid and containing a transducer with a diaphragm whose one side is exposed to the internal liquid and whose other side communicates with the internal liquid through a half wave length rigid-walled tube.

U. S. No. 2,832,058. R. W. Samsel. Iss. 4/22/58. App. 9/10/48. Assign. General Electric Co.

Electroacoustic Transducer. A hydrophone having a plastic plate with piezoelectric crystal elements cemented to the back face and a plano-convex plastic lens cemented to the front face.

U. S. No. 2,832,952. S. M. Bagno. Iss. 4/29/58. App. 10/1/56. Assign. Walter Kidde & Co., Inc.

Electroacoustic Transducer. A transducer having a hemispherical shell with magnetostriction rods spaced from and parallel to the edge plane of the shell and connected to the shell by impedance matching strips.

U. S. No. 2,834,422. F. A. Angona. Iss. 5/13/58. App. 6/21/56. Assign. Socony Mobil Oil Co., Inc.

Seismic Data Producing System. A device for making a synthetic seismogram from a velocity well log by generating a pulse in a metal rod and detecting reflections produced by abrupt variations in rod diameter corresponding to variations in the logged velocity.

U. S. No. 2,835,746. O. C. Montgomery. Iss. 5/20/58. App. 4/7/52. Assign. Phillips Petroleum Co.

Amplifier with Automatic Volume Control. A seismograph amplifier avc system in which the

output is rectified and applied to voltage dividers in different stages of the filter through different RC circuits, and also applied to a relay which cuts out a low-pass filter.

U. S. No. 2,835,759. S. M. Waldow. Iss. 5/20/58. App. 12/2/55. Assign. Bendix Aviation Corp.

Accelerometer Apparatus. An acceleration actuated switch having a ball in an insulating cylinder between two helical springs so that acceleration causes the ball to leave one of the springs and break an electrical circuit through the ball and springs.

U. S. No. 2,835,772. M. M. Di Giovanni. Iss. 5/20/58. App. 7/2/56. Assign. Statham Instruments, Inc.

Motion Sensing Device. An accelerometer having a mass suspended on a cantilever spring supported at one end and contacted by knife edges at a point a short distance out from the support, and with unbonded wire strain gauges detecting bowing of the cantilever between the support and the knife edges.

U. S. No. 2,835,774. L. D. Statham. Iss. 5/20/58. App. 5/17/54. Assign. Statham Instruments, Inc.

Electrical Accelerometer. A liquid damped linear accelerometer having a spring-suspended mass which is also connected to the case through another spring in series with unbonded strain wires whose change in resistance is detected.

U. S. No. 2,835,877. R. V. Walker. Iss. 5/20/58. App. 5/31/55.

Safety Device for Electrical Detonators. A short-circuiting device for cap wires, the wires being bared and clamped in grooves cut in the adjacent faces of two blocks which are bolted together and clamp a T-shaped bar across the wires.

U. S. No. 2,835,973. R. H. Schmuck. Iss. 5/27/58. App. 8/15/55. Assign. Esso Research and Engineering Co.

Three Dimensional Seismic Computer. A geometric device for setting up the plane of a subsurface reflector having a plate mounted on a vertical post by a ball joint, the orientation of the plate being determined by vertical arms that can be set at radii corresponding to seismic spreads and having calibrated vertical adjustments corresponding to the step-out.

U. S. No. 2,836,719. R. A. Manhart. Iss. 5/27/58. App. 8/23/55. Assign. California Research Corp.

Methods and Apparatus for Shifting Seismic Record Timing Pulses. A system for zeroing timing lines at a particular point during reproduction of a seismic record by reproducing the line impulses through two multivibrator circuits, one having a delay equal to the time by which the first preceding timing line precedes the point and the other having a delay equal to the time by which the first preceding tenth-second timing line precedes the point.

U. S. No. 2,836,803. G. E. White and E. W. Grant. Iss. 5/27/58. App. 3/30/53. Assign. Statham Instruments, Inc.

Inductive Transducer. A motion detector having a helical bifilar winding excited by a-c and a secondary helical winding suspended so that it moves from proximity of one primary helix to proximity of the other primary helix.

WELL LOGGING

U. S. No. 2,826,066. R. G. Piety. Iss. 3/11/58. App. 5/1/50. Assign. Phillips Petroleum Co.

Flowmeter. A well flowmeter having a calibrated motor-driven impeller that causes fluid to flow through a channel across a packer, and a heating coil and thermocouples to detect flow in a second channel across the packer, the motor current being observed for zero flow in the second channel.

U. S. No. 2,826,736. H.-G. Doll. Iss. 3/11/58. App. 4/21/55. Assign. Schlumberger Well Surveying Corp.

Methods and Apparatus for Exploring Boreholes. A water entry detector for a well having a pair of electrodes that contact the borehole wall and are rotated in an annular path by a motor with the resistance between the electrodes indicated.

U. S. No. 2,827,572. A. Blanchard. Iss. 3/18/58. App. 7/9/54. Assign. Schlumberger Well Surveying Corp.

Measuring Apparatus. A radioactivity logging system in which detected pulses are transmitted to the surface and recorded on an endless magnetic tape from which they are reproduced by two longitudinally spaced magnetic heads connected to two multivibrator circuits producing respectively positive and negative pulses which are fed to a condenser whose voltage is recorded.

U. S. Re. 24,446 (Original No. 2,704,364). G. C. Summers. Iss. 3/25/58. App. 10/28/50, 3/15/55 and 3/11/57. Assign. Socony Mobil Oil Co., Inc.

Velocity Well Logging. An acoustic logging system using a transmitter and one or two detectors and initiating either coincident with the source impulse or its arrival at the first detector a monotonically changing voltage which is cut off when the impulse arrives at either the first or second detector and the accumulated charge on a condenser indicated.

U. S. No. 2,828,548. J. S. McCune. Iss. 4/1/58. App. 8/30/51. Assign. Eastman Oil Well Survey Co.

Apparatus for Surveying Lateral Holes Extending from Earth Bores. An articulated stem for a well survey instrument to facilitate its penetration into a lateral hole and permit determination of its position in the hole from the position of its upper end in the main borehole.

U. S. No. 2,829,441. E. W. Bagnell. Iss. 4/8/58. App. 4/30/56. Assign. Johnston Testers, Inc.

Bottom Caliper Support. A device mounted on the lower end of a calipering device to keep the caliper centered in the hole and having umbrella-type arms connected to a common spring-actuated collar on the central mandrel.

U. S. No. 2,829,443. A. J. Abs. Iss. 4/8/58. App. 4/25/55. Assign. Technical Oil Tool Corp., Ltd.

Inclination and Directional Recorder. A well surveying apparatus having a pendulum and compass-oriented record chart, the chart being held off its pivot until a record is about to be made when it is lowered onto the pivot for magnetic azimuthal orientation and thereafter lifted off the pivot and brought into contact with the end of the pendulum.

U. S. No. 2,829,518. R. C. Rumble and P. H. Monaghan. Iss. 4/8/58. App. 12/17/53. Assign. Esso. Research and Engineering Co.

Subsurface Flow Meter. A well flow meter having a coil in an oscillator circuit through which the flow passes and a solenoid pump that forces a suspension of paramagnetic material into the flow stream some distance from the coil, the time between operation of the pump and detection of the material in the coil being recorded.

U. S. No. 2,830,184. S. A. Scherbatskoy. Iss. 4/8/58. App. 12/24/53. Assign. PGAC Development Co.

Radiation Detector. A radioactivity logging device for simultaneously measuring fast neutrons and gamma rays and having a detector of neutrons and gamma rays surrounded by a detector sensitive only to gamma rays, with an anticoincidence circuit and a coincidence circuit connected to both detectors and to separate counting-rate circuits.

U. S. No. 2,830,185. S. A. Scherbatskoy. Iss. 4/8/58. App. 1/4/54.

Radiation Detector. A neutron-gamma logging system using a neutron source below a shield with an air gap to allow only horizontal radiation to enter into a chamber inside the shield, the chamber having a scintillation counter in line with the air gap and additional counters located so as to respond only to Compton-scattered photons from the first scintillator, the counters being connected to a coincidence circuit that controls a gate so that the energy initially lost by the photon is recorded.

U. S. No. 2,830,186. S. A. Scherbatskoy. Iss. 4/8/58. App. 1/21/54. Assign. PGAC Development Co.

Neutron Detector. A thermal neutron detector having a scintillation-type detector sensitive to thermal neutrons, fast neutrons, and gamma rays surrounded by the crystals of other scintillation-type detectors sensitive to fast neutrons and gamma rays, with the detectors connected to an anti-coincidence circuit and counting rate meter.

U. S. No. 2,830,187. S. A. Scherbatskoy. Iss. 4/8/58. App. 1/22/54.

Radiation Detector. A directional radioactivity detector for a borehole having two scintillating crystals with a shield between them, the photomultipliers being connected to frequency meters whose d-c outputs are connected in opposition so that no response is obtained in a direction normal to the line joining the crystals.

U. S. No. 2,830,188. S. A. Scherbatskoy. Iss. 4/8/58. App. 1/11/54. Assign. PGAC Development Co.

Neutron Detector. A neutron detector having an anthracene crystal and photomultiplier surrounded by other anthracene crystals and photomultipliers with an outer shield for attenuating soft gamma rays, and a light reflector between the two sets of crystals, the photomultipliers being connected to an anticoincidence circuit and counting rate meter.

U. S. No. 2,830,266. P. F. Southwick and M. R. J. Wyllie. Iss. 4/8/58. App. 6/1/54. Assign. Gulf Research & Development Co.

Method of and Apparatus for Measuring Mud Filter Cake Resistivity. A device with an annular chamber having a permeable, conical inside wall of sintered metal so that when lowered into the well a filter cake forms on the conical surface, and when removed from the well a conducting cone can be placed against the filter cake and the electrical resistance measured.

U. S. Re. 24,471 (Original No. 2,670,442). G. Herzog. Iss. 5/6/58. App. 4/25/50, 2/23/54 and 10/29/57. Assign. The Texas Co.

Radioactivity Bore Hole Logging Apparatus. A neutron-gamma logging system using a source of neutrons and measuring the intensity of gamma rays induced in the formations close to the neutron source and simultaneously measuring the intensity of gamma rays naturally emitted from the formations in a zone far from the neutron source.

U. S. No. 2,833,982. G. P. Maly. Iss. 5/6/58. App. 1/14/57. Assign. Union Oil Co. of Calif.

Water Entry Detection Method and Apparatus. A device for locating zones of water entry in a well whose casing is perforated and having on the production tubing below the pump an expandible rubber matrix with horizontal channels communicating with the production tubing and with electrodes connected to the surface for measuring the resistivity of the fluid.

U. S. No. 2,834,421. G. C. Summers. Iss. 5/13/58. App. 1/7/54. Assign. Socony Mobil Oil Co., Inc.

Low Noise Level Acoustic Logging System. An acoustic logging system using a piezoelectric receiver and a magnetostrictive transmitter having two adjacent cylinders of magnetostrictive material with

oppositely-wound series-connected toroidal exciting coils so as to minimize the external stray field of the transmitter.

U. S. No. 2,835,819. G. Herzog. Iss. 5/20/58. App. 11/18/53. Assign. The Texas Co.

Apparatus for Locating a Zone of Lost Circulation. A device for detecting where fluid leaves a borehole having a radioactivity detector curtained by flexible radioactive streamers that normally hang close to the detector but are sucked away from the detector by fluid flow into the zone of loss.

U. S. No. 2,835,821. R. E. Fearon. Iss. 5/20/58. App. 6/22/51. Assign. Well Surveys, Inc.

Method of Observing and Classifying the Spectrum of Gamma Rays. A radioactivity detector for use at high temperatures having a nonradioactive monatomic gas such as mercury vapor in which scintillations are detected by a photocathode having a high electronic work function.

U. S. No. 2,836,359. R. P. Mazzagatti. Iss. 5/27/58. App. 11/1/54. Assign. The Texas Co.

Integration of Electrical Signals. A system for obtaining a log of average occurrence of events in which the events are recorded on magnetic tape and played back by a series of equally-spaced reproducers whose outputs are applied to an RC integrating circuit.

MISCELLANEOUS

U. S. No. 2,828,485. R. S. Finn. Iss. 3/25/58. App. 9/9/54. Assign. Seismograph Service Corp.

Radio Location System. A phase-comparison type of position determining system in which the receivers at the two link transmitting stations each have two antennas located equidistant on opposite sides of the transmitter so that the carrier wave from the nearby transmitter can be blocked out without affecting reception from the distant transmitter.

U. S. No. 2,829,515. H. E. Johnson. Iss. 4/8/58. App. 7/21/54.

Porosimeter. A core-testing method in which the core is evacuated and known volume of gas at high pressure is allowed to expand into the core and the remaining gas again brought to its original pressure and the volume difference measured.

U. S. No. 2,829,824. N. A. Schuster. Iss. 4/8/58. App. 7/1/52. Assign. Schlumberger Well Surveying Corp.

Automatic Computer. A computing device having a light beam or c-r beam that is deflected according to one variable with the beam passing through a moving screen having openings formed according to the other variable and a photocell that counts the light pulses.

U. S. No. 2,829,825. H.-G. Doll. Iss. 4/8/58. App. 7/1/52. Assign. Schlumberger Well Surveying Corp.

Automatic Computing Apparatus. A computing device having a light beam or c-r beam whose deflection follows one variable and which passes through a moving screen having openings formed according to another variable, and is detected by a photocell that counts the pulses, a second beam and set of openings on the same screen being used to control the pulse counter.

U. S. No. 2,831,347. J. E. Yancey. Iss. 4/22/58. App. 8/23/54. Assign. Drillograph Co., Inc.

Apparatus for Recording Drilling Operations. A drilling rate recorder having a clock-driven record tape and stylus that is moved to one side during drilling but which returns to zero and records operations other than drilling on the opposite side of the zero line.

U. S. No. 2,835,888. R. L. Frank. Iss. 5/20/58. App. 9/27/56. Assign. Sperry Rand Corp.

Multiple Pulsed Navigation System. A loran radio navigation system in which groups of pulses are used and the pulses in the respective groups are integrated at the mobile receiver-indicator station.

SELECTED LIST OF U. S. PATENTS ISSUED DURING MARCH, APRIL AND MAY OF 1958

Patent No.	*Subject**	*Patent No.*	*Subject**	*Patent No.*	*Subject**
2,825,227	16	2,827,622[a]	492	2,829,363	188
2,825,228	16	2,827,623	224	2,829,437	200
2,825,229	16	2,827,626	68	2,829,441[a]	44
2,825,502	68	2,827,627	316	2,829,443[a]	520
2,825,533	392	Re.24,446[a]	8	2,829,515[a]	88
2,825,621[a]	364	2,827,716	288	2,829,518[a]	148
2,825,763	484	2,827,786	16	2,829,520	288
2,825,805	308	2,827,787	484	2,829,521	16
2,825,861	68	2,827,788	16	2,829,522	16
2,825,884	108	2,827,789	16	2,829,523	16
2,825,885[a]	352	2,827,824	420	2,829,556[a]	352
2,825,901	316	2,827,978	12	2,829,618	224
2,825,977[a]	232, 216	2,828,070	68	2,829,619	16
2,826,066[a]	148	2,828,118	4	2,829,823	68
2,826,068	148	2,828,367	224	2,829,824[a]	68
2,826,358	68	2,828,368	224	2,829,825[a]	68
2,826,476	444	2,828,422	200	2,829,827	68
2,826,485	136	2,828,423[a]	308	2,829,828	68
2,826,634	224	2,828,425	308	2,829,829	68
2,826,642	224	2,828,459	224	2,829,847	16
2,826,643	224	2,828,467	228	2,829,848	16
2,826,699	148, 308	2,828,468	308	2,830,114	324
2,826,700	148, 308	2,828,485[a]	312	2,830,130	224
2,826,706	484	2,828,548[a]	520	2,830,131	324
2,826,726	108	2,828,621	496	2,830,165	484
2,826,736[a]	116	2,828,628	16	2,830,183	308
2,826,749	484	2,828,629	16	2,830,184[a]	304
2,826,750[a]	360	2,828,916	16	2,830,185[a]	304
2,826,753	316	2,828,961	224	2,830,186[a]	304
2,826,912	8, 148	2,829,025	324	2,830,187[a]	304
2,826,913	148	2,829,026	324	2,830,188[a]	304
2,826,914	148	2,829,047	484	2,830,189[a]	304
2,826,915	148	2,829,202	484	2,830,190	308
2,826,916	148	2,829,207	224	2,830,201	484
2,827,233	68	2,829,208	224	2,830,202[a]	4
2,827,245	224	2,829,209	224	2,830,204	484
2,827,249	16	2,829,210	484	2,830,207	224
2,827,250	16	2,829,259	236	2,830,263[a]	132
2,827,355	224	2,829,260	236	2,830,266[a]	252
2,827,539	196	2,829,264[a]	308	2,830,274	484
2,827,572[a]	304	2,829,270[a]	308	2,830,283	484
2,827,573	68	2,829,275	196	2,830,453	460
2,827,605	16	2,829,319	484	2,830,762	68
2,827,619	108	2,829,330	16	2,830,777	16
2,827,620	108, 436	2,829,361[a]	484, 436	2,830,865	324

* A key to the subject classification system will be found in GEOPHYSICS, v. 12, pp. 256–264 (April, 1947).

[a] Abstracted on preceding pages of this issue.

Patent No.	Subject*
2,830,866	324
2,830,867	324
2,831,068	224
2,831,107	68
2,831,118	420
2,831,121	308
2,831,132	484
2,831,155	16
2,831,175	484
2,831,177[a]	484, 376
2,831,180	224
2,831,186	316
2,831,187	316
Re.24,464[a]	124
2,831,347[a]	100
2,831,348	148
2,831,349	148
2,831,351	148
2,831,429	48
2,831,670	4
2,832,041[a]	232
2,832,058[a]	484
2,832,063	224
2,832,214	12
2,832,218	148
2,832,536	68
2,832,551	16
2,832,552	16
2,832,581	428
2,832,599	224
2,832,839	224
2,832,842	484
2,832,886	68
2,832,937	68
2,832,944	436, 108
2,832,952[a]	484
Re.24,471[a]	304
2,833,046	484
2,833,147	200
2,833,148	200
2,833,213	48
2,833,214	48
2,833,215	48
2,833,469	68
2,833,470	68
2,833,471	68
2,833,472	68
2,833,475	224
2,833,476	68
2,833,538	224
2,833,928	68, 196
2,833,929	308
2,833,931	308
2,833,932[a]	308
2,833.979	484
2,833,982[a]	508
2,833,999	484
2,834,000	484
2,834,200	496
2,834,201	188
2,834,209	148
2,834,214	16
2,834,215	16
2,834,217	200
2,834,236	12
2,834,245	136
2,834,246	416
2,834,421[a]	8
2,834,422[a]	360
2,834,543	68
2,834,561	16
2,834,562	16
2,834,563	16
2,834,564	16, 312
2,834,565	16
2,834,689	196
2,834,831	324
2,834,888	416
2,834,891	196
2,834,929	16
2,834,935	68
2,834,939[a]	232
2,834,943	484
2,834,952	484
2,834,953	288
2,834,955	316
2,834,956	316
2,834,957	16, 312
2,835,116	196
2,835,131	16
2,835,132	16
2,835,444	68
2,835,549	324
2,835,699	308
2,835,742	224
2,835,743	224
2,835,744	484
2,835,746[a]	344
2,835,749	68
2,835,759[a]	4, 16
2,835,772[a]	492
2,835,773	68
2,835,774[a]	4
2,835,819[a]	304
2,835,820	416
2,835,821[a]	308
2,835,839[a]	308
2,835,858	68
2,835,861	16
2,835,877[a]	136
2,835,882	224
2,835,888[a]	312
2,835,973[a]	352
2,836,059	140
2,836,061	428
2,836,062	428
2,836,067	288
2,836,071	16
2,836,072	68
2,836,147	224
2,836,356	68
2,836,357	68
2,836,358	68
2,836,359[a]	68, 308
2,836,479	324
2,836,719[a]	368
2,836,726[a]	308
2,836,737	484
2,836,738	484
2,836,739	200
2,836,791[a]	232
2,836,803[a]	484
2,836,810	316
2,836,811	316
2,836,815	312
2,836,816	16, 68
2,836,817	316

REVIEWS

REVIEWS COMMITTEE

FRANKLYN K. LEVIN, Chairman, Jersey Production Research Company, Tulsa, Oklahoma
W. T. BORN, Geophysical Research Corporation, Tulsa, Oklahoma
THOMAS A. ELKINS, Gulf Research and Development Company, Pittsburgh, Pennsylvania
W. W. GARVIN, California Research Corporation, La Habra, California
SIGMUND I. HAMMER, Gulf Research and Development Company, Pittsburgh, Pennsylvania
CHWAN-CHANG LEE, Temco Aircraft Corporation, Dallas, Texas
JOHN E. NAFE, Lamont Geological Observatory, Palisades, New York
CARL H. SAVIT, Western Geophysical Company of America, Los Angeles, California
VICTOR VACQUIER, Scripps Institution of Oceanography, La Jolla, California
J. E. WHITE, The Ohio Oil Company, Littleton, Colorado

CONTENTS

An Introduction to the Theory of Random Signals and Noise, Wilbur B. Davenport, Jr. and William L. Root, by *Carl H. Savit* 848
Analysis of a Multiple Receiver Correlation System, Melvin J. Jacobson, by *Carl H. Savit* 849
Direct Methods for the Evaluation of Gravity Measurements in the Case of Two-Dimensional Mass Distribution, Aivars Celmiņš, by *Thomas A. Elkins* 849
Stoneley-Wave Velocities for a Solid-Solid Interface, A. S. Ginzbarg and E. Strick, by *J. E. White* 850
On Rayleigh Waves Propagated over the Surface of a Medium with Elastic Afterworking, Kohei Nakamura, by *J. E. White* 850
Investigations of the Interior of the Earth, L. Egyed, by *Asger Lundbak* 851
The Geology and Geophysics of Cooke and Grayson Counties, Texas. Joint Activities Committee of the Dallas Geological and Geophysical Societies, by *Vernon L. Redding* 851
Self-Reciprocity Transducer Calibration in a Solid Medium, R. M. White by *J. E. White* 852

An Introduction to the Theory of Random Signals and Noise, Wilbur B. Davenport, Jr., and William L. Root, McGraw-Hill Book Company, Inc., New York, New York. 393+ix pp., 1958, $10.00.

Spurred by the growing importance and universality of the subject, books on various approaches to signal and noise theory are now becoming increasingly available. Davenport and Root have set down in book form an excellent résumé of the present state of knowledge in the field of the statistical treatment of signals and noise. While there is always at least a two-year lag between a book and the literature, this book comes satisfyingly close to the frontiers of the field.

Only one other book covering the general statistical theory of signals and noise is known to this reviewer. A comparison between the work of Davenport and Root and the other publication, *Random Processes in Automatic Control* by Laning and Battin, McGraw-Hill, 1956, is inevitable. Much of the material covered by the two books is common; differences are largely of emphasis and approach. Laning and Battin, being in the Aeronautical Engineering Department at MIT, concern themselves largely with the problems of signals and noise in servomechanisms and guidance and use corresponding language and examples. Davenport and Root, on the other hand, are associated with the Lincoln Laboratory of the Department of Electrical Engineering, also at MIT. Their approach and language are thus taken from communications and radar. The two books clearly complement each other by reason of their diverse approaches and by covering different phases of the newer disciplines.

Random Signals and Noise significantly omits reference to the modern field of information theory but does devote two chapters to nonlinear devices. A relatively small amount of space is devoted to the problem of statistical operations on finite data, a subject which, by contrast, occupies a considerable chapter in Laning and Battin.

Davenport and Root treat each chapter in a straightforward matter-of-fact manner with little

or no attempt to discuss the conflicts behind the theory. As a result, the book is excellent both as an introductory text and a handbook for those interested in applying statistical techniques to signals and noise. Those who prefer some philosophy and a critical discussion of inherent assumptions are well advised to consult Laning and Battin. Nowhere is the textbook nature of *Random Signals* better shown than in the multiplicity of graded exercises to be found at the end of each chapter. Specific examples to illustrate the theory are, however, rather infrequent in contrast to the situation in *Random Processes*, in which there is at least one illustrative example for almost every section.

Research geophysicists would be well advised to add *Random Signals and Noise* to their libraries as a supplement to *Random Processes in Automatic Control*. In combination, these two excellent works contain the basic concepts underlying most of the research underway today in statistical filter theory and related subjects.

CARL H. SAVIT
Western Geophysical Company of America
Los Angeles, California

Analysis of a Multiple Receiver Correlation System, Melvin J. Jacobson. *The Journal of the Acoustical Society of America*. Vol. 29, pp. 1342–1347. 1957.

It is well known that high directivity may be obtained from an array of two acoustical receivers f the outputs of the two receivers be cross-correlated. If now each of the two receivers be replaced by a linear-additive array and the resulting outputs again be cross-correlated, we would expect to achieve further improvement in directivity.

Dr. Jacobson shows that detection of a signal from a given direction in the presence of uncorrelated noise is improved by increasing the number of detectors in the composite array. Signal-to-noise improvement is shown to be bounded below by a quantity proportional to the square root of the number of elements in the composite array.

Generalized expressions of the mean value of the output for broad-band signals are presented from which qualitative conclusions may be drawn indicating that directivity increases with signal band width and, of course, with the physical size of the array.

The conclusions of this paper have a tendency to fall into the class of the "intuitively obvious." However, so far as this reviewer knows, no direct proof has heretofore been published. From the standpoint of exploration seismology one may now conclude that the directivity improvement of multiple-seismometer arrays is at least preserved under cross-correlation of independent groups.

CARL H. SAVIT
Western Geophysical Company of America
Los Angeles, California

Direkte Verfahren zur Auswertung von Schweremessungen bei zweidimensionaler Massenverteilung (Direct methods for the evaluation of gravity measurements in the case of two-dimensional mass distribution), Aivars Celmiņš, *Geofisica pura e applicata*, Vol. 38, 1957, pp. 81–122.

This paper, which is an excerpt from the dissertation presented by the author to the Clausthal Bergakademie, is a comprehensive summary of methods available for inferring mass distributions from gravity surveys in the two-dimensional case. The author, formerly with Seismos G.m.b.h., Hannover, is now with Petrobrás-Depex, Rio de Janiero.

The paper is divided into five sections. The first section is introductory. The author distinguishes three methods of solving the problem: direct, indirect, and mixed. The direct methods make use of processes, such as analytic continuation, which are applied to the gravity data and lead to inferences about the mass distribution. In the indirect methods a plausible mass distribution is assumed and the gravity effect calculated. If it does not agree closely with the observed effect, the assumed mass distribution is varied and a trial-and-error procedure followed until a sufficiently good agreement is reached. Finally, the mixed methods are those which use a combination of the first two types. For the purpose of his paper, the author introduces a more significant classification of methods into those which use a constant density and those which use a variable density.

The second section assembles some basic formulas from potential theory for later use, while the third section considers direct methods for inferring mass distributions from gravity, both those previously given in the literature and those devised by the author.

The first group considered is that of methods using a variable density. To cut down on the possible multiplicity of solutions it is necessary with such methods to fix ahead of time the domain in which the mass distribution is supposed to occur. If this is done, the problem reduces to the solution of an integral equation linear in the density. Three cases are considered. The first is that of a surface-density distribution on a plane a fixed depth below the surface (actually a line, since this is the two-dimensional case), a problem whose solution has been available in the literature for some time. The second case treated is that in which the mass distribution is required to lie between two given fixed depths z_0 and z_1 and the density depends only on the horizontal co-ordinate. The third case, tailored especially for salt domes, again assumes two given bounds of z_0 and z_1, but it also takes the density to be of the form

$$w(x) \cdot (1 + bz) \cdot D_1,$$

where z is the depth, b and D_1 are given constants, and $w(x)$ is a horizontally variable weighting factor which is to be determined. This case thus allows for variation of the density with respect to depth.

The second group considered is that of methods using a constant density. Here the problem is the finding of the domain which contains the mass distribution, basically a much more difficult problem than that of the first group of methods. Some attention is devoted to the case in which a good first approximation to the outline of the domain is known and it is desired to find small variations for a closer approximation. Otherwise the methods described are of the now classic type in which the geometric shape of the mass boundary is assumed and the necessary parameters are deduced from the gravity data either in its entirety or from selected characteristic values. This process is carried out for a step and for a block, both two-dimensional.

The fourth section considers the problem of the lack of uniqueness, while the fifth section applies the methods of the third section to some theoretical gravity curves. Specifically, the examples are a horst, a graben, a salt dome, and a fault.

The list of references has twenty-four items. The complete absence of references to the Russian literature is surprising and is perhaps the only weak point in this stimulating paper on an important problem.

THOMAS A. ELKINS
Gulf Research and Development Company
Pittsburgh, Pennsylvania

Stoneley-Wave Velocities for a Solid-Solid Interface, A. S. Ginzbarg and E. Strick, *Bulletin of the Seismological Society of America*, Vol. 48, 1958, pp. 51–63.

Stoneley-wave velocities for a solid solid interface were calculated for a wide range of elastic parameters. In contrast to the rather meager numerical calculations of Stoneley-wave velocities previously available in the literature, the twenty sets of curves presented here will permit one to read the velocity of Stoneley waves propagating along an interface between any two media, or to see at a glance that such waves are not permitted by the contrast in properties of the two media.

J. E. WHITE
The Ohio Oil Company
Littleton, Colorado

On Rayleigh Waves Propagated over the Surface of a Medium with Elastic Afterworking, Kohei Nakamura, *Science Reports of the Tohoku, University, Fifth Series, Geophysics*, Vol. 9, 1957, pp. 36–44.

Two models are used in describing elastic afterworking, one specified only by the time of relaxation of shearing stress (τ), the other by two relaxation times respectively for shearing stress and symmetrical stress. For the first model, a plot indicates that as frequency decreases below $\omega\tau = 1$,

Rayleigh-wave velocity decreases indefinitely and attenuation rises rapidly. The axis of the ellipse describing particle motion at the surface of the solid is shown to tilt away from the vertical by an angle which reaches a maximum near $\omega\tau = 1$. It is concluded that deviations from the vertical of the axes for observed particle trajectories due to small explosions considerably exceed the tilts which could be attributed to the loss mechanisms considered here.

J. E. WHITE
The Ohio Oil Company
Littleton, Colorado

Investigations of the Interior of the Earth, L. Egyed, *Annales Universitatis Scientiarum Budapestinensis, Sect. Geol.*, Tom. 1, 1957, p. 37–77.

A new theory about the constitution of the Earth and its dynamic character has been presented by Professor Egyed on earlier occasions, rather elaborately in the Hungarian *Acta Geologica* (Tom. IV, Fasc. 1, 1956), and more fragmentarily in the Italian *Geofisica Pura e Appli.* (Vol. 33, p. 42–48, 1956) and the English *Nature* (Vol. 178, p. 534, 1956). The central point in the theory is that the radius of the Earth has been steadily increasing since the formation of the Earth, and that it is still growing at a rate of about 0.5 mm a year.

The hypothesis of an increasing radius has been presented by others in a vaguer form, but Professor Egyed has succeeded in giving this hypothesis a highly reliable form. He states how this hypothesis or theory is able to explain such different phenomena as the proportion between the areas of continents and ocean basins, the much disputed Wegener drift, the steady decrease of the Earth's angular velocity, the origin of tectonic energies, and the formation of mountains, deep-sea troughs, and sub-oceanic rifts.

The theoretical starting-point is that the core of the Earth with its high values of density is in a primeval state, i.e., the inner and solid core in a first ultrahigh pressure state, the outer and liquid core in a second ultraphase state. The mantle is supposed to present a third and more final stage. As the core aims at this final stage with lower density, the result must be expansion of the Earth.

Although the theory may at the first glance seem somewhat speculative, Professor Egyed has founded it on much quantitative material, and he has himself pointed out some parts of the theory which must still be considered uncertain. As an example, one can mention that part of the theory which deals with the source of the Earth's main geomagnetic field. This field is here proposed to originate from some kind of uniform arrangement of the protons and neutrons in the inner core caused by the existing high pressures. Such an explanation deviates greatly from the common views which are dealing with electrical and material current systems in the outer core; but also this geomagnetic part of Professor Egyed's theory is grounded quantitatively.

ASGER LUNDBAK
Danish Meteorological Institute
Copenhagen, Denmark

The Geology and Geophysics of Cooke and Grayson Counties, Texas, published by the Joint Activities Committee of the Dallas Geological and Geophysical Societies, 1957, 211 pp.

This publication, an integrated series of articles by different authors, is a general, yet sufficiently detailed, compilation of geological and geophysical knowledge concerning these two North Texas counties. The report is directed much more strongly toward the geological aspects than the geophysical. This relative emphasis is perhaps unfortunate for geophysicists interested in the area, but the wealth of geologic data presented should be of great help in the interpretation of any new geophysical surveys.

Each of the two counties is treated separately in descriptions of the structural, historical, and petrographic geology. Several of the more important oil fields are described in more or less detail.

The two counties are considered jointly in the rest of the publication. A respectable amount of

core analysis data is given on several formations from several fields. One important reservoir horizon is described from core and sample analyses and other log data from many wells.

The role of the gravity meter in exploration of Cooke and Grayson Counties is outlined in a rather short article. Apparently, the large structural features and massive changes in the character of the older rocks make the gravity meter an important tool in this area.

The chapter on seismic reflection techniques points out some of the difficulties involved and suggests techniques which have been used with most success in overcoming these difficulties.

The publication is the result of much work by, and cooperation between, the various authors and the committee responsible for its issuance. It should be invaluable to those who are now engaged in or contemplating exploration for oil and gas in Cooke and Grayson Counties, Texas.

VERNON L. REDDING
Humble Oil & Refining Company
Houston, Texas

Self-Reciprocity Transducer Calibration in a Solid Medium, R. M. White, *Journal of the Acoustical Society of America*, Vol. 29, 1957, pp. 834–836.

A procedure is described for the absolute calibration of reversible transducers such as those which have been used widely for seismic model work and ultrasonic inspection of solids. A sinusoidal pulse of compressional waves is sent out by the transducer, an appropriately spaced plane reflector directs the waves back to the transducer, and the pulse is observed with the transducer acting as a detector. From the current fed into the transducer when sending, the open circuit voltage generated by the reflected wave, and the known geometry, the strength as a source and the sensitivity as a detector can be computed, making use of reciprocity relations for reversible transducers coupled to infinite media. Although the discussion considers only a transducer imbedded in an infinite medium, having no boundaries other than the plane which serves as a perfect reflector, it is implied that this calibration procedure applies as well when the transducer is coupled to the solid at a boundary.

J. E. WHITE
The Ohio Oil Company
Littleton, Colorado

PUBLICATIONS RECEIVED

American Journal of Science, v. 256, nos. 6 & 7 (July & Summer, 1958)
Annales de Géophysique, v. 14, nos. 1 & 2 (1958)
Annali di Geofisica, v. 10, nos. 3 & 4 (July & October, 1957)
Boletin de la Asociacion Mexicana de Geologos Petroleros, v. 10, nos. 3 & 4 (March & April, 1958)
Bulletin of the Chinese Association for the Advancement of Science, v. 6, nos. 1 & 2 (February & April, 1958)
Bulletin of the Earthquake Research Institute (Tokyo University), v. 36, n. 1 (March, 1958)
Bulletin of the Seismological Society of America, v. 48, n. 3 (July, 1958)
Bulletin of the Seismological Station (Copenhagen), n. 71 (January–March, 1958)
Chronique de l'Union Géodésique et Géophysique Internationale, n. 11 (May, 1958)
Deutsche Hydrographische Zeitschrift, v. 11, n. 1 (1958)
Economic Geology, v. 53, nos. 4 & 5 (June–July & August, 1958)
Egyptian Journal of Geology, v. 1, n. 2 (1957)
Erdöl und Kohle, v. 11, nos. 5 & 6 (May & June, 1958)
Geofizikai Közlemények, v. 7, n. 1 (1958)
Geofysiske Publikasjoner, v. 20, n. 3 (May, 1958)
Geological Abstracts, v. 6, n. 2 (June, 1958)
Geologisches Jahrbuch, v. 73 (1958)
Geološki Glasnik (Sarajevo, 1956)

Geophysical Abstracts, v. 172 (January–March, 1958)
Geophysical Digest, v. 5, n. 3 (July, 1957)
Geophysical Notes, v. 11, n. 1 (1958)
Geophysical Prospecting, v. 6, n. 2 (June, 1958)
Institute of Petroleum Review, v. 12, nos. 138 & 139 (June & July, 1958)
Journal of the American Society of Safety Engineers, v. 3, n. 3 (August, 1958)
Journal of Earth Sciences (Nagoya University), v. 5 n. 2 (September, 1957)
Journal of Geomagnetism and Geoelectricity, v. 9, n. 3 (1957)
Journal of the Institute of Petroleum, v. 44, nos. 414 & 415 (June & July, 1958)
Journal of Petroleum Technology (June–August, 1958)
Journal of Technology (Bengal Engineering College), v. 2, n. 2 (December, 1957)
Mining Engineering, v. 10, nos. 6–8 (June–August, 1958)
Mining Review (Department of Mines of South Australia), nos. 103 & 104 (December, 1955, & June, 1956)
Proceedings of the Cambridge Philosophical Society, v. 54, part 3 (July, 1958)
Quarterly Journal of the Geological Society of London, v. 113, n. 451 (May, 1958)
Review of Scientific Instruments, v. 29, nos. 5–7 (May–July, 1958)
Science, v. 127, nos. 3311–3313 (June 13–27, 1958); v. 128, nos. 3314–3321 (July 4–August 22, 1958)
Science Reports of the Tohoku University (5th Series, Geophysics), v. 9, nos. 2 & 3 (October, 1957, & March, 1958)
Soviet Physics JETP, v. 6, nos. 3–6 (March–June, 1958)
Tecnica (Universidad Nacional de Tucuman, Mexico), v. 2, n. 3 (January, 1958)
Tellus, v. 10, n. 2 (May, 1958)
Transactions of the American Geophysical Union, v. 39, nos. 3 & 4 (June & August, 1958)
Transactions and Proceedings of the Geological Society of South Africa, v. 60 (1957)
Veröffentlichungen des Institutes für Bodendynamik und Erdbebenforschung in Jena, vols. 59 & 61 (1958)
Zeitschrift für Geophysik, v. 24, n. 2 (1957)

DISCUSSIONS AND COMMUNICATIONS

LETTERS TO THE EDITOR

COMMENTS ON "THE MOVEOUT FILTER"

The casual reader may draw erroneous conclusions from this paper. In particular, I would like to comment on three points:

1. The apparent great difference between the results of Parr and Mayne (P & M) and Savit, Brustad, and Sider (S B & S) shown here.
2. The importance of length as well as number of elements in a pattern.
3. The importance of an "optimum" rejection filter.

I shall draw upon the data of three papers in GEOPHYSICS:

1. Savit et al., "The Moveout Filter" (January, 1958),
2. Parr & Mayne, "A New Method of Pattern Shooting" (July, 1955),
3. White, "Transient Behavior of Patterns" (January, 1958).

First, let us compare the P & M and the S B & S criteria. They differ in that the former minimize the peak rebounds while the latter minimize the rms output in the rejection band. Figure 6 (p. 14) of "The Moveout Filter" purports to show responses of P & M and S B & S filters having a "common reject band." Let us use the P & M definition of the rejection band (Reference 2, p. 542) as the ratio of the longest to the shortest wave lengths between which the *rebound* amplitudes are less than some prescribed value, "R." In Figure 6 for the P & M pattern, $R=0.15$; and the band width,

$$W = \frac{20 - 0.82}{0.82} = 23^{+}.$$

From Figure 2 (p. 10), corresponding values for an unweighted line are:

$$R = 0.22; \qquad W = \frac{20 - 0.84}{0.84} = 23^{-}.$$

From either Figure 6 or Figure 2, corresponding values for the S B & S filter are:

$$R = 0.06; \qquad W = \frac{20 - 1.3}{1.3} = 13.5.$$

It seems to me that S B & S have applied the P & M definition of band width to the P & M data and a different (half-power?) definition to their own data. Figure 6 is not a comparison of two patterns with common rejection bands. As P & M state (Reference 2, p. 546–547, Figures 5 and 6), for any given number of elements a greater band width must sacrifice rejection. Actually, the P & M array in Figure 6 has as wide a rejection band as the unweighted array in Figure 2, yet only $\frac{2}{3}$ the rebound amplitude. The wide band results because of the un-

usually strong end elements in the P & M weighting (Figure 13, p. 19). For $W = 13.5$, the P & M technique would give a smooth taper, similar to the S B & S taper.

Second, starting with the last paragraph on p. 15 and continuing on p. 17, S B & S compare s/n ratios for several lines. The authors state that the length "S" was held constant for the groups compared. S is constant only for the 21-element lines. The length of the continuous line is only one-half that of the 21-element lines. For an equal-length continuous line, s/n would be about 0.82 (as it is for the 21-element unweighted line in Figure 11). Figure 10 indicates that the use of a shorter continuous line has destroyed low (spatial) frequency rejection. To some extent the 3-element line is not a good comparison because of the length difference, either. Making this line longer would improve the response for low S/λ, but the response for higher S/λ would be worse. The s/n might not change appreciably. Increasing length in Figures 8 to 13 changed the s/n ratio by a factor of 10. Weighting improved the s/n ratio by a factor of 3. (Here, the P & M weighting suffers because it has too wide a band for the noise spectrum. I feel sure that P & M would not recommend this band width filter for the noise spectrum of Figure 7.)

Third, both the P & M and S B & S papers imply an optimum noise suppression by utilizing certain weighting techniques. Their steady-state response curves show considerable improvement over unweighted elements. However, White's transient responses using short pulses do not indicate striking differences among several weighted continuous distributions (Reference 3, Figure 11). Let us compare the Jones parabolic (Reference 3, equation (10)) and the "housetop" (Reference 3, equations (6) and (9)) distributions of White, with the P & M and S B & S distributions. For simplicity, let us weight only five elements to approximate the distributions in accordance with the various authors' criteria. Table I below indicates these weighting factors. I have attempted to obtain roughly equal bandwidths for all except an inverted housetop. (The housetop is composed of three parts triangle and one part rectangle. The inverted housetop is composed of one part triangle and six parts rectangle. The values for S B & S are graphic samples from a plot of the 21-element weights.)

The steady-state response curves in Figure 1 below may err in detail (I computed only a limited number of points), but the salient features will stand, I believe. Note first that the strong-end-weak-center weighting of the inverted housetop widens the band and increases the rejection rebounds, with respect to equal weights. This is the effect of using too wide a band, as S B & S have done, with the P & M weighting. Note next that the P & M and S B & S data differ appreciably only over that part of the rejection band between

$$2 < \frac{n \cdot s}{\lambda} < 3.$$

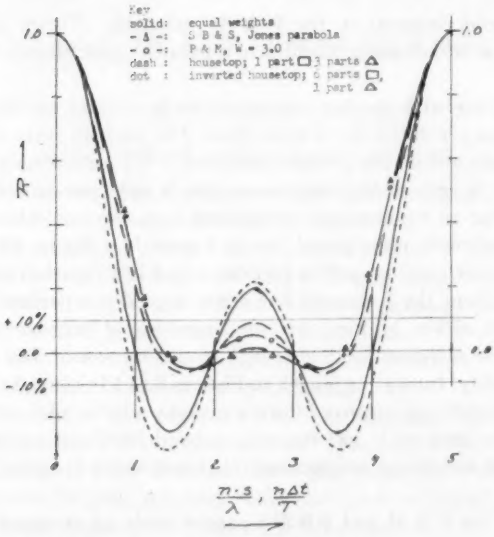

FIG. 1. Steady-State Rejection Curves for Five-Element Lines.

This plot shows the response "R" for lines relative to that of a bunched group of equal number as a function of the line length to apparent wavelength ratio. Length, here, is the number "n" times spacing "s." The ratio of n times the moveout between elements "$n\Delta t$" to the period T is equivalent to $(n \cdot s)/\lambda$ White's $\Delta\tau$ is the same as $n\Delta t/T$ here.

The maximum difference is at $n \cdot s/\lambda = 2.5$, where the difference ratio is

$$\frac{0.06}{0.01} = \frac{P \,\&\, M}{SB \,\&\, S}.$$

The "housetop" has nearly as good response (within two percent) except over the range

$$2 < \frac{n \cdot s}{\lambda} < 3$$

where R is as great as 0.09. The Jones data are essentially identical with that of S B & S, from which one might conclude that they are based on similar criteria. Table I indicates the rejection band "W" and rejection amplitude "R" for these curves.

Now, if we were to increase the number of elements, the differences here would be accentuated. However, larger fractions of the rejection bands would become almost equal, and all would widen an equivalent amount. I suggest that one could devise almost any weighting technique to give response characteristics that compare favorably with those of P & M or S B &S. The big problem is not

TABLE I
WEIGHTING FACTORS WITH W AND R VALUES

Distribution	Weights for elements					W	R
	1	2	3	4	5		
Equal	1.0	1.0	1.0	1.0	1.0	5.3	.25
S B & S	0.35	0.81	1.00	0.81	0.35	2.9	.06
P & M	0.40	0.80	1.00	0.80	0.40	3.0	.06
Jones	0.36	0.84	1.00	0.84	0.36	2.9	.06
Housetop	0.46	0.80	1.00	0.80	0.46	3.3	.09
Inverted Housetop	1.00	0.87	0.75	0.87	1.00	6.1	.30

devising the weights. The big problem is how to insure getting the weights one wants!

P. L. LAWRENCE
Magnolia Petroleum Company
Dallas, Texas

Received by Editor April 11, 1958

REPLY TO COMMENTS OF MR. P. L. LAWRENCE

Since at least one erroneous conclusion has apparently been drawn from our paper, "The Moveout Filter," and this by an obviously non-casual reader, we must apologize for having failed to set forth clearly the viewpoint and fundamenal hypothesis of this paper.

To begin, a summary of the circumstances under which this paper was written and of the philosophy upon which it is based would appear to be in order. It should first be pointed out that "The Moveout Filter" was completed, as a paper, before the publication of "A New Method of Pattern Shooting" by Parr and Mayne. "The Moveout Filter" was presented to the Annual Meeting of the SEG in New York in the spring of 1955. It was submitted for publication in GEOPHYSICS almost coincidentally with the publication of the paper of Parr and Mayne. As originally submitted, our paper, naturally enough, contained no reference to the Parr-Mayne paper. It was only upon the suggestion of the referees that the material comparing the Parr-Mayne criteria to ours was prepared and inserted into the manuscript.

Throughout "The Moveout Filter" the approach has been functional and operational. Fundamentally, the theoretical studies are based on the assumption that the system has to operate on real, not idealized, data. It was hoped that the results of the study would enable a field geophysicist to select the weighting or sensitivity system which would optimize signal-to-noise ratio in a given locality. We intended that our design criteria should be directly applicable to field data

without further experimentation. Thus if a party chief in the field found his problem to be that of noise having wave lengths of 25 to 300 ft, it was intended that he be able to choose his tapering system using that knowledge directly. His "reject band" would correspond to the wave-length band from 25 to 300 ft inclusive. It is this definition of "reject band" which was applied both to our equations and to those of Parr and Mayne. As pointed out in our paper (p. 14), we used the Parr-Mayne formula uncritically to apply to the maximum wave length of noise which it was desired to reject. This was the same criterion which was used in designing the weighting system of Table I (p. 9). While Parr and Mayne do not specifically state in their paper that the reject band for the system coincides with the observed noise band, this interpretation is strongly implied. Furthermore, Parr's 1955 patent (U.S. 2,698,927, to which he refers in the paper) specifically sets forth (column 7, lines 14–27) the identity of the two.

The two taper systems of Figure 6 were thus designed to fit the same set of noise data, each according to its own appropriate criterion. Relative quality of the results was judged on the basis of the effect of each pattern upon the same noise system. The comparison intended is an over-all comparison of definitions, applicability criteria, and final design. It was not intended to determine whether, by judicious choices of parameters in the two systems, it would be possible to achieve substantially similar results. Figures 12 and 13 finally show what would happen if a field man proceeded to use each of the systems precisely as set forth.

Comparison of the relative effectiveness of various weighting systems on the basis of the maximum value of R in the reject band assumes that the noise to be rejected consists of isolated high-amplitude bursts randomly distributed over the reject band, an assumption directly contrary to fact in most cases. In fact, Parr and Mayne (p. 540) themselves strongly imply a continuous noise distribution. Far greater improvement in signal-to-noise ratio results from keeping the rebound amplitudes down as much as possible over as much of the reject band as possible even if the rebound amplitude escapes to a high value at isolated wave lengths. The RMS criterion is far better suited to the design of a taper system to be used against real noise than the minimum-maximum criterion which produces the Tchebycheff expansion of Parr and Mayne.

The objection to the sequence of examples (p. 15 through 17 and Figures 8 through 13) of our paper on the basis that S is not constant indicates that our explanation of the construction of the examples was insufficient. The sequence of examples was intended to represent historical progress. Figure 7 represents a basis of comparison while Figure 8 represents the best that can reasonably be accomplished with electronic filtering alone. Figure 9 represents normal, non-pattern shooting with optimum electronic filtering. Three seismometers per group on a group length of 100 ft is at least comparable to prevailing techniques in non-pattern areas. Figure 10 represents the optimum to be expected with areal groups of many seismometers as used contemporaneously in the more difficult pattern areas. Figure 11 is simply inserted to show the effect of increased group length

without taper so that the effect of the taper of Figure 12 may be compared with a non-tapered group of the same length. Figure 13, of course, represents the Parr-Mayne array designed to fit the observed noise pattern according to the Parr-Mayne criteria.

In order that all illustrations be comparable, it was necessary that a given wave length appear at the same S/λ value in all figures. To achieve this end it was assumed that in all cases S was 400 ft but that outside the group illustrated in each specific example, a weighting of zero prevailed out to the 400-ft limit. Thus the example of Figure 9 is intended to represent the output of an array of 9 elements having sensitivities, 0, 0, 0, 1, 1, 1, 0, 0, 0.

The next contention is that White's paper implies no striking differences among several weighted continuous distributions. This topic has been extensively discussed in a Letter to the Editor in GEOPHYSICS, April, 1958 (Savit, "Transient Behavior of Patterns," p. 360–362). To summarize, White studied only the pass-bands of the various distributions and did not concern himself with the reject-bands. White's conclusions are, therefore, inapplicable to the present discussion.

The comparisons prepared by Mr. Lawrence for the case of five elements do not afford an adequate comparison of the two weighting systems under discussion largely because of the small number of elements and the approximate nature of the computations. The larger the number of elements, the greater is the relative difference between the two criteria. It is also improper to determine the optimum tapering for five elements by averaging or sampling the optimum tapering for twenty-one. If one desires to compare five-element groups under the two criteria, one must calculate the RMS best-fit directly, as, for example, by the use of formula (20), p. 9. Quite obviously, the use of the Parr-Mayne design criterion alone to evaluate the relative effectiveness of different tapers will always prove that the Parr-Mayne weighting is superior. Conversely, the use of our design criterion alone to evaluate the relative effectiveness of moveout filters will produce a superiority for our weighting.

Even with all these handicaps and using Mr. Lawrence's own figures, we note that for the three rebound peaks in the reject band our taper yields equality of two peaks and a six-to-one improvement for the third peak as compared to the Parr-Mayne taper. The two band-widths are identical under the Parr-Mayne definition.

It is hard to see how a six-to-one improvement in noise rejection over one-third of the reject band can lightly be dismissed as unimportant. For larger numbers of elements the portion of the reject band over which there is improvement increases approximately as $(n-4)/(n-2)$.

Mr. Lawrence is indeed correct in stating that the major problem is not necessarily devising the weights. It certainly is the problem of insuring that the weights we desire are actually applied. If we are willing to pay the cost, the desired weights may be obtained to a reasonable degree of accuracy. It is only necessary to record the outputs of the individual seismometers on magnetic tape

(or other reproducible medium), base-level the reproduced outputs, and then combine the signals in proper proportion. Unfortunately, for application to the areas described in our paper, a minimum of 94 independent recording channels would be required for a 24 trace recording. The cost of such a setup precludes its general use, particularly since very good results can be obtained with the taper applied directly. An additional improvement of about 2 to 1 in signal-to-noise ratio could probably be expected by the use of the individual recording and base-leveling technique.

CARL H. SAVIT
Western Geophysical Company of America
Los Angeles, California

Received by the Editor April 26, 1958

RESIDUAL AND SECOND DERIVATIVE OF GRAVITY AND MAGNETIC MAPS

There has been considerable discussion regarding the merits and demerits of the "smoothers" and the "gridders" in preparation of residual and second derivative maps. The controversy is probably unnecessary, as it appears that, basically speaking, the "smoothers" determine or tend to determine the residual, whereas the "gridders" aim at the second derivative. Following are the reasons for this statement.

(1) Some authors (Henderson and Zeitz, 1949; Nettleton, 1954) have pointed out the fact that the so-called residual as computed by grids are numerically proportional to the second derivatives computed from the same grid. Compare the following expressions:

$$\text{Second Derivative} \equiv (C/S)^2(W_0H_0 + W_1\overline{H}_1 + W_2\overline{H}_2 + \cdots) \quad \text{General formula (Nettleton, 1954)}$$

$$\text{Residual} = H_0 - \overline{H}(s) \equiv (W_0H_0 + W_1\overline{H}_1 + W_2\overline{H}_2 + \cdots) \quad \text{(Griffin, 1949)}$$

(?)

$$\text{Residual} = [\overline{H}(r_1) - \overline{H}(r_2)]/[r_2 - r_1]$$

(?)

$$\equiv (D/S)(W_0H_0 + W_1\overline{H}_1 + W_2\overline{H}_2 + \cdots) \quad \text{(Saxov-Nygaard, 1953)}$$

where C and D are constants, S the spacing, W the weights, and other symbols have the usual meanings. The proportionality, which is so obvious from the above formulas, seems to be an absurd result, because the residual can only be related to the second derivative as g is to $\partial^2 g/\partial z^2$. Residual is the field at the surface due to the isolated structure or stratigraphy we are interested in, and the second derivative is the same thing twice differentiated with respect to the vertical direction. The two can hardly be simply proportional. It is true that some of the highs and lows of a second derivative map will coincide with those of the

residual in position, but they will not be proportional to the residual. Further, by its very nature, the second derivative map will have more maxima and minima than the corresponding residual.

(2) Slotnick (1932) proved that the $\partial^2 g/\partial z^2$ map is proportional to the mean curvature of the g-surface, and Nettleton (1954) demonstrated that "the operation of any grid system is rather closely analogous to determining the curvature of the potential field or 'surface'." The obvious conclusion seems to be that all grid calculations yield second derivatives or quantities proportional to it. Griffin's (1949) and Saxov-Nygaard's (1953) formulas, therefore, do not appear to relate to residuals but are really different forms (as are the formulas by Elkins, 1951, Rosenbach, 1953, and others) for the differentiation that $\partial^2 g/\partial z^2$ involves.

(3) The determination of the residual or the regional is fundamentally indeterminate (Vajk, 1951) because it involves the separation of an integral potential field into its components, whereas the second derivative is quite determinate because this consists of only the numerical differentiation of a given set of data.

Vajk (1951) rightly states that the grid procedures for regional correction have no physical basis. It seems meaningless to search for an objective criterion for something that has no objective basis. Steenland's (1952) view that the physical basis for the computation of $\partial^2 g/\partial z^2$ supplies the basis for the grid residuals because the two are proportional does not seem valid in the face of what has been said above. As a matter of fact, the proportionality between the second derivative and the grid-residual is an indication that the latter is not a residual at all. The constants of proportionality or the dimensions in Griffin's and Saxov-Nygaard's formulas are not right because these relationships are only assumed, not derived from valid physical concepts.

I would like further to draw your attention to a statement in Saxov-Nygaard's paper (1953, p. 927): "As far as the second and the fourth derivatives are concerned, we should like to state that these figures do not represent a depth gradient, but a residual anomaly." The converse seems to be the true state of affairs.

AMALENDU ROY
Indian Institute of Technology
Kharagpur, West Bengal, India

Received by the Editor April 16, 1958

REFERENCES

Elkins, T. A., 1951, The second derivative method of gravity interpretation: Geophysics, v. 16, p. 29–50.

Griffin, R. W., 1949, Residual gravity in theory and practice: Geophysics, v. 14, p. 39–56.

Henderson, R. G., and Zeitz, I., 1949, The computation of second vertical derivatives of geomagnetic fields: Geophysics, v. 14, p. 508–516.

Nettleton, L. L., 1954, Regionals, residuals, and structures: Geophysics, v. 19, p. 1–22.

Rosenbach, O., 1953, A contribution to the computation of the "second derivative" from gravity data: Geophysics, v. 18, p. 894–912.

Saxov, S., and Nygaard, K., 1953, Residual anomalies and depth estimation: Geophysics, v. 18, p. 913–928.
Slotnick, M. M., 1932, Curvature of equipotential surfaces: Early Geophysical Papers, p. 410–419.
Steenland, N. C., 1952, Review of Vajk's paper (see Vajk): Geophysics, v. 17, p. 409.
Vajk, R., 1951, Regional corrections of gravity data: Geofisica Pura e Applicata, v. 19, p. 129–143.

SOLICITED REPLY TO PROFESSOR AMALENDU ROY

Professor Roy's letter points out the mathematical similarity of expressions for "residual" values and those for derivatives and that what appear to be essentially the same quantities have been expressed, in the geophysical literature, in different units.

There can be little argument in Roy's contention that all the numerical or grid schemes of calculating "residual" values are qualitatively similar to derivative calculations. Their origin, however, is largely empirical rather than analytical, and it is more or less an accident that they are so similar. They are retained, in spite of their lack of analytical foundation, partly because of their simplicity and effectiveness and partly because the analytically complex derivative systems have been found to be more difficult to understand.

All the various residual or derivative systems are attempts to increase the discrimination of a potential field and to make a map which is more directly related to the geological irregularities of interest than is the map of the original data. Basically, this means separating a field into components from different sources presumably at different depths or otherwise distinguishable. Such a separation is never exact because of the ambiguity in the source of potential fields.

To clarify the different procedures and maps which are used in the interpretation of potential fields, the following definitions are suggested.

Residual Maps show the difference between an observed field and a "regional" field. The units of a residual are the same as those of the observed data (i.e., milligals or gamma).

The "regional" is empirical because the inherent ambiguity of the source of a potential field makes it impossible, without other assumptions, to define the boundaries of density or magnetic contrasts, except within certain outer (or deeper) limits (Skeels, 1947; Nettleton, 1940, p. 101). Therefore, there is no firm theoretical basis for separating the field into regional and local components. In spite of their ambiguity, residual maps are very useful, but they are relatively laborious to make and require a high degree of skill and experience. They can be used for quantitative analysis of possible geometric or geological forms which cause the disturbance.

Derivative Maps are based on computations of the type

$$\frac{\partial^n H}{\partial Z^n} = \frac{C}{S^n}\left(W_0\overline{H}_0 + W_1\overline{H}_1 + W_2\overline{H}_2 + \cdots\right),$$

where $(W_0+W_1+W_2+\cdots)=0$ and $\overline{H}_1, \overline{H}_2 \cdots$ are average values at different distances from the point of calculation. S is the grid spacing (on the ground), and C is a derived constant. They are usually computed for second derivatives ($n=2$) but first and fourth vertical derivatives are mentioned in the literature (Evjen, 1936; Peters, 1949). The units are those of the original field divided by S^n (e.g., gals/$\overline{\text{cm}^2}$, gamma/$\overline{\text{mile}^2}$, for second derivatives, etc.).

Derivative calculations represent approximations to the calculations of a definite mathematical function from a given potential field. They are approximate because, for practical purposes, the field is represented by a grid of discrete points. Also, the values for the constant, C, and for the weighting factors or coefficients (i.e., W_0, W_1, etc.) are dependent on the mathematical procedure used for their derivation and on the limiting assumptions used. The different derived formulas for the same quantity give widely different results (Nettleton, 1954, Figures 7–13). Also, the computed magnitudes vary considerably with grid spacing, although, theoretically, they should not as the spacing is taken into account by the $1/S^n$ term in the formula. Theoretically, they should be suitable for quantitative calculation, but practically their usefulness for quantitative analysis is very limited because of their dependence on the type of formula used.

Grid Residual Maps are based on computations of the type

$$H_0 - \overline{H}(S) = (W_0H_0 + W_1\overline{H}_1W_2\overline{H}_2 + \cdots),$$

where $(W_0+W_1+W_2+\cdots)=0$ and $\overline{H}_1, \overline{H}_2 \cdots$ are average values at one or more distances from the point of calculation. The units are those of the original field.

Grid Residual calculations were originally developed empirically (Griffin, 1949) as a practical expedient to approximate the results of a true residual by a routine numerical operation which can be done quickly by mechanical methods and relatively unskilled labor. The results are very greatly dependent on the grid spacing and to a small degree on the grid pattern. With properly chosen spacing, they will give maxima and minima closely matching those given by a true residual. Their relation to Second Derivative Maps has been pointed out by Henderson and Zietz (1949). They are not suitable for quantitative analysis.

Derivative and Grid Residual Maps are very much alike, and, in particular, have nearly the same zero contour if the weighting formula and spacing are similar (Henderson and Zietz, 1949; Nettleton, 1954). The difference in units comes from the inclusion, in the derivative calculations, of the C/S^2 coefficient and its omission from the grid residual calculations.

L. L. NETTLETON
Gravity Meter Exploration Company
Houston, Texas

Received by the Editor May 20, 1958

REFERENCES

Evjen, H. M., 1936, The place of the vertical gradient in gravitational interpretations: Geophysics, v. 1, p. 127.

Griffin, W. Raymond, 1949, Residual gravity in theory and practice: Geophysics, v. 14, p. 39.

Henderson, Roland G., and Zeitz, Isidore, 1949, The computation of second vertical derivatives of geomagnetic fields: Geophysics, v. 14, p. 508.

Nettleton, L. L., 1940, Geophysical prospecting for oil: New York, McGraw-Hill Book Company, Inc.

————, 1954, Regionals, residuals, and structures: Geophysics, v. 19, p. 1.

Peters, L. J., 1949, The direct approach to magnetic interpretation and its practical applications: Geophysics, v. 14, p. 290.

Skeels, D. C., 1947, Ambiguity in gravity interpretation: Geophysics, v. 12, p. 43.

CONTRIBUTORS

JAMES AFFLECK

JAMES AFFLECK received his primary and high school education in Scotland. He obtained the degree of B.S. in Electrical Engineering in 1930 from the Carnegie Institute of Technology and the M.S. in Mathematics in 1934 from the University of Pittsburgh. In 1930 Mr. Affleck joined the Gulf Research and Development Company as a geophysicist, and he is now Section Head in charge of Magnetic Interpretation and Research.

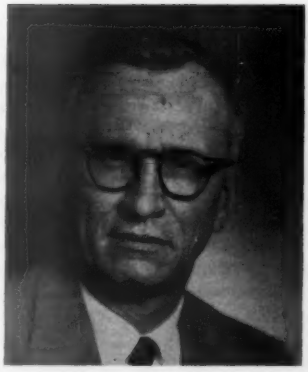

WILLIAM B. AGOCS

WILLIAM B. AGOCS received his B.S. degree in Mining Engineering with Honors from Lehigh University in 1934, his M.S. in Physics in 1944, and his Ph.D. in 1946. From 1934 to 1940 he was associated with the Gulf Research and Development Company as a geophysicist and a Party Chief on seismic parties in Venezuela and the United States. From 1940 to 1944, he was a graduate student and an Instructor in Physics at Lehigh University. During the years 1944 to 1946 and 1948 to 1950, he was the Chief Geophysicist for the Venezuela Atlantic Refining Company, and he organized its Geophysical Department. From 1946 to 1948, he was Associate Professor of Physics at Lehigh University, and, from 1950 to 1953, he was Professor of Physics and Geophysics at the University of Tulsa. Dr. Agocs has been a consultant on problems in the exploration for minerals and petroleum, and since 1953 he has been the Chief Geophysicist for the Aero Service Corporation and its affiliates.

He is a member of SEG, EAEG, AGU, GSA, the American Institute of Mining and Metallurgical Engineers, the American Physical Society, and the Society of Sigma Xi.

S. NORMAN DOMENICO

S. NORMAN DOMENICO was born in 1925 at Louisville, Colorado. His undergraduate studies were interrupted during World War II, at which time he served as a radio technician in the Navy for two years. In 1948 he received a degree in Geological Engineering (geophysics option) from the Colorado School of Mines, and in 1951 he was awarded the D.Sc. in Geophysics from the same institution. In 1949 he took the M.S. in Geophysics from the California Institute of Technology.

In 1951 he joined the Pan American Petroleum Corporation as a geophysicist, and he has advanced through the grade of Party Chief to charge of experimental crews. He has recently been made the Geophysical Technical Supervisor for the Canadian operations of the Pan American Petroleum Corporation. During a leave of absence in 1951, he conducted theoretical studies in underwater sound for the Naval Electronics Laboratory.

Dr. Domenico is a member of SEG, EAEG, and the Seismological Society of America.

JOSEPH W. HAMMOND is a graduate in electrical engineering from Purdue University. In 1939 he joined the Seismograph Service Corporation as a trainee; and, after being promoted to observer and transferred to Venezuela in 1941, he became the company's Instrument Supervisor in both Venezuela and Colombia. In 1949 he returned to the United States as Senior Research Engineer, and he was later promoted to Manager of Field Research for the firm's international operations.

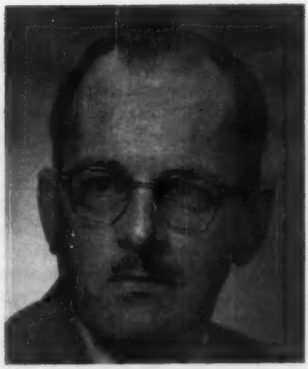

JOSEPH W. HAMMOND

JAMES E. HAWKINS

JAMES E. HAWKINS is a native of Canada and a naturalized citizen of the United States. In 1932 he graduated from the University of Alberta with the degree of B.Sc. (E.E.). From 1936 to 1940 he did graduate work at the Colorado School of Mines, and there he obtained the degrees of Master of Geological Engineering and Doctor of Geophysical Engineering. During these years he was a Graduate Instructor in Geophysics; in 1940–1941 he was made a full Instructor, and he gave courses in electrical and seismic geophysics. From 1936 to 1941 he was employed part time in various capacities by the Heiland Research Corporation; and he also spent a considerable amount of time in geophysical instrument design and field application, particularly with electrical prospecting methods for mining work.

In 1941, Dr. Hawkins joined the Seismograph Service Corporation as an Instrument Research Engineer, and in 1945 he was made a Vice-President and Director of Research, Manufacturing, and Supply.

Dr. Hawkins is a member of SEG, EAEG, the Geophysical Society of Tulsa, the Institute of Radio Engineers, the Acoustical Society of America, and the American Institute of Electrical Engineers.

RALPH D. HUTCHISON

RALPH DELAMERE HUTCHISON was born in Toronto, Canada, in 1917 and grew up there. After five years on the editorial staff of a Toronto newspaper, he joined the Royal Canadian Naval Volunteer Reserve as a sub-lieutenant and served at sea from 1941 to 1945.

During the next five years he qualified for the degree of B.A.Sc. (in engineering physics) at the University of Toronto and spent several summers as observer in Arctic magnetic surveys then being carried out jointly by the Dominion Observatory, Ottawa, and the Royal Canadian Air Force. During the same period he began, at the Dominion Observatory, a program of investigation into the character of magnetic secular change as observed in Canada between 1900 and 1950.

In 1952 he left the Dominion Observatory for employment in mining geophysics. He has since worked on surveys in various parts of Canada and the United States, and in South America and Ireland. He is now practising in Toronto as a consulting geophysicist. He belongs to the Association of Professional Engineers of the Province of Ontario and to the Canadian Exploration Geophysicists.

KAISER S. KUNZ

KAISER S. KUNZ, a native of Indiana, received the A.B. degree in Physics from Indiana University in 1936; the A.M. degree in 1937, and the Ph.D. degree in Theoretical Physics from the University of Cincinnati in 1939. The following three years he served as Instructor in Mathematics in the Engineering College of the latter University. From 1942 to 1945 he was a member of the staff of the Officer's Training School (pre-radar) at Harvard University. In 1945 he entered the research program set up at Harvard University under Division 13 of the Office of Scientific Research and Development, where his field of investigation was a study of slot antennas for high-speed aircraft.

Early in 1946, Dr. Kunz received an appointment as Research Fellow in Communications at the Electronics Research Laboratory of Harvard University. One of his chief researches during this period was a mathematical study of the radiation from the open end of waveguides. In 1947 he was appointed lecturer in applied mathematics at the Computation Laboratory of Harvard University.

He left Harvard in 1949 to accept an Associate Professorship in Engineering at Case Institute of Technology. In 1951 he joined the Schlumberger Well Surveying Corporation as a Research Physicist and is now Technical Assistant to the Head of Research. His book on numerical analysis was published last year by the McGraw-Hill Book Company. He is a member of the Phi Beta Kappa Society, the Society of Sigma Xi, the Institute of Radio Engineers, the American Physical Society, and the American Mathematical Society.

FRANKLIN K. LEVIN

FRANKLIN K. LEVIN received the B.S. in Physics from Purdue University in 1943. After graduate work at Columbia University and the University of Wisconsin, he was awarded the Ph.D. in Physics in 1949 by the latter university.

Except for a year when he served as Assistant Director of the Hudson Laboratories, he has been associated with The Carter Oil Company from 1949 to 1958 as a research physicist. He is now a Senior Physicist with the Jersey Production Research Company.

Dr. Levin is a member of SEG, the American Physical Society, the Acoustical Society of America, the Geophysical Society of Tulsa, and the Society of Sigma Xi.

RALPH D. LYNN

RALPH D. LYNN graduated from the University of Oklahoma with a B.A. degree in Physics in 1931, and in 1933 he received the M.S. in Physics from the same institution. He taught physics and mathematics at Cameron State Agricultural College (at Lawton, Oklahoma) for one year. From 1934 to 1937 he was a seismograph operator for The Carter Oil Company, and from 1937 to 1958 he has been a research physicist at the company's research laboratory except during the years of his military leave (1942 to 1946) with the U. S. Army. He is presently associated with the Jersey Production Research Company as a Research Physicist.

Mr. Lynn is a member of SEG, AGU, the Geophysical Society of Tulsa, the Seismological Society of America, the American Physical Society, the Institute of Radio Engineers, and the Society of Sigma Xi.

JAMES H. MORAN

JAMES H. MORAN, a native of Montana, received his B.S. from the California Institute of Technology in 1945. After two years with the engineering department of the Anaconda Copper Mining Company he began graduate work in electrical engineering at the Case Institute of Technology in Cleveland. In 1949 he received his M.S. and in 1952 his Ph.D., both in Electrical Engineering, from Case. He remained there as an Assistant Professor in the electrical engineering department until 1953, when he joined the research department of Schlumberger Well Surveying Corporation in Ridgefield, Connecticut. With Schlumberger he has worked on a variety of theoretical problems associated with well logging.

Dr. Moran is a member of the American Physical Society, the Institute of Radio Engineers, Eta Kappa Nu, and the Society of Sigma Xi.

DONALD R. OKSA

DONALD R. OKSA received the Associate of Arts degree from Gogebic Junior College and the B.S. in Geological Engineering from the Michigan College of Mining and Technology. He served in the Air Force from 1943 to 1946 in flight and maintenance engineering. He was employed by the Atlantic Refining Company in 1947, and in 1951 he joined the Sinclair Oil and Gas Company. With Sinclair, Mr. Oksa was first in the Land Department, but in 1952 he was transferred to the Research Section and there has been engaged in seismic interpretation problems.

FREDERICK E. ROMBERG graduated from the University of Texas in 1929 with the B.A. degree and from Harvard University in 1932 with the A.M. In 1932–1933, he was an Instructor in Physics at Harvard.

In 1933 Mr. Romberg was employed by Geophysical Service Inc. From 1941 to 1951 he was actively engaged in the manufacture and development of gravity meters with the firm of LaCoste and Romberg in Austin, Texas. In 1951, after rejoining Geophysical Service Inc., he became Manager of its Southern Division in Houston, and in 1954 he was made the Manager of the company's Gravity Department.

Mr. Romberg is a member of SEG, AGU, GSA, and the Society of Sigma Xi.

FREDERICK E. ROMBERG

CLARENCE H. SANDBERG

CLARENCE H. SANDBERG was born in Fullerton, Nebraska, in 1895. He graduated from University of Idaho in 1918 where he received the degree of B.S. in Chemical Engineering.

He served in World War I as a Second Lieutenant in the Engineers. From 1920 to 1930 he was employed in the Sales Department of the Standard Oil Company of California. After leaving the employ of that company, he took a year's geological training at the Montana School of Mines followed by two years at the University of Arizona.

For the past 15 years he has been a geophysicist in the U. S. Bureau of Mines and the U. S. Geological Survey.

Mr. Sandberg is a member of SEG, AGU, GSA, AAAS, and the Society of American Military Engineers.

WILLIAM SCHRIEVER

WILLIAM SCHRIEVER was born in 1894 at Dakota City, Nebraska.

He received the degree of Bachelor of Arts from Morningside College in 1916. He received a scholarship at the University of Iowa for graduate study in physics and was awarded the degree Master of Science in 1917. His graduate study was interrupted by World War I when he served in the newly-created science and research division of the Signal Corps from January, 1918, to February, 1919. His graduate study was again interrupted during 1919–1920 when he served as Assistant Professor of Physics at the University of Oklahoma. He was awarded the degree of Doctor of Philosophy in 1921 at the University of Iowa. He returned to his position at Oklahoma in 1921. He was advanced to Associate Professor in 1924 and to Professor of Physics in 1927.

He served as Chairman of the Department of Physics from 1942–1952 and as Director of the School of Engineering Physics from 1942–1948.

Dr. Schriever is a member of SEG, AGU, and the American Association of Physics Teachers. He is a Fellow of the American Physical Society and of the American Association for the Advancement of Science. He served as first president of the Oklahoma Chapter of the Society of Sigma Xi.

SOCIETY ROUND TABLE

COMMITTEES FOR THE YEAR ENDING IN OCTOBER 1958

Executive Committee

President: O. C. Clifford, Jr., The Atlantic Refining Co., Dallas, Texas
Vice-President: Ben F. Rummerfield, Century Geophysical Corp., Tulsa, Oklahoma
Secretary-Treasurer: Howard E. Itten, Empire Geophysical Inc., Ft. Worth, Texas
Editor: Lawrence Y. Faust, Amerada Petroleum Corp., Tulsa, Oklahoma
Past President: Roy F. Bennett, Sohio Petroleum Co., Oklahoma City, Oklahoma

Nominations

O. C. Clifford, Jr., *Chairman*
Roy F. Bennett
R. C. Dunlap, Jr.

Tellers

J. V. Franklin, *Chairman*

Education

Joshua L. Soske, *Chairman*
Victor J. Blum, S.J.
P. E. Dehlinger
G. D. Garland
J. W. Hoover
J. B. Hudson
V. Vacquier

Student Membership

W. H. Courtier, *Chairman*

Subcommittee on Student Membership

Fred J. Agnich, *Chairman*

Subcommittee on Scholarships

Richard Brewer, *Chairman*

Subcommittee on Essays

Charles W. Oliphant, *Chairman*

Distinguished Lectures

M. E. Denson, Jr. ('58), *Chairman*
R. A. Peterson ('58)
John Bemrose ('59)
Milton Born ('59)
A. J. Hintze ('60)
J. Weldon Thomas ('60)

Radio Facilities

B. D. Lee, *Chairman*
W. M. Rust, Jr., *Vice-Chairman*
C. B. Bazzoni
Richard Brewer
V. Robert Kerr
E. M. Shook
Daniel Silverman
Bart W. Sorge

Membership

John C. Hollister, *Chairman*
C. L. Barker
L. H. Boyd
G. A. Grimm

Honors and Awards

Sigmund Hammer ('58) *Chairman*
Curtis H. Johnson ('59)
Roy L. Lay ('60)
Paul L. Lyons ('61)

Publications

Cecil H. Green, *Chairman*
Sigmund I. Hammer
H. B. Peacock
Sidney Schafer
Robert J. Watson

Subcommittee on Translation of Russian Publications

Irwin Roman, *Chairman*
Eugene M. McNatt
Paul P. Reichertz

Reviews

Franklyn K. Levin, *Chairman*
W. T. Born
Thomas A. Elkins
W. W. Garvin
Sigmund I. Hammer
Chwan-Chang Lee
John E. Nafe
Carl H. Savit
V. Vacquier
James E. White

Geophysical Activity

H. G. Patrick, *Chairman*
Kenneth L. Cook
R. J. Copeland
Herbert Hoover, Jr.
Santos Figueroa Huerta
C. N. Hurry
Kumiji Iida
C. C. Lister
L. R. Tucker

Safety

C. C. Sellers, Jr., *Chairman*
R. N. Brantley
J. W. Brown
J. W. Green
P. M. Hanahen
R. C. Henderson
G. M. Kintz
W. H. Newton
E. L. Wells

Mining Geophysics

Ralph C. Holmer, *Chairman*
Kenneth L. Cook
H. V. W. Donohoo
Walter E. Heinrichs, Jr.
LeRoy Scharon
R. Maurice Tripp
Stanley H. Ward

Case Histories

Dave P. Carlton, *Chairman*

Mining Case Histories

H. LeRoy Scharon, *Editor*

Constitution and Bylaws

W. M. Rust, Jr., *Chairman*
Cecil H. Green
W. W. Hardy
Paul Lyons
L. L. Nettleton

Membership in American Institute of Physics

Norman H. Ricker, Liaison Member

Research

W. T. Born, *Chairman*
F. G. Boucher
J. M. Crawford
C. Hewitt Dix
C. H. Green
John C. Hollister
L. L. Nettleton
T. J. O'Donnell
A. L. Parrack
R. A. Peterson
Daniel Silverman
Noyes D. Smith, Jr.

R. R. THOMPSON
J. E. WHITE
J. P. WOODS

Subcommittee on Thesis Study

L. L. NETTLETON, *Chairman*
C. H. GREEN

Subcommittee on Rice Symposium

NOYES D. SMITH, JR., *Chairman*
C. HEWITT DIX
L. L. NETTLETON
R. A. PETERSON
A. L. PARRACK

Index of Wells

V. U. GAITHER, *Chairman*

Magnetic Recording

J. D. SKELTON, *Chairman*
KEITH R. BEEMAN
ROLAND F. BEERS
K. E. BURG
J. D. EISLER
J. E. HAWKINS
K. M. LAWRENCE
B. D. LEE
G. B. LOPER
R. A. PETERSON
R. R THOMPSON
E. B. TICKELL
F. A. VAN MELLE

Magnetic Recording Subcommittee on Definitions & Measurement

L. W. ERATH, *Chairman*
R. A. ARNETT
FRANK COKER
J. M. CUNNINGHAM
J. J. DURAPAU
F. J. FEAGIN
H. R. FRANK
ROGER HARLAN
R. W. KELLEY
L. B. MCMANIS
R. C. MOODY

Magnetic Recording Subcommittee on Recorder Characteristics

S. KAUFMAN, *Chairman*
A. L. PARRACK

American Geological Institute Directors

R. C. DUNLAP, JR. ('58)
ROY F. BENNETT ('59)

AGI Glossary

R. A. GEYER, *Chairman*
L. W. BLAU
D. S. HUGHES
PAUL L. LYONS
L. L. NETTLETON
D. C. SKEELS
I. A. VAN WEELDEN
J. TUZO WILSON

AGI Committee on Licensing

A. E. MCKAY, SEG MEMBER

Business Office

CRAIG FERRIS, *Chairman*
JAMES F. JOHNSON
FRANK E. BROWN

National Research Council Div'n of Earth Sciences Representative

R. D. WYCKOFF

AAAS Council Representative

ROLAND F. BEERS

Radioactive Mineral Exploration

BEN F. RUMMERFIELD, *Chairman*
E. R. GORDON
A. J. HINTZE
JOHN C. HOLLISTER
F. H. LAHEE
PAUL L. LYONS
L. W. MACNAUGHTON
JOHN MASTERS
A. GARCIA ROJAS
STAN. L. ROSE

SEG Committee on IGY

PAUL L. LYONS, *Chairman*

Publicity and Public Relations

BART W. SORGE, *Chairman*
SAM W. ALLEN, JR.
G. A. BOLLINGER
J. M. COCHRANE
S. R. FAUST
STANLEY E. GIULIO
J. A. HALL
GLENN R. HARRIS
B. A. HEIDT
D. T. MCCREARY
W. H. NEWTON
M. L. PUGH
G. A. ROUSSEL
H. B. SMITHWICK
J. C. WATERMAN
RAY H. WRIGHT
W. C. WOOLEY

Sustaining Membership

L. O. SEAMAN, *Chairman*
C. W. PAYNE

LOCAL SECTIONS

Geophysical Society of Tulsa

Chartered February 2, 1948
Frank Searcy, *pres.*
T. S. Green, *1st v-pres.*
F. R. Kittredge, *2nd v-pres.*
P. M. McNally, *treas.*
R. L. Frossard, *editor*
S. E. Giulio, *secty.* The Carter Oil Co., Box 801, Tulsa 2, Okla.
Meetings: Monthly, 2nd Thursday, 7:00 P.M., meeting only, University of Tulsa, room 224, Petroleum Science Hall

Geophysical Society of Houston

Chartered February 14, 1948
John F. Anderson, *pres.*
S. Brooks Stewart, *1st v-pres.*
Paul Farren, *2nd v-pres.*
John R. Monkhouse, *treas.*
Bernard G. Hubner, Jr., *secty.* Atlantic Refining Company, Box 1346, Houston 1, Texas
Meetings: Monthly, Noon luncheon ($1.65), Rice Hotel

Pacific Coast Section SEG

Chartered April 12, 1948
Dean Walling, *pres.*
Robert B. Moran, Jr., *v-pres., S.D.*
James A. Kurfess, *v-pres., N.D.*
Robert D. Brace, *secty.* Std. Oil Co. of Calif., P.O. Box 278, Olldale, California
Meetings: Monthly, 2nd Thursday, Noon luncheon ($2.00), Biltmore Hotel, Los Angeles

Dallas Geophysical Society

Chartered August 7, 1948
Martin C. Kelsey, *pres.*
John A. Cathey, *1st v-pres.*
Wm. C. Wooley, *2nd v-pres.*
Mark K. Smith, Jr., *secty.* Geophysical Service, Inc., P.O. Box 35084, Airlawn Station, Dallas 35, Texas
Meetings: Monthly, usually 2nd Monday, 8:00 P.M., Fondren Science Building, Southern Methodist University

Fort Worth Geophysical Society

Chartered August 7, 1948
Paul H. Ledyard, *pres.*
L. V. Lombardi, *v-pres.*
Burl J. Boring, *treas.*
H. G. McCleary, *secty.* Woodson Oil Company, 2600 6th Avenue, Fort Worth 4, Texas
Meetings: Monthly, 4th Monday, Noon luncheon ($1.50), Texas Hotel

Ark-La-Tex Geophysical Society

Chartered March 12, 1949
C. P. Bragg, *pres.*
Bill C. Tucker, *v-pres.*
S. T. Spradlin, *secty.* The Ohio Oil Company, P.O. Box 1129, Shreveport Louisiana
Meetings: Monthly, last Monday, Noon luncheon ($1.50), Captain Shreve Hotel, Shreveport

Permian Basin Geophysical Society

Chartered January 30, 1950
B. F. Owings, *pres.*
R. A. Baile, *1st v-pres.*

J. E. Clark, *2nd v-pres.*
J. M. Armstrong, *treas.*
S. L. Hake, *secty.* Box 1018, Midland, Texas
Meetings: Monthly, 2nd Tuesday 7:30 P.M., free coffee & donuts, Midland Women's Club, Midland, Texas

Denver Geophysical Society

Chartered May 19, 1950
J. E. Thompson, *pres.*
John C. Hollister, *v-pres.*
Fred L. Travis, *secty-treas.* Tower Exploration Inc., 3600 S. Huron St., Englewood, Colorado
Meetings: Monthly, 1st Monday, Noon luncheon ($2.35). Petroleum Club, Denver

Canadian SEG

Chartered January 24, 1952
George J. Blundun, *pres.*
John Fuller, *v-pres.*
N. E. Klinck, *secty-treas.* Seismotech Limited, 320—39th Avenue S.E., Calgary, Alberta
Meetings: Monthly, no set schedule

Geophysical Society of Oklahoma City

Chartered September 30, 1952
W. B. Robinson, *pres.*
G. E. Anderson, *1st v-pres.*
R. H. Peacock, *2nd v-pres.*
C. L. Howell, *treas.*
H. R. DeVinna, *secty.* Central Exploration Co., 13 NE 28th, Okla. City, Okla.
Meetings: Monthly, 2nd or 3rd Monday. Time and place to be announced

Casper Geophysical Society

Chartered May 23, 1953
Dupree McGrady, *pres.*
A. C. Austin, *v-pres.*
R. L. Billings, *secty.* Forest Oil Corp., 254 N. Center St., Casper, Wyoming
Meetings: Monthly, 1st Monday, 7:00 P.M., dinner ($2.75), Townsend Hotel, Casper, Wyoming

Geophysical Society of South Texas

Chartered November 9, 1953
W. Harry Mayne, *pres.*
Jack W. E. Edmonson, *v-pres.*
P. J. Rudolph, *secty-treas.* Petty Geophysical Engineering Company, P.O. Drawer 2061, San Antonio, Texas
Meetings: 1st and 3rd Wednesdays, Noon luncheon, Sommers Cafeteria, Main Plaza, San Antonio

Southeastern Geophysical Society

Chartered April 1, 1954
I. B. Murray, Jr., *pres.*
M. H. Dingman, *1st v-pres.*
J. D. Keese, *2nd v-pres.*
Clark E. Allen, *secty-treas.* Geophysical Service Inc., 414 Carondelet Building, New Orleans 12, Louisiana
Meetings: Monthly, 3rd Monday, Noon luncheon ($1.50), St. Charles Hotel, New Orleans

Montana Geophysical Society

Chartered April 12, 1954
W. T. Langstroth, *pres.*
W. L. Holloway, *1st v-pres.*
A. J. Newton, *2nd v-pres.*
N. L. Hull, *secty-treas.* Mobil Prokucing Company, P.O. Box 2548, Billings, Montana
Meetings: Monthly, 2nd Monday, 7:30 P.M., Billings Petroleum Club

Jackson Geophysical Society

Chartered May 12, 1955
Ralph C. Cole, *pres.*
Joel E. MacGregor, *v-pres.*
Robert L. Nelson, *secyMtreas.* Pan American Petroleum Corporation, P.O. Box 689, Jackson, Mississippi
Meetings: Monthly, during 3rd week, 5:30 P.M., refreshments, 6:30 P.M., dinner ($2.00), Roof Garden of Robert E. Lee Hotel, Jackson, Mississippi

Four Corners Geophysical Society

Chartered June 19, 1958
R. P. Thomas, *v-pres.*
J. W. Rogers, *v-pres.*
V. Frank Hinson, *treas.*
John P. Badami, *secty.* Box 1121, Durango, Colorado

Southwest Louisiana Geophysical Society

Chartered January 4, 1956
Lawrence N. Ott, *pres.*
Neal Clayton, *1st v-pres.*
G. E. Tilley, *2nd v-pres.*
James M. Moore, *secty.* Skelly Oil Company, Lafayette, Louisiana
Meetings: to be announced

Utah Geophysical Society

Chartered October 29, 1956
J. R. Cheney, *pres.*
R. J. Lacy, *1st v-pres.*
D. E. Smith, *2nd v-pres.*
E. W. Morris, *secty.* General Petroleum Corporation, 53 East 4th South, Salt Lake City, Utah

Dakota Geophysical Society

To be chartered
W. E. Phillips, *pres.*
Hugh McCain, *1st v-pres.*
Quin Hayes, *2nd v-pres.*
R. R. Phair, *secty.* Roundup Powder Company, Box 452, Bismarck, North Dakota
Meetings: Monthly, 1st Friday, 7:30 P.M., Petroleum Club, Prince Hotel, Bismarck, North Dakota

New Mexico Geophysical Society

Chartered September 18, 1957
W. B. Scaife, *pres.*
J. A. Hall, Jr., *1st v-pres.*
R. A. Nixon, *2nd v-pres.*
E. J. Medley, *secty-treas.* Magnolia Petroleum Company, 714 Roswell Petroleum Bldg., Roswell, New Mexico

STUDENT SOCIETIES AFFILIATED

Colorado School of Mines Society of Student Geophysicists

Ernest Berkman, *secty.* Department of Geophysics, Colorado School of Mines, Golden, Colorado
Meetings: Monthly, 2nd Monday, 4:00 P.M.

Geophysical Society of Saint Louis University

Norman J. Guinzy, *secty.* 410 Vandalia, Collinsville, Illinois
Meetings: Monthly, 2nd Wednesday 7:30 P.M., meeting only, Institute of Technology

SEG Houston Student Section

Reed B. Kubena, *secty.* 1816 Lynnview, Houston 24, Texas
Meetings: to be announced

University of Toronto Geophysical Society

John E. Hogg, *secty.* 49 St. George Street, Toronto 5, Ontario
Meetings: Bi-weekly, alternate Thursdays, 4:00 P.M., 49 St. George Street

University of Tulsa Student Geophysical Society

Hugh Hayes, *secty.* Department of Geophysics, 600 South College, Tulsa, Oklahoma
Meetings: Weekly, Thursday, 4:00 P.M., Petroleum Science Bldg.

Trans-Pecos Student Section

John T. Sample, Jr., *secty.* Box 56, Texas Western College, El Paso, Texas
Meetings: to be announced

Pennsylvania State University Geophysical Society

Wm. R. England, *secty.* College of Mineral Industries, University Park, Pa.
Meetings: to be announced

University of Utah Geophysical Society

James D. Morgan, *secty.* College of Mines and Mineral Industries, Salt Lake City 1, Utah
Meetings: Monthly, 1st Thursday, Noon, Mines Building. Other special meetings to be announced

A & M College of Texas Student Geophysical Society

Edward C. Hanson III, *secty.* Geology and geophysics dept., A & M College of Texas, College Station, Texas

SOCIETY AFFILIATIONS

American Association for the Advancement of Science

SEG is affiliated under Section E, Geology and Geography
1515 Massachusetts Avenue
Washington 5, D. C.
Wallace R. Brode, *President*
Paul A. Scherer, *Treasurer*
Dael Wolfle, *Executive Officer*

The American Association of Petroleum Geologists

A Cooperative relationship
Box 979
Tulsa 1, Oklahoma
G. S. Buchanan, *President*
G. I. Atwater, *Vice-President*
H. T. Morley, *Secretary-Treasurer*
S. A. Wengerd, *Editor*
G. B. Moody, *Past President*
R. H. Dott, *Executive Director*

American Geological Institute

SEG is a charter member society
2101 Constitution Ave., N.W.
Washington 25, D. C.
J. V. Howell, *President*
Paul L. Lyons, *Vice-President*
J. L. Gillson, *Past President*
Donald H. Dow, *Secretary-Treasurer*
R. C. Stephenson, *Executive Director*

European Association of Exploration Geophysicists

Mutually affiliated
30, Carel Van Bylandtlaan
The Hague, Netherlands
L. Solaini, *President*
J. M. Bruckshaw, *Vice-President*
B. Baars, *Secretary-Treasurer*
O. Koefoed, *Editor*
E. H. Hedström, *Past President*

National Research Council, Division of Earth Sciences

SEG is a member society
2101 Constitution Ave., N.W.
Washington 25, D. C.
John N. Adkins, *Chairman*
Harry H. Hess, *Past Chairman*
Edward B. Espenshade, Jr., *Chairman-Designate*
William R. Thurston, *Executive Secretary*

MEMBERSHIP APPLICATIONS RECEIVED

Applications for active membership have been received from the following candidates. This publication does not constitute an election but places the names before the membership at large, in accordance with Bylaws, Article III, Section 4. References are listed in parentheses following the name of each candidate. If any member has information bearing on the qualifications of these candidates he should send it to the president within thirty days.

APPLICATIONS FOR ACTIVE MEMBERSHIP

Kenneth H. Amdall (P. P. Conrad, J. B. McKee, W. Lee Moore, Homer Roberts)
Harry W. Barbee, Jr. (Gene C. Conley, Stefan Von Croy, David F. Jewell, Jr., T. J. Thomas)
H. Raymond Brannon, Jr. (L. G. Howell, F. J. Feagin, D. H. Gardner, R. R. Thompson)
G. D. Causey (J. C. Pollard, Robert H. Ray, Robert S. Duty, Jr.)
Fred E. Fowler (Warren H. Westphal, George R. Rogers, John C. Hollister, Ralph Holmer)
J. R. Hume (Jack F. Hartman, John P. Paschall, George J. Blundun, Eugene T. Cook)
Jack Hutchins (H. W. McDonnold, C. C. Zimmerman, J. J. Schneider, Jr.)
Kenneth J. Killgore (James M. Watson, W. W. Clark, J. T. Williams)
A. F. King (E. M. Peacock, C. C. Lellers, C. L. Howell, C. C. Lilley)
Eugene P. Lane (C. D. Roemer, David E. Reed, R. W. Baltosser, R. A. Pohly)
Helmut Linsser (George Brinchkmeier, Alfred Schleusener, Otto Rosenback, Dr. W. Zettel)
Wayne H. Mack (R. N. Gsell, J. A. Lester, W. S. Hawes, C. D. Smith)

M. H. Morsi (James B. Meadours, Winston H. Schulte, John R. Locke)
John H. Oberwortmann (S. E. Giulio, W. H. Dawson, W. E. Martin, S. R. Marsh)
E. S. O'Driscoll (Richard A. Pohly, Elmer W. Ellsworth, Norman S. Morrisey)
Wesley Pustejovsky (E. L. Greene, U. E. Neese, T. T. Pope, G. T. Crosby)
Herbert C. Robertson, Jr. (Lewis C. Foote, John H. Hoke, Justus V. Price, T. E. Dennis)
James M. Sanders (Stefan Von Croy, L. B. Tromble, R. H. Glover, D. F. Jewell)
Edwin K. Simmons (O. K. Juller, Jr., A. A. Moore, Jr., D. B. Moore)
Bobby G. Turner (R. B. Cornell, R. M. Nugent, Evan Watts, James C. Eley)
William R. Woolner (W. Harlan Taylor, O. P. Gill, L. N. Ott)

APPLICATION FOR TRANSFER TO ACTIVE MEMBERSHIP

Patton Condren (C. M. Moore, J. L. Stephens, R. D. Everett, Sam Zimerman)
Wm. Duchscherer, Jr. (C. V. A. Pittman, E. C. Reagor, Wm. Ransone)
John A. Dunn (J. M. Watson, W. W. Clark, Marvin Romberg, J. T. Williams)
Ned E. Duval, Jr. (P. L. Terrasson, J. T. Hartman, Josiah Taylor, Richard C. Hilton)
Hugh Evans (E. L. Erickson, C. A. Wilner, S. M. Crawford, L. E. Whitehead)
Patrick J. Farrell (R. H. Wright, T. A. Halbrook, W. E. Dickson)
Maxwell O. Graham (Bryan A. Duby, Earl Hinson, Jr., S. R. Marsh, E. J. Laurent)
Vernon Frank Hinson (Walter J. Osterhoudt, C. A. Swartz, W. A. Meszaros, W. K. Hastings)
Joe H. Jones (Donald R. Oksa, A. C. Reid, James F. Johnson, S. T. Algermissen)
Barry W. Koch (C. C. Butler, James Divelbiss, Dupree McGrady, Frank Byrne)
D. G. Koppel (H. B. Peacock, R. F. Bennett, C. C. Sellers, Neal Clayton)
Robert M. Treacy (R. D. Holland, F. B. Wallis, R. F. Zimmerly)
John J. Wallace (J. A. Harris, J. E. MacGregor, R. E. Connelly, T. O. May)
Hartmut Arno Winkler (H. M. Houghton, H. O. Seigel, D. M. Wagg, R. K. Moyse)
T. Eugene Young (H. L. Thomsen, R. C. Kendall, J. M. Nash, F. R. Versaw)

PROPOSED AMENDMENTS OF THE SEG CONSTITUTION

The first group of amendments is:

Item 1 can be handled either of two ways. Perhaps the best method is to amend the Constitution by adding to Article XI, Section 4, the sentence:

"If a District Representative ceases to be a member of the Local Section he represented or is unable to perform his duties, the Executive Committee of the Local Section may appoint an Active or Honorary Member of the Society to fill the unexpired term."

And adding to Article XII, Section 2:

"If a Representative-at-large is unable to perform his duties, the Executive Committee may appoint an Active or Honorary Member of the Society to fill the unexpired term."

The second group of amendments is:

Article VI, Section 1

The first sentence to read:

"The officers of the society shall be a President, *a First Vice-President*, a Vice-President, a Secretary-Treasurer, and an Editor."

Article VII, Section 2

To read:

"The *First* Vice-President shall assume the office of President in case of a vacancy from any cause in that office and shall assume the duties of the President during the absence or disability of the latter. *The further line of succession is to Vice-President to Secretary-Treasurer to Editor.* (He shall also be responsible for all national meetings of the society.) (He) *The First Vice-President and the Vice-President* shall perform such (other) duties as may be delegated (to him) by the President *or the Executive Committee.*"

Article VIII, Section 3

Omit first sentence except for the words "The Secretary-Treasurer" and the word "the" at the start of second sentence.

Article IX, Section 1

To read:

"The Executive Committee shall consist of the President, *the First Vice-President*, the Vice President, the Secretary-Treasurer, the Editor, and the Past President."

The third group of amendments is:

After the first sentence of By-Laws Article IV, Section 2, add the sentence:

"In lieu of annual dues, an Active Member may make a single payment of two hundred dollars ($200.00) in full payment of his dues for life."

If this is done, it might be desirable to formalize the action that some past Executive Committees have taken of granting "Life" membership for meritorious service to SEG in cases where Honorary membership did not seem appropriate. This could be done by adding the following sentence:

"In case of exceptionally meritorious service to the Society, the Executive Committee may by unanimous vote remit the dues of any Active or Associate Member for life."

ANNOUNCEMENTS

RECENTLY ELECTED OFFICERS OF SEG

The new members of SEG's Executive Committee of 1958–1959 who were elected this past summer and who will assume their duties at the San Antonio Meeting are: Mr. E. V. McCollum of Tulsa, President; Mr. William M. Erdahl of Tulsa, Vice-President; and Mr. Robert Dyk of San Francisco, Secretary-Treasurer. Mr. O. C. Clifford, Jr., of Dallas will become the Past President; and Dr. Lawrence Y. Faust of Tulsa will continue as Editor through the coming year.

TWENTY-FIRST INTERNATIONAL GEOLOGICAL CONGRESS

Copies of the First Circular for the Twenty-First Session of the International Geological Congress to be held in August of 1960 in the Nordic Countries are now available and may be obtained on request from the American Geological Institute, 2101 Constitution Avenue, N.W., Washington 25, D. C. Those who request this First Circular will be placed on the mailing list to receive travel literature and other pertinent information.

NEW BUREAU OF STANDARDS PUBLICATION IN APPLIED MATHEMATICS

Integrals of Airy Functions, National Bureau of Standards Applied Mathematics Series 52, issued last May 15, 28 pages in length, is available from the Superintendent of Documents, U. S. Government Printing Office, Washington 25, D. C., at the price of 25 cents.

This pamphlet gives tables of integrals of the Airy function which are of basic importance in the asymptotic theory of linear ordinary differential equations containing a parameter. In particular, the tables provide approximate solutions to differential equations of the second order in the neighborhood of a turning point, and they are often needed in the evaluation of definite integrals by the method of stationary phase.

NEWLY REVISED BIBLIOGRAPHY OF GEOLOGY THESES

The Pruett Press of Boulder, Colorado, has announced the publication of a revised and up-to-date edition of *Bibliography of Theses in Geology*, a preliminary edition of which appeared in 1953. The new work was prepared by John Chronic, Associate Professor of Geology in the University of Colorado, and Halka Chronic, with the assistance of the Petroleum Research Corporation.

This bibliography includes descriptive titles of more than 11,000 theses prepared in the universities and colleges of the United States and Canada. Each entry also has the name of the author,

the date, and the university where the thesis is kept. There is an index classifying the theses by geographic location as well as by geologic time and subject matter.

PERSONAL ITEMS

Dr. WILLIAM SCHRIEVER, Professor of Physics in the University of Oklahoma, became the first Honorary Life Member of the Geophysical Society of Tulsa on April 17, 1958, at the opening session of the 11th Annual Midwestern Exploration Meeting which was held in Tulsa.

Due to a serious illness, Dr. Schriever was unable to attend the meeting and to accept the award and present his paper. The presentation of the award was made by Mr. FRANK SEARCY, President of the Geophysical Society of Tulsa, and Mr. V. L. JONES accepted it for Professor Schriever.

Dr. SYLVAIN J. PIRSON, Professor of Petroleum Engineering in the University of Texas, has spent the past summer giving lectures on oil reservoir engineering in France, England, and Italy.

Beginning in August, 1958, Dr. J. CL. DE BREMAECKER will be on leave from the Institute for Scientific Research in Central Africa, and he will spend one year on a research fellowship at the Dunbar Laboratory of Harvard University.

The Robert H. Ray Company of Houston has announced the appointment of Mr. WAYNE H. LEE as Geophysical Supervisor of its newly opened office in Bakersfield, California. Prior to his California assignment, Mr. Lee had been the company's Canadian supervisor since 1951. The company also announced the appointment of Mr. JESSE O. SIMS as the Seismic Supervisor of its newly opened district office in the Four Corners Area at Durango, Colorado. Mr. Sims has previously been the Ray Company's Seismic Supervisor in Pakistan and Houston.

Dr. VANNEVAR BUSH, Corporation Chairman of the Massachusetts Institute of Technology, has announced the appointment of Mr. CECIL H. GREEN as a term member of that corporation. Mr. Green, an alumnus of MIT, received his B.S. and M.S. degrees in Electrical Engineering there in 1924. He is Chairman of the Board of Geophysical Service Inc.

The Jersey Production Research Company has announced the appointments of Mr. WARREN A. ALEXANDER and Mr. STANLEY E. GIULIO as Research Associates in the Geophysical Research Division.

The Iraq Petroleum Company Ltd. and its associated companies have established an Exploration Headquarters office in Baghdad, Iraq. Attached to this office are Dr. C. E. THIEBAUD, Exploration Manager-Iraq and Mr. N. H. BANTA, Senior Geophysicist-Iraq.

Dr. GABOR DESSAU has terminated his two years' assignment with the Technion, Israel Institute of Technology, in Haifa, where he had been sent by UNESCO, for the establishment of a Mineral Engineering Department. He is now back in Italy and is Chargé de Cours in Mineral Deposits at the Geological Institute of the University of Pisa.

R. D. TOOLEY has completed his work for the Ph.D. at MIT and has accepted an appointment as Research Physicist with the California Research Corporation at its Oil Field Research Center in La Habra.

Dr. JAMES W. HIGGINS has been appointed Senior Research Geologist, Staff, and transferred to the San Francisco office of the California Research Corporation.

Dr. GERHARD HERZOG, Assistant General Manager of the Research and Technical Department of The Texas Company, is the patentee of a recently issued patent, U. S. 2,824,233, assigned to The Texas Company and directed to a method for cooling a well logging scintillometer. He has been awarded 79 patents in the field of exploration and production.

TWO LEADERS IN EXPLORATION

SEG President O. C. CLIFFORD, JR., is shown here talking with AAPG President GEORGE S. BUCHANAN at the 11th Annual Midwestern Exploration Meeting in Tulsa which the two presidents addressed.

Mr. R. B. PRATT has recently been named Vice-President of the Petty Geophysical Company of San Antonio. He is now in his 25th year with the firm.

Dr. J. A. PEOPLES, JR., has resigned his position as Chief, Terrestrial Sciences Laboratory, Geophysics Research Directorate, Air Force Cambridge Research Center, and has accepted an appointment as Associate Professor in the Geology Department of the University of Kansas at Lawrence, Kansas. He will teach and do research in geophysics.

Mr. LESTER W. LOUDER is now Vice-President, Manager, of Geofisicos Asociados Internacionales C.A. His address is Apartado Chacao 4196, Caracas, Venezuela.

Mr. FRED J. AGNICH, President of Geophysical Service Inc., has announced the appointment of Mr. PIERSON M. RALPH as the company's Personnel Director. Dr. MARK K. SMITH, the Research Director of Geophysical Service Inc., has announced that Dr. MILO M. BACKUS has been named

FIRST RECIPIENTS OF THE CECIL H. GREEN MEDAL

At the 84th Commencement of the Colorado School of Mines on last May 23, Mr. CECIL H. GREEN of Dallas presented gold medals to the first two recipients of the prize which he has recently established there for graduates in geophysical engineering. Shown here (left to right) are DONALD G. JOHNSON, of the Class of 1957, Mr. GREEN, and ROBERT H. HAMILTON, of the Class of 1958. In 1953, for his work in promoting research and education in the earth sciences, this institution conferred on Mr. Green the honorary degree of Doctor of Engineering.

Chief Research Geophysicist and that Mr. FRED A. BROCK has been appointed Chief Research Engineer.

Mr. VICTOR V. GRAF, former Manager of Research, Engineering and Supply for the Seismograph Service Limited in England, has been appointed Assistant to the President of the Seismograph Service Corporation.

Mr. KENNIS WITT GILBERT has been named District Geophysicist of the Pan American Petroleum Corporation's Lubbock District. He has been with the company since 1950 and has held various geophysical positions in San Angelo and Midland.

Mr. J. RYAN WALKER has opened his office at 554 Broadmoor Boulevard, Shreveport, Louisiana, for geophysical consultation. He is specializing in seismic interpretation and crew supervision.

MR. WALTER E. HEINRICHS, JR., has announced the formation of the Heinrichs Geoexploration

Company of which he is the President. The new company is offering consulting and contracting service in mineral engineering. Its offices are located at 806-808 West Grant Road, Tucson, Arizona.

Mr. GEORGE C. HOWARD, formerly Executive Vice-President of Georesearch Inc., has been appointed the Director of Exploration for the Titan-Tex Drilling and Production Corporation of Shreveport, Louisiana.

Mr. ROGER H. PEMBERTON has been appointed Senior Technical Representative to the Mining Industry for Canadian Aero Service Limited. His offices are at 347 Bay Street, Toronto.

CSEG'S 6TH ANNUAL "DOODLEBUG" GOLF TOURNAMENT

Under the able guidance of Mr. ROBERT A. BOULWARE, Chairman of the Tournament Committee, the 6th Annual "Doodlebug" Golf Tournament was voted by the 160 odd participants the most successful held to date.

Sponsored by the Canadian Society of Exploration Geophysicists, the tournament, held at the Banff Springs Hotel Golf Course, Banff, Alberta, on September 6–8, saw Mr. DOUG DRYSDALE of the Texaco Exploration Company come up Winner of the "Doodlebug" (Championship) Flight. Runner-up was Mr. VIC FAMILINOW of Colorado Oil & Gas Limited. All flights were keenly contested and some very fine scores were turned in.

A special event, held last year for the first time and repeated again this year, was the prize of a Cadillac to any participant scoring a "hole in one" on the famous 9th hole (The Cauldron). Although no player was successful, several near misses caused a great deal of excitement and interest.

A bridge tea on Saturday and a scenic boat ride on Sunday was well patronized by the ladies.

A cocktail party, an excellent stage show put on by the hotel orchestra, and a windup buffet dinner provided well organized added entertainment.

Mr. FRANCIS A. HALE, President of the CSEG presented prizes to all flight winners and runners-up.

Tournament Winners. Left to right, Mr. VIC FAMILINOW, Runner-up, Championship Flight Mr. DOUG DRYSDALE, Winner, Championship Flight; Mr. D. K. SEAMAN, Winner, Consolation Championship Flight; Mr. ALEX FRAME, Runner-up, Consolation Championship Flight.

CALENDAR OF MEETINGS

1958

October

13–16 Society of Exploration Geophysicists, 28th Annual International Meeting, Hotel Gunter, San Antonio (Weldon L. Crawford, General Chairman, Motex Oil Company, Drawer 2061, San Antonio, Texas)

22–24 American Association of Petroleum Geologists, Southwest Regional Meeting, City Auditorium, Mineral Wells, Texas

November

1–21 First Arab Petroleum Congress and Exhibition, Cairo, Egypt. (Sponsored by the Secretariat General of the Arab League. Reference: Research and Translations Office, P.O. Box 1224, Beirut, Lebanon)

6–7 American Association of Petroleum Geologists, Pacific Section Annual Meeting, Los Angeles

1959

February

15–19 American Institute of Mining, Metallurgical, and Petroleum Engineers, Inc., Annual Meeting, San Francisco

March

16–19 American Association of Petroleum Geologists—Society of Economic Paleontologists and Mineralogists, National Convention, Memorial Auditorium, Dallas

October

28–30 American Association of Petroleum Geologists, Mid-Continent Regional Meeting, Broadview Hotel, Wichita, Kansas

November

9–12 Society of Exploration Geophysicists, 29th Annual International Meeting, Biltmore Hotel, Los Angeles (Flint H. Agee, General Chairman, United Geophysical Corporation, 1200 South Marengo Avenue, Pasadena 15, California)

1960

November

7–10 Society of Exploration Geophysicists, 30th Annual International Meeting, Moody Convention Center, Galveston (Walter B. Lee, Jr., General Chairman, Gulf Oil Corporation, Drawer 2100, Houston 1, Texas)

1961

November

5–9 Society of Exploration Geophysicists, 31st Annual International Meeting, Denver (Colin C. Campbell, Box 1536, Tulsa 1, Oklahoma)

1962

September

17–20 Society of Exploration Geophysicists, 32nd Annual International Meeting, Calgary, Alberta (Colin C. Campbell, Box 1536, Tulsa 1, Oklahoma)

* * * * *

July 1, 1957 to December 31, 1958

International Geophysical Year (Worldwide) *vide* GEOPHYSICS, v. 21, p. 257–259, and v. 21, p. 681–690 (H. Odishaw, National Academy of Sciences, Washington 25, D.C.)

PROFESSIONAL DIRECTORY

CALIFORNIA

H. WAYNE HOYLMAN
Consultant
Petroleum and Mining Exploration
Aerogeophysics Company — 816 W. 5th St.
Mutual 6428 — Los Angeles 17, Calif.

L. F. IVANHOE
Consulting Geologist and Geophysicist
Domestic and Foreign Exploration
Phone: FA 50283 — 2810 Elmwood Avenue
Cable: IVANHOE — BAKERSFIELD, CALIFORNIA

CURTIS H. JOHNSON
Geophysical Consultant
Domestic & Foreign
816 WEST FIFTH ST. LOS ANGELES 17, CALIFORNIA
Phone: MAdison 6-0020

WILLIAM CROWE KELLOGG
Geological Engineer
Kellogg Exploration Company
Geologists — Geophysicists
Electrical — Magnetic — Gravity — Radioactivity
Air-Ground Surveys Interpretation
3301 NORTH MARENGO ALTADENA, CALIFORNIA

HENRY SALVATORI
Western Geophysical Company of America
1116 Pacific Mutual Bldg.
523 W. 6th Street
LOS ANGELES 14, CALIFORNIA

JOSHUA L. SOSKE
Geologist and Geophysicists
SCHOOL OF MINERAL SCIENCES
Stanford University
STANFORD, CALIFORNIA

CALIFORNIA

ELLIOTT SWEET
Gravity Meter Surveys
Gravity and Seismic Interpretation
SWEET GEOPHYSICAL CO.
21544 Rambla Vista Drive
MALIBU, CALIFORNIA

GEO. SHUMWAY
GEOLOGICAL DIVING CONSULTANTS, INC.
Underwater studies of bedrock and sediments
P.O. Box 6571 — San Diego 6, California

COLORADO

Milt Collum — Wes Morgan
PETROLEUM GEOPHYSICAL COMPANY
Contract Seismograph Crews
Seismic Review and Interpretations
Rocky Mountain Area
KEystone 4-0253
620 19th Street — Denver 2, Colorado

KANSAS

CHARLES C. (RUSTY) WILLIAMS
Geologist-Geophysicist
Williams Seismograph, Inc.
252 South Green Street
WICHITA, KANSAS

LOUISIANA

CARL L. BRYAN
Consulting Geophysicist-Geologist
804 Texas Eastern Bldg. — Telephone
SHREVEPORT, LA. — 5-1924

MISSISSIPPI

EWIN D. GABY
Delta Exploration Company
Jackson — Mississippi

MISSOURI

LEROY SCHARON
Mining and Engineering Geophysics
567 Brookhaven Court
Kirkwood 22 Phone
St. Louis, Missouri KIrkwood 1578-W

NEW YORK

ROLAND F. BEERS
ROLAND F. BEERS, INC.
Petroleum and Minerals Exploration Consultants
Ground and Airborne Surveys
Data Reduction and Analysis
P.O. Box 1019 Troy, New York
Ashley 2-6478; 2-2351

OKLAHOMA

THOMAS J. BEVAN
Geophysicist
914 American Airlines Bldg. Phone CHerry 2-7508
TULSA 3, OKLAHOMA

ARNOLD H. BLEYBERG
Petroleum Exploration Consultant
Domestic & Foreign Services
MID-AMERICA BANK BLDG.
OKLAHOMA CITY 2, OKLA. PH.: CENTRAL 2-0913

JULIAN M. BUSBY
Geological Engineer—Geophysicist
SPECIALIZING IN MAGNETICS
OKMULGEE, OKLAHOMA
529 COMMERCE BLDG. PHONE 2568

OPIE DIMMICK
Century Geophysical Corp.
Tulsa, Oklahoma Phone 5-7111

R. W. DUDLEY
Oil Exploration Consultant
Geologist *Geophysicist*
608 First National Bldg. Telephone FOrest 5-5255
OKLAHOMA CITY 2, OKLAHOMA

OKLAHOMA

CRAIG FERRIS
Geophysicist
E. V. McCollum & Co. GeoSeis, Inc.
515 Thompson Bldg.
TULSA 3, OKLA.

TOM D. MAYES
Mayes-Bevan Co.
Gravity Meter Surveys
and Interpretations
305 Kennedy Building
TULSA, OKLAHOMA

E. V. McCOLLUM
Geophysicist
E. V. McCollum & Co.
515 Thompson Building
TULSA, OKLAHOMA

GLENN M. McGUCKIN
Seismograph Consultant
Data Interpretation Current Supervision
SALES: McGUCKIN (Patented) SEISMOGRAPH
SECTION PLOTTER (DIP MIGRATOR)
23 Years Experience:
Supervising, Contracting, Consulting
Phone JEfferson 4-0853 1304 Ann Arbor
NORMAN, OKLA.

RICHARD A. POHLY
Gravity Surveys and Re-interpretation
POHLY EXPLORATION COMPANY
1135 E. 38th St. RIverside 2-2009
TULSA 5, OKLAHOMA

BEN F. RUMMERFIELD
Geologist and Geophysicist
CENTURY GEOPHYSICAL CORPORATION
503 Jenkins Building 1105 7th Ave., W.
Tulsa 3, Okfahoma Calgary, Alberta

JOHN J. RUPNIK
RUPNIK AND BALLOU
Petroleum Exploration Consultants
GEOPHYSICAL & GEOLOGICAL COORDINATION
1102 HUNT BLDG., TULSA 3, OKLAHOMA
LUther 7-2435

OKLAHOMA

HUGH M. THRALLS
Consulting Geophysicist
Box 9577 GIbson 7-3921
TULSA, OKLAHOMA

PENNSYLVANIA

W. B. AGOCS
Geophysical Consultant
Aero Service Corp.
236 E. Courtland
PHILADELPHIA 20, PENNSYLVANIA

TEXAS

JOHN F. ANDERSON
ANDERSON & COOKE
Oil Exploration Consultants
Geological Consulting
Seismic Surveys & Interpretations
665 San Jacinto Bldg. Houston 2, Texas

WALTER D. BAIRD
Consulting Geophysicist
NEIL P. ANDERSON BUILDING
PHONE EDison 6-8400 FORT WORTH 2, TEXAS

KEITH R. BEEMAN
Electronic Consultant
Seismograph and Allied Equipment
P.O. Box 13058
Houston, Texas

JOHN L. BIBLE
Southern Geophysical Company
Seismic—Gravity—Magnetics
3339 N. Rice Ave. Houston, Texas

HART BROWN
Brown Geophysical Company
Gravity-Meter-Surveys
Interpretations
5300 Brownway Rd. Houston 19, Texas

TEXAS

JOHN W. BYERS
Byers Exploration Company
Seismic, Gravity and Magnetic Surveys
709 M. & M. Building Phone
HOUSTON, TEXAS CApitol 4-2425

R. A. CRAIN
Texas Seismograph Company
Panhandle Building
WICHITA FALLS, TEXAS

PAUL D. CRAWFORD
Askania Magnetometer
Surveys
1421 Milam Bldg. San Antonio, Texas

R. H. DANA
Dana Explorations, Inc.
1301 W. T. Waggoner Bldg.
Fort Worth, Texas

PAUL FARREN
Geophysical Consultant
Specializing in Seismic Interpretation,
Review, and Supervision
1528 Bank of the Southwest
HOUSTON 2, TEXAS FA 3-1356

L. F. FISCHER
Exploration Consultant
Geophysicist
Geologist
621-A City National Bank Bldg. Houston, Texas

J. F. FREEL
RESEARCH EXPLORATIONS, INC.
5134 Westheimer Road
Houston, Texas

TEXAS

E. JOE SHIMEK — LLOYD PAITSON

GEOPHYSICAL ASSOCIATES

P.O. Box 6005 — Houston 6, Texas

Seismic

JOHN A. GILLIN

National Geophysical Company

8800 Lemmon Avenue

Dallas 9, Texas

IRVING M. GRIFFIN, JR.

Consultant in
Seismic Review and Interpretation
and
Field Crew Supervision

FAirfax 3-9111 — 1331 Esperson Bldg.
JAckson 2-4558 — Houston 2, Texas

T. I. HARKINS

Independent Exploration Company

1973 West Gray
P.O. Box 13237
Houston 19, Texas

J. G. HARRELL

Mid-Continent Geophysical Co.

Contract Seismograph Crews
Seismic-Reinterpretations

2509 West Berry — Fort Worth, Texas

SIDON HARRIS

Southern Geophysical Company

6640 Camp Bowie Blvd. — Fort Worth, Texas

J. O. HOARD

HOARD EXPLORATION COMPANY

Esperson Building — Houston, Texas

TEXAS

W. B. HOGG

Geophysical Consultant

1915 Adolphus Town Bldg.
DALLAS 1, TEXAS

LEO HORVITZ

Geochemical Prospecting

Horvitz Research Laboratories
3217 Milam Street
HOUSTON, TEXAS

JOHN S. IVY

Niels Esperson Building

HOUSTON, TEXAS

J. C. KARCHER

Geophysicist

Adolphus Tower
DALLAS, TEXAS

MARTIN C. KELSEY

Rayflex Exploration Company

6923 Snider Plaza — Dallas 5, Texas

H. KLAUS

Geologist and Geophysicist

Klaus Exploration Company
Gravimetric and Magnetic Surveys
and Interpretations

P.O. Box 1617 — Lubbock, Texas

PAUL H. LEDYARD

Mid-Continent Geophysical Co.

Contract Seismograph Crews
Seismic-Reinterpretations

2509 West Berry — Fort Worth, Texas

TEXAS

C. T. MacALLISTER
Geophysical Consultant
Seismic Interpretations and Field Supervision
6327 Vanderbilt, Houston 5, Texas — Telehpone: MA 3-4181

HAYDON W. McDONNOLD
Geologist & Geophysicist
Keystone Exploration Company
2813 Westheimer Road
HOUSTON, TEXAS

A. E. "SANDY" McKAY
Geologist and Geophysicist
Continental Geophysical Co.
FORT WORTH, TEXAS
2111 Continental Life Bldg. Phone EDison 2-9231

GEORGE D. MITCHELL, JR.
Geologist and Geophysicist
911 Mercantile Securities Bldg. Dallas, Texas

P. E. NARVARTE
Consulting Geophysicist
Seismic Interpretations
Current Supervision and Review
Frost National Bank Building
San Antonio, Texas

L. L. NETTLETON
Gravity Meter Exploration Co.
Interpretation of Gravity Surveys
Interpretation of Aeromagnetic Surveys
340 M. Esperson Bldg.
HOUSTON 2, TEXAS

W. W. (IKE) NEWTON
Geophysicist
823 Corrigan Tower
DALLAS, TEXAS

TEXAS

J. O. PARR, JR.
Consulting Geophysicist
Methods & Instrumentation
for
Seismic & Radiometric Surveys
202 Janis Rae — San Antonio, Tex.

C. W. PAYNE
Payne & Warren
Geophysical Consultants
2210 Continental Life Bldg.
Fort Worth — TEXAS

H. B. PEACOCK
Consulting Geophysicist
8400 Westchester
DALLAS 25, TEXAS

J. C. POLLARD
GEOPHYSICAL ENGINEERING
●
SEISMIC . . . GRAVITY . . . MAGNETIC SURVEYS
●
2500 Bolsover Rd., P.O. Box 6557, Houston 5, Tex.

ROBERT H. RAY
GEOPHYSICAL ENGINEERING
●
SEISMIC . . . GRAVITY . . . MAGNETIC SURVEYS
●
2500 Bolsover Rd., P.O. Box 6557, Houston 5, Tex.

SAM D. ROGERS
Rogers Geophysical Company
Rogers Explorations, Sociedad Anonima
3616 West Alabama — Houston 6, Texas

C. WHITNEY SANDERS
Consulting
Petroleum Geologist-Geophysicist
U. S. and European Exploration
1132 Bank of the Southwest Building
HOUSTON 2, TEXAS

TEXAS

RAYMOND L. SARGENT
Magnetometer Surveys
Interpretations
M & M Bldg.
HOUSTON 2, TEXAS

SIDNEY SCHAFER AND COMPANY
Geophysicists and Geologists
EXPLORATION CONSULTANTS
Domestic and Foreign
Sidney Schafer — 2200 Welch Avenue
Jack C. Weyand — Houston 19, Texas

HUBERT L. SCHIFLETT
States Exploration Company
Seismic, Gravity and Magnetic Surveys
5313 Richmond Road — Highway 75 North
HOUSTON, TEXAS — SHERMAN, TEXAS

H. B. SMYRL
Portable Seismograph, Inc.
706 Frost National Bank Bldg.
San Antonio 5, Texas

NELSON C. STEENLAND
Gravity Meter Exploration Company
Geophysicist
340 Mellie Esperson Building — Houston, Texas

R. C. SWEET
Geophysicist
1111 Bering Dr. — Houston, Texas

R. MAURICE TRIPP
Oil and Mineral Exploration Research
3525 Beverly Drive — Dallas, Texas

TEXAS

F. RITCHIE WALLACE
Geophysical Consultant
701 Polk — Off. FAirfax 3-7719
Houston 2, Texas — Res. MOhawk 5-5542

KIRBY J. WARREN
Payne & Warren
Geophysical Consultants
2210 Continental Life Bldg.
Fort Worth — Texas

E. DARRELL WILLIAMS
Geophysicist
Specializing in Radiometric Exploration for Oil
3114 PRESCOTT ST., HOUSTON 25, TEXAS
PHONE MA 3-3991

JOHN H. WILSON
Exploration Consultant
1201 Sinclair Bldg.
FORT WORTH, TEXAS

CHARLES C. ZIMMERMAN
Geologist & Geophysicist
Keystone Exploration Company
2813 Westheimer Road
HOUSTON, TEXAS

WYOMING

Exploration Geology — Seismic Reviews
Evalutions — Seismic Supervision
JOHN F. PARTRIDGE, JR.
Consulting Geologist—Geophysicist
P.O. Box 258 — Room 211 O-S Building
Phones 2-6485 and 2-3328 CASPER, WYOMING

CANADA

R. E. DAVIS
Farney Exploration Company, Ltd.
830-8th Avenue West
CALGARY, Alberta, Canada

Please mention GEOPHYSICS when answering advertisers

CANADA

JOHN O. GALLOWAY

Petroleum Consultant

627 8th Ave., W. Calgary, Alberta

THEODORE KOULOMZINE

Geologist & Geophysicist

Koulomzine, Geoffroy & Co.

P.O. Box 870

VAL D'OR Que. Canada.

LUNDBERG EXPLORATIONS LIMITED

Consulting Geologists and Geophysicists

Specialty—Airborne, Radiation, Electrical & Magnetic Surveys

96 Eglinton Avenue E.
Toronto 12, Canada

CANADA

D. BRUCE McDOUGALL

Geophysicist

201 OIL EXCHANGE BLDG. CALGARY, CANADA

GEORGE W. SANDER

Consulting Geophysicist

174 Douglas Ave. N., Oakville, Ontario Phone VIctor 4-6345

DR. W. F. STACKLER

Consulting Geophysicist

Phone 447303
1937 25th Avenue S.W.
CALGARY, ALBERTA

- **TURNKEY OPERATION—includes trailers, personnel and supplies.**
- **Specialists in trailers built for use abroad.**
- **Check our foreign lease plan.**

Complete Trailer Camps

for your field crew. Kitchen trailers, diners, showers, offices, sleepers, power plants, water tank and gasoline trailers.

ELDER TRAILER and BODY, INC. 4830 Race • Denver, Colorado
Phone: AMherst 6-1781

For Better Seismograph Service

TEXAS SEISMOGRAPH CO.

PANHANDLE BLDG. WICHITA FALLS, TEXAS

Review of Scientific Instruments

Since 1923, the leading publication in the field of scientific instrumentation. Over 1,000 pages annually of the latest original research material on new instruments for measurement and control. Written and edited by experts, the "Review" is the most widely quoted and referenced publication in its field. Indexed annually by subject. Circuits, computers, counters, electrical measurement, laboratory techniques, mechanics, microwaves, nuclear machines, vacuum techniques, X-Ray diffraction, many others. Over 88 subjects covered. Annually, 12 issues, $9.00. Single copy, $1.25

AMERICAN INSTITUTE OF PHYSICS

335 East 45 Street New York 17, N.Y.

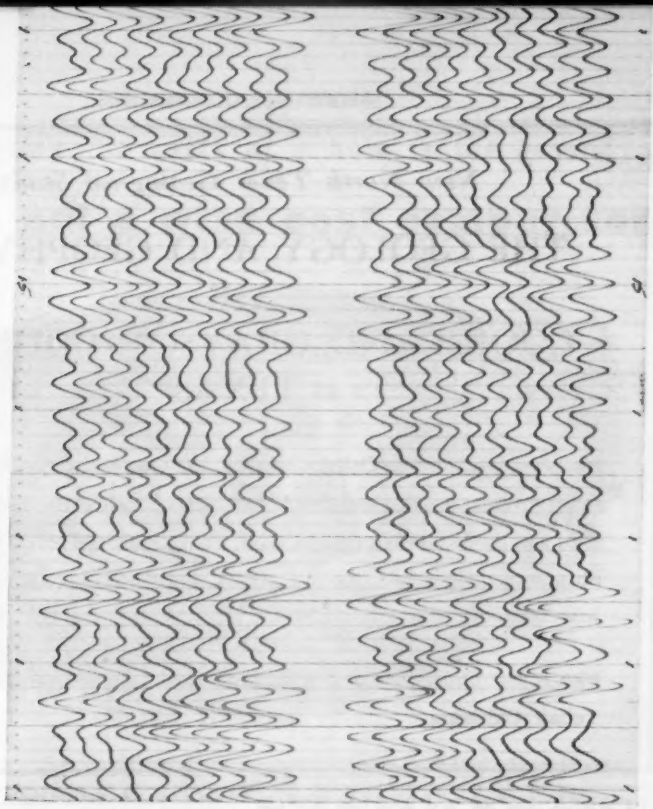

For easy-to-read records . . .
use Kodak Linagraph 480 Paper

In seismic recording your essential need is for clean, easy-to-read records.

Kodak Linagraph 480 Paper gives you what you need. Traces are sharp, strong blacks against clean whites. And with Linagraph 480 you get these results consistently under the wide range of field conditions you meet in prospecting.

The paper comes to you in metal slip-cover cans that effectively guard against moisture and damage.

Your Kodak dealer can supply all your needs for Kodak Linagraph Papers and Chemicals. Keep in touch with him.

The new booklet "Kodak Materials for Geophysical Exploration" gives you complete information on Kodak Linagraph Materials. See your Kodak dealer.

EASTMAN KODAK COMPANY, Rochester 4, N. Y.

Kodak

New North Texas Geological Study

THE GEOLOGY AND GEOPHYSICS OF COOKE AND GRAYSON COUNTIES TEXAS

Published jointly by the Dallas Geological and Geophysical Societies, a 200-page report covering regional geology and tectonics, a history of the discovery, development and production of principal fields, stratigraphic and sedimentary characteristics, core analysis data, regional gravity, and the application of the reflection seismograph.

PRICE $10. Order from Society of Exploration Geophysicists, P. O. Box 1536, Tulsa 1, Oklahoma.

INSTRUMENT FABRICATION

To Your Specifications for:

EXPLORATION EQUIPMENT
LOGGING EQUIPMENT

. . . by experienced craftsmen and fabrication engineers

CUSTOM FABRICATION CORPORATION

2711 Dawson Road — Tulsa, Oklahoma
P.O. Box 3391, Whittier Station — Madison 6-6716

Issued Feb. 1956

FIFTIETH ANNIVERSARY
Economic Geology
1905-1955
(in two parts)

This publication comprises some 24 review papers by specialists in their fields, on wide phases of economic geology, including ore deposits and ore genesis, sedimentary deposits of rare metals, uranium deposition, coal petrology, time of oil and gas accumulation, oxidation of copper sulphides and secondary sulphide enrichment, pegmatite deposits, carbonate mineralogy of limestones and dolomites, engineering geology, influence of geological factors on the engineering properties of sediments, geochemistry and geophysics in prospecting, hydrothermal deposits, metallogenetic epochs and provinces, mineral synthesis, geologic thermometry, developments in clay mineralogy and technology, temperature in and near intrusions, and other important topics of interest to the professions of geology, mining and engineering. All of the authors are specialists in their field, and present a critical and stimulating review of the literature.

Price to Subscribers (including members, non-member Journal subscribers, and students whether subscribers or not) $6.00
Price to Non-Subscribers to Journal 8.00

Order from: Economic Geology Publishing Company
105 Natural Resources Building
Urbana, Illinois

When measuring the costs of a hole in the ground...

Price is not a wise cost comparison

"Blue Demon" Bit performance gives proven cost reduction

U.S. Patents
2,615,684 & 2,666,622 —
Others Pending

FIGURING bit cost on the price of the bit does not give a true cost comparison, since a number of variables are involved . . . rate of penetration, footage per bit, round trips required, bit service and finally bit cost per foot of hole drilled.

Hawthorne's "Blue Demon" Carbide Insert Rock Bit has become the leading all-formation drill bit in the exploration industry . . . used by more drillers than all other drag-type bits combined.

These field-proved replaceable blades, with superior inserts on the self-sharpening cutting edges, give faster, smoother penetration in hard formations . . . drilling from top to bottom without tripping between soft and hard formations.

Ample stocks of popular bit sizes are maintained in every active exploration area to give you prompt, low-cost on-the-drill bit service, and experienced field service engineers will help you with your special drilling problems.

Drill more footage faster, smoother with long-lasting "Blue Demon" Bits, and cut your cost per foot of hole.

WRITE FOR ILLUSTRATED CATALOG.

HERB J. HAWTHORNE INC.

P. O. BOX 7366, HOUSTON 8, TEXAS

Seismic Engineering COMPANY

ENGINEERED SEISMIC SURVEYS

6111 MAPLE AVENUE • DALLAS • TEXAS

R. D. Arnett C. G. McBurney J. H. Pernell

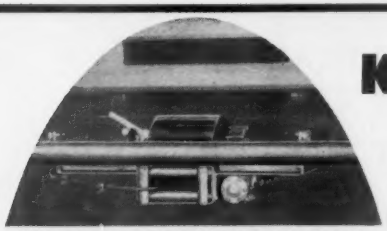

Model A-11 King Winch on A-120 (4x4) all-wheel-drive International truck.*

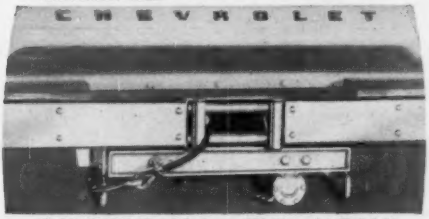

Model CD-8116 King Winch on 1958 Chevrolet Model 31 (4x4).

Model 151J King Winch on Willys Jeep.

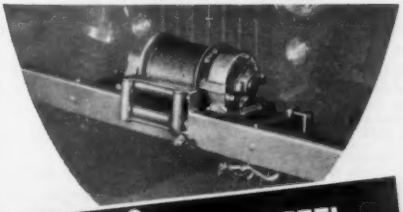

KING WINCHES

. . . for Willys, International, Chevrolet, GMC, Ford, Land Rover and other vehicles

COMPLETE, READY-TO-INSTALL KING FRONT-MOUNT WINCH ASSEMBLIES FEATURE:

- winch side arms to reinforce truck frame
- bronze-bushed, 4-way cable guide rollers
- cable drum guard
- heavy-duty pipe bumper
- needle-bearing, universal-joint spline-shaft drive assembly
- Timken bearings on worm

King Winches keep you moving through the most difficult terrain . . . you get action where there's no traction with dependable pulling power. King power winches have pulling capacities of 8,000 to 19,000 lbs.

* *King Winches for International trucks are available through International-Harvester dealers.*

Koenig ALL-STEEL CABS FOR JEEPS

FULL AND HALF CABS

Koenig Jeep cabs and King Winches for Willys vehicles are available through Willys Motors, Inc., and Willys-Overland Export Corp. distributors or dealers. Write for free descriptive literature.

Full Cab and Model 151J King Winch Illustrated.

KOENIG ALL-STEEL CABS HAVE THESE SUPERIOR FEATURES:

- PROTECTION
- SAFETY
- COMFORT
- CONVENIENCE

Roll-down windows, full opening . . . full panel-board head lining and masonite door lining . . . safety glass throughout . . . all-steel welded construction . . . door locks.

Koenig

IRON WORKS, Inc.

P. O. BOX 7728 HOUSTON 7, TEXAS

AVAILABLE PUBLICATIONS OF

The American Association of Petroleum Geologists

1947	**Comprehensive Index of the Publications of the A.A.P.G., 1917-1945.** Compiled by Daisy Winifred Heath. 603 pp. 6.75 x 9.50 inches. Cloth. **To members, $3.00**	4.00
1957	**Comprehensive Index of Publications of the A.A.P.G., 1946-1955.** Compiled by Daisy Winifred Heath and June McFarland. 302 pp., 6.75 x 9.50 inches. Cloth. **To members, $3.00**	4.00
	Both Indexes at once, covering all Association publications, 1917-1955 at special price. **To members, $5.00**	7.00
1948	**Structure of Typical American Oil Fields.** Vol. III. McCoy Memorial Volume. 24 papers. 516 pp. 219 illus. Cloth. **To members, $3.50**	4.50
1948	**Appalachian Basin Ordovician Symposium.** From August, 1948, *Bulletin*. 264 pp. 72 illus. 6 x 9 inches. Cloth. **To members, $1.50**	2.00
1949	**Possible Future Oil Provinces of the United States and Canada.** 4th printing. From August, 1941, *Bulletin*. 154 pp., 83 figs. 6 x 9 inches. Paper. **To members, $1.00**	1.50
1949	**Problems of Petroleum Geology. 2d printing.** Originally published, 1934. 43 papers. 1,073 pp. 200 illus. 5.75 x 8.5 inches. Cloth. **To members, $4.00**	5.00
1951	**Possible Future Petroleum Provinces of North America.** From February, 1951, *Bulletin*. 360 pp., 153 figs. 6 x 9 inches. Cloth. **To members, $2.50**	4.00
1954	**Geological Cross Section of Paleozoic Rocks: Central Mississippi to Northern Michigan.** Prepared under auspices of Geologic Names and Correlations Committee. 5 cross sections, vertical scale 500 feet to the inch. 29 pp. of explanatory text, index. 8 x 10 inches. Pressboard, sections folded in pocket. **To members, $2.00**	2.50
1955	**Miocene Stratigraphy of California (1938).** By Robert M. Kleinpell. 450 pp., 14 figs., 22 pls., 18 tables. Offset reprinted. 5.5 x 8.5 inches. Cloth. **To members, $4.50**	5.00
1955	**Stratigraphic Type Oil Fields (1941).** 37 papers. 902 pp., 304 figs., 3 pls. Offset reprinted. 5.5 x 8.5 inches. Cloth. **To members, $4.50**	5.00
1956	**Petroleum Geology of Southern Oklahoma.** 24 articles. 402 pp., 110 figs., 6 pls., 27 tables. 6.75 x 9.5 inches. Cloth. **To members, $5.00**	6.00
1957	**Structure of Typical American Oil Fields.** Vol. I (1929). 4th printing. 510 pp., 190 illus. 5½ x 8½ inches. Cloth. **To members $4.00**	4.50
1957	**Structure of Typical American Oil Fields.** Vol. II (1929). 4th printing. 750 pp., 235 illus., 5½ x 8½ inches. Cloth. **To members $5.00**	5.50
1957	**Geology of California (1933).** By R. D. Reed. 355 pp., 58 figs., 26 tables. **Structural Evolution of Southern California (1936).** By R. D. Reed and J. S. Hollister. 157 pp., 57 figs., 14 photographs, 9-color tectonic map. Both offset reprinted. 2d printing. 5½ x 8½ inches. Clothbound together. **To members $6.00**	6.50
1957	**Western Canada Sedimentary Basin. Rutherford Memorial Volume.** Edited by Leslie M. Clark (1954). 30 papers. 521 pp. 2d printing. **Stratigraphy of Plains of Southern Alberta. Dowling Memorial Volume (1931).** A symposium. 14 papers. 166 pp. 2d printing, by offset. 6¼ x 9½ inches. Clothbound together. **To members $6.00**	6.50
1958	**Jurassic and Carboniferous of Western Canada. Allan Memorial Volume.** Edited by A. J. Goodman. 24 papers. 514 pp. Cloth. **To members $6.00**	6.50
1958	**Habitat of Oil.** Edited by Lewis G. Weeks. 1,364 pp., cloth bound. 56 papers on oil occurrence—20 on North America; 5 on South America; 7 on Europe; 5 on Middle East; 4 on Far East; 9 topical papers on oil occurrence and migration, hydrocarbons, and basin development; and an analysis by the Editor. **To members $9.00**	11.00

Bulletin of The American Association of Petroleum Geologists. Official monthly publication. Each number, approximately 150 pages of articles, maps, discussions, reviews. Annual subscription, **$18.00** (outside United States, **$19.00**). Descriptive price list of back numbers on request.

(Prices, postpaid. Write for discount to colleges and public libraries.)

THE AMERICAN ASSOCIATION OF PETROLEUM GEOLOGISTS

BOX 979, TULSA 1, OKLAHOMA, U.S.A.

Information to *complete* the sub-surface picture

The SIE MS-12 **Geo**physical **Data** (GeoData) Processing System, makes the handling of magnetically recorded sub-surface information economically practical. **GeoData** equipment presents **all** of the geophysical information acquired with modern wide-band seismic techniques, in geologically oriented form at half the instrumentation cost of early laboratory systems!

Magnetic recordings are sequentially processed in the MS-12, and presented on a pen-written record, ready for interpretation. Up to 15 recordings can be processed in one hour by one operator . . . an important reduction in exploration cost. To get the **complete** sub-surface picture, make certain SIE **GeoData** equipment is part of your geophysical exploration program.

SIE

SOUTHWESTERN INDUSTRIAL ELECTRONICS COMPANY

2831 Post Oak Road • P. O. Box 13058 • Houston 19, Texas

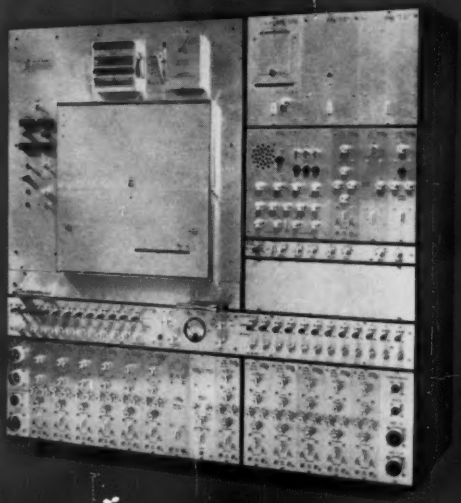

SIE MS-15 MAGNETIC-SEISMIC FIELD RECORDING SYSTEM

...a completely unitized FM installation for use in any field location.

The MS-15 Magnetic Seismic Field Recording System is a completely new and economical "one-package" unit for magnetic recording and monitoring in the field. All of the high fidelity advantages of the time proven frequency modulation method are obtained at the same cost as AM instruments. The unique "one-package" design of the MS-15 eliminates interconnecting cabling, providing dependability characteristics so necessary in a field system.

Twenty-four broad-band, linear phase shift seismic amplifier-FM modulator combination channels are specifically designed for magnetic recording to take advantage of the inherent qualities of the famous standard SIE tapes. Bridged-T hi-line filters are available. The twenty-four seismic data channels and four voice or data channels can be played back through an SIE GA-3 or GA-85 seismic amplifier sequentially and displayed on a monitor screen to verify record quality. Either pen or electro-stylus reproducing methods are available, and no photographic processing processes are required. A dry reproduction of the seismic recording is available only 2½ minutes after the shot is fired. The system is packaged in one sturdy unit and since no darkroom and developing facilities are required, the MS-15 is easily installed as a portable recording unit and transported in a small pickup truck or marsh vehicle.

In every characteristic—FM high-fidelity, dependability and ease of maintenance, operating convenience and flexibility, the MS-15 establishes the standards which have made SIE geophysical instrumentation THE STANDARD OF THE INDUSTRY.

SOUTHWESTERN INDUSTRIAL ELECTRONICS CO.

2031 Post Oak Road • P.O. Box 13058 • Houston 19, Texas

SIE

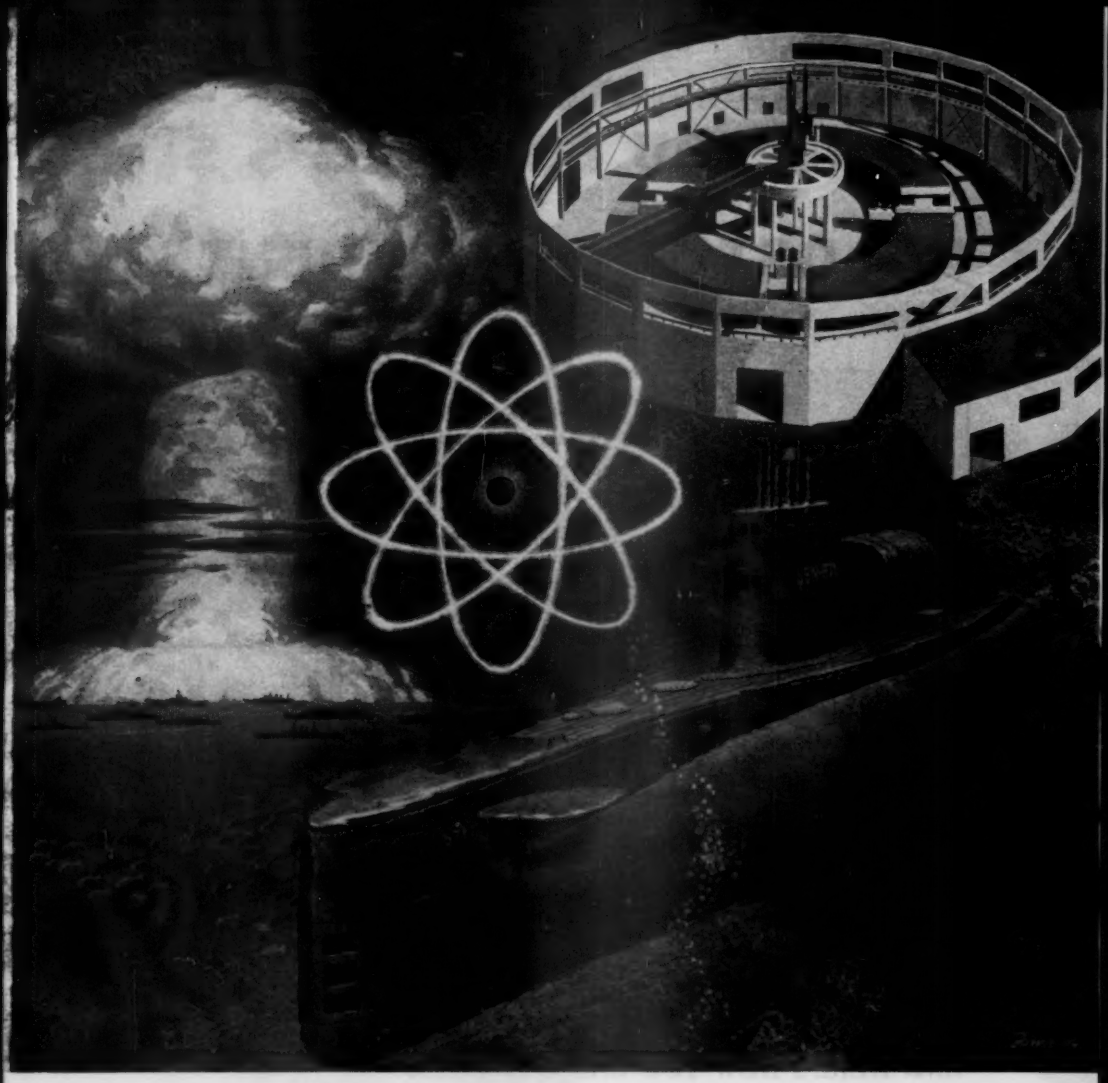

Small but significant. The minute atom abruptly revolutionized scientific theories with its significance. General's automatic plotter and computer—the *Geopac*—has also revised modern thinking. This *compact unit* presents an entirely *new concept* in seismic interpretation. Offering speed and accuracy, the *Geopac* frees the seismologist from numerous routine details. *Geopac*—the efficient, economical method of processing and presenting seismic data.

General
GEOPHYSICAL COMPANY
HOUSTON CLUB BUILDING • HOUSTON, TEXAS
In Canada: 10508 81st Avenue, Edmonton, Alberta, Canada
General Geophysical Company de France (SARL), 4 Square Rapp • Paris 7, France
General Geophysical Company de Venezuela, C. A., Sociedad A. Camejo No. 16 • Caracas, Venezuela
General Geophysical Company (Bahamas) Ltd.

WHEN YOUR CONTRACT IS WITH GENERAL, THE PERCENTAGE FOR SUCCESSFUL EXPLORATION IS IN YOUR FAVOR

ARE YOU LOSING $ $ $

IN LOST-TIME ACCIDENTS?

Misfires, snake bites, strained backs, lopped off fingers, attacks by wild animals . . . few other professions present the occupational hazards faced by geophysical field parties. Time is money in exploration, and lost-time accidents cost you $ $ $.

Now the SEG Committee on Safety has available a series of 35 mm color slides which can help you bring home to your field people the value of good safety practices.

HERE'S WHAT YOU CAN GET . . .

Shot Point Boners (set of 12)	$12.50
Drilling Boners (set of 12)	$12.50
Doodlebug Boners (set of 12)	$12.50
Pre-departure Checkout (set of 35)	$37.50
It Could Happen To You (set of 56)	$42.50

AND HERE'S HOW YOU CAN GET THEM . . .

The SEG Committee on Safety has these five sets of 35 mm color slides available immediately. To order any one or all of the series write, enclosing payment, to:

Mr. Colin Campbell, *Business Manager*
Society of Exploration Geophysicists
Post Office Box 1536
Tulsa, Oklahoma

Please mention GEOPHYSICS when answering advertisers

we'll show you where

. . . to locate your next well and give you an accurate picture of oil-producing possibilities.

For positive results and high production, you can depend on Tidelands' experienced crews.

A COMPLETE GEOPHYSICAL SERVICE

9233 WESTHEIMER ROAD HOUSTON 27, TEXAS

W & T Sensitive SURVEYING ALTIMETERS

DURABLE

SELF-BALANCING

CUSTOM CALIBRATED

ACCURACY 0.1%

STANDARD RANGES

Minus 1000 to 3000 feet
Minus 1000 to 6000 feet
Minus 1000 to 15000 feet
Special Ranges Available

Write for additional information

WALLACE & TIERNAN INCORPORATED

25 MAIN STREET, BELLEVILLE 9, NEW JERSEY

In Canada, Wallace & Tiernan, Ltd. — Toronto

A-118.42

transistorized voltage supply for seismic amplifiers

Here is a *completely static* unit which is far more dependable than vibrators or dynamotors. The ARNOLD power supply is used as a regulated supply for vacuum tube or transistorized seismic amplifiers. Inherent in the design and construction are these advantages:

No radiated interference
No ripple below 1KC
Low output impedance from 0 to 1KC
Shock resistant and hermetically sealed
Operates from −65°F to +160°F
No moving parts—hence long life and no maintenance.

SPECIFICATIONS
Input: 6, 12 or 24 volt batteries.
Output: Any voltage from 6 to 1200 volts, regulated 2% for discharging battery and variations of load, simultaneously.
Weight: 19 ounces.
Size: 3" diameter x 3 1/16" high.

Arnold power supplies are used by Pan American Petroleum Corp., Seismic Explorations, Inc., and other leading companies. *Write for literature on the Model 591-E.*

ARNOLD MAGNETICS CORP.
4613 West Jefferson Boulevard, Los Angeles 16, California
Telephone REpublic 1-6344

BERT & RALPH DUESING

"Selling Atlas Explosives"

BIG LAKE, TEXAS — HASKELL, TEXAS

GEOPHYSICAL CASE HISTORIES, VOLUME II

Contents

General and historical papers	6
Salt dome case histories	6
Reef case histories	6
Anticline case histories	23
Stratigraphic trap case histories	3
Mining case histories	3
New uses case histories	5
Total number of papers	52

WITH GENERAL INDEX AND INDEX TO MAPS

$6.00 to SEG, AAPG and AIME members—$10.00 to others

Payment must accompany order No C.O.D. orders accepted

SOCIETY OF EXPLORATION GEOPHYSICISTS

Box 1536 Tulsa 1, Oklahoma

Your
FIRST CHOICE...

MAYES-BEVAN
SEISMOGRAPH and GRAVITY METER SURVEYS

MAYES-BEVAN
GRAVITY METER
M
B
SEISMOGRAPH
COMPANY

KENNEDY BUILDING • TULSA, OKLAHOMA

EUROPEAN ASSOCIATION
OF
EXPLORATION GEOPHYSICISTS

The E.A.E.G. was founded in December 1951

The aims of the Association are to promote the science of exploration geophysics by establishing contacts and encouraging co-operation and fellowship between geophysicists in Europe and elsewhere and by disseminating knowledge of the science through the agency of regular meetings and the publication of technical papers.

MEMBERSHIP

Active Members pay an annual membership fee of Neth. fls. 15.—, increased by Neth. fls. 0.50 collecting charges. In U.S. currency this charge amounts to $4.10.

Prospective Members. Anybody interested in geophysics can apply for membership by sending in an Application Form, duly filled out. Forms will gladly be supplied by the Secretary-Treasurer of the E.A.E.G. but may also be obtained through the kind assistance of the Business Manager of the S.E.G.

GEOPHYSICAL PROSPECTING

Official Journal of the European Association of Exploration Geophysicists

This journal is issued quarterly and contains articles written in English, French or German. English, however, is predominant and each article is preceded by an abstract in that language.

Active members receive the journal free of charge.

In accordance with the Terms of Affiliation with the Society of Exploration Geophysicists, members of that Society may enter a current subscription to the journal for the normal membership fee.

The Subscription Rate for non-members is Neth. fls. 22.—(U.S. $5.80) per annum. Single copies are available at Neth. fls. 6.—(U.S. $1.60). These rates include packing and postage and are payable in advance. A limited quantity of previous issues is still available at the same price.

Advertising rates will be sent upon request.

All communications to be directed to:

THE SECRETARY-TREASURER E.A.E.G.

30, C. VAN BYLANDTLAAN • THE HAGUE • NETHERLANDS

HERE and ABROAD

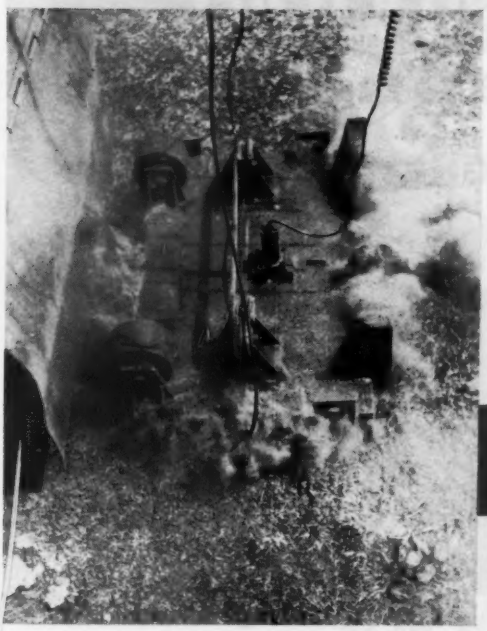

THE

RED WEIGHT

IS

GEOGRAPH

Searching for OIL

FIRST IN THE FIELD OF WEIGHT DROPPING

In Canada, Algeria, all over the world, McCollum GEOGRAPH crews are proving the weight drop technique's speed, safety, economy and accuracy in the search for oil. The versatility of GEOGRAPH in hard rock areas, frozen terrain, desert sand, etc., illustrates its advantages over conventional methods in obtaining accurate seismic data while completely eliminating the need for shot holes and explosives. Seventeen years of research and development on GEOGRAPH assures the world market the most effective and economical exploration method.

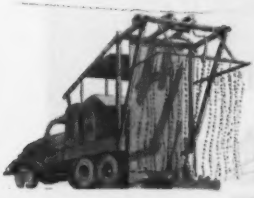

McCOLLUM SINCE 1923
Exploration Company
1025 S. Shepherd Drive, JAckson 8-5427, Houston, Texas

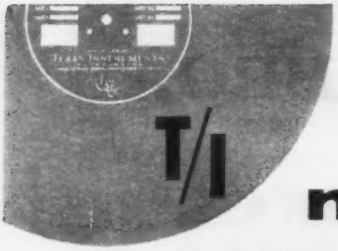

magneDISC*

DISC-TYPE MAGNETIC RECORDER

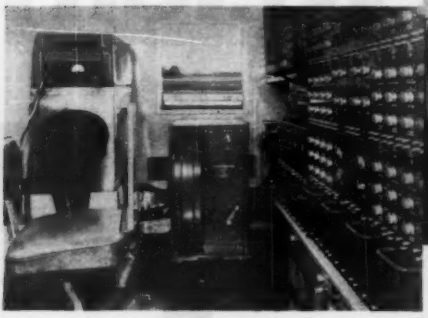

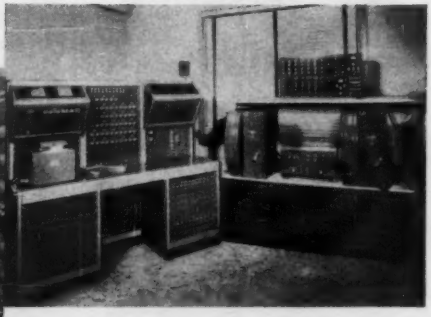

Best in the Field!

The magneDISC has proved its operational superiority in exacting seismic data recording conditions throughout the world.

Greater Capacity—Record up to 115 data and auxiliary traces at one time.

Reliable and Rugged—No pampering required . . . no air-conditioned, dust-free, humidity-controlled environment is needed for accurate performance of the magneDISC.

No "Barber-Poling"—The disc is the most stable geometric design for magnetic recording . . . no skewing of tape to affect accuracy.

Recording Heads stay in precise alignment—discs can be played interchangeably on any magneDISC—tolerances are maintained to insure timing accuracy of ±½ millisecond trace to trace.

Best in the Central Processing Office!

The versatility of the magneDISC is unsurpassed in the CPO, used in conjunction with the seisMAC for automatic data reduction.

Speed of Processing—utilizing two 115 head magneDISC Transducer Units, data may be played from one through the seisMAC and re-recorded on the other in one continuous operation.

Greater Operational Latitude—two T/D Units provide 230 channels of information for mixing, compositing, or stacking as desired—no necessity for synchronization of several drums as with other systems.

Easier Handling and Storage—one movement of lever accurately positions disc in the T/D Unit—eject button pushes disc out for easy removal. magneDISCS take up less storage space than any other type of magnetic recording medium.

For complete information and the many other advantages of the magneDISC, write for Bulletin ___S-307; or request a visit from the TI representative!

TEXAS INSTRUMENTS INCORPORATED
INDUSTRIAL INSTRUMENTATION DIVISION
3609 BUFFALO SPEEDWAY • HOUSTON, TEXAS • CABLE: HOULAB

* T/I system

7090

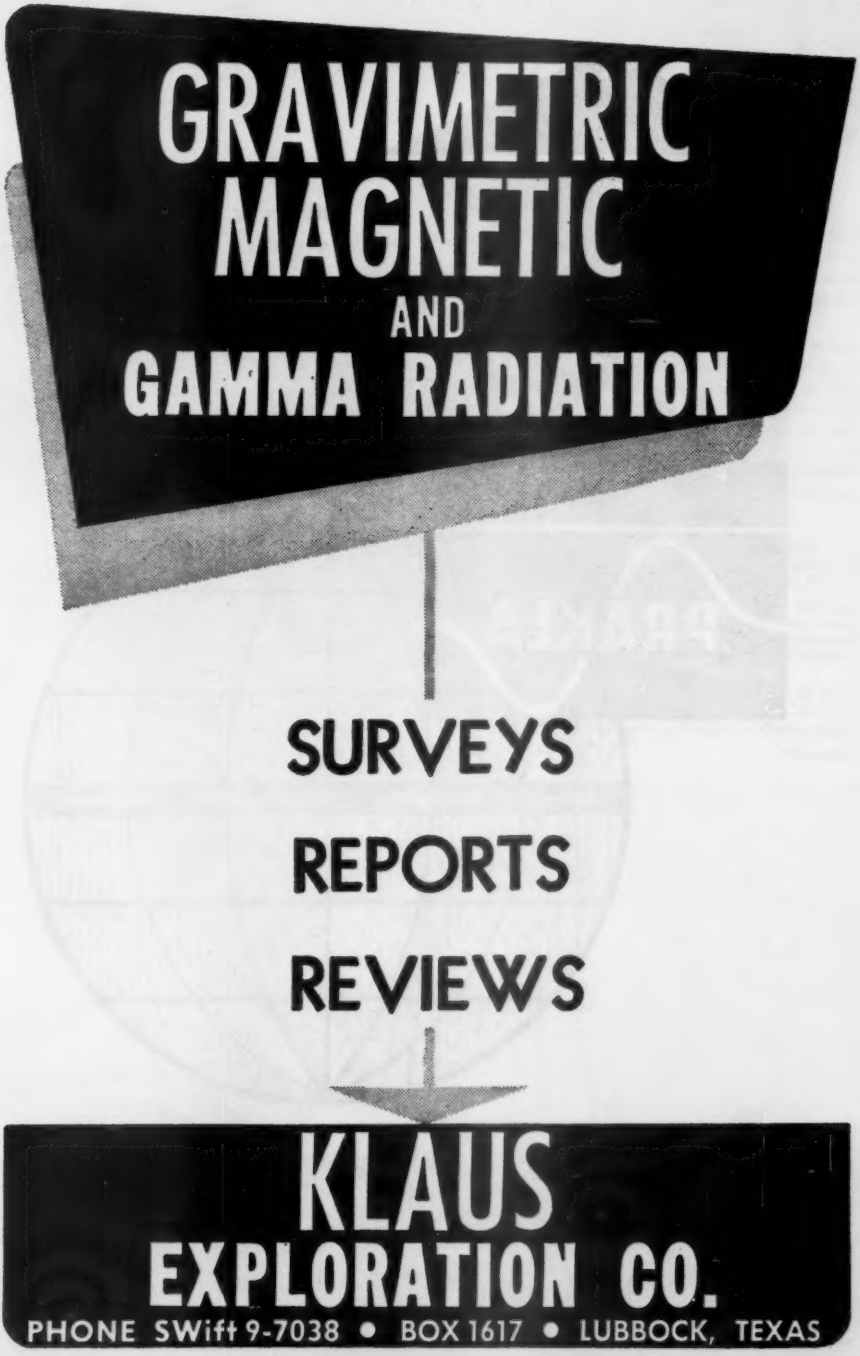

Please mention GEOPHYSICS when answering advertisers

PRAKLA-PARTIES
ALL OVER THE WORLD

PRAKLA

HANNOVER · HAARSTRASSE 5

PHONE: 8 6 6 6 1 · TELEX: 9 2 2 8 4 7 · CABLE: PRAKLA

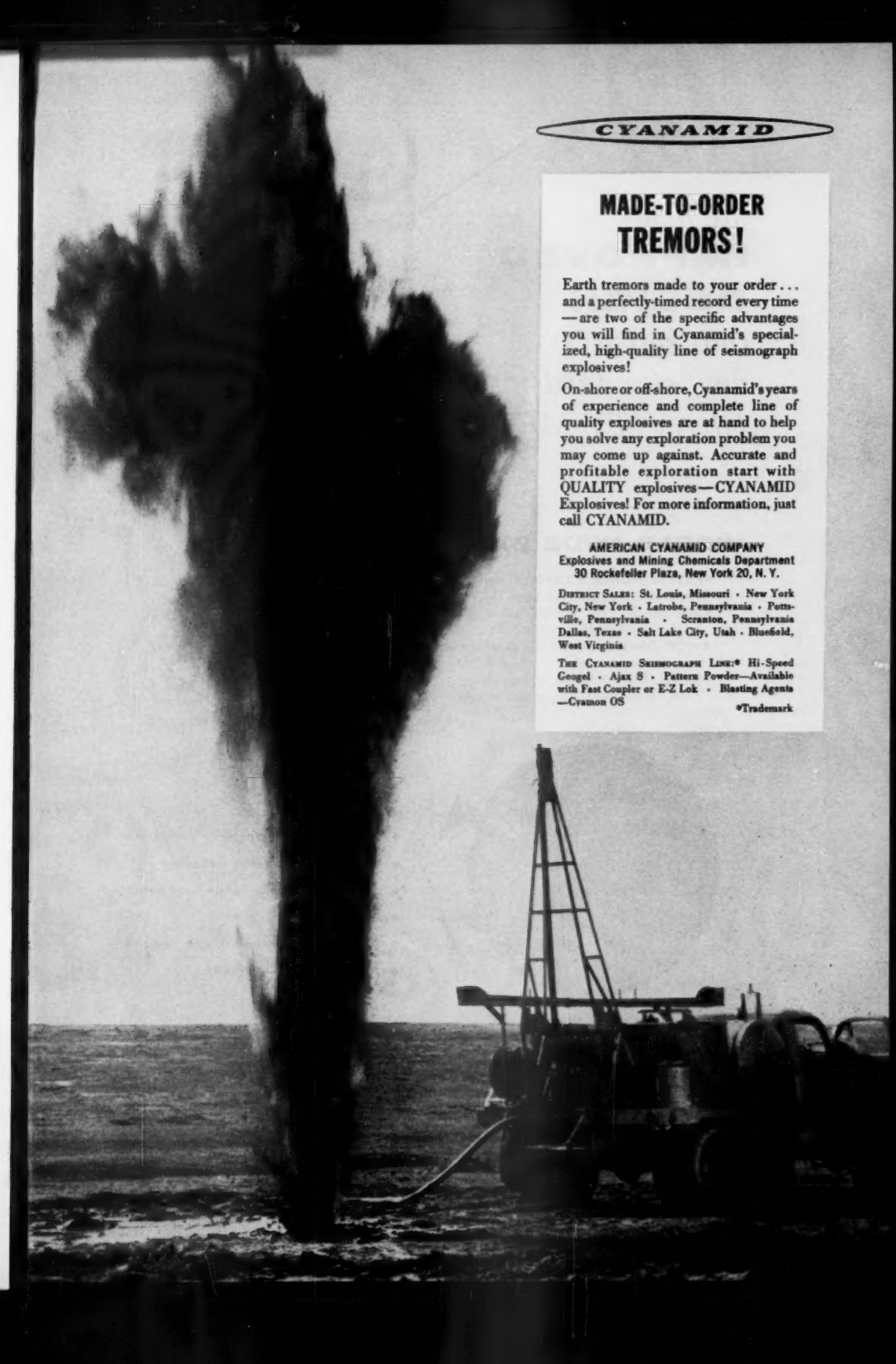

CYANAMID

MADE-TO-ORDER TREMORS!

Earth tremors made to your order . . . and a perfectly-timed record every time —are two of the specific advantages you will find in Cyanamid's specialized, high-quality line of seismograph explosives!

On-shore or off-shore, Cyanamid's years of experience and complete line of quality explosives are at hand to help you solve any exploration problem you may come up against. Accurate and profitable exploration start with QUALITY explosives—CYANAMID Explosives! For more information, just call CYANAMID.

AMERICAN CYANAMID COMPANY
Explosives and Mining Chemicals Department
30 Rockefeller Plaza, New York 20, N. Y.

DISTRICT SALES: St. Louis, Missouri • New York City, New York • Latrobe, Pennsylvania • Pottsville, Pennsylvania • Scranton, Pennsylvania Dallas, Texas • Salt Lake City, Utah • Bluefield, West Virginia

THE CYANAMID SEISMOGRAPH LINE:* Hi-Speed Geogel • Ajax S • Pattern Powder—Available with Fast Coupler or E-Z Lok • Blasting Agents —Cyamon OS

*Trademark

the new
IMPROVED DESIGN
that sets a new standard in GRAVITY METERS

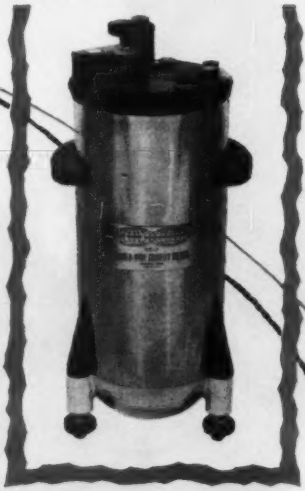

WORLD-WIDE EXCLUSIVE FEATURES

- **EASY READING COUNTER** enables the operator to read the meter without removing from the tripod.
- **RECESSED LEVEL BUBBLE** avoids direct sunlight thereby eliminating level bubble creep.
- **WORLD-WIDE RANGE** for all meters regardless of latitude, without returning to laboratory for further range adjustments.
- **SMALL DIAL RANGE** of approximately 100 milligals minimizes resetting instrument in rugged terrain.

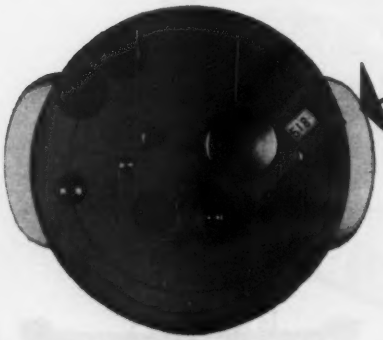

- Lightweight, completely portable
- .01 milligal reading accuracy
- Thoroughly temperature compensated
- Direct digital reader
- No external power source required
- Full two year warranty

• Direct reading digital counter facing upwards, and read like an automobile mileage recorder, enables operator to read without removing from tripod. Small dial range approximately 100 milligals.

WORLD-WIDE INSTRUMENTS, INC.

3802 South Shepherd—Houston 6, Texas U.S.A.
Cable Address: WRLDWIDINS HOUSTON

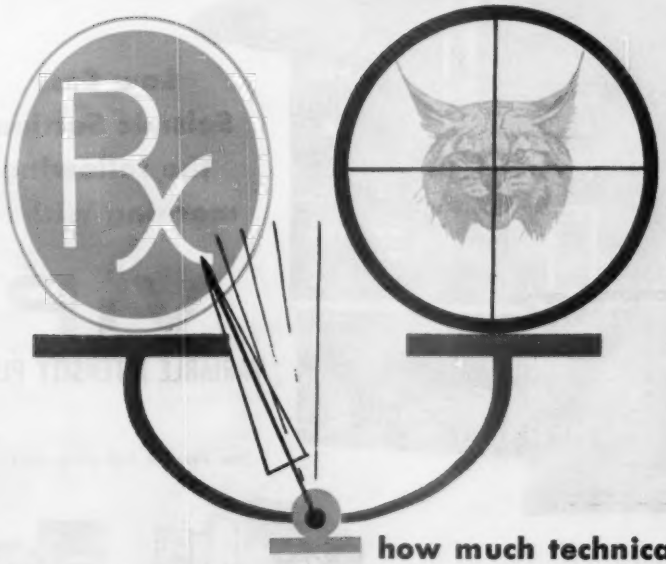

how much technical assistance is needed to increase your wildcat hits? . . .

ALL YOU CAN GET! Technical assistance, in the form of sound geological and geophysical counsel could easily be the difference between a "rich strike" or an "expensive miss".

National statistics bear this out — when technical advice, either geological or geophysical, or both, are used to locate drilling sites, the wildcatter's chances for success are increased by nearly 300%. Think that over . . . then call REPUBLIC. The latest in magnetic equipment and modern methods are at your disposal.

A map of the U. S. showing major geological features is now available to you. Write: Republic, Dept. B, Box 2208, Tulsa. Okla.

REPUBLIC EXPLORATION COMPANY
TULSA, OKLAHOMA — MIDLAND, TEXAS

Please mention GEOPHYSICS when answering advertisers

Low Cost Seismic Sections the following morning with...

VIP*

VARIABLE INTENSITY PLOTTER

VIP's speed, low initial cost and lowest processing cost per profile, make it ideally suited for day-to-day processing of seismic data in the field office. It is easily transported from prospect to prospect, and, of most importance, *VIP* is compatible and operative with all makes of amplifier and magnetic transducer systems.

This first ALL-ELECTRONIC system devised for variable density presentations rapidly corrects for time or depth and compresses wide areas of seismic data into section form. The *VIP* cross section closely approaches a geologic section and is easily comprehended.

Operating directly from any magnetic record, the *VIP* processes 24 channels at one time (or sequentially) over full record length — corrections may be viewed as applied — maintains timing accuracy of ± one millisecond. For complete information on the field-proved *VIP*, write for Bulletin No. S-322.

Use Versatile VIP everywhere . . .

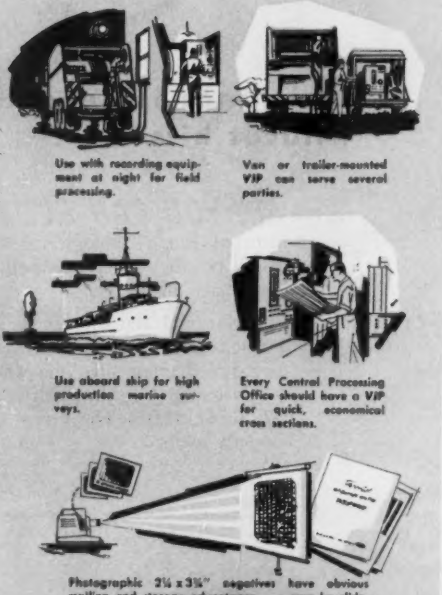

Use with recording equipment at night for field processing.

Van or trailer-mounted VIP can serve several parties.

Use aboard ship for high production marine surveys.

Every Central Processing Office should have a VIP for quick, economical cross sections.

Photographic 2¼ x 3¼" negatives have obvious mailing and storage advantages . . . may be slide-projected, or blown up to report size or working size sections.

TEXAS INSTRUMENTS
INCORPORATED
INDUSTRIAL INSTRUMENTATION DIVISION
3609 BUFFALO SPEEDWAY • HOUSTON, TEXAS • CABLE: HOULAB

a "Seismafloat" system

*Trademark of Texas Instruments Incorporated

182

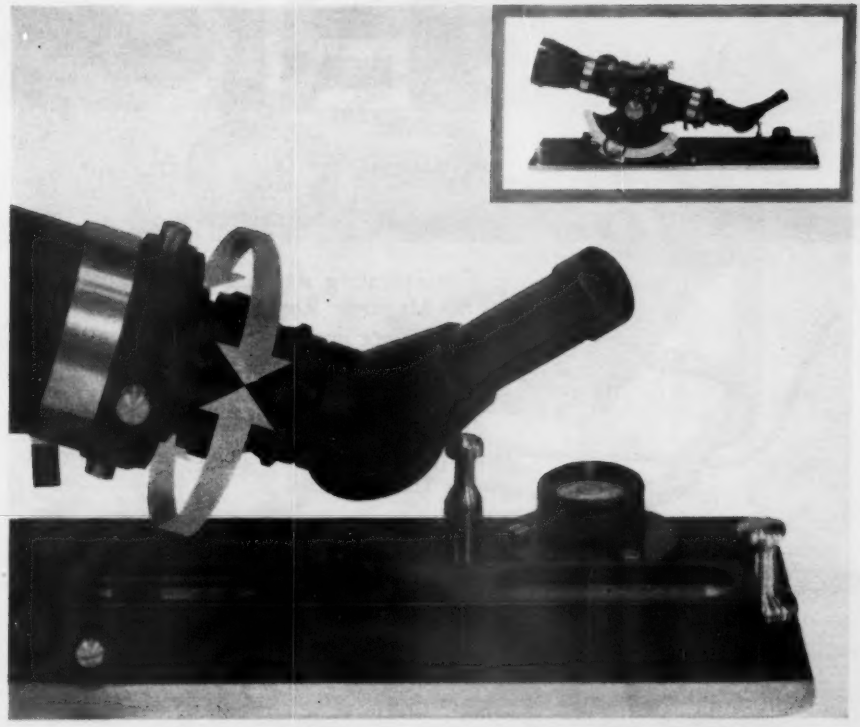

New elbow eyepiece for Gurley Alidades

Permits faster set-up... easier reading—even with glasses

Gurley Alidades are now available with a new swivel-type elbow eyepiece in place of the standard diagonal prism eyepiece. This eyepiece may be turned to permit reading from the top or either side, and adjusted for easy viewing.

Engineers who are using the new Gurley Alidade Eyepiece in the field report a saving in time...less danger of knocking the instrument out of position...and much greater convenience in reading—especially for those wearing eyeglasses.

The new swivel-type elbow eyepiece is available on the Gurley Standard Alidade (Model 582) and the Gurley Explorers Alidade (Model 580). It can also be added to Gurley Alidades now in use. For complete information on the eyepiece, write W. & L. E. Gurley.

GURLEY W. & L. E. GURLEY, ALIDADE DEPARTMENT, TROY, N.Y.

Please mention GEOPHYSICS when answering advertisers

EIC DR-50

Incorporating standard EIC features, the DR-50 Magnetic Recording System provides new versatility in direct recording. The system can be constructed with from 25 to 50 seismic and information channels.

Tape speed is 3.6 inches per second; head spacing is ¼ inch. The power supply is completely transistorized.

Write, wire or phone for detailed information.

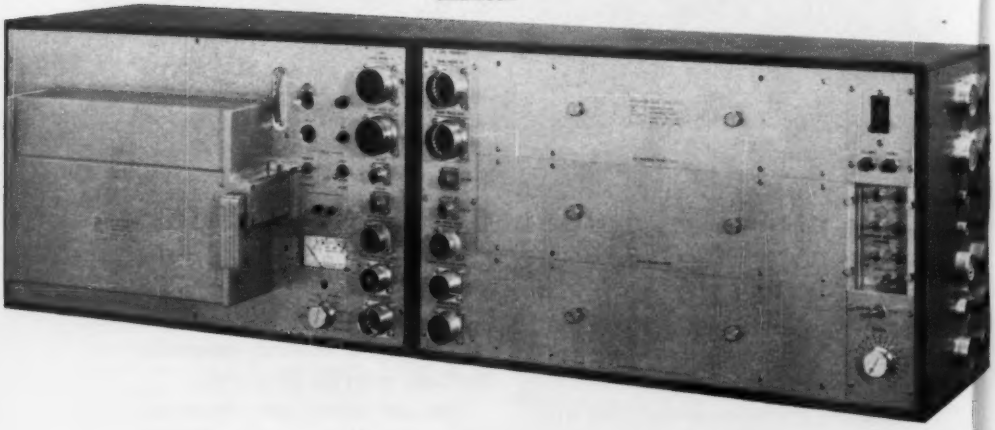

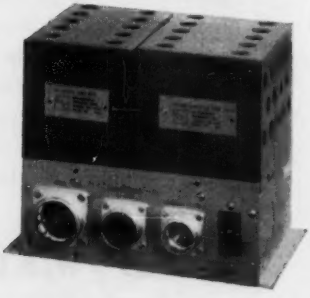

ELECTRODYNAMIC INSTRUMENT CORPORATION

2508 Tangley Road
Houston 5, Texas

Novelty

ASKANIA

GRAVIMETRIC MEASUREMENTS AT SEA

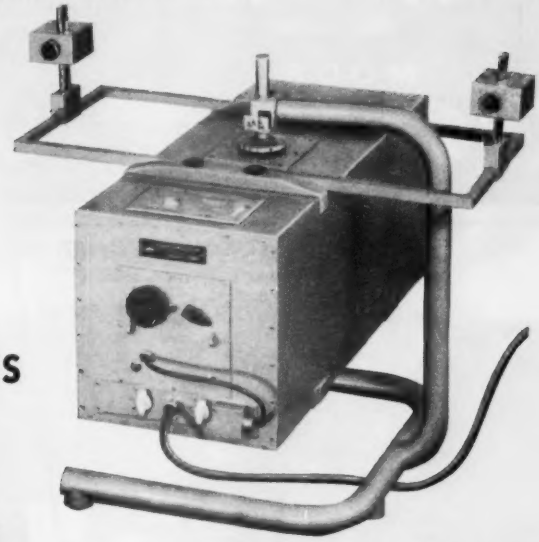

FROM MOVING SURFACE SHIPS BY MEANS

OF THE

ASKANIA SEA GRAVIMETER AFTER GRAF

ATTAINABLE ACCURACY: 1 mgal

U.S. BRANCH ASKANIA-WERKE AG
4913 CORDELL AVE BETHESDA, MD.

ASKANIA-WERKE AG · BERLIN-FRIEDENAU

DALLAS
MAYHEW
TEXAS

MODEL 200-T

See us in Booth 59 at the Convention.

featuring maximum application versatility . . .

SHOOTING UNIT

Transports explosives, shooting equipment, and water for shot-tamping in seismic operations. Includes racks for loading poles, casing or drill stem.

★HOT-HOLE DRILL

Light-weight rotary type utilizing chain pull-down, double-drum drawworks, 4½ x 5 mud pump. Pump provides uphole water velocity of 300 ft. per minute with a 4" bit.

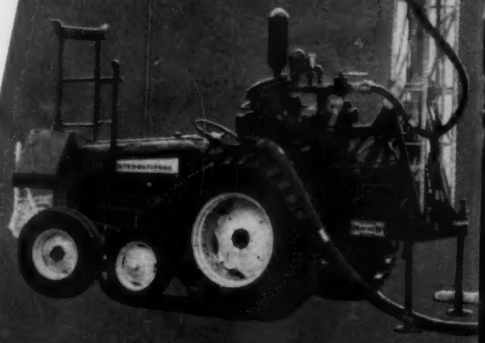

WATER TANK

All-steel body incorporates water tank, racks to carry drill stem, loading poles, or casing.

TRACTOR-MOUNTED

to permit year-round operations in most areas formerly inaccessible to truck-mounted equipment.

★ Choice of International 350 or Ford 820 tractor. Half-tracks optional.

HOME OFFICE

MAYHEW SUPPLY CO., INC.

4700 SEVENTH ROAD • DALLAS, TEXAS

SALES AND SERVICE

CASPER, WYOMING • TULSA, OKLAHOMA • SIDNEY, MONTANA • LUBBOCK, TEXAS • GRAND JUNCTION, COLORADO GALLUP, NEW MEXICO • EXPLORATION EQUIPMENT CO. INC., HOUSTON, TEXAS

CANADA

SEISMIC SERVICE SUPPLY, LTD., CALGARY AND EDMONTON, ALBERTA

EXPORT

IOSCO — MEADOWS BLDG., DALLAS, TEXAS, P. O. BOX 1331

SEI

EXPERIENCE

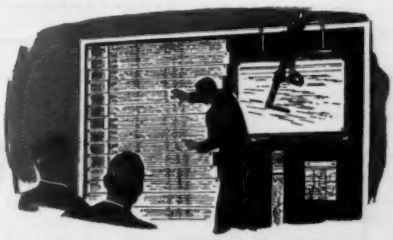

INTERPRETATION

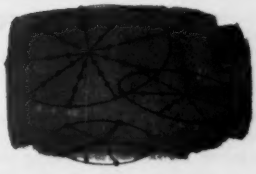

TECHNIQUE

For twenty-six years, SEI has specialized in subsurface studies of the domestic oil provinces . . . from Canada to the Gulf. Numerous innovations in instrumentation, interpretation, and field technique have kept SEI in the forefront. For example, in difficult areas, SEI has been a pioneer in the use of patterns of multiple shot holes and geophone arrays.

Your exploration program is in capable hands at SEI.

SEISMIC EXPLORATIONS INCORPORATED

1017 SOUTH SHEPHERD • HOUSTON, TEXAS

Area Offices: Midland, Texas • Shreveport, Louisiana • Oklahoma City, Oklahoma • Billings, Montana

An easily read, clearly illustrated text on
Modern Geophysical Techniques

EXPLORATION GEOPHYSICS

by J. J. Jakosky, Sc. D.

In more than 1200 pages and with 715 illustrations, the 1957 revised printing of *Exploration Geophysics* covers the entire field of exploration by modern geophysical methods. It is concisely and clearly written by an internationally known geophysicist, in close collaboration with 39 other leading authorities.

Thirteen fact-packed chapters fully cover all contemporary methods; plus permit, trespass and insurance problems. A basic textbook for every geologist, geophysicist, engineer and physicist concerned with exploration, well logging and production. Adopted by many leading universities.

FREE EXAMINATION

Send your money order or check for $12.50 for a copy of Exploration Geophysics on 5-day approval. If you are not fully satisfied, merely return the book in its original condition and your money will be promptly refunded.

TRIJA PUBLISHING COMPANY, 2500 W. COAST HIGHWAY, NEWPORT BEACH, CALIFORNIA

OLSEN SEISMOGRAPH SUPPLIES

GROUNDHOG DRILL BITS

YOURS FOR FASTER AND CHEAPER FOOTAGE

GARLAND, TEXAS
BOX 428

PHONES
BROADWAY 6-5117
NITE BROADWAY 6-2808

AUTO-SEIS

a new milestone in seismic exploration

AUTO-SEIS is streamlined for efficient operation with automatic cable handling equipment.

ON DISPLAY at Booths 79-80 at the S.E.G. National Convention in San Antonio.

THE AUTO-SEIS in-cable geophone makes automatic planting a practical reality. The result of an extensive research program conducted by the same engineers who developed the small, light weight detector that made multiple geophone operations practical, the Hall-Sears AUTO-SEIS opens a new era of high production, low labor cost exploration.

AUTOMATIC PLANTING . . . with optimum effectiveness due to careful weight vs. contact area design.

AUTOMATIC ORIENTATION . . . positive perpendicular positioning. Ingenious design eliminates fragile and troublesome gimbals.

SIMPLICITY OF DESIGN is a major factor in the reliable performance and low maintenance of the AUTO-SEIS.

DAMPING is not significantly affected by external loads. Little if any movement is induced by the other detectors in the system, thus minimizing the possibility of "motor effect."

CLEAN, UNDISTORTED OUTPUT surprisingly high in a unit of this size. Any spurious resonances which might exist, considered inherent in most similar devices, are effectively eliminated by the use of silicon damping meduim.

RUGGED, FIELDWORTHY . . . made to stand up under hard field service. Streamlined for through-cable handling. Generous flex points guard against lead breakage.

LOW COST . . . close spacing, the key factor in self-planting systems, is now economically feasible with the extremely low cost AUTO-SEIS.

Contact us, or the closest member of the H-S International Group for further details and demonstrations.

H/S

HALL-SEARS, INC.

2424 BRANARD • HOUSTON, TEXAS, U.S.A.
Phone: JAckson 6-2975 • Cable Address: HALSEA

"WORLD WISE" IN SEISMIC INSTRUMENTATION

ONE OF A SERIES PRESENTING THE MEMBERS OF THE HALL-SEARS INTERNATIONAL GROUP.

Above: Headquarters of Hall-Sears Europa, N.V. Below: Views of portions of the offices and shops.

At the Crossroads of World Trade

Hall-Sears Europa, N.V. is located at Banstraat 2, The Hague, Holland. In this busy center of international oil activity Hall-Sears maintains a fully staffed office, engineering and manufacturing facilities, and a supply division unique in Europe.

Besides the numerous materiel and technical advantages of this region, the liberal policies of the Netherlands government make it possible to trade here in almost any currency. Many Hall-Sears customers find this a distinct advantage on transactions where the crossing of frontiers is often a problem.

The Hall-Sears world-wide organization brings a new standard of service to the geophysical industry

The Hall-Sears organization is devoted exclusively to the field of seismic instrumentation. Built around a staff whose accomplishments include the development and practical application of some of the most widely used instruments in seismic exploration, the parent company closely coordinates the activities of its far-flung affiliates. Thus, each of the six Hall-Sears offices not only maintains its own facilities, but each receives as well the full benefit of this accumulated staff experience and engineering skill. Hall-Sears is proud of the growing acceptance and reputation of its instruments throughout the industry, and of the character and scope of its world-wide network of facilities serving that industry.

Throughout the world, wherever there is oil exploration, the Hall-Sears Group stands ready to serve you.

HALL-SEARS INTERNATIONAL
P. O. Box 1841, Houston, Texas, U.S.A.
Cable Address: HALSEA

HALL-SEARS EUROPA, N.V.
Kanstraat 2, The Hague, Holland
Cable Address: HALSEA

HALL-SEARS FRANCE, S.A.
Business Office: 82 13e Haussmann, Paris, France
Works: Gaillard, France

SEISMIC INSTRUMENTS LIMITED
Granta Works, Cambridge, England

HALL-SEARS ALBERTA, LTD.
830 Eighth Avenue West
Calgary, Alberta, Canada

HALL-SEARS PACIFIC
Box 455
Goleta, California, U.S.A.

HALL-SEARS, INC.

2424 BRANARD • HOUSTON, TEXAS, U.S.A.

"WORLD WISE" IN SEISMIC INSTRUMENTATION

HALL-SEARS
Model HS-100
SEISMIC AMPLIFIER SYSTEM

the first really new and improved equipment of its kind in years

Remote Control Unit.

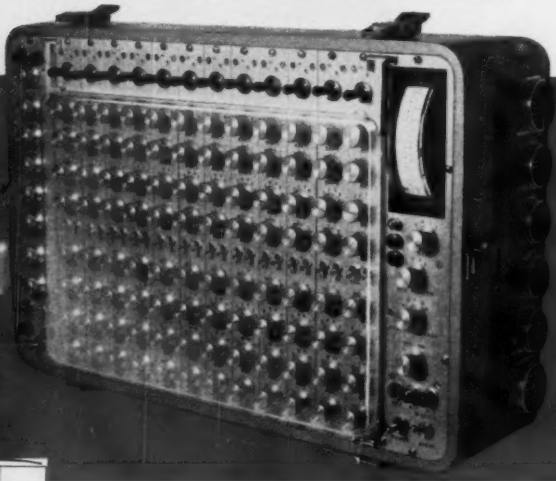

Amplifier with cover removed, showing clear plastic control cover in place. Overall amplifier dimensions (with cover) 12½" x 19½" x 7".

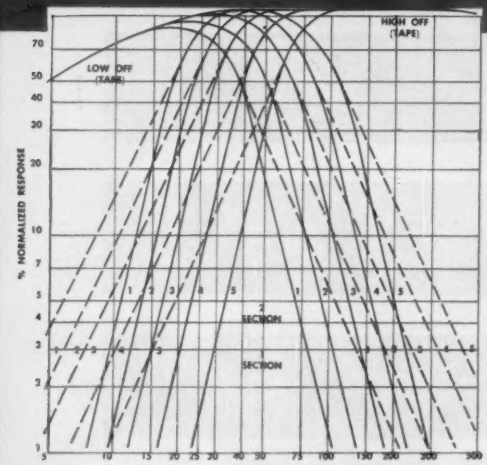

Steady State Sinusoidal Filter Response

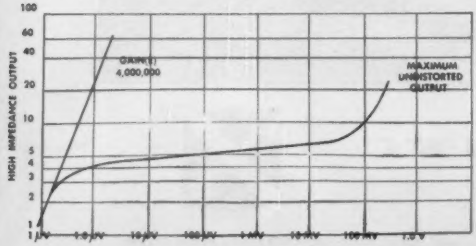

Steady State AGC Characteristics

The HS-100 Seismic Amplifier is being acknowledged as today's most modern seismic field recording amplifier system.

Some of the exceptional features of the HS-100 include first break filter switching • unusually wide range of filtering-mixing-AGC combinations • signal handling capacity without distortion better than .5 volt • built-in transistorized power supply • remote control operation • adaptability to magnetic recording equipment • simplified cabling • extensive moisture-proofing • rugged cast aluminum case • light weight. (Complete 12-channel unit weighs only 57 pounds.)

See this new amplifier in operation to appreciate how fully it meets the most demanding requirements of modern geophysical operations. A demonstration will be arranged at your convenience.

ON DISPLAY at Booths 79-80 S.E.G. National Convention in San Antonio.

H/S

HALL-SEARS, INC.

2424 BRANARD • HOUSTON, TEXAS, U.S.A.
Phone: JAckson 6-2975 • Cable Address: HALSEA

"WORLD WISE" IN SEISMIC INSTRUMENTATION

In longitudes East and West, in latitudes North and South . . . on each of the six continents . . . Robert H. Ray crews are at work. During every minute of the day, somewhere RHR men are busy recording, computing, and interpreting geophysical data. These many and varied man hours create direct and efficient methods . . . produce detailed and accurate results.

Expertly manned and completely equipped for either Seismic (Reflection and Refraction), Magnetometer, or Gravity methods, Robert H. Ray Co. is prepared to carry your explorations to any geographical location.

This vast experience is cumulative. It works for *You* in every contract with Robert H. Ray Co.

ROBERT H. RAY CO.

2500 Bolsover Road • Houston 5, Texas

RHR CO. SEISMIC • MAGNETIC • GRAVITY

ROBERT H. RAY ROBERT S. DUTY JR. JACK C. POLLARD NORMAN P. TEAGUE

TEX-TUBE

SHOT HOLE CASING
16 GAGE - 19 GAGE
With The
EXCLUSIVE SPEED
COUPLER JOINT

Strong, and light-weight **Tex-Tube** Shot Hole Casing with the exclusive Speed Coupler Joint will solve your shot hole problems! Light enough to carry in—strong enough to drill with! Each length of 16 gage **Tex-Tube** Shot Hole Casing weighs only 20 pounds. Each length of 19 gage weighs 13 pounds. The exclusive **Tex-Tube** Speed Coupler Joint makes up fast—without collars. Only two quick turns make a water tight connection strong enough for high pressure jetting. Field tests prove **Tex-Tube** best.

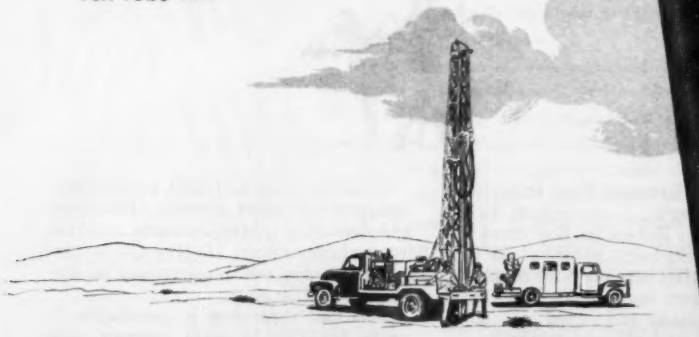

H & T Sales Co.	Beeville, Texas	FLeetwood 8-1642
Bilderback Dynamite Co.	Lafayette, Louisiana	CEnter 4-6184
	Houma, Louisiana	UPtown 2-0861
Par-Tain Exploration Co.	Bakersfield, California	FAirview 5-3764
Deupree Distributing Co.	Oklahoma City, Oklahoma	JAckson 8-6740
Grove Hardware Co.	Oklahoma City, Oklahoma	JAckson 8-4886
Teton Tool Co.	Mills, Wyoming	CAsper 2-7181
Seismic Service Supply, Ltd.	Calgary, Alberta, Canada	5-5691
Venezuelan Supply, C. A.	Caracas, Venezuela	71-53-21
National Supply Co. Export Division	New York City	Circle 6-3232

Tex-Tube, Inc.

Houston, Texas
UN 9-3411

Baton Rouge, Louisiana
ELgin 5-1430

Houma, Louisiana
UPtown 2-0569

LIBYA REVISITED
in 60,000 square mile Aero surveys

Two new air surveys in Libya, totaling 60,000 sq. mi., are now being added to the 165,000 sq. mi. already logged there by veteran AERO crews.

One survey, for Mobil Oil Company of Canada Ltd. and Oasis Oil Company of Libya, will be used for photogeological studies of their concessions. Air photos are made at 31,000 ft. from an AERO B-17. AERO photomosaics will later aid logistical planning.

The other survey, for Pan American International Oil Company, involves both photo coverage and airborne magnetometer studies to aid in determining basement depths and sedimentary structures. To offset turbulent air at low altitudes over the desert, the magnetometer flights are made with DC-3 fixed tail-cone magnetometer installation. Monitoring stations check for magnetic storms.

Both surveys are being conducted over remote desert areas —400 to 500 miles distant from air bases in Bengasi and Tripoli. It's the tough jobs like these that call for the experience and equipment of AERO—pioneer and leader in the field.

AERO SERVICE CORPORATION
Oldest Flying Corporation in the World
Philadelphia 20, Pa.

AIRBORNE GEOPHYSICAL STUDIES • PRECISE AERIAL MOSAICS • PHOTO INTERPRETATION
RELIEF MODELS • TOPOGRAPHIC AND PLANIMETRIC MAPPING

RUSKA MAGNETOMETERS

Now with New Type Temperature Shielding

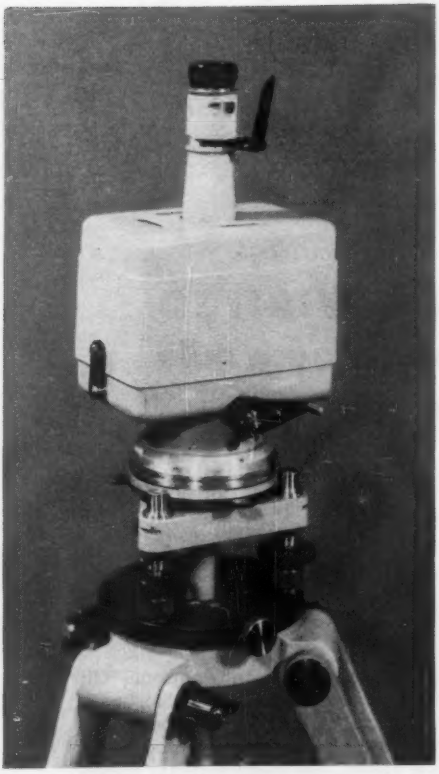

TYPE V—Vertical Magnetic Field Balance

TYPE H—Horizontal Magnetic Field Balance

TYPE VR—Vertical Magnetic Recording Balance

TYPE HR—Horizontal Magnetic Recording Balance

Standard Sensitivity
10 gamma per scale division —visual

10 gamma per millimeter— recorded

"SCOUT"—a light-weight vertical reconnaissance magnetometer

Standard Sensitivity
25 gamma per scale division

All Ruska magnetometers are equipped with temperature compensated systems with sapphire knife-edges.

ALSO: HOTCHKISS TYPE SUPER-DIP

BETTER BECAUSE THEY ARE MADE TO BE BETTER

A superior product plus a program of continual improvement keeps Ruska instruments unsurpassed. Built to remain accurate and to stand hard use, they are the choice of prospectors the world over.

RUSKA INSTRUMENT CORPORATION

4607 MONTROSE BLVD. HOUSTON 6, TEXAS

IF YOU WANT TO
RING THE BELL

CALL Milligal

Milligal can help you solve the problem of a difficult, unproven location through our accurate, reliable, scientific service.

Specify an E. V. McCollum & Co. GRAVITY SURVEY first for prompt, precise, dependable investigation.

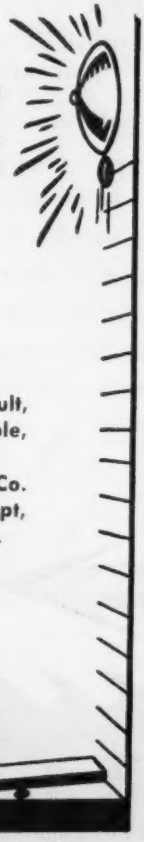

E.V.McCOLLUM & CO.
WE WEIGH THE EARTH

E. V. McCollum Craig Ferris
515 Thompson Bldg. Phone CHerry 2-3149
Tulsa, Oklahoma

Foreign Affiliate: NAMCO INTERNATIONAL

Electro-Tech Gravity Meters

(FORMERLY MANUFACTURED BY NORTH AMERICAN GEOPHYSICAL CO.)

Accurate Control of Temperature Guarantees Lowest Drift-Rate

Electro-Tech Portable Gravity Meters are manufactured in several models, each specially designed for particular applications. Sensitivities and accuracies of 0.01 milligal are provided on all meters except for tidal recording use where one microgal sensitivity and accuracy is usual. No barometric or temperature corrections are necessary.

LAND GRAVIMETERS AG-1 standard exploration model has reading range of approximately 100 milligals. Quick reset mechanism allows use in any latitude or elevation.

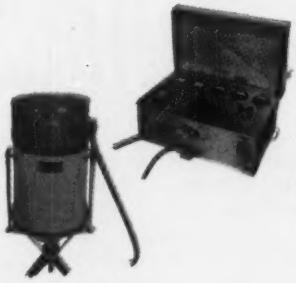

MARSH GRAVIMETERS Remote controlled RM-1 is unequalled for work in shallow water, mud or swamp areas. Small movements of operator, boat or vehicle do not disturb readings.

ELECTRO-TECH

RENT OR RENTAL PURCHASE

ELECTRO-TECHNICAL LABS

Division of Mandrel Industries, Inc.

P. O. Box 13243 Houston 19, Texas

SEISMOGRAPH SURVEYS*

**long and short term contracts*

C. N. PAGE A. E. "SANDY" McKAY C. J. LOMAX

Central Office
2111 Continental Life Bldg.
Fort Worth, Texas

Division Offices

WEST TEXAS
Midland, Texas

GULF COAST
Houston, Texas

ROCKY MTS.
Denver, Colorado

Foreign Affiliate: namco INTERNATIONAL

GET NEW BUSINESS . . . EXPAND YOUR SERVICES

with the

OMNITAPE

MAGNETIC MEDIA TRANSCRIBING SYSTEM...

Places every Major Magnetic Recording at your finger tips...

- Carter Pulse Width
- Electro Tech DS-7
- Electrodynamic F M and Direct
- SIE F M and Direct
- Techno Direct
- Texas Instruments magneDISC
- Others as specified

OMNITAPE transcribing data from Texas Instruments magneDISC to SIE FM tape.

NOW, you can transcribe data at will from any magnetic recording to any other, regardless of type tape or disc, speed, recording method, track spacing or number of channels. The *OMNITAPE*, in effect, places every magnetic transport in use today in your processing office, and at a fraction of the cost of the individual magnetic systems.

The *OMNITAPE* is fast, flexible, easy to operate . . . maintains accuracy and fidelity of the original recordings. This first successful instrumentation for standardizing magnetic media offers new and profitable advantages to Geophysical Contractors, Oil Companies, and Independent Processing Agencies alike. Write today for complete information.

Be sure to see the OMNITAPE at the SEG Show in San Antonio!

HALE *Instruments Inc.*

343 West 23rd St. • P. O. Box 7487 • Houston • UN 1-7574

105

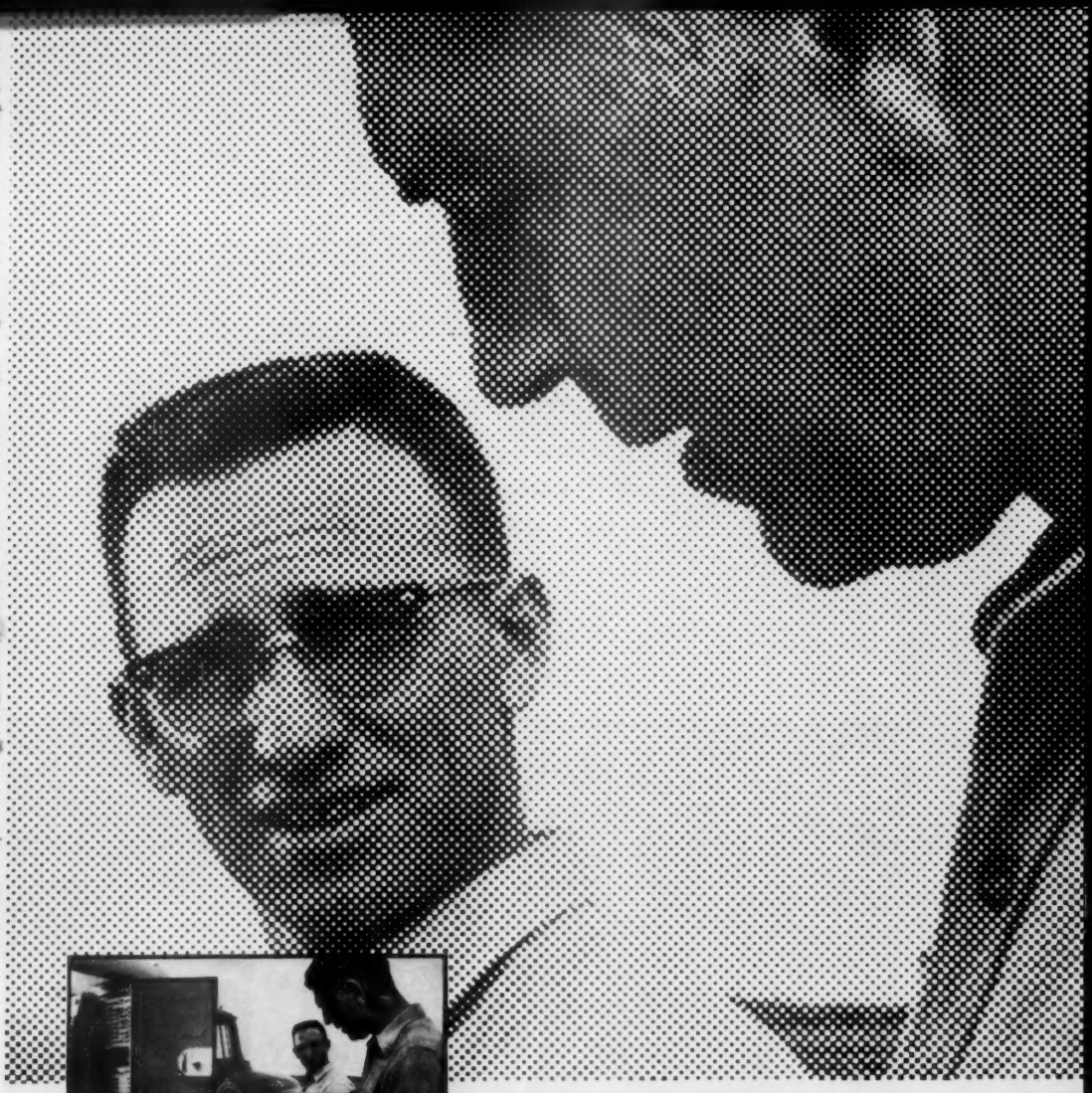

THE QUALITY OF HUMAN JUDGMENT

is the important part of your survey picture

The superiority of IX surveys is a matter of skill and experience. Independent has the finest seismic exploration equipment available. In the final analysis, however, it's the demonstrated ability of IX personnel that makes the difference. Independent has proved itself to virtually every independent and major oil company. More than 1763 man years of experience go into every exploration job. Next time, call in IX.

POINTING THE WAY IXO FOR THE DRILL

INDEPENDENT EXPLORATION CO.

1973 West Gray, Houston, Texas
1 Frederick's Place, Old Jewry, London, E.C.2, England
12 Rue Chabanais, Paris, France

Geophysical Surveys

OVER 1763 MAN YEARS OF EXPERIENCE

oedip

The only discoveries

in the Sahara make it

obvious :

Wherever oil hides,

CGG finds it

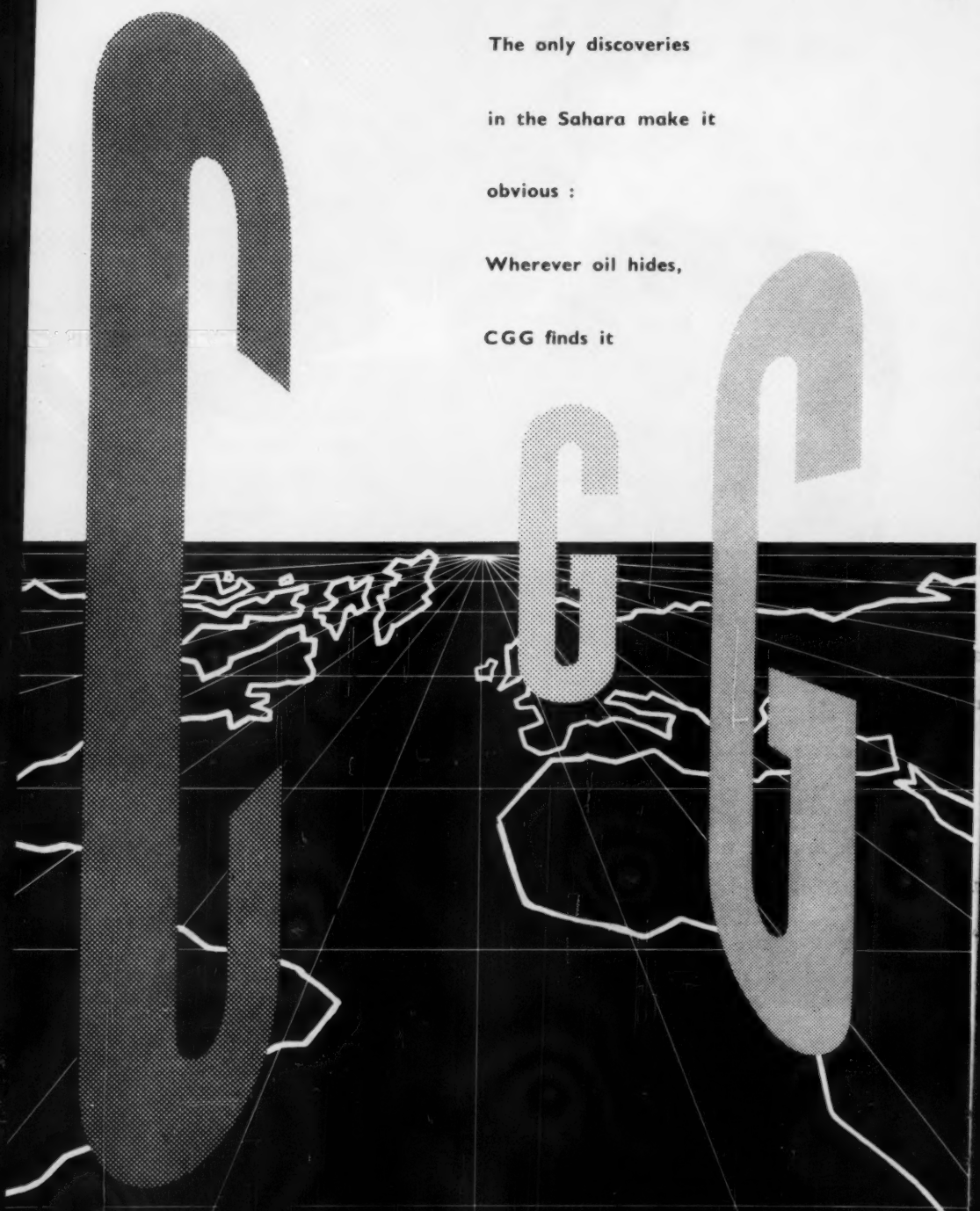

COMPAGNIE GÉNÉRALE DE GÉOPHYSIQUE, 50, RUE FABERT - PARIS-7e

One of the leading geophysical contractors

There's a Petty crew below

In areas like this, fifty-feet is a cross-country trip; yet the world's tough terrain is just routine to Petty. Unexplored areas are no obstacle to our modern methods of exploration . . . in mountain, jungle, desert or offshore. If you're looking for oil, at home or abroad, get the most for your dollar by putting Petty in your picture.

33 YEARS EXPLORATION

IN ALL TERRAIN

Petty GEOPHYSICAL ENGINEERING CO.

SAN ANTONIO 5, TEXAS

District Offices: Houston, Tulsa, Denver, Lafayette

You can believe it when you see it

When you are faced with the question "Will it make a producer?", the Schlumberger Formation Tester gives the answer.

From the soft sands of the Coastal Areas to the hardrock country of the Mid-Continent, more than 3,000 successful tests have given clear decisions — *each test pin-pointed exactly in the interesting section shown by the log.*

It's a natural combination — a Schlumberger Log that indicates presence of oil followed by a Schlumberger Formation Test that puts oil in your hand.

The Schlumberger Formation Tester provides:

- Fluid Recoveries
- Gas-Oil Ratios
- Gas-Oil and Oil-Water Contact Levels
- Flowing and Shut-In Pressures
- Pressure Build-Up for Formation Pressure and Permeability Studies

It's quick, safe and economical. Ask your Schlumberger Representative for details on the Formation Tester.

THE EYES OF THE OIL INDUSTRY*

SCHLUMBERGER

Here are the best two reasons for the REFRACTION REVIVAL!

TI **VLF VERY LOW FREQUENCY SEISMOGRAPH** AND **S-36 HIGH-OUTPUT 2-CYCLE SEISMOMETER**

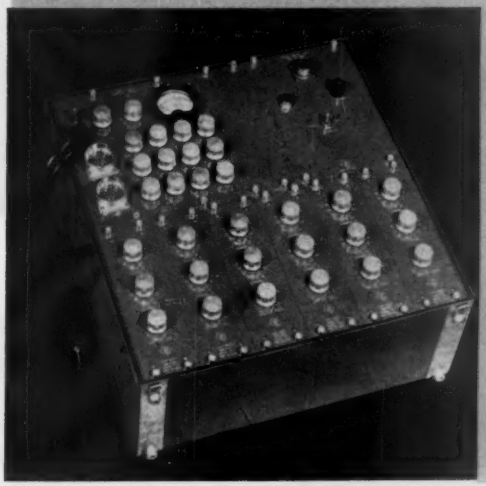

Although the Refraction Seismograph was used as an exploration tool many years before the Reflection method, it was virtually abandoned during the thirties because of the inability of existing equipment to record low frequencies and build up a satisfactory signal-to-noise ratio.

SAVE UP TO 50% ON DYNAMITE — SHOOT ANY TIME OF THE DAY!

Now, the thoroughly field-proved *VLF* Refraction System provides highly usable results for large area surveys or in areas unworkable by the reflection method. Excellent first breaks and second arrivals have been recorded while using less than half the dynamite required by other systems. Furthermore, the *VLF's* high signal-to-noise ratio permits shooting during the usually windy mid-day hours when other systems cannot produce usable results. With frequency response down to one cycle on the amplifiers and to two cycles on the S-36 seismometers, the versatile *VLF* system is equally satisfactory for the most difficult petroleum exploration programs, mining surveys, and civil engineering projects.

You can be sure of the best attainable refraction results with the compact and portable 12-channel *VLF* system. Write for complete information — specify Bulletin S-308.

TEXAS INSTRUMENTS
INCORPORATED
INDUSTRIAL INSTRUMENTATION DIVISION
3609 BUFFALO SPEEDWAY · HOUSTON, TEXAS · CABLE: HOULAB

a Seismation system

183

Don't miss the premiere showing of

a new line of magnetic recording instruments by

TECHNO

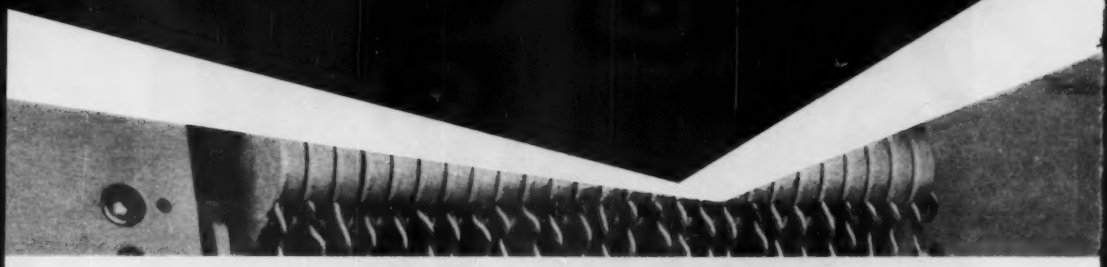

featuring

- greater productivity
- single-unit portability
- increased versatility
- simplified installation
- complete transistorization

SEE THEM AT SAN ANTONIO / BOOTHS 13 and 14

Techno Instrument Company 6666 LEXINGTON AVE., LOS ANGELES 38, CALIFORNIA / HOllywood 5-3304

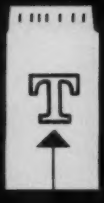

Toll free in most cities / ENterprise 3304

Rogers crews go everywhere . . . .

If your proposed petroleum province lies along the Po, or on the Pampas; if it's in the states or the Sahara . . . Rogers crews are there now (or have been). For these are the crews that operate worldwide, that assure you accurate geophysical surveys.

Consult Rogers about your potential province, regardless of its location.

Rogers *Geophysical Companies*

3616 WEST ALABAMA • HOUSTON, TEXAS

Edificio Republica • Caracas, Venezuela
Mogadiscio • Somalia
34 Ave. de. Champs Elysees • Paris, France
1-3 Arlington St., St. James's • London S.W. 1, England

Geophysics abroad

Ask SEISMOS GmbH HANNOVER-GERMANY

Central Processing Office with seismac system

equipped to process
HTL Magnetic Discs
SIE Magnetic Tapes

Geophysikalische Messungen überall

SEISMOS GmbH HANNOVER

Refraktion · Reflexion · Gravimetrie (zu Lande und zu Wasser)
Geoelektrik (Eigenpotential · Widerstand · Induktion)
Szintillometrie (carborne)
Magnetik

Please mention GEOPHYSICS when answering advertisers

TRANSFORMER NEWS FROM TRIAD

GEOPHYSICAL TRANSFORMER RELIABILITY

Every coil on every Triad Geophysical Transformer is tested (1) before impregnation, (2) before assembly, and (3) after completion. Induction tolerances are held within ±5% of standard. In addition to the Triad Geophysical Transformers listed in our catalog (all especially designed to meet the peculiar and difficult conditions of geophysical prospecting) we will supply units to *your* specifications—at reasonable cost and in reasonable time.

These are some of the reasons why Triad Geophysical Transformers have long been the standards of excellence for geophysical prospecting. We'll gladly send you our catalog. Please ask for **TR-58.**

TRIAD

4055 REDWOOD AVENUE, VENICE, CALIFORNIA
812 E. STATE STREET, HUNTINGTON, INDIANA

A SUBSIDIARY OF LITTON INDUSTRIES

Please mention GEOPHYSICS when answering advertisers

CLEVITE
CORPORATION
TEXAS DIVISION

for the best

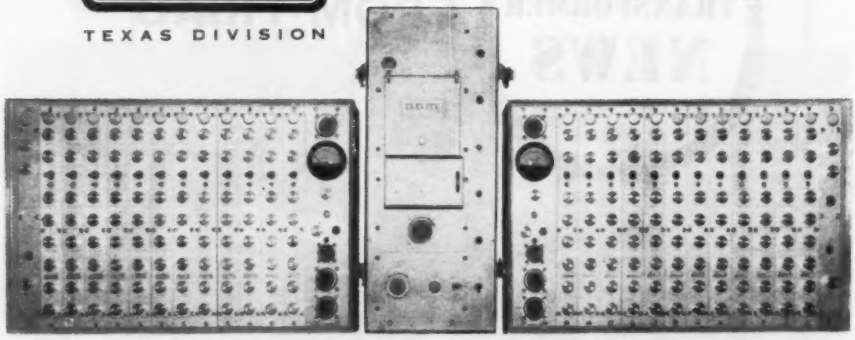

The Clevite Universal Seismic Recording System . . .

This truly universal system can be used for either FM or direct recording. The seismic amplifiers have outputs for both magnetic recorder and oscillograph, permitting *simultaneous recording* of magnetic and photographic tapes. Monitoring may be accomplished by sequential teledeltos monitor (using ink or electric stylus) or conventional oscillograph.

The Clevite Recording System is well suited to portable or mobile use. The system consists of: (1) Tape Transport (FM or direct), (2) Two Seismic Amplifier Banks, (3) Transistorized Power Unit, (4) 28-channel Modulator Bank and (5) Direct Writing Monitor or Oscillograph. No single unit weighs over 55 lbs.

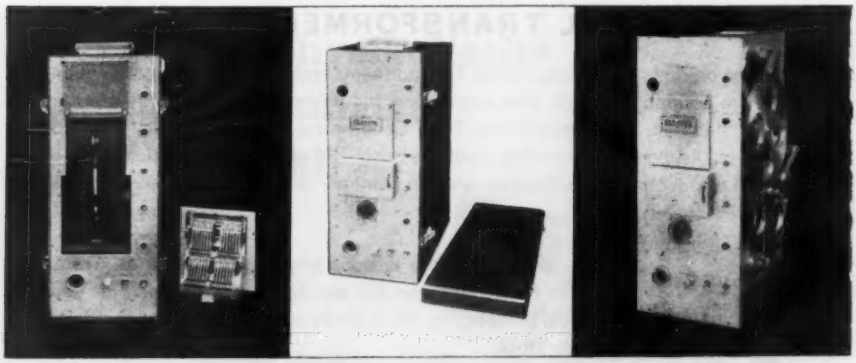

Complete Head Bank, mounted on precision ways, is removable without tools. Single channel may be replaced and phased in the field.

MFR-1 Tape Transport has submersible, lightweight fiberglass case. Dimensions: 8" wide x 22" high x 17" deep.

Unique Belt Drive System of stainless steel is servo-controlled and locked to precision fork frequency standard. Operation is noiseless.

Please mention GEOPHYSICS when answering advertisers

...in Universal Seismic Systems

POWER UNIT
MODEL TFP-1

Size: 15½" wide x 13" high x 11" deep.
Weight: 20 lbs.
Power Requirements: 6.5 amps.
Output: plus 170 v. minus 150 MA — 100 v. bias.
Dual regulated.

OPTIONAL EQUIPMENT

DIRECT WRITING MONITOR
four-inch teledeltos paper with preprinted timing lines.
Electric or ink stylus.
Drum shaft quick-coupled to magnetic drum shaft.
Any trace in any sequence available for monitoring from single front panel control.
Sequential operation.
Size: 8" wide x 22" high x 17" deep.

PHOTOGRAPHIC OSCILLOGRAPH
May be used for monitor (with demodulator or playback amplifiers)

MODULATOR BANK, MODEL MM-4 (FM System)
Fourteen dual channels plus control and metering panel. Less than 1% distortion, 3 v. input at 1 megohm for full modulation.
Size: 23¼" wide x 16¾" high x 7" deep.

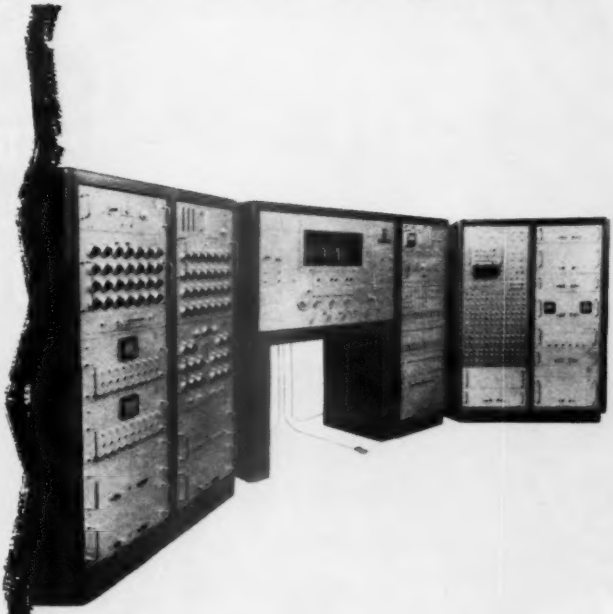

The Clevite Universal Seismic Analog Computer ...

enables the geophysicist to extract an unprecedented amount of significant information from field-recorded seismic tapes. And he can do so with greater accuracy and less time lag between tape and mapped results. Moreover, the analog computer technique permits a wider range of electronic inputs.

The computer continuously derives variable and fixed corrections and inserts these corrections in field data simultaneously. Time or depth scaled records may be run off with all corrections made. Compositing by pairs, to eight pairs, may be accomplished using raw or corrected tapes from the same or different shot points. Flexible filtering or mixing combinations are available.

The Clevite (MRA-2) Computer combines the best features and accuracy of analog computation with the most flexible servo mechanization. Ask for literature and a demonstration.

CLEVITE CORPORATION

9820 South Main Street, Houston 25, Texas

TEXAS DIVISION

Now Available

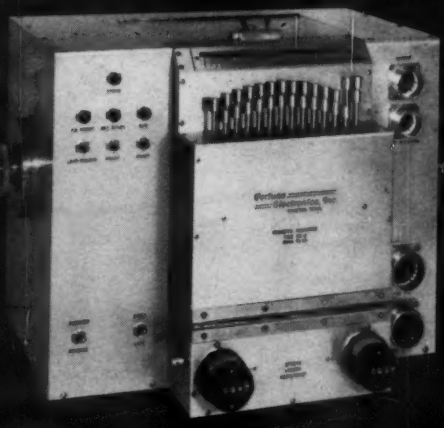

FORTUNE ELECTRONICS' DC-2

. . . the economical record-playback unit for office and field use

Fortune Electronics' new dynamic correction record-playback unit makes it possible for you to obtain accurate, corrected playbacks in the office or on location with a minimum initial investment. *The compact DC-2 handles any shot spread configuration. Spread length adjustments are calibrated directly in feet.* The unit accommodates standard six and one-half or seven inch tapes. Weighing only 82 pounds, the DC-2 is easy to handle—requires minimum space.

SPECIFICATIONS

Physical Characteristics

Maximum Dynamic Correction	150 ms
Static Correction	±50 ms
Drive	400 cycle Hysteresis Motor Gear Coupled to Drum
Size	15 x 18 x 14 inches
Weight	82 pounds
No. of Traces	26 or 28

Electrical Characteristics

Power Requirements	8 amperes @ 12 volts
Signal/Noise Ratio	50 db RMS to RMS
Timing Accuracy	±1 ms
Total Harmonic Distortion	2½% @ 100% Record Level
Crossfeed	−60 db @ 10 cycles

See The DC-2 on Display—Booth No. 34-SEG Convention Oct. 13-16—San Antonio, Texas

For complete details on the all new DC-2 write or call:

Fortune Electronics, Inc.

H. H. HAPPEL—H. H. HAPPEL, JR.
2505 SOUTH BOULEVARD, HOUSTON, TEXAS

Represented in Dallas, Texas and Tulsa, Oklahoma by Indel Supply Company

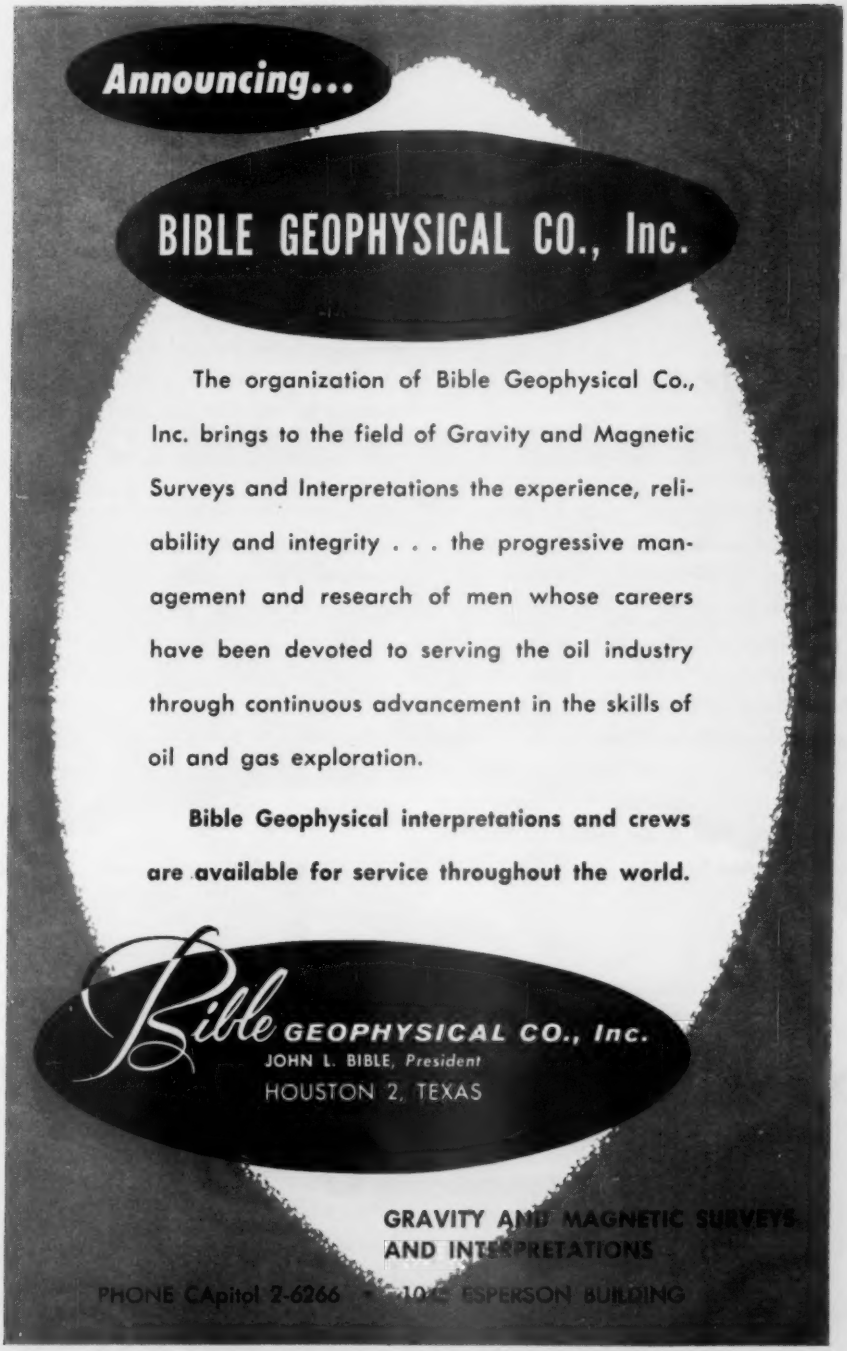
Announcing...
BIBLE GEOPHYSICAL CO., Inc.
The organization of Bible Geophysical Co., Inc. brings to the field of Gravity and Magnetic Surveys and Interpretations the experience, reliability and integrity . . . the progressive management and research of men whose careers have been devoted to serving the oil industry through continuous advancement in the skills of oil and gas exploration.
Bible Geophysical interpretations and crews are available for service throughout the world.
Bible GEOPHYSICAL CO., Inc.
JOHN L. BIBLE, President
HOUSTON 2, TEXAS
GRAVITY AND MAGNETIC SURVEYS AND INTERPRETATIONS
PHONE CApitol 2-6266
ESPERSON BUILDING

The Forest and The Trees

The old expression of not being able to see the forest for the trees has its application in exploration work as well as in forestry. As an extreme example, consider the effect on the reflection seismograph of a piercement salt dome. As a rule, the local complications of the structure eliminate usable data over the dome. On the other hand, the gravity method being "blind" to the small details gives its most satisfactory results in that same area. The case history of the Hawkins field is an excellent example of where, because of the complicated faulting, the trees almost caused the forest to be overlooked.*

This reasoning is not confined to salt domes. The principle is universal in that we may say that the gravity meter is looking at the mass of the structure while the seismograph is looking at its surface detail. Both points of view are necessary for the most thorough analysis of the subsurface.

The nature of the gravity method also assists in giving a more complete view of the "setting" of the local structure in relation to its surroundings; for example, its relationship to nearby structures or its position relative to the axis of the basin.

In order then, to see the forest *and* the trees, we believe that we can be of valuable assistance to you in your exploration efforts.

* A.A.P.G. Vol. 30, p. 1856, map insert.

Thomas J. Bevan
910 South Boston

Ed M. Handley
Tulsa, Oklahoma

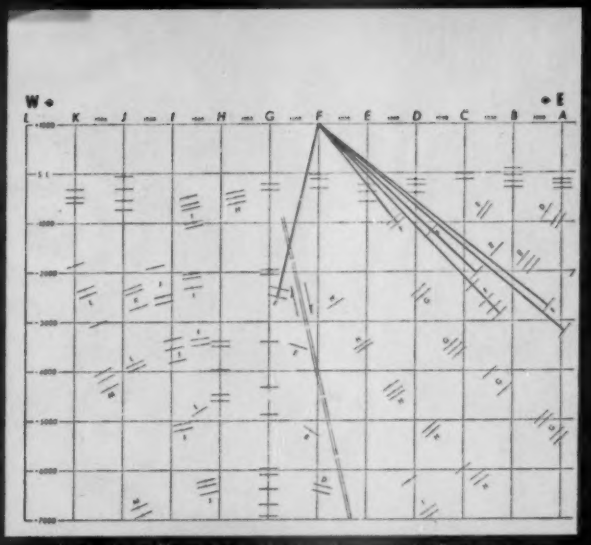

A seismic profile section in depth with migrated reflecting points.

SSC ACCURATELY DETERMINES GEOLOGIC STRUCTURES...

SSC's Seismic Replay Center in combination with the Sinclair Dip Plotter provides completely interpreted seismic data.

This service is now available for your magnetic or photographic field data.

Contact SSC TODAY for more complete information.

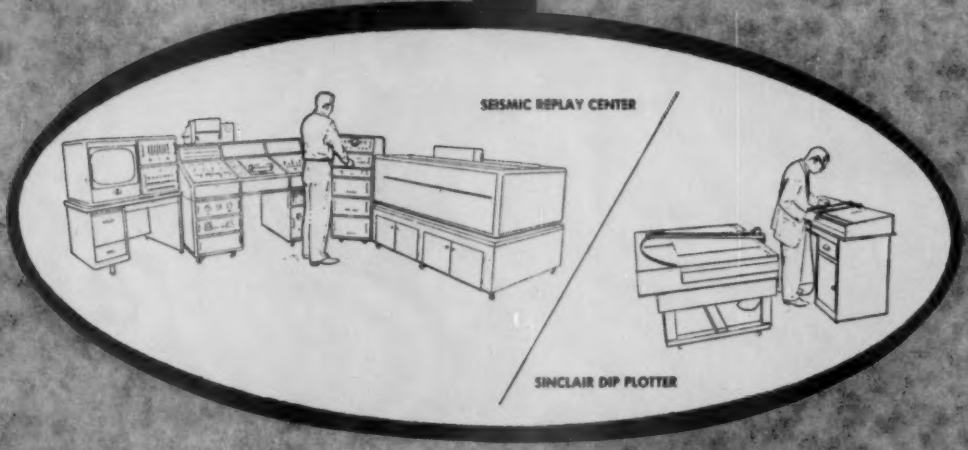

SEISMIC / GRAVITY AND MAGNETIC SURVEYS / LORAC / CONTINUOUS VELOCITY LOGGING

Seismograph Service Corporation

6200 East 41st Street • TULSA, OKLAHOMA • Riverside 7-1181

WORLD-WIDE SUBSIDIARIES

SSC of Canada / SSC of Colombia / SSC of Bolivia / SSC of Libya / SSC of Mexico
SSC of Venezuela / SSC International
Seismograph Service Limited — England
Seismograph Service Italiana / Compagnie Française de Prospections Sismique

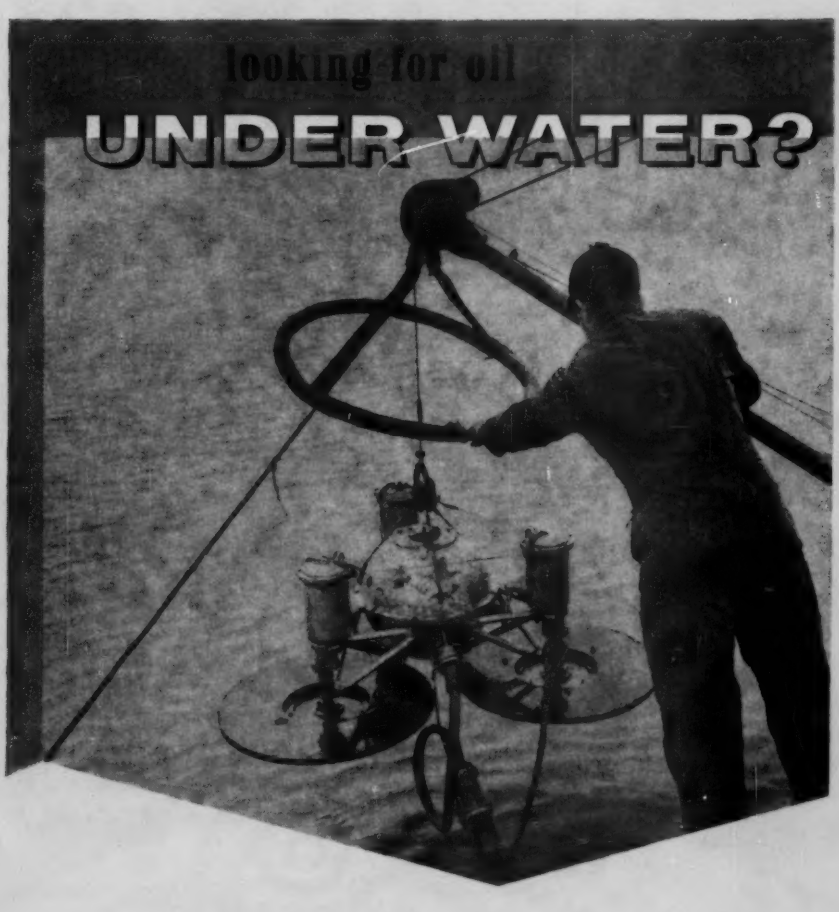

Murky or clear, water can't cloud the answers to your exploration problems when a GSI underwater gravity party goes in search of them.

Data integration makes the difference. GSI cooperates with your exploration staff by interpreting data in the light of all available geophysical and geological information.

Remember... we not only work *for* you, we work *with* you.

Write today for Bulletin G 58-1 "Underwater Gravity Surveys"

GSI... continuing leadership through research and growth

GEOPHYSICAL SERVICE INC.

100 EXCHANGE PARK NORTH • DALLAS 30, TEXAS